UNIVERSITY OF LONDON

IMPERIAL COLLEGE OF SCIENCE AND TECHNOLOGY

DEPARTMENT OF ELECTRICAL ENGINEERING

STEADY STATE AND TRANSIENT STABILITY ANALYSIS

OF

A.C. - D.C. POWER SYSTEMS

Thesis submitted for the Degree of
Doctor of Philosophy
in the Faculty of Engineering

by

Tam Cheuk Cheung, B.Sc. (Eng.)

London, England

September, 1969

ABSTRACT

The outlook for h.v. d.c. in the next decade is promising with three schemes close to commissioning and four more planned. The total capacity of these seven new schemes will be over 12,000 MW.

Ever since the beginning of h.v. d.c. activities the need to analyse the different aspects of mixed a.c./d.c. power systems has led to many different methods of representing d.c. converters and systems. A classification of these methods is proposed and forms the basis for an extensive discussion of these methods.

The interaction between d.c. converters and weak a.c. systems is considered and its effect on d.c. link power transfer limit is studied. Converter characteristics are discussed and causes of possible power oscillations are explained. A method for co-ordinating system transformer and converter taps is developed. An operation chart for a simple d.c. link is presented.

An a.c./d.c. load flow program is developed which can accommodate both single and double pole d.c. links with full conventional controls and has a comprehensive tap changer subroutine. This program provides the initial conditions for the transient analysis of a.c./d.c. systems. It has also been used to investigate the effect of the slope of converter characteristics, and a particular problem of non-convergence when an a.c. line outage is simulated.

For the transient analysis of a.c./d.c. systems a method using matrix algebra is developed and applied to a simple system. A transition matrix method for solving the d.c. line equations and a recursive method for representing d.c. link controls is described.

The particular problem of suddently isolating a generator onto a d.c. link is considered and two methods of control in order to limit voltage and machine frequency excursions are studied.

Methods of digital solution of differential equations using ordinary programming language and digital analog simulation languages are described. The advantages and disadvantages of these two approaches are discussed, and an extensive discussion of the desirable features of digital analog simulation languages is presented.

ACKNOWLEDGEMENTS

The author wishes to thank Mr. B.J. Cory, B.Sc.(Eng.), F.I.E.E., for his supervision, advice and encouragement throughout the course of the work described in this thesis.

He also acknowledges the helpful discussions with colleagues at Imperial College and the Central Electricity Generating Board.

The bursary from the Imperial College and the studentship from the Science Research Council are gratefully acknowledged. A special appreciation is due to the Central Electricity Generating Board, who sponsor this project, for providing useful data as well as the typing and reprographic facilities in the preparation of this thesis.

TABLE OF CONTENTS

LIST OF SYMBOLS

The most commonly used symbols are defined below; those not listed are explained in the text.

In general, upper case letters denote variables in practical units, while lower case letters denote variables in per unit.

Main Symbols

A	Slope of converter characteristics
B	Number of bridges in a converter group or susceptance
C	Capacitance
E	E.M.F. or voltage
H	Machine inertia constant
I	Current
I_{ds}	Current order of converter
P	Real power
Q	Reactive power
R	Resistance
V	Voltage
X	Reactance
Z	Impedance
Y	Admittance
T_d	Synchronous machine direct axis short circuit time constant
T_{do}	Synchronous machine direct axis open circuit time constant
T_{qo}	Syncrhonous machine quadrature axis open circuit time constant
f	Frequency
h, k, n	Transformer tap ratio
p	$\frac{d}{dt}$
s	Laplace transform operator or slip
t	Time
u	Commutation angle

α	Firing angle of converter
β	Angle of advance of inverter
γ	Extinction angle of inverter
δ	Load angle of synchronous machine
θ, ϕ	Phase angle
ω	Angular velocity in radians per second
ψ	Flux linkage

Subscripts

a	Phase a or armature
b	Phase b
c	Phase c or commutation (e.g. x_c)
d	Direct axis or d.c. converter or system
q	Quadrature axis
f_ℓ	Field winding leakage
md	Direct axis mutual
mq	Quadrature axis mutual
kd	Damper winding on direct axis
kq	Damper winding on quadrature axis
ℓ(or 1)	D.C. line
p	Positive sequence
n	Negative sequence
o	Zero sequence or minimum value (as in α_o)
1	Rectfier
2	Inverter

Superscripts

'	Transient
''	Subtransient
*	Conjugate

CHAPTER 1

INTRODUCTION

1.1 General survey of the place of h.v.d.c. in electric power transmission

It is 15 years since the first commercial h.v.d.c. scheme using the modern type of mercury arc valves was commissioned in Gotland in 1954. In this period the rating of mercury arc valves has increased from 20 MW (Gotland) to 270 MW (Nelson River) and the application of h.v.d.c. has become world-wide. Table 1.1 gives all h.v.d.c. schemes in operation and proposed for the future. Fig. 1.1 is a histogram of the rating of the schemes and Fig. 1.2 is a plot of the total installed capacity of h.v.d.c. schemes in the world. From this information the following conclusions can be drawn:

(1) Individual h.v.d.c. schemes are increasing in rating, the highest (Ekibastaz USSR) being 300 times that of the Gotland scheme.

(2) The elapsed time between the announcement of a project and its commissioning is about 5 years for schemes of less than 1000 MW (e.g. Kingsnorth, Nelson River Stage I), and more than 10 years for larger schemes (e.g. Caborra Bassa, Ekibastaz). This is an indication of the complexity of h.v.d.c. projects, bearing in mind that only 5 years are usually required for the design and construction of a modern 2000 MW power station.

(3) High capacity schemes (2000 MW and above) are usually installed in large countries like the U.S.S.R. and Canada where there are cheap power sources remote from load centres, and where the economic advantage of high power long distance d.c. transmission are overwhelming.

(4) Smaller schemes (1000 MW and below) were usually chosen because of the technical merits of d.c., eg Sakuma (frequency changing), Kingsnorth (no increase in fault level). Others exploited both the economic and technical advantages of d.c. eg Cross-Channel and New Zealand (submarine crossing).

(5) In the decade 1960 - 1970 the rate of installation of h.v.d.c. schemes was nearly one every other year. For the next decade 1970 - 1980 present information suggests that this rate of installation will be roughly maintained but the total capacity to be installed will be more than double that of this decade. The outlook is therefore fairly optimistic, although there exists an element of speculation. This aspect of h.v.d.c. will be discussed further in Section 1.3.

Project	Capacity MW	Direct Voltage kV	Distance Miles	Date of commissioning	Date of project announcement
Operational					
Moscow-Kashira (USSR)	30	200	72	1950	
Gotland (Sweden)	20	100		1954	
Gotland (Add thyristor bridge)	30	150	72	1970	
Cross-Channel (UK & France)	160	±100	34	1961	
Volgograd-Donbass (USSR)	750	±400	295	1964	
New Zealand (New Zealand)	600	±250	385	1965	
Sakuma (Japan)	300	±125	0	1965	
Konti-Skan (Sweden)	270	250	102	1965	
Sardinia (Italy)	200	200	258	1967	
Vancouver, Stage I (Canada)	78	130	43	1968	
Under construction					
Vancouver, Stage II (Canada)	312	260	43	1969	
Pacific Intertie, Stage I (US)	1440	±400	875	1970?	1965
Kingsnorth (UK)	640	±266	37,51 (2 poles)	1971	1965
Nelson River, Stage I (Canada)	810	+150, -300	570	1971	1965
Planned					
Vancouver, Stage III (Canada)	624	±260	43	?	
Nelson River, Stage II (Canada)	3240	±450	570	?	
Snettisham, Stage I (US)	40	125	45	1972	1968
Snettisham, Stage II (US)	80	±125	45	?	1968
Caborra Bassa, Stage I (Mozambique & South Africa)	960	±266	900	1974	1968
Caborra Bassa, Stage II (Mozambique & South Africa)	1440	±400	900	1976	1968
Pacific Intertie, Stage II (US)	2880	±400	875	1977?	
Caborra Bassa, Stage III (Mozambique & S.A.)	1920	±533	900	1978	1968
Ekibastuz (USSR)	6000	±750	1800	1980	1969
New Brunswick (Canada)	350	?	?	?	1969

Table 1.1 H.V.D.C. schemes in operation, under construction and planned.

(The total capacity at each stage is shown).

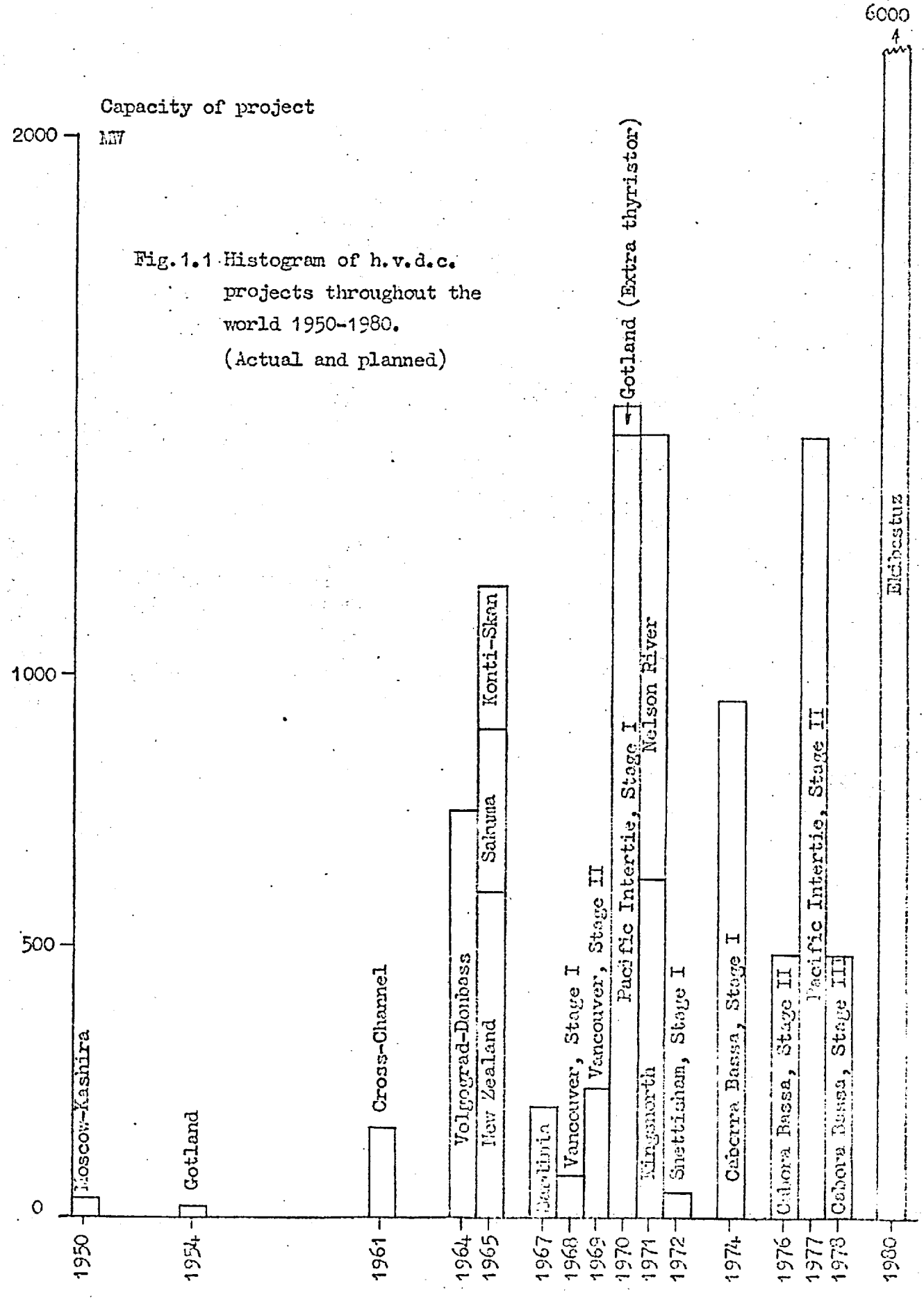

Fig.1.1 Histogram of h.v.d.c. projects throughout the world 1950-1980. (Actual and planned)

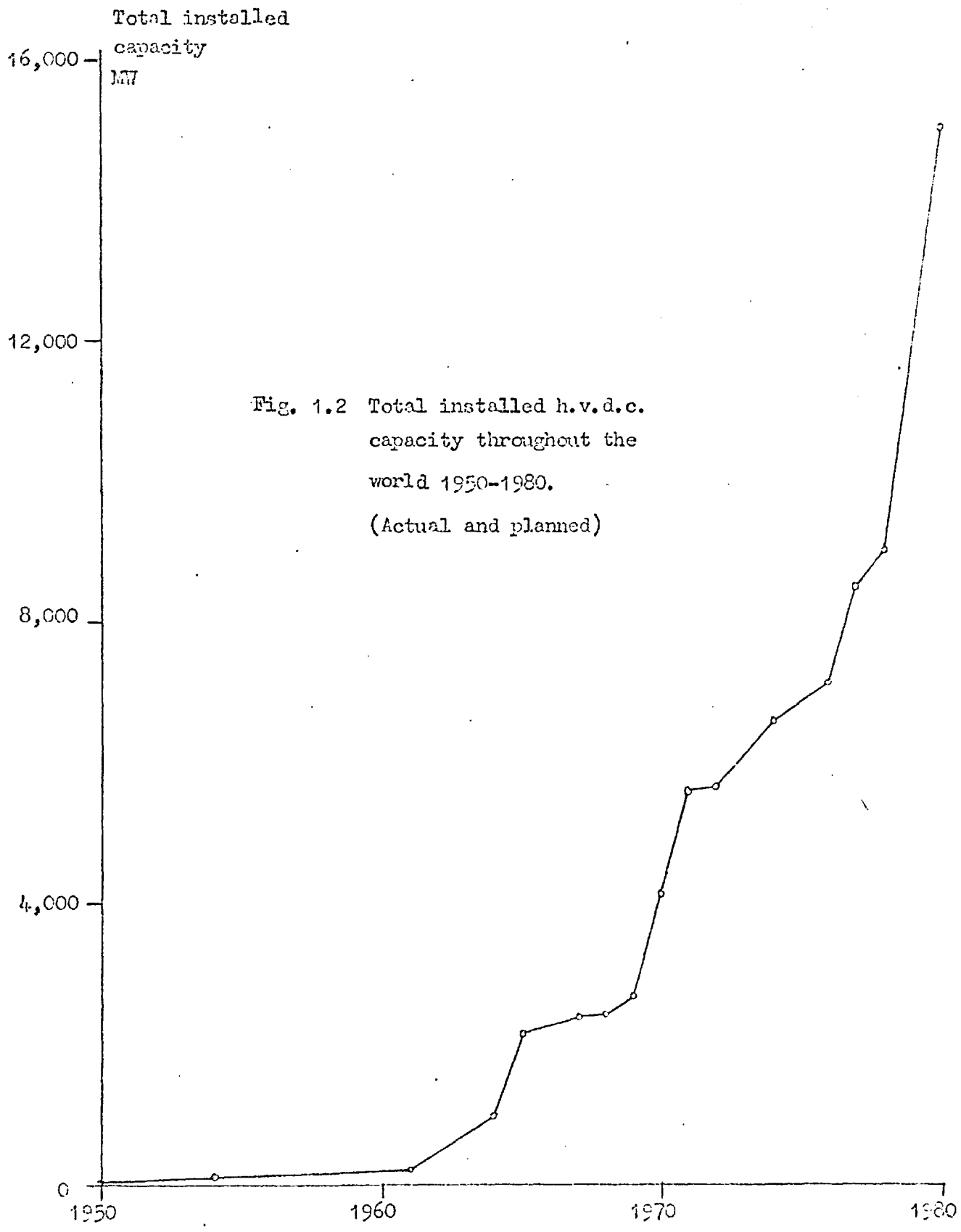

Fig. 1.2 Total installed h.v.d.c. capacity throughout the world 1950-1980. (Actual and planned)

The promising but speculative future of h.v.d.c. leads one to associate it with the saying 'solution in search of a problem' which was once used to describe the laser. In this connection it is perhaps worthwhile to summarise the most likely applications of h.v.d.c. in the future, these are

(1) Bulk power transmission over long distances

(2) Reinforcement of existing a.c. systems without raising fault level

(3) Undergrounding high voltage circuits where overhead lines are objectionable

(4) Asynchronous link between two power systems

(5) Reinforcement of distribution systems from high voltage system to bypass intermediate voltages

(6) Submarine crossing

Bulk power transmission over long distances will of course have more scope in countries like the U.S.S.R. and Canada. In the U.S.S.R. the load centre is essentially in the European part to the West and the cheap power sources are in the Urals and Siberia to the East separated by a distance of over 1000 miles. A h.v.d.c. link in a East-West direction therefore provides the extra advantage of different time zones. Even the Cross-Channel link took advantage of the different peak times between England and France before British Standard Time was introduced. In Canada, however, natural resources in the form of hydro-electric power are abundant in the North while the load centres are mainly in the South so that all major transmission lines are in a North-South direction.

In countries like Britain, where the high voltage system is closely interconnected the use of h.v.d.c. for reinforcement has special appeal when it is essential to keep the fault level down. However, it is important to recognise that there are other means of limiting fault level, e.g. resonance links[64], which can be more economical.

On the other hand h.v.d.c. will have a place in undergrounding high voltage circuits in countries where amenity is held in high esteem, although again the economics has to be competitive with alternative solutions such as intermediate reactive compensation of high voltage underground cables.

H.V.D.C. links, because their operation is independent of a.c. system frequency, are eminently suitable as interties between systems not under one central system control (e.g. Cross-Channel link) or between systems of different frequencies (e.g. Sakuma frequency changer). Thus there seems to be scope for d.c. interties between Canada, where there is abundant hydro-electric resources, and the U.S. The use of d.c. links as frequency changers will, of course, apply only to countries with mixed frequencies like Japan and perhaps Venezuela and is therefore limited.

The use of d.c. to reinforce distribution systems was first proposed by Brewer and Fraser [65] in 1966. The idea is that a high capacity rectifier from the high voltage system can feed several smaller inverters in series or in parallel at distribution voltage level thus bypassing several intermediate voltage levels. The economic case for this proposal is, however, debatable. In a recent paper by Brewer and Kidd[66], a 50% reduction of the cost of the thyristor has to be assumed before a marginal economic advantage can be obtained. Besides, the problems of harmonics at distribution level and the need to dissipate the heat from the losses in the inverter are some of the objections that have to be considered, even cheap and reliable thyristor valves are available. Mercury arc valves of single anode construction, sealed for oil immersion and arranged for outdoor mounting are available[67] at the right rating (30-90 MW) for use as distribution inverters, but they are probably just as costly. A limitation of this scheme is that it can only be introduced into distribution networks which are secure and strong in order to obtain the required reactive power supply, otherwise the need to provide for artificial commutation would add heavily to the cost.

For long submarine crossings d.c. links remain the only answer since it would be very difficult to provide intermediate reactive compensation, but the scope for this application seems limited.

To reduce fault levels on the high voltage system Knight[68] has suggested that the system may be segregated into two or more 'overlaid' systems. In this way a higher load density can be sustained at the same fault level, but the price to pay is a lower security for the same capital expenditure. The security can be improved, however, by connecting the overlaid systems at points of high load density with zero distance d.c. links or other short-circuit limiting coupling.

In recent years it has been suggested that nuclear power stations can be built to such safety standards that they may be sited in or near big cities and would thus relieve the need for bulk power transmission. Leaving aside the probable objection by the public to live and work in close proximity to a nuclear station there is still the requirement of large source of cooling water which would rule out many big cities. The more cogent argument against nuclear stations near cities is the cost and complexity of their demolition at the end of their useful life. Bainbridge[69] estimated that the cost would be a few per cent of the original station cost, and suggested that automatic or remote-control equipment would be necessary. Therefore it is more likely that nuclear power stations will continue to be built in less populated areas near the sea or rivers, and bulk transmission will still be required. Whether h.v.d.c. is chosen for this purpose or not will be entirely determined on its economic and technical merits.

1.2 Application of thyristors to h.v.d.c.

In recent years the application of thyristors to h.v.d.c. seems to have aroused considerable interest in many manufacturers and research establishments all over the world. This may be due to the lower capital cost of thyristor research compared with the mercury arc valve. Despite the actual operation of a thyristor valve in the Gotland scheme and the forthcoming

English Electric trial thyristor valve for the Lydd Converter station, the real advantages of thyristor valves over mercury arc valves have not really been established. The usual advantages given for thyristors are:-

(1) freedom from arc backs

(2) smaller and therefore cheaper converter stations

(3) reduced filter requirements (thyristor valve built up from 12-pulse groups to reduce harmonics; and filters can be connected to secondary of converter transformer)

(4) smaller converter transformer required (reduced harmonics and reactive power)

Several recent papers, however, provided sufficient information to cast doubt on the real value of these advantages. Calverley[70] stated that present day mercury arc valves are fairly free from arc backs and consequential arc backs are practically eliminated; and in any case d.c. transmission scheme using mercury arc valves can be designed to recover from arc back with minimum disturbance. Gavrilović et al[71] gave the sizes of a 200 kV 200 MW converter station as follows:-

Mercury arc valve station	115 m x 162 m
Thyristor valve station (indoor)	115 m x 154 m
" " " (outdoor)	115 m x 132 m

Thus an indoor thyristor valve station is only marginally smaller than an equivalent mercury arc valve station, and an outdoor thyristor station is only about 20% smaller. The authors also stated that even allowing for savings in converter building cost, damping circuits filters and converter transformers, a thyristor station is still not competitive with mercury arc valve, especially when the higher thyristor losses are included in the consideration. Jones et al[67] compared two designs using thyristors and mercury arc valves respectively of a 90 MW converter station for distribution system application. They showed that the mercury valve design is both cheaper and smaller.

Using single anode mercury arc valves sealed for oil immersion and outdoor mounting, one converter bridge can be made into a tank occupying 9' x 3.5' x 11' high as against a comparable thyristor converter bridge which occupies 12' x 7' x 10' high. They therefore concluded that there is little prospect of thyristors being competitive with mercury arc valves for reinforcing distribution systems, and added that a.c. methods based on the resonance link appears to be more appropriate.

Against this background of questionable advantages, the thyristor valve still faces considerable technical problems. A large number of thyristors has to be connected in series and parallel in order to achieve the required voltage and current rating (typically 20 - 80 kV 30 - 90 MW for distribution reinforcement). The major problem is to ensure even voltage and current distribution, and the correct firing of many thyristors in unison. Over-voltage exceeding the transient voltage rating of the thyristor valve would cause unrepairable damage. Moreover, each of the many thyristors requires its own voltage divider and firing circuit and these must be as reliable as the thyristors themselves in order to achieve an acceptable overall reliability.

Weighing the uncertain benefits of the thyristor against its known disadvantages it seems safe to assume that mercury arc valves will remain dominant in h.v.d.c. transmission.

1.3 Commercial aspects of h.v.d.c.

Lane[72] has summed up the commercial hazards of h.v.d.c. as a 'tantalising situation in which projects are large but infrequent, engineering demand intense but highly variable, competition is limited but international, and the future is speculative but promising'. He pointed out that of all the h.v.d.c. projects in operation or under construction hardly any two are similar. Projects, as can be seen from Fig. 1.1, only occur at the rate of one every other year in the decade 1960 - 70 and in the next, but requirements differ and become more complicated with each succeeding scheme.

This, he said, creates a situation which tests the nerve of the present manufacturers and deters new competitors. A case in point which illustrates the speculative and uncertain future of h.v.d.c. transmission is the U.S. Pacific Intertie project. It was announced recently [73] that Stage II of this project is being delayed until at least 1977 due to a postponement of a loan from Congress. Consequently the contract with ASEA and G.E. is being terminated.

15 years after the Gotland scheme there are still only two manufacturers of converter valves (both mercury arc and thyristor) in the Western world, viz: ASEA and English Electric. Commercial research into valve construction and h.v.d.c. system behaviour and control are more diversified and may be summarised as:-

Britain	Central Electricity Generating Board
	English Electric
Sweden	ASEA
Germany	400 kV Forschungsgemeinshaft
U.S.	Edison Electric Institute
	General Electric
	Bonneville Power Administration
Canada	Canadian Westinghouse
	Hydro Quebec
Japan	Electrotechnical Laboratory
	Mitsubishi

While in the U.S.S.R. research and protection work on h.v.d.c. are in the hands of several institutes.

The new-comers in this group of commercial research establishments are the Canadian Westinghouse and Hydro Quebec. It was reported [74] that the former made the decision after a market survey suggested that there exists in Canada a potential market of h.v.d.c. apparatus valued at $200 M in the next 10 years and that an even bigger market may exist in the U.S.

This is really intriguing since the parent Westinghouse Company in the U.S. had closed down its h.v.d.c. activities 2 years ago. Hydro Quebec enters into h.v.d.c. research in view of the proposed James Bay and other long distance bulk power transmission schemes. If the judgement of these two firms are correct, then North America will see more h.v.d.c. projects before long.

1.4 Relevance of interaction of h.v.d.c. link and weak a.c. system

There are, in general, two different manners in which h.v.d.c. transmission is applied to power systems. In the first place a d.c. link can be used to bring power into an existing a.c. system that is strong with plenty of internal generation. This approach is favoured by the Russians, and in a recent paper [75] they stated that the rating of any d.c. link from power stations in Central U.S.S.R. to the European part should be of the order of 2 - 3% of the total receiving system capacity so that loss of a d.c. link produces acceptably small disturbances. Since the total generating capacity in the European part of the U.S.S.R. is estimated to be about 100,000 MW doubling to more than 200,000 MW in 1980, the rating of any d.c. link may be of the order of 3000 - 6000 MW. System reinforcement of this nature is apparently limited to the U.S.S.R. where the load centres already have abundant local generation and yet there are cheap power sources to be exploited thousands of miles away.

A different situation arises when d.c. transmission is used to supply power to an area which is weak and has little internal generation so that the rating of the d.c. link is comparable to the receiving system generating capacity, examples being the Kingsnorth and Nelson River projects. In the former the receiving systems at Beddington and Willesden have little generation near-by, and the ratio of short circuit fault level at these two stations to the d.c. link rating (320 MW) is about 6 under minimum plant condition. (This ratio will be lowered if there are circuits out on fault). Studies on this scheme already indicated voltage rises exceeding the permissible 10% if the entire link (2 poles) is blocked under light load condition, and would therefore require the link to be operated below rating

under such conditions. In the Nelson River project, the d.c. link will supply 810 MW in Stage I to southern Manitoba which has a total generating capacity of only 1500 MW although there are interconnection to smaller systems to the east and west. Thus it is necessary, according to Scott[76], to install substantial synchronous condenser capacity to supply reactive power to the valve, to maintain adequate short circuit fault level and to contain transient over-voltage arising from blocking of valve groups. Another feature arising from the high proportion of supply from the d.c. link is the necessity to provide fast switching facilities (of the order of 750 msec) for parallelling healthy valve groups in case of d.c. line faults. Common between the two schemes is the provision of frequency control of d.c. link power. In the Kingsnorth scheme frequency control is used to regulate machine frequency at Kingsnorth in the isolated generator mode; at the receiving ends a rise of frequency about a certain limit causes the link to be blocked. In the Nelson River project frequency control alters the d.c. link power to help maintain constant frequency at the receiving end.

Reinforcement of either a strong or weak a.c. system with d.c. has many problems in common, but some of these are particularly acute when the a.c. system is weak. They have been mentioned above and can be summarised again as:-

(i) voltage instability

(ii) d.c. link power transfer limit

(iii) frequency control of direct current order

(iv) harmonic instability

The last problem has been considered by Ainsworth[43] who suggested a phase-locked oscillator control system producing symmetrical three-phase converter current even when the a.c. voltage is unbalanced or distorted. This thesis considers the other problems listed.

1.5 Isolated generator mode

In several h.v.d.c. schemes in operation or proposed the sending end generators are isolated and asynchronously connected to an a.c. system by the d.c. link, examples are the Sardinia, Nelson River and Snettisham projects. In the first of these, described by Cahen et al[21], the frequency of the sending end (Sardinia) is regulated by frequency-control of the d.c. link power. On the other hand, frequency control of the Nelson River d.c. link [76] will be relied upon to maintain the frequency of the receiving end.

The Kingsnorth scheme is not an isolated generator scheme like those mentioned since the generators will be normally connected to the 400 kV supergrid. Under certain fault or test conditions, however, one machine may be isolated from the system and only connected to the d.c. link. Since this condition can arise when this machine is supplying real and reactive power different from those demanded by the d.c. link, it may cause fluctuations in speed and voltage of the machine. For this sudden isolated condition, this thesis considers the effect of frequency control, and other methods of controlling the d.c. link, in order to limit the disturbances.

1.6 Analysis of a.c./d.c. system in the transient state

The analysis of pure a.c. systems in the transient state is well established with machines represented by voltages behind transient or subtransient reactances and transmission system and loads represented as impedances. For the d.c. system the dynamic simulation by Hingorani et al[30] provides a most comprehensive representation of converter operation featuring the individual firing of the valves. A combination of these representations of a.c. and d.c. systems will produce the most rigorous method of analysing mixed a.c./d.c. systems. Unfortunately the converter representation of Hingorani is, although simple in principle, not often suitable due to the considerable programming effort and computing time required. A compromise is to use an approximate representation which neglects the individual valve firings and treats the rectifier and inverter as d.c. motors and generators whose e.m.f's are continuously controllable by means of the firing angle contro By adopting this approximation the representation of converters is greatly simplified.

The justification of using this approximate representation is discussed in Chapter 2 where all known methods of converter and d.c. system representations are discussed and classified.

1.7 AC/DC load flow program

Before any transient analysis of a system can start it is necessary to establish the initial conditions. In the case of a mixed a.c./d.c. system the initial conditions of machine outputs, voltages and power flows are obtained from a load flow program. One such program was developed and is described in this thesis. This program has the following features:

(i) a tap changer routine which produces the required d.c. link voltage and firing angle

(ii) ability to simulate effect of current margin crossing

(iii) ability to simulate blocking of valve groups

(iv) single-pole or double-pole d.c. link

This program has also been used to investigate an interesting problem of non-convergence for certain mixed a.c./d.c. systems. It was noticed that for some a.c./d.c. systems which produce convergent load flow, the removal of a line to simulate outage causes the voltage over the system to oscillate and not converge. This is thought to be due to the voltage sensitivity of the weak a.c. system to changes of reactive power and has been overcome by adjusting the d.c. link power or current order.

1.8 Digital solution of differential equations - digital analog simulation

Analysis of the dynamics of a system usually entails the solution of a set of simultaneous differential equations. Before the advent of the digital computer this was often accomplished by means of an analog computer. As the use of the digital computer spreads, so the methods of numerical integration using the well-known Runge-Kutta, predictor-corrector, or other formulae to solve differential equations tend to replace the analog computer. Although the digital computer is entirely satisfactory in this task,

the ordinary scientific programming languages such as FORTRAN or ALGOL are not particularly suitable to deal with dynamic systems which are often represented in the form of transfer functions and which the analog computer is better equipped to tackle. It was not long, however, before special programming languages were written which provided this special feature, and allow the user to program directly from the block diagram of a dynamic system. These languages are a break-through in simplifying the use of the digital computer for dynamic analysis. Two of these, MIMIC and DSL/90, have been used in the course of the work of this thesis. An appendix is included to describe and discuss the methods of numerical integration, the advantages and disadvantages of digital analog simulation. An improvised simulation method developed by the author is also presented.

CHAPTER 2

METHODS OF REPRESENTATION OF H.V.D.C. CONVERTERS AND SYSTEMS IN ANALYSIS

2.1 Introduction

The analyses of a.c./d.c. systems were often performed by treating d.c. links as simple resistances or simple T-circuits and converters as equivalent current generators. Although this method of representation is widely used, other methods had been employed in the analyses of the many and varied problems of h.v.d.c. As with the analyses of so many other problems there is always the fundamental choice between building a physical model and developing a mathematical model. With few exceptions the present trend seems to favour the latter and digital computers are inevitably used to implement the analyses. This is so with h.v.d.c. where simulators are still few and far between,[1,2,3,4] Although they are extremely useful in certain specific applications, e.g. in developing and testing of control circuits. The conclusion is, therefore, that more analyses of h.v.d.c. problems will be in the form of mathematical modelling, and the present chapter is devoted to the review of the known methods of representing, mathematically, d.c. links and converters. To facilitate discussion, a classification of all known methods is proposed as follows:

(1) Steady state representations
    (a) as equivalent current generator
    (b) as equivalent circuit
(2) Transient state representations
    (a) for small signal analysis
    (b) for large signal analysis

The steady state representations are essentially single phase representations and are commonly used in load flow and fault current analyses. Application is simple in both balanced and unbalanced a.c. systems, although an iterative process is necessary when the converter terminal is not an infinite bus with fixed voltage.

The transient state representations are necessary in the studies of a.c./d.c. system transient stability, a.c./d.c. system faults, valve faults, and the response of control systems. These representations are essentially three phase and can therefore deal with balanced and unbalanced a.c. systems, but in some simplified situations these representations can be implemented in single phase terms.

2.2 Steady-state Representations

The basis of these representations is the steady-state relationships between the alternating voltage and current at the converter terminals, the direct voltage and current of the converter, and the firing and commutation angles of the converter. Excellent expositions of these relationships can be found in Read,[5] Calverley,[6] and Uhlmann[7]. By taking only the fundamental components of alternating voltage and current at the converter terminals, a converter can be represented either as an equivalent current generator or an equivalent circuit.

2.2.1 Equivalent current generator representation in symmetrical a.c. system

Uhlmann[8] was the first to propose this method of representation of d.c. links and converters for use on a network analyser. Although the direct voltage is freely related to the alternating voltage through the firing angle so that there is no fixed relationship between them, he argued, such a fixed relationship, to a good approximation, exists between the direct current I_{dc} and the magnitude of the fundamental component of the alternating current I_{ac} viz:

$$|I_{ac}| \doteq \frac{\sqrt{6}}{\pi} I_{dc} \qquad (2.1)$$

for a 6-pulse converter group. The error in this approximation is greatest for a firing angle of 0°, but it is not greater than 1-1.5%. On this basis the converter can be represented as a current generator with no mechanical inertia and supplying current at the same frequency as the a.c. network connected to it, i.e. a rectifier can be regarded as a motor and an inverter as a generator with no inertia.

Uhlmann[8] made the distinction between E_o, the r.m.s. line voltage at an imaginary feeding point of the a.c. network where the voltage remains sinusoidal even when supplying the converter, and E_1 the r.m.s. value of the fundamental voltage waveform on the valve side of the converter transformer which in general is non-sinusoidal. The displacement factor (i.e. the ratio of active to apparent power of the fundamental voltage and current) between the current I_{ac} and the voltage E_1 are related to the direct voltage V_{dc} by

$$E_1 \cos\varphi_1 = \frac{\Pi}{3\sqrt{2}} \text{ Vdc} \qquad (2.2)$$

The value of $\cos\varphi_1$ must be less than a maximum $(\cos\varphi_1)$ max corresponding to the minimum firing angle α_o of a rectifier or the minimum extinction angle γ_o of an inverter. The value of $(\cos\varphi_1)$ max is obtained as follows:

$$\cos\alpha_o \text{ or } \cos\gamma_o \doteq \frac{\cos\varphi_1{}^1 + e_{xm}\frac{Idc}{Im}\frac{Eom}{E_1}}{\left[1 + 2\left(\frac{6}{\Pi} e_{xm}\frac{Idc}{Im}\frac{Eom}{E}\right)\sin\varphi_1{}^1 + \left(\frac{6}{\Pi} e_{xm}\frac{Idc}{Im}\frac{Eom}{E}\right)^2\right]^{\frac{1}{2}}} \qquad (2.3)$$

where Im = rated value of Idc

Eom = rated value of Eo

$$e_{xm} = \frac{ImX}{\sqrt{2}Eom}$$

X = phase reactance of a.c. network including the converter transformer

and $\cos\varphi_1{}^1 = (\cos\varphi_1)$ max (See Fig. 2.1)

Uhlmann in this paper showed that $\cos\varphi_1{}^1$ depends substantially on the value of α_o and γ_o, and is virtually independent of I_{dc} and E_1 except for small values of α_o (or γ_o) and Idc. He also emphasised that the firing angles and extinction angles are related to the sinusoidal voltage E_o.

If the value of $\cos\varphi_1$ from Eq. 2.2 does not satisfy the condition

$$\cos\varphi_1 \leq (\cos\varphi_1) \text{ max} \qquad (2.4)$$

the voltage E_1 must be increased by tapping up on the converter transformer; if the tap limit is reached, the rectifier will lose current control to the inverter.

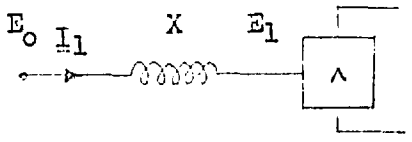

(a) Schematic diagram of converter connection

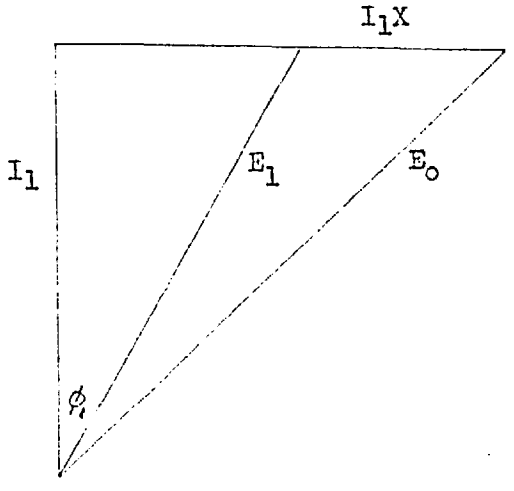

(b) Phasor diagram of converter voltage and current

E_o phase voltage at imaginary feeding point
E_1 " " " converter terminal
I_1 " current to converter
X commutating reactance

Fig. 2.1 Converter voltage & current

Breuer et al[9,10] applied Uhlmann's equation but did not take advantage of the fact that $\cos\varphi_1{}^1$ is virtually independent of I_{dc}. For each value of I_{dc} and E_t an iterative procedure was used to calculate $\cos\varphi_1{}^1$ by rearranging Eq. 2.3. This is no doubt a contributary factor to the high computing time quoted (110 minutes on the IBM 7094 computer to simulate 1.5 sec). A much greater simplification can be obtained by assuming the voltage at the converter busbar to be sinusoidal by virtue of the reactive compensation provided by the filters or compensators. This is then the voltage Eo in Uhlmann's paper and its value is known at each stage of the load flow iteration. The voltage E_1 is no longer required, and the power factor of the converter referred to Eo can be obtained by

$$E_o \cos\varphi_o = \frac{\Pi}{3\sqrt{2}} V_{dc} \qquad (2.4)$$

To determine the movement of converter transformer tap it is only necessary to check the value of V_{dc} against

$$(V_{dc})_{max} = \frac{3\sqrt{2}}{\Pi} E_o \cos a - \frac{3X}{\Pi} I_{dc} \qquad (2.5)$$

where $a = \alpha_o$ for rectifier and γ_o for inverter. If the limit of tap position is reached the rectifier loses current control to the inverter. In a later paper Breuer et al[3] reported that such modifications had been made, although the expected improvement in computing speed was not mentioned.

Incidentally the programs written by Breuer et al treated the converters as equivalent active and reactive loads which are derived from the equivalent alternating current I_{ac} from Eq. 2.1 and power factor from Eq. 2.2. Hingorani and Mountford[11] retained the equivalent current concept and treated the converter as current injections at the converter nodes. Their method is eminently suited to be incorporated into a.c. load flow programs which use the nodal currents explicitly, e.g. the method of Glimm and Stagg[12], and was the method adopted in Chapter 4.

Gavrilovic and Taylor[13] used the same method to represent converters in their analysis of the regulation characteristics of d.c. systems. In this paper a useful per unit system was presented which simplifies the conventional converter equations. This system requires two different base systems for the a.c. and d.c. systems:

A.C. base quantities

$$ECB = kVv \tag{2.6}$$

$$PcB = N.mvaT \tag{2.7}$$

$$IvB = N.mvaT/\sqrt{3}\ kVv \tag{2.8}$$

D.C. base quantities

$$VdB = \frac{3\sqrt{2}}{\Pi}\ N.kVv \tag{2.9}$$

$$PdB = N.mvaT \tag{2.10}$$

$$IdB = \frac{\Pi}{3\sqrt{2}}\ \frac{mvaT}{kVv} \tag{2.11}$$

where kVv = nominal voltage of valve winding of converter transformer

$mvaT$ = rating of one converter transformer

N = number of converter bridges

The voltage and current equations expressed in this per unit system are

$$v_d = e_c \cos\alpha - \frac{\Pi}{6} x_{cid} \tag{2.12}$$

$$i_v \doteq i_d \tag{2.13}$$

$$i_p = \frac{v_d i_d}{e_c} \tag{2.14}$$

$$i_q = (i_v^2 - i_p^2)^{\frac{1}{2}} \tag{2.15}$$

where v_d = average direct voltage across N bridges in p.u.

i_d = direct current in p.u.

i_v = fundamental component of alternating current of N bridges in p.u.

i_p, i_q = active and reactive components of i_v with respect to e_c in p.u.

e_c = voltage behind commutating reactance in p.u.

$x_c = \frac{mvaT}{kVv^2} X_c$

X_c = commutating reactance in ohms/phase

2.2.2 Equivalent current generator representation in asymmetrical a.c. systems

Uhlmann's representation of converters has one limitation, i.e. it is valid only when the a.c. system is symmetrical, although the equivalent current generator concept itself can be extended to cater for asymmetrical a.c. systems. Under this condition the voltage waveform at the converter terminals is unbalanced with asymmetrical voltage cross-over points. The unequal commutating voltages therefore cause unbalanced converter currents. The relations between voltage and current in this case can be studied in three phase terms by using the three phase voltages and currents, or in single phase terms by means of symmetrical components and this was the approach used by Arrillaga and Efthymiadis[14] in their study on the performance of converters under unbalanced conditions. From an alternating voltage with a specific degree of asymmetry in terms of positive and negative sequence components the converter currents in the three phases are calculated and injected into a three phase representation of the network, alternatively these three phase currents are transformed into positive and negative components and injected into the corresponding sequence networks. Since converter transformers do not allow the flow of zero sequence current this component of current is absent.

The calculations required are summarised by the following steps as given in the paper:

(a) derive ideal voltage cross-over points

$$\text{e.g. } C_{RY} = \tan^{-1} \frac{E_{SR} \sin \theta_{SR} - E_{SY} \sin \theta_{SY}}{E_{SR} \cos \theta_{SR} - E_{SY} \cos \theta_{SY}} \qquad (2.16)$$

for a star-star connected converter transformer

(b) Calculate the commutation-angle overlaps

$$\text{e.g. } u_{13} = \cos^{-1} \left(\cos\alpha_{13} - \frac{2X_{RY}}{E_{SRY}} I_d\right) - \alpha_{13} \qquad (2.17)$$

(c) calculate limits of commutation currents

$$\text{e.g. } \left.\begin{aligned} L_1 &= \alpha_{51} \\ L_2 &= \alpha_{51} + u_{51} \\ L_3 &= \alpha_{13} + C_{13} - C_{13} \\ L_4 &= \alpha_{13} + C_{13} - C_{13} + u_{13} \end{aligned}\right\} \qquad (2.18)$$

For the positive half of current in R phase

(d) derive phase-current wave shapes

e.g. the R phase current in the star-star converter transformer is

$$\left.\begin{aligned}
&\text{Between } L_1L_2 \quad i'_{SR} = \frac{\cos\alpha_{51} - \cos wt}{\cos\alpha_{51} - \cos(\alpha_{51} + u_{51})} I_d \\
&\text{Between } L_2L_3 \quad i''_{SR} = I_d \\
&\text{Between } L_3L_4 \quad i'''_{SR} = \left[1 - \frac{\cos\alpha_{13} - \cos wt - C_{13} + C_{51}}{\cos\alpha_{13} - \cos(\alpha_{13} + u_{13})}\right] Id
\end{aligned}\right\} \quad (2.19)$$

(e) calculate the fundamental components of the current wave shapes

e.g. the R phase current in the star-star converter transformer is

$$i_{SR} = \sqrt{2}\, I_{SR} \sin(wt + \phi_{SR}) \qquad (2.20)$$

where $\sqrt{2}\, ISR = \sqrt{A_R^2 + B_R^2}$

and $\phi_{SR} = \tan^{-1}\left(\frac{A_R}{B_R}\right) + C_{51}$

and A_R and B_R are dependent variables of the direct current and the firing and commutation angles.

Fig. 2.2 illustrates the meaning of some of the principal symbols.

(f) for three phase solution inject the three phase currents from the converter into a three phase representation of the network.

(g) for single phase solution transform the phase currents into positive and negative sequence components and inject these into the corresponding sequence networks.

(h) if the converter terminal voltage is not fixed and the converter is supplied from an unbalanced a.c. voltage source through an impedance then a process of iteration is required by repeating the above steps until a convergent value of converter terminal voltage is reached. The process is started by assuming the converter terminal voltage to be balanced and calculate the converter current, which would also be balanced, for use as the first current injection.

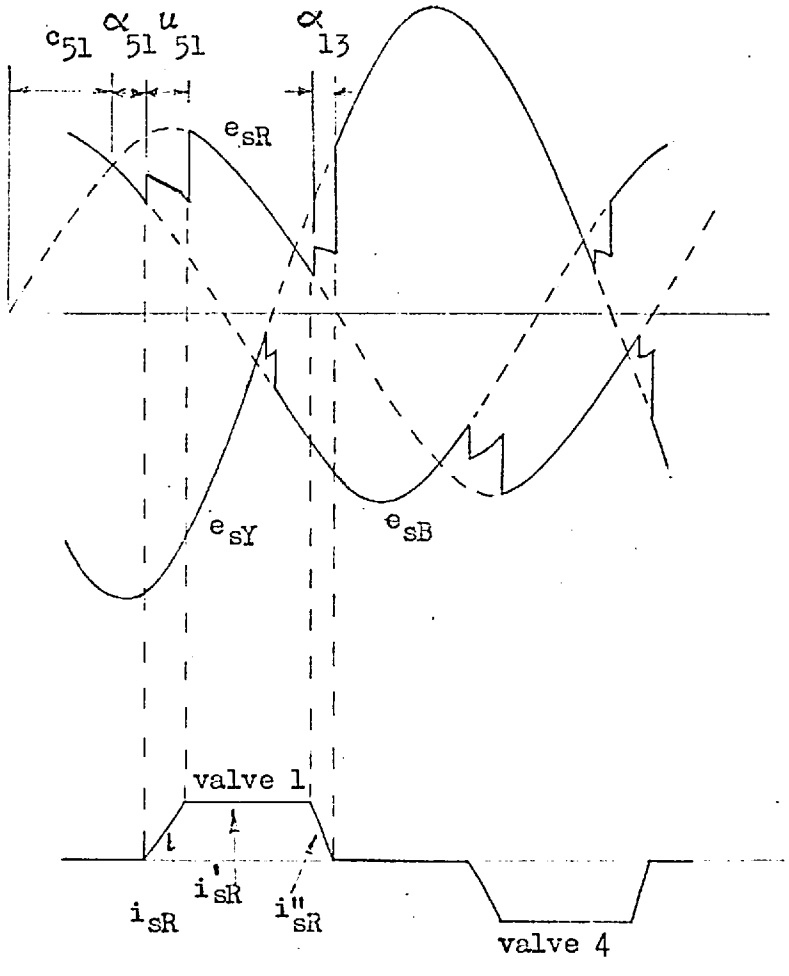

Fig. 2.2 Valve voltage & current waveshapes

e_{sR}, e_{sY}, e_{sB} --secondary phase voltage for star/star connection.

Incidentally this paper did not consider the effect of converter controls and the direct current setting, while firing angle and extinction angle were regarded as fixed.

2.2.3 Equivalent circuit representation in symmetrical a.c. systems

The idea of representing a converter as an equivalent circuit is in fact an extension of the equivalent current generator concept, since an equivalent impedance or admittance can be readily found from the phasor relationship between converter voltage and current as shown in Fig. 2.3. A possible equivalent impedance may be derived as follows for a 6-pulse three-phase converter:

For a rectifier

$$V_d = \frac{3\sqrt{2}}{\Pi} |V_1| \cos\alpha - \frac{3X}{\Pi} I_d \qquad (2.21)$$

$$I_1 \doteq \frac{\sqrt{6}}{\Pi} I_d \qquad (2.22)$$

$$\cos \phi_1 \doteq \tfrac{1}{2} [\cos\alpha + \cos (\alpha + u)] \qquad (2.23)$$

where V_d, I_d = direct voltage and current

V_1, I_1 = alternating voltage and current

X_1 = commutating reactance

α_1, u_1 = rectifier firing and commutation angle

ϕ_1 = phase angle between V_1 and I_1

Equivalent impedance of rectifier is:-

$$Z_1 = \frac{V_1}{I_1}$$

$$= \frac{\frac{\sqrt{3}}{2} X_1 |V_1|}{\frac{3\sqrt{2}}{\Pi} |V_1| \cos\alpha_1 - V_d} \cdot \exp (-j\phi_1) \qquad (2.24)$$

$$\text{or} = \frac{\Pi^2}{3\sqrt{3}} \cdot \frac{1}{\cos\alpha_1 + \cos (\alpha_1 + u_1)} \frac{V_d}{I_d} \cdot \exp (-j\phi_1) \qquad (2.25)$$

Similarly, the equivalent impedance of an inverter is:-

$$Z_2 = \frac{\frac{\sqrt{3}}{2} X_2 |V_2|}{\frac{3\sqrt{2}}{\Pi} V_2 \cos\alpha_2 - V_d} \cdot \exp (-j\phi_2) \qquad (2.26)$$

$$\text{or} = \frac{\Pi^2}{3\sqrt{3}} \frac{1}{\cos\alpha_2 + \cos (\alpha_2 + u_2)} \frac{V_d}{I_d} \cdot \exp (-j\phi_2) \qquad (2.27)$$

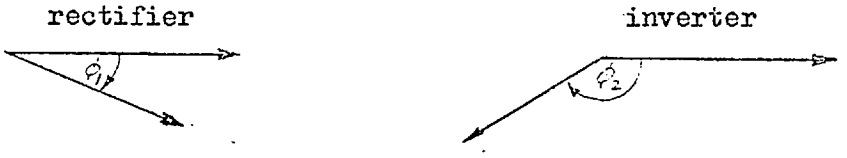

Fig. 2.3 Phasor relationship of converter voltage and current.

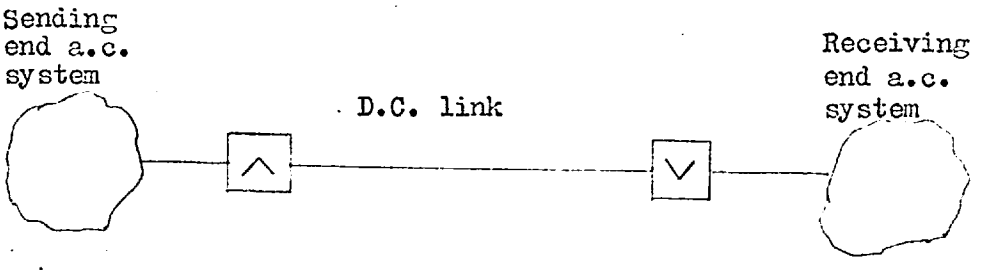

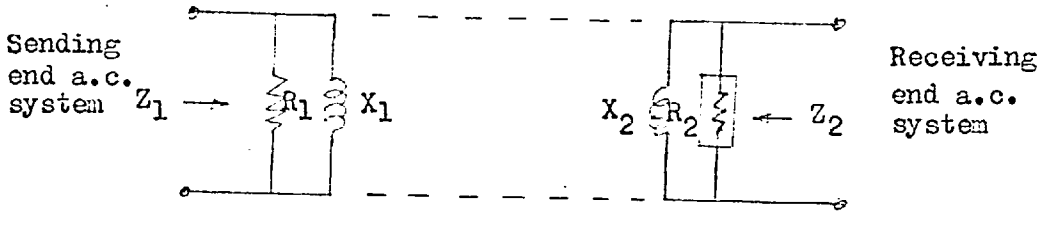

R_2 = negative resistance

Fig. 2.4 Equivalent circuit of d.c. link

Fig. 2.4 shows the equivalent circuit of the rectifier and inverter as obtained above. It is important to note that both Z_1 and Z_2 are non-linear functions of the terminal a.c. and d.c. voltage and current, as well as the firing angles. If these equivalent impedances are used to represent a d.c. link in an a.c./d.c. load flow program, their values must be calculated for each iteration of the voltage.

For load flow analysis the equivalent admittance $Y = I/E$ can be used where Y must be calculated every time E is iterated. This representation is useful therefore in those methods which use nodal admittances, e.g. the method of Glimm and Stagg[12], and would not be suitable for methods which use nodal impedances, e.g. the method of Brameller and Denmead[12].

Instead of considering the terminals of a d.c. links separately as above, Horigome[15] and later Horigome and Reeve[16] considered a d.c. link in its entirety by transforming a d.c. link into an equivalent 4-terminal a.c. network. Depending on the source of reactive currents three types of equivalent circuits are possible as shown below:

Type A equivalent circuit - reactive current source at sending end

The matrix equation for this equivalent circuit is

$$\begin{bmatrix} E_s \\ I_s \end{bmatrix} = \begin{bmatrix} \frac{1}{\beta} & 0 \\ 0 & \beta \end{bmatrix} \begin{bmatrix} 1 & 0 \\ 0 & (\frac{1}{\beta\delta} - 1) + 1 \end{bmatrix} \begin{bmatrix} 1 & Z_{dr} \\ 0 & 1 \end{bmatrix} \begin{bmatrix} E_r \\ I_r \end{bmatrix} \qquad (2.28)$$

where on the right hand side the first matrix represents as ideal transformer, the second a reactive current source, and the third an impedance. This equivalent circuit is shown in Fig. 2.5a.

Type B equivalent circuit - reactive current source at receiving end

The matrix equation for this equivalent circuit is:-

$$\begin{bmatrix} E_s \\ I_s \end{bmatrix} = \begin{bmatrix} 1 & Z_{ds} \\ 0 & 1 \end{bmatrix} \begin{bmatrix} \frac{1}{\beta} & 0 \\ 0 & \beta \end{bmatrix} \begin{bmatrix} 1 & 0 \\ 0 & (\frac{1}{\beta\delta} - 1) + 1 \end{bmatrix} \begin{bmatrix} E_r \\ I_r \end{bmatrix} \qquad (2.29)$$

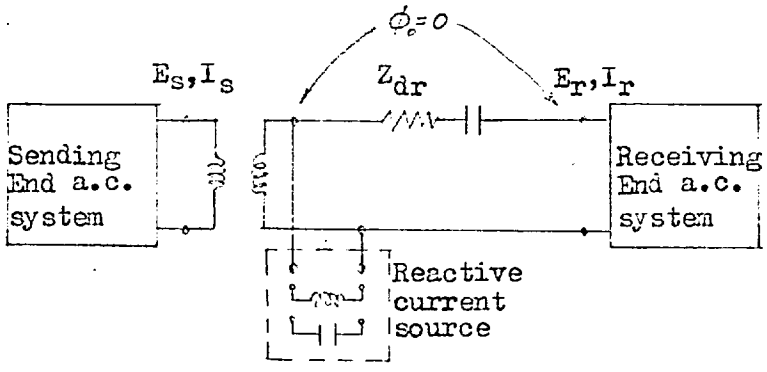

(a) Type A equivalent circuit -- Reactive current source at sending end.

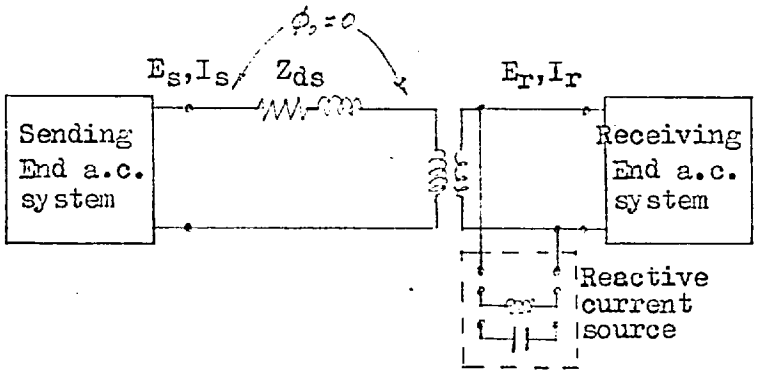

(b) Type B equivalent circuit-- Reactive current source at receiving end.

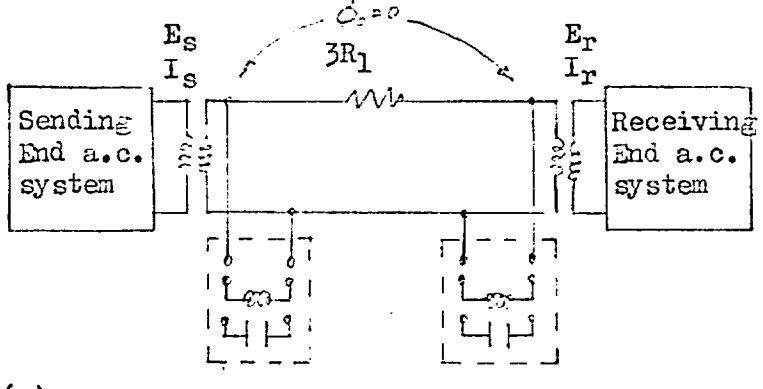

(c) Type C equivalent circuit-- Reactive current sources at sending & receiving ends

Fig. 2.5 Four-terminal a.c. equivalent circuits of d.c. link.

where on the right hand side the first matrix represents an impedance, the second an ideal transformer and the third a reactive current source. This equivalent circuit is shown in Fig. 2.5b.

Type C equivalent circuit - reactive current sources at both ends

The matrix equation is:-

$$\begin{bmatrix} E_S \\ I_S \end{bmatrix} = \begin{bmatrix} \frac{1}{K_1 \cos\phi s} & 0 \\ 0 & K_1 \cos\phi s \end{bmatrix} \boxed{MD} \begin{bmatrix} K_2 \cos\phi r & 0 \\ 0 & \frac{1}{K_2 \cos\phi r} \end{bmatrix} \begin{bmatrix} E_r \\ I_r \end{bmatrix} \qquad (2.30)$$

where

$$\boxed{MD} = \begin{bmatrix} 1 & 0 \\ 0 & \frac{3K_4}{K_1 \cos\phi s} \exp(-j\phi s) \end{bmatrix} \begin{bmatrix} 1 & 3R_e \\ 0 & 1 \end{bmatrix} \begin{bmatrix} 1 & 0 \\ 0 & \frac{K_2 \cos\phi r}{3K_3} \exp(-j\phi r) \end{bmatrix} \qquad (2.31)$$

In Eq. 2.30 the first and third matrix on the right hand side represent ideal transformers and the matrix MD represents a loss network with reactive current sources at both sending and receiving ends as shown in Fig. 2.5c. The symbols in these equations are defined as follows:-

E_S, I_S = voltage and current at sending end

E_r, I_r = " " " " receiving end

$$\beta = \frac{K_1 \cos\phi s}{K_2 \cos\phi r} = \left[\frac{K_1 \cos\alpha}{K_2 \cos\beta} \right]$$

$$\delta = \frac{K_3}{K_4} \exp\left[j(\phi s + \phi r) \right]$$

where K_1, K_2 = constants dependent on the valve connections of the rectifier and inverters respectively

$= \frac{3\sqrt{2}}{\Pi}$ for one bridge connected converter

K_3, K_4 = constants which are functions of firing and commutation angles of the rectifier and inverter respectively

$\doteq \frac{\sqrt{6}}{\Pi}$ for bridge connected converter

ϕs = phase angle of I_S w.r.t. E_S

ϕr = " " " I_r " E_r

$$Z_{dr} = \frac{Re}{K_2 K_3 \cos\phi r} \cdot \exp(-j\phi r) = \left[\frac{R^1}{K_2 K_3 \cos\delta} \cdot \exp(-j\phi r) \right]$$

$$Z_{ds} = \frac{Re}{K_1 K_4 \cos\phi s} \cdot \exp(j\phi s) = \left[\frac{R^1}{K_1 K_4 \cos\alpha} \cdot \exp(j\phi s) \right]$$

where R_e = resistance of d.c. line

$$R^1 = R_\ell + \frac{3X_1}{2\Pi} + \frac{3X_2}{2\Pi}$$

X_1, X_2 = commutating reactances of rectifier and inverter respectively.

The expressions in brackets are alternative formulae of the variables.

The three types of equivalent circuits are convenient for the study of an interconnected system. There are occasions, however, when only the sending end or receiving end needs to be considered. A simplified representation is therefore necessary and is achieved by suitably transforming the voltage and current at one end to eliminate the reactive current source. If the receiving end only is considered then the sending end can be represented by the equivalent voltage and current E_S' and I_S' respectively as shown below:

where E_S is assumed constant

$$\begin{bmatrix} E_S \\ I_S \end{bmatrix} = \begin{bmatrix} \frac{1}{\beta} & 0 \\ 0 & \frac{1}{\delta} \end{bmatrix} \begin{bmatrix} E_S' \\ I_S' \end{bmatrix} \qquad (2.32)$$

$$\begin{bmatrix} E_S' \\ I_S' \end{bmatrix} = \begin{bmatrix} 1 & Z_{dr} \\ 0 & 1 \end{bmatrix} \begin{bmatrix} E_r \\ I_r \end{bmatrix} \qquad (2.33)$$

Similarly if the sending end only is considered the receiving end is represented by the equivalent voltage and current E_r' and I_r' as shown below where E_r is assumed constant.

$$\begin{bmatrix} E_S \\ I_S \end{bmatrix} = \begin{bmatrix} 1 & Z_{ds} \\ 0 & 1 \end{bmatrix} \begin{bmatrix} E_r' \\ I_r' \end{bmatrix} \qquad (2.34)$$

$$\begin{bmatrix} E_r' \\ I_r' \end{bmatrix} = \begin{bmatrix} \frac{1}{\beta} & 0 \\ 0 & \frac{1}{\delta} \end{bmatrix} \begin{bmatrix} E_r \\ I_r \end{bmatrix} \qquad (2.35)$$

The equivalent circuits for these two cases are shown in Fig. 2.6. In the derivation of these circuits the voltages E_S and E_r had been assumed to be in phase ($\phi_o = 0$), but this is not a necessary assumption. If E_S and E_r are not in phase the same derivation still applies.

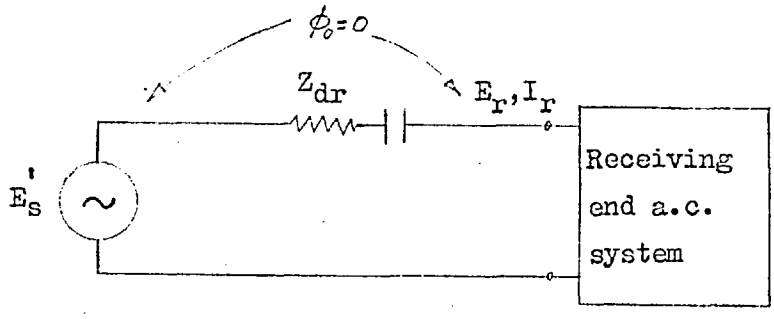

(a) Simplified equivalent circuit -- receiving end only is considered.

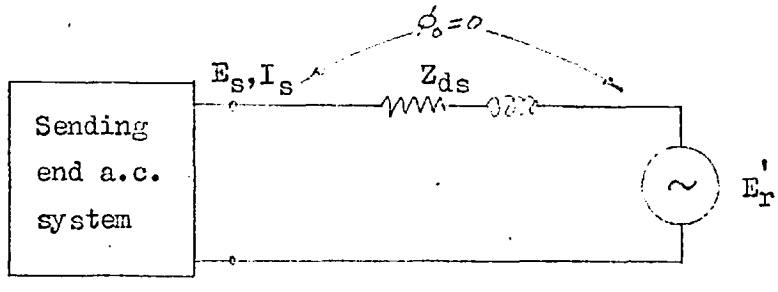

(b) Simplified equivalent circuit-- sending end only is considered.

Fig. 2.6 Simplified equivalent circuits of d.c. link when only one end is considered.

It is important to note that the transformation factors β and δ and the equivalent impedances Z_{dr} and Z_{ds} are all dependent on the firing angles or phase angles at the terminals so that a process of iteration is necessary for the solution of these equivalent networks. Horigome and Ito[17] used these equivalent circuits in an a.c./d.c. load flow program where each d.c. terminals are treated separately by the simplified representations given above in Eq. 2.32 - 2.35. Some of the equations used in this paper can be greatly simplified by using Uhlmann's approximation in Eq. 2.1, and would result in reduced computing time.

2.2.4 Equivalent circuit representation in asymmetrical a.c. systems

The equivalent circuit representation described so far is only valid when the a.c. system is symmetrical, but it may be used as a rough approximation for the analysis of fault currents in an a.c. system with unbalanced fault as by Horigome and Adamson[18]. More often it is used to provide a first approximation in a more exact analysis of fault currents during an asymmetrical fault in the a.c. system as shown by Horigome and Ito[19]. In the process described in that paper the converter phase currents were transformed into positive and negative components, which were then used with the sequence components of the converter terminal voltage to calculate the corresponding sequence impedances. These impedances were connected to the sequence network as shown in Fig. 2.7 and a new set of converter phase currents obtained. A process of iteration was performed until convergence was reached. This method is similar to that of Arrillaga and Ethymiadis[14] and it is also necessary to calculate the voltage cross-over points, commutation angles, etc.

Phadke and Harlow[20] applied the same concept of positive and negative sequence impedances for the analysis of converter operation when the alternating voltages are unbalanced. They pointed out, however, that these equivalent impedances are merely ratios of sequence voltages and currents, and are not composed of physically realisable R, L, and C elements.

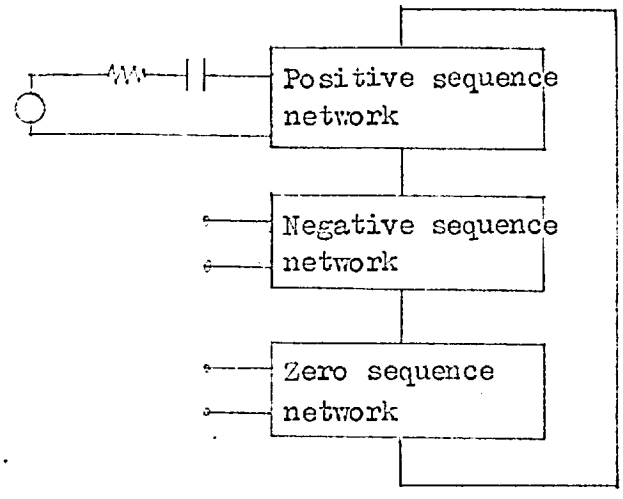

(a) First approximation using equivalent circuit of d.c. link

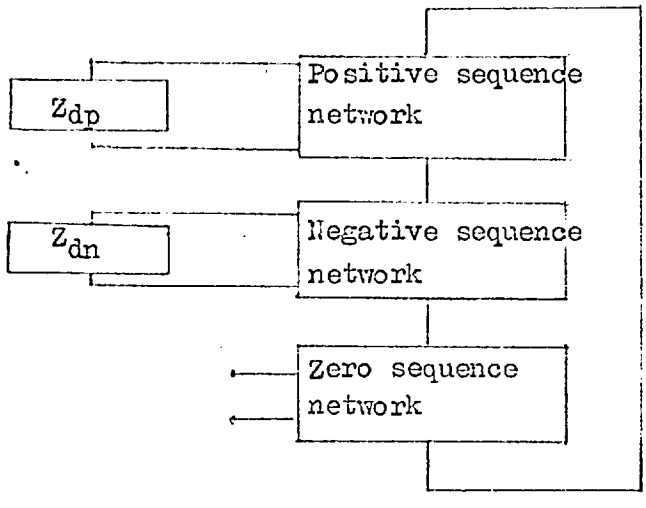

(b) Better approximation using equivalent sequence impedances of d.c. link.
Z_{dp} & Z_{dn} are equivalent sequence impedances of d.c. link.

Fig. 2.7 Representation of d.c. link in a.c. system with asymmetrical fault.

2.3 Transient-state Representations

Transient problems in an a.c./d.c. system can be divided into two groups - those dealing with small disturbances, e.g. small changes in current setting, and those dealing with large disturbances, e.g. valve faults. Studies of small disturbances (small signal analyses) are usually effected by applying small changes to a steady condition and evaluating the increments in the variables, thus the steady state voltage and current equations of a d.c. link can be transformed into similar equations in terms of increments of the variables, linearising where necessary. For large signal analyses, i.e. the study of large disturbances, the use of incrementals and linearisation is no longer valid, and problems of this nature in an a.c./d.c. system are usually tackled in two different ways. The converters can be represented as generators and motors with their voltages continuously controllable by the firing angles so that analyses can proceed in exactly the same way as indicated in Section 2.2.1. Alternatively the discrete nature of converter control through firing angles is recognised and the converter valves are represented as on-off switches; analysis then proceeds with actual instantaneous values of voltage and current, and not with average values as in the first approach. The following sections explain these points in greater detail.

2.3.1 Transient-state representations for small signal analyses in balanced a.c. systems

Reider[20,23] considered the stability of d.c. control systems by deriving equations of incremental e.m.f.s. of the rectifier and inverter. By assuming the firings of the values to be uniform at steady state and changing by small amounts during a transient, it was shown that over regular intervals of 60° (for one bridge) the actual bridge output voltage waveform (saw-tooth waveform) can be replaced by a step voltage waveform, the height of which is given by:

for rectifier $$e = \frac{3\sqrt{2}}{\Pi} E_1 \cos\alpha - \frac{3X_1}{\Pi} I_d \qquad \text{or} \qquad (2.36)$$

for inverter $$e = \frac{3\sqrt{2}}{\Pi} E_2 \cos\beta + \frac{3X_2}{\Pi} I_d \qquad (2.37)$$

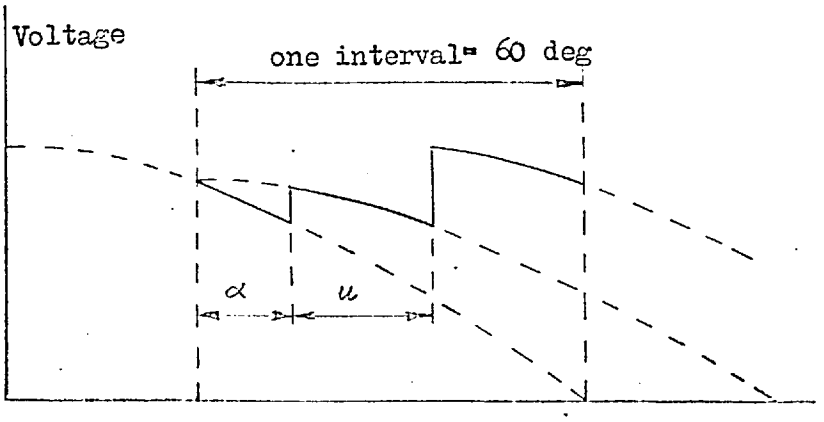

(a) Rectifier voltage waveform (saw-tooth)

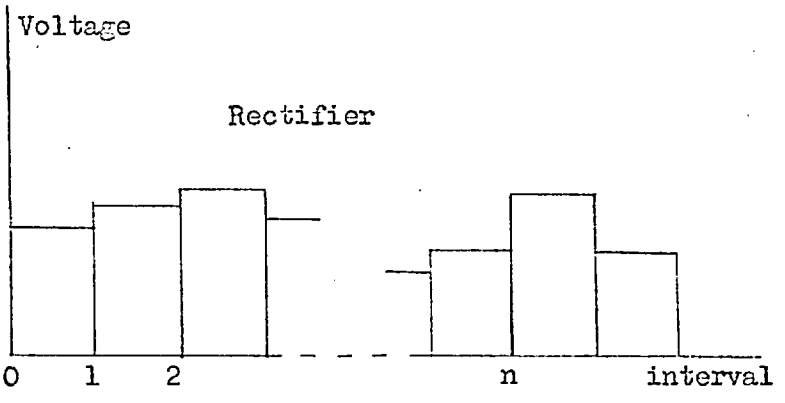

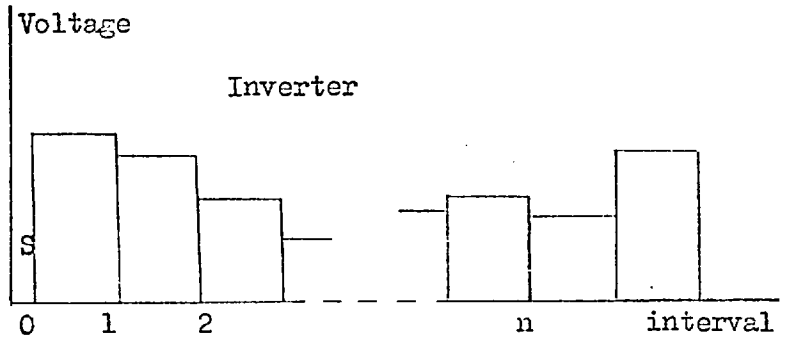

(b) Rectifier & inverter equivalent step voltage waveform with phase shift S

Fig. 2.8 Actual and equivalent step voltage waveforms

Fig. 2.8 shows these two waveforms. In Fig. 2.8a the 60° interval of the saw-tooth waveform is measured from the voltage cross-over, and it appears that this argument would only apply if $\alpha + u$ (sum of firing and commutation angles) or β (advance angle for inverter) is less than 60°. In fact the interval can begin at any point of the waveform, as long as there is no more than one commutation within one interval. For normal operation the commutation-angle is less than 60° for a rectifier and less than $(60-\gamma)^\circ$ for an inverter, hence by suitable choice of the beginning of the interval the actual saw-tooth waveform can always be replaced by a step voltage waveform for cases even with α or β exceeding 60°. If the rectifier step voltage waveform has a different start reference point on the actual waveform from that of the inverter, there would be an additional phase shift between the two step waveforms over and above that which arises from the phase angle difference between the alternating voltages at the two terminals (See Fig. 2.8) However, the effect of this phase shift was proved by Reider to be small.

The last term in Eqs. 2.36 and 2.37 may be regarded as resistance voltage drops so that a hypothetical resistance $\frac{3X}{\Pi}$ can be added to the equivalent circuit of the d.c. line represented as a single T-circuit. The equivalent e.m.f.s. of the rectifier and inverter are simply $\frac{3\sqrt{2}}{\Pi} E_1 \cos\alpha$ and $\frac{3\sqrt{2}}{\Pi} E_2 \cos\beta$ respectively.

Reider also showed that the effect of system impedance $(r + jw\ell)$ between the a.c. source and converter (including converter transformer) for normal range of firing and commutation angles can be included in the d.c. line equivalent circuit as:

$$r^1 = 1.85r \qquad (2.38)$$

$$\ell^1 = 1.85\ell \qquad (2.39)$$

By adding the equivalent resistance $\frac{3X}{\Pi}$ from Eqs. 2.36 and 2.37 to the line resistance the parameters of the equivalent d.c. link are shown in Fig. 2.9.

For the analysis of control system stability Reider recognised that the action of the firing angle control is discrete, i.e. the converter output voltage is fixed after each firing and cannot be changed until the

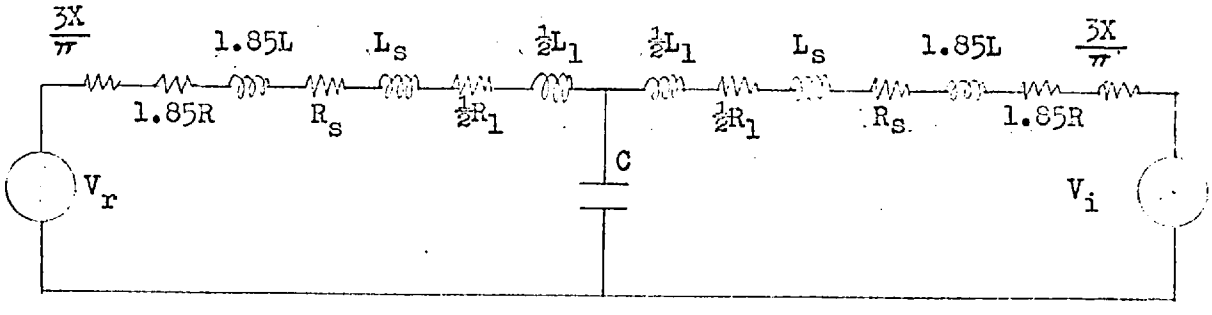

Fig. 2.9 Approximate lumped parameter representation of d.c. line

V_r, V_i rectifier & inverter terminal voltages

R, L a.c. system resistance & inductance

R_l, L_l d.c. line " "

R_s, L_s d.c. smoothing reactor resistance & inductance

X commutating reactance

C d.c. line capacitance

next firing. He therefore adopted the technique of discrete operator (Z transform) which is defined as

$$z = e^{-sT}$$

where z = z transform operator

s = Laplace transform operator

$T = \frac{60^{\circ}}{\omega}$ corresponding to an interval of 60°

Berlin[24] also analysed control system stability by an incremental method and used the same equations of converter voltages and the same equivalent circuit as Reider. However, Berlin implicity assumed the converter voltages to be continuously controllable by the firing angles so that these voltages were treated as continuous variables and not as discrete variables whose values hold for an interval of 60°. The operational equations were given in terms of Laplace operators.

Norton and Cory[25,26] studied small signal stability of control systems for multi-terminal h.v.d.c. links. Reference 25 presented a digital simulation program for calculating the direct current in each branch of the multi-terminal d.c. system, the a.c. system was represented merely as infinite busbars behind commutating reactances. The d.c. systems were represented as distributed parameter lines, and the currents were obtained by means of the Bergeron travelling wave equations. The main advantage of this method was said to be economy of computation, and the ease with which the complicated voltage waveform across d.c. terminals and attentuation can be included. However, the actual voltage waveform was not used; only the change in the steady-state voltage as a result of change of firing angle was considered. This was expressed as a time integral of the d.c. terminal voltage. Calculation proceeded on a step by step basis with a time step of τ which was ideally a common factor of all the transit times of the d.c. line branches. Linear interpolation and extrapolation were used to obtain values of direct current when firing instants of valves did not coincide with intervals of τ. Computing time was quoted as 1.6 min. on the IBM7090 for 80 msec real time, compared with a computing time of 12 min. on the KDF9 to simulate 100 msec. as required

by the program of Hingorani et al[30]. However, this method was not suitable for studying valve faults and d.c. line faults.

In Reference 26 the same two authors developed an alternative method for studying control system stability in multi-terminal h.v.d.c. systems. Using linearised equations a stability criterion in terms of operational admittance of the entire system seen from a junction was derived. Small perturbations from steady state condition was simulated by treating the small variations of d.c. terminal voltage resulting from small changes in firing angles as a train of modulated δ functions as shown in Fig. 2.10. Each branch of the d.c. line was represented by a single Π - equivalent circuit since the frequencies of interest are below 100 Hz. The discrete nature of the d.c. controllers were incorporated by expressing their transfer functions in terms of z transforms of sampled voltages and currents. Expressions of the operational admittance were derived in terms of d.c. line constants and controller transfer functions. By plotting these admittances as functions of frequency, stability limits and margins for different controller transfer functions were obtained. This method of control system stability analysis was used to check the results in the first paper[25] and agreement was shown to be good.

These two papers, therefore, provide two alternative methods for the preliminary study of control of multi-terminal h.v.d.c. systems. Computing times required are favourably short compared with other methods, although accuracy is not as high.

All the above papers on small signal analyses of control systems in d.c. transmission confined their attention to the variations in the d.c. system only, e.g. firing angles, direct voltage and current, and treated the a.c. system as a source of balanced and constant e.m.f. Hence the effect of a.c. system unbalance and the interaction between a.c. and d.c. systems in the transient-state were not considered. These two aspects, as well as other topics, are considered in the following sections on large signal analysis.

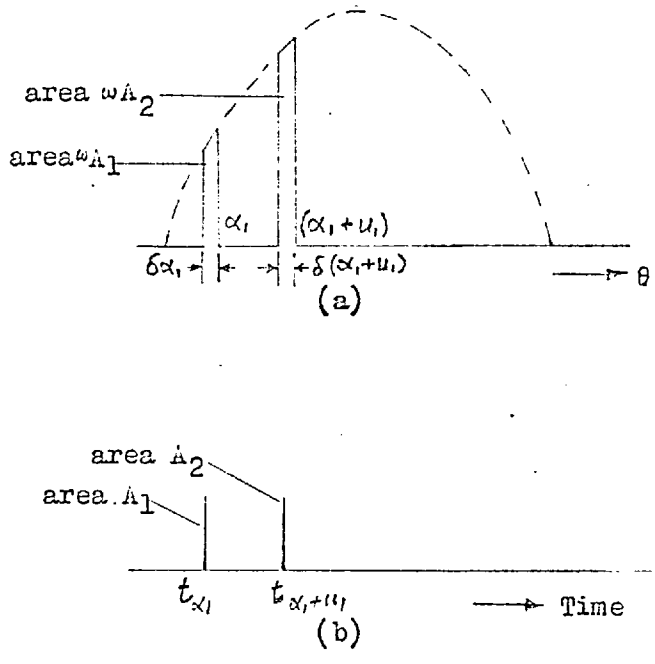

Fig. 2.10 Incremental terminal direct voltage represented as modulated delta functions

2.3.2 Transient-state representation for large signal analyses

In cases where it is required to determine the actual instantaneous values of voltage and current in an a.c./d.c. system during normal operation or following a large disturbance the values of a converter are represented as perfect on-off switches controlled by the firing pulses and the polarity of the voltage across them. Forward voltage drop across a conducting valve and reverse current through a non-conducting valve are both neglected. Freris[27] adopted this approach when analysing the conduction modes of a multi-group a.c. - d.c. converter. Similarly Reeve[28] used the same representation to establish the logic behaviour of converters during normal and abnormal operations. Phadke et al[29] analysed the transient fault currents from a rectifier following a line to ground fault on the d.c. line close to the rectifier terminals, the rectifier values being again represented as perfect switches.

The a.c. system is usually represented as three-phase e.m.f.s. supplying the converter through system impedance and converter transformers. The instantaneous voltages and currents of the three phases can be found by starting from these e.m.f.s. The d.c. line, if involved in the study is represented as an equivalent T - or Π - circuit, and differential or operational equations set up to relate the instantaneous currents to the actual voltage waveforms from the converter terminals. This lumped parameter representation of the d.c. line is only valid for slow transients below about 1 kHz which is deemed to be sufficient for most purposes. Fast transients on d.c. lines can be studied by using a distributed parameter representation and a travelling wave method of solution.

Hingorani et al[30,31,32] developed a very comprehensive procedure for the dynamic simulation of h.v.d.c. systems under all conditions of operations, both normal and abnormal, that are likely to occur in practice. The key to this procedure is that, like Reeve[28], they realised that under all conditions the operation of a converter can be divided into a limited number of easily recognisable patterns all of which can be further simplified for the purpose of analysis down to one single equivalent

circuit called the central-process equivalent circuit. In a converter with 1 bridge, the authors argued that only a maximum of four out of the seven valves (including the bypass valve) may conduct at any one instant and concluded that, out of a possible 86 conduction patterns with one to four values conducting, only 12 are likely in practice, and these can be represented by 7 equivalent circuits as shown in Fig. 2.11. These equivalent circuits show the connection from the three phases of the a.c. system to the d.c. line, and can be further simplified into a central-process equivalent circuit as shown in Fig. 2.12. In this circuit the 7 valves of the bridge are shown and their conduction states would correspond to one of the 12 possible circuits. Each of the 7 circuits required a set of differential equations to relate the voltages and currents and these were solved with a Kutta-Merson variable step integration subroutine.

In Fig. 2.12 valves n, n-1, and n-2, termed primary valves, are associated with normal operation, and valves n-3, n-4, n-5, and 7 conduct only during abnormal operation and are therefore called secondary valves. To relate the valves in this equivalent circuit with the actual valves in the bridge, a process of iteration is necessary to adjust the value of process number n until the conduction pattern corresponds to one of the 12 shown in Fig. 2.11.

The firing angles were determined from the conventional control characteristics shown in Fig. 2.13 and were expressed by the following equations:

$$\left.\begin{aligned} &\alpha = \alpha_o \quad \text{if} \quad \frac{\sqrt{2}\omega L I_d}{E} - \cos\gamma_o + \frac{X(I_d)}{\sqrt{2}E} > \cos\alpha_o \\ &\text{otherwise} \quad \alpha = \cos^{-1}\left\{\frac{\sqrt{2}\omega L I_d}{E} - \cos\gamma_o + \frac{X(I_d)}{\sqrt{2}E}\right\} \end{aligned}\right\} \qquad (2.40)$$

in which $X(I_d) = 0$ if $I_d > I_{ds}$

otherwise $X(I_d) = A(I_d - I_{ds})$

where α_o = minimum firing angle of rectifier

γ_o = minimum extinction angle of inverter

L = commutating inductance per phase

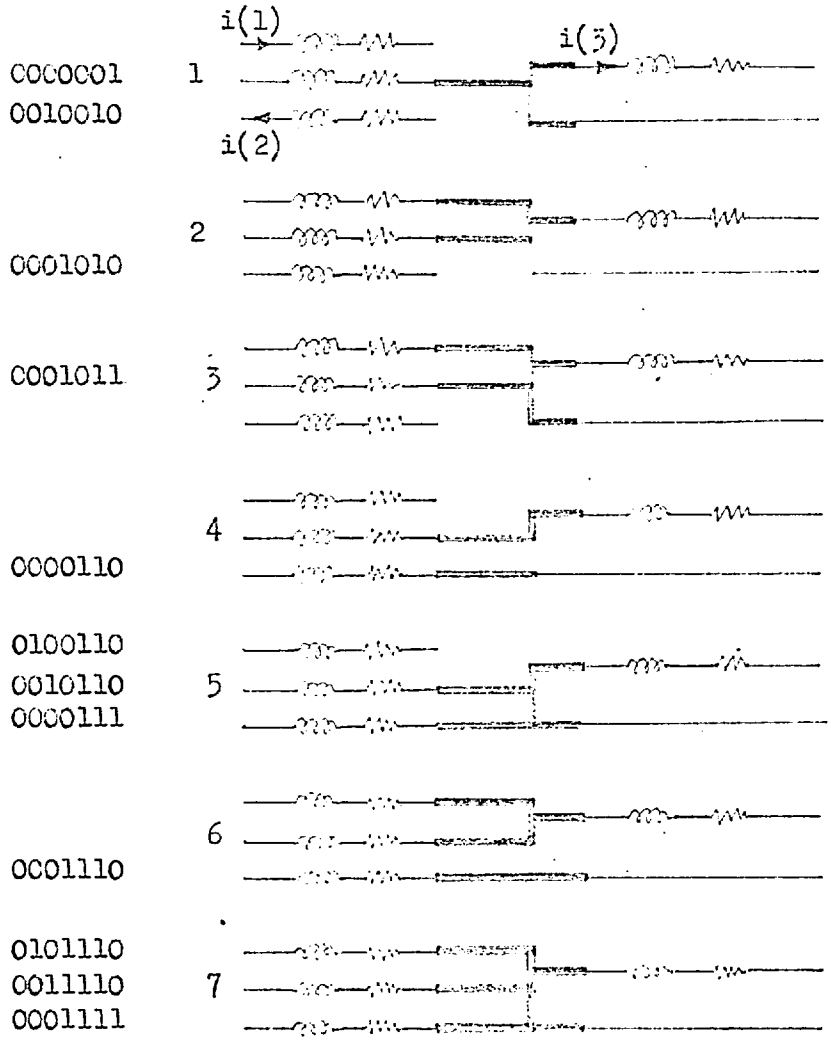

Fig. 2.11 Practical equivalent circuits .
1 & 0 in the conduction patterns denote the conducting & non-conducting states of the 7 valves of a bridge.

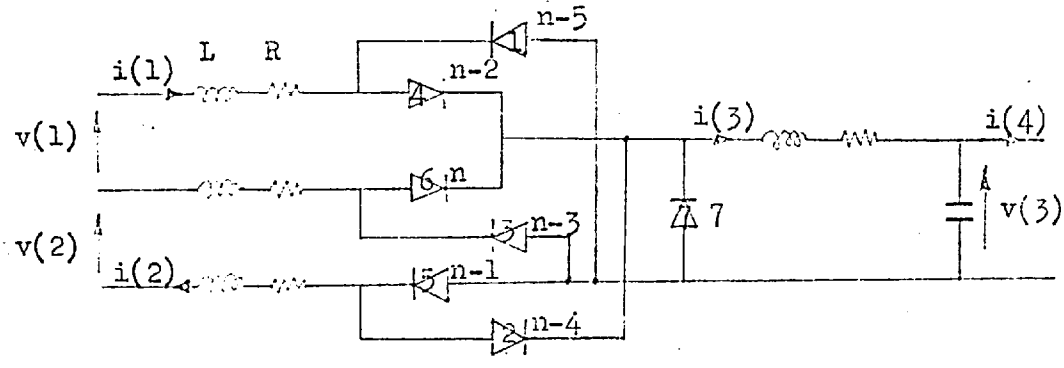

Fig. 2.12 Complete central-process equivalent circuit

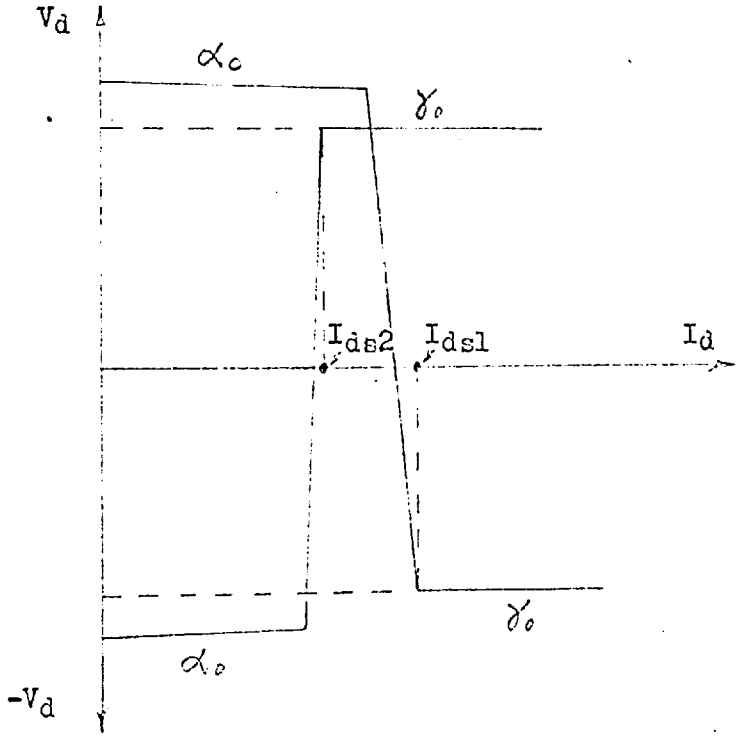

Fig. 2.13 Converter control characteristic

A = slope of converter characteristic

E = r.m.s. line voltage at converter

Since the firing of a valve or the introduction of a fault marked the end of one typical process, as defined in Fig. 2.11, and the beginning of another, the program was designed to check the occurance of such events. This was achieved by using the Kutta-Merson integration process to go backward and forward in time with reducing time steps until the process transition point was fixed to within a certain accuracy in time. This is the part of the program that consumes most computing time and is one area where improvement can be made. As a first attempt fixed time step integration may be used instead. If the fixed step is small, say 0.3 msec. or below, the firing instants can be located with an accuracy of up to 5.4 electrical degrees, which is smaller than the value of α_o (7 degrees) or γ_o (17 degrees).

Valve faults were introduced by interfering with the normal sequence of grid pulses or by modifying the voltages across the valve, e.g. fire through was represented by supplying the appropriate grid pulse, and arcback was introduced by supplying grid pulse and assuming the voltage across that valve to be positive.

The description of Hingorani et al was based on a 6-pulse 2-terminal d.c. link although their representation is perfectly general and can be extended to cover 12-pulse converters, although at the expense of increased computing time. Valve faults and d.c. line faults can be studied fairly easily. But as Norton and Cory[25] pointed out, their method would be cumbersome to extend to multi-terminal systems with electrically long d.c. interconnections, because of the rapid rise in the number of differential equations for simultaneous solution.

The above method is a true three phase representation of both converters and a.c. systems so that unbalance of a.c. system voltage in magnitude and phase can easily be catered for in the three phase voltage equation. However, Hingorani et al assumed the a.c. systems to be infinite busbars thus excluding from their investigations the effect of

interaction between the a.c. and d.c. systems. When it is required to study the transient behaviour of machines connected near d.c. terminals the effect of this interaction would be crucial, particularly if the a.c. systems connected to the converters are weak. In these cases the three phase representation of Hingorani et al must be complemented with a three phase (or equivalent) representation of the machines and the a.c. systems. The Hingorani representation of converters yields instantaneous three phase currents at the converter busbar and these can be used directly in the a.c. system solution if the machine equations are expressed in three phase terms, or, if they are expressed in d-q components, a transformation would be required to link the converter phase quantities with the d-q components in the rest of the system. For a simple case of a converter connected to one single generator as shown in Fig. 2.14 the following set of equations in d-q components may be used:

(a) Flux equations (from Harley[33])

$$\omega\psi_d = x''_d\, i_d + \omega(x''_d - x_a)\left(\frac{\psi_f}{x_{f\ell}} + \frac{\psi_{kd}}{x_{kd}}\right)$$

$$\omega\psi_q = x''_q\, i_q + \omega(x''_q - x_a)\,\frac{\psi_{kq}}{x_{kq}}$$

$$p\psi_{kd} = \frac{1}{T''_{do}}\left(\frac{x'_d - x_a}{\omega}\cdot i_d + \frac{x'_d - x_a}{x_{f\ell}}\cdot\psi_f - \psi_{kd}\right)$$

$$p\psi_{kq} = \frac{1}{T''_{qo}}\left(\frac{x_{mq}}{\omega}\cdot i_q - \psi_{kq}\right)$$

$$p\psi_f = e_f + \frac{1}{T'_{do}}\left\{\frac{x''_d - x_a}{x'_d - x_a}\left(\frac{x_{md}}{\omega}\cdot i_d + \frac{x_{md}}{x_{kd}}\cdot\psi_{kd}\right) - \psi_f\left[1 + \frac{(x''_d - x_a)x_{md}}{x_{kd}x_{f\ell}}\right]\right\}$$

(b) Voltage equations (from Adkins[34])

$$e_d = \omega\psi_q + r_a i_d$$

$$e_q = \omega\psi_d + r_a i_q$$

The $p\psi_d$, $p\psi_q$ terms have been ignored in the above equations because they are small compared with the $\omega\psi$ terms under normal operation.

(c) Current equations

From the three phase representation of the converter given by Hingorani et al[32] it is fairly straight-forward to identify the phase currents with those in the central-process equivalent circuit of Fig. 2.12.

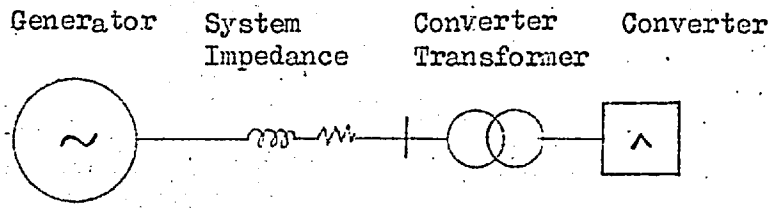

Fig. 2.14 Single generator feeding converter

For example, when the process number n = 6, and a valve firing pattern given by equivalent circuit number 6 in Fig. 2.11 (i.e. two valves commutating)

$$i_a = i(1)$$

$$i_b = i(3) - i(1)$$

$$i_c = - i(2)$$

where the currents i(1), i(2) and i(3) are for this particular process, given by:-

$$\begin{bmatrix} pi(1) \\ pi(2) \end{bmatrix} = \begin{bmatrix} 2\ell & -\ell \\ -\ell & 2\ell+\ell d \end{bmatrix}^{-1} \left[\begin{bmatrix} v(1) \\ v(2)-v(3) \end{bmatrix} - \begin{bmatrix} 2r & -r \\ -r & 2r+r_d \end{bmatrix} \cdot \begin{bmatrix} i(1) \\ i(2) \end{bmatrix} \right]$$

$$pv(3) = \frac{1}{c_d} [i(3) - i(4)]$$

$$i(3) = i(2)$$

$$v(1) = e_b - e_a$$

$$v(2) = e_c - e_b$$

where e_a, e_b and e_c are the e.m.f.s. at the generator terminals. It should be noted that the variables r and ℓ in this case are the total resistance and inductance per phase between the generator and the converter terminals, including that of the converter transformer. The equation for i(4) will depend on the representation of the d.c. line.

Each of the equivalent circuits of Fig. 2.11 will have its own set of differential equations to describe the currents i(1), i(2) and i(3) as explained in Reference 32. Also the correlation between phase voltages and currents with their counterparts in the equivalent circuits depend on the process number and firing pattern.

(d) Transformation of voltages and currents (from Adkins[34])

The differential equations of currents i(1), i(2) and i(3) are in terms of the voltages v(1) and v(2) and hence on the phase voltages e_a, e_b and e_c. Since voltages are only calculated in terms of d-q components a voltage transformation of the following form is required:-

$$\begin{bmatrix} e_a \\ e_b \\ e_c \end{bmatrix} = \begin{bmatrix} \cos\theta & \sin\theta \\ \cos(\theta - 120) & \sin(\theta - 120) \\ \cos(\theta + 120) & \sin(\theta + 120) \end{bmatrix} \begin{bmatrix} e_d \\ e_q \end{bmatrix}$$

where θ is the angle between rotor axis and a synchronously rotating reference frame, and is found from the mechanical equation of rotation of the machine.

When the instantaneous values of the phase currents have been obtained by solving the differential equations of i(1), i(2) and i(3) and relating them to phase quantities, another transformation is needed to get the d-q components of current for use in the flux and voltage equations. Thus:-

$$\begin{bmatrix} i_d \\ i_q \end{bmatrix} = \frac{2}{3} \begin{bmatrix} \cos\theta & \cos(\theta - 120) & \cos(\theta + 120) \\ \sin\theta & \sin(\theta - 120) & \sin(\theta + 120) \end{bmatrix} \begin{bmatrix} i_a \\ i_b \\ i_c \end{bmatrix}$$

To summarise it may be said that the machine equations (in d-q components) are linked with the d.c. converter and system equation (in a-b-c components) by a d-q to a-b-c transformation of voltages and a reverse transformation of currents. A simple case of one machine feeding a single converter has been taken as example, but the same idea can be adopted to incorporate d.c. links in more complex a.c. systems with more than one machine. Extra complications will arise, however, if more than one generator is connected to a converter busbar so that the converter phase currents cannot be related to the d-q voltages and currents of one generator alone. In this case some iterative process must be used at each step of numerical integration to establish convergent conditions throughout the system.

2.3.3 Transient-state representation for large signal analysis in symmetrical a.c. systems only

The three phase representation of Hingorani et al is the only one known that would rigorously model the operation of converters on a firing by firing basis, and would therefore simulate all types of valve faults found in practice. Unfortunately the implementation of this representation requires considerable programming effort and the program itself requires long running time. For this reason this representation of converters had not been used in the transient analysis of large a.c./d.c. systems with balanced a.c. condition. In these cases the d.c. systems are dealt with by ignoring the complex voltage waveforms at the d.c. converter terminals arising from individual valve firing, and replacing these waveforms with their average values. Moreover the steady state relationship between currents on the a.c. and d.c. sides of the converter and the phase angle between converter voltage and current are assumed to hold in the transient state for the purpose of analysis. i.e.

$$V_d = \frac{3\sqrt{2}}{\Pi} E \cos\alpha - \frac{3X}{\Pi} I_d$$

or $$V_d = \frac{3\sqrt{2}}{\Pi} E \cos\gamma - \frac{3X}{\Pi} I_d$$

$$I_{ac} = \frac{\sqrt{6}}{\Pi} I_d$$

$$\frac{3\sqrt{2}}{\Pi} E \cos\phi = V_d$$

The voltage V_d is a function of the firing angle or extinction angle which is assumed to be continuously acting and affects V_d at each step of the calculation. The values of these angles are determined by the d.c. controls. Peterson et al[35] and Breuer at al[9,10] both adopted this simplification and used firing angle controls of the form:

$$\cos\alpha_R = \frac{K_R(I_r - I_R)}{V_R}$$

and $$\cos \alpha_I = -\cos \gamma_o + \frac{\frac{6X_I}{\pi} I_I + e^*_{CI}}{V_I}$$

with $$e^*_{CI} = K_I(kI_r - I_I) > 0$$

where α_R = rectifier firing angle

α_I = inverter firing angle

I_r = d.c. link current order

I_R = rectifier side direct current

I_I = inverter side direct current

K_R = gain of rectifier controller

K_I = gain of inverter controller

k = multiplier $(= \frac{I_r\text{-current margin}}{I_r})$

X_I = inverter commutating reactance

V_R = rectifier a.c. voltage

V_I = inverter a.c. voltage

Breuer et al in a later paper compared the results obtained from a computer program using such simplified representation of the converters in the transient state with results obtained from a simulator for a.c. and d.c. system faults and claimed good agreement. This is most probably due to the firing intervals of the valves (1.67 msec for 12 pulse operation) being small compared with the time constants of generators (10-100 msec for T''_{do} and a.v.r. time constant). The significance of their finding is that representation of converters in such detail as that of Hingorani et al would seem unjustified unless effect of valve faults are to be studied. Hence Chapter 5 and 6 adopted this simplified representation of converters.

2.3.4 Representation of converters on analog or hybrid computers

To close this chapter it is worthwhile to mention briefly the representation of converters on an analog computer[36] which may be regarded as halfway between a simulator and a digital model. In this case the converter valves are represented by clamping circuits which produce

an output to correspond to the firing of a valve whenever the forward voltage and the grid pulse are positive. The d.c. link and converter controllers are easily set up as transfer functions on the analog computer. The a.c. system can be represented either by a three-phase oscillator or by a simulation of a synchronous machine, in both cases unbalanced voltages or a.c. systems with different frequencies are easily simulated by changing the parameters of the representation. Both a.c. and d.c. transmission lines can be represented as lumped parameter equivalent circuits. Thus this method of representing a.c. and d.c. systems provides a rigorous simulation without the expenditure of considerable programming effort. However, due to the lumped parameter representation of transmission lines, a high time-scale factor would be required (A factor of 1000 was used in Reference 36, i.e. 1000 seconds of analog computer time was required to simulate 1 sec. of real time). Therefore practical investigations using analog computers have been limited to a matter of 1 sec. real time.

This problem of excessive computing time is largely avoided if the transmission lines are represented as distributed parameters and the equations solved on a digital computer, while retaining the analog representation of converters and their controls. A hybrid computer, which has a digital computer linked to an analog computer through digital-analog converters, is ideal for this purpose. Krause and Carroll[37] reported that, using a hybrid computer, a reduction of time-scale factor to 100 was possible, although the actual factor used was 500.

CHAPTER 3

STEADY-STATE STABILITY OF A.C./D.C. SYSTEMS

3.1 Introduction

This Chapter considers the stability of an a.c./d.c. system in the steady - and semi-steady state, the latter referring to the short period after a disturbance but before operation of tap changers. The factors considered are changes in local a.c. load, changes in d.c. power transfer, changes in a.c. system connection and sudden changes in direct voltage. Steady-state characteristics of d.c. transmission systems are discussed and a voltage stability limit is derived. Effects of tap changers on power transfer and current margin on voltage are considered. Finally, some results from an actual system test are given.

3.2 Interaction of d.c. converters and weak a.c. system

When one terminal of a h.v.d.c. link is connected to a weak a.c. power system there would be strong mutual influence, in terms of voltage and harmonics, between the d.c. converters and the a.c. system. In this connection a weak a.c. system may be defined as one having a short circuit fault level at the converter station bus which is not great compared with the power rating of the d.c. link, say 5 times and below. If a large a.c. load is also connected to the converter busbar the sum of the d.c. and a.c. power demands can also cause the a.c. system to appear weak. For the present study a 2 - terminal h.v.d.c. link was considered. One object of the study was to find the maximum permissible d.c. power import and export with different a.c. system fault levels and different a.c. loads. And, since the d.c. power transfer depends on the method of control as well as the condition of the a.c. system, a second object was to determine the necessary control requirements to match existing or anticipated a.c. system conditions. The operation of the d.c. link was considered under both steady-state and semi-steady-state conditions: the former refers to the condition when the a.c. system condition and d.c. power transfer are fixed; while the latter refers

to the interval of time after a disturbance but before transformer tap-changer operation, i.e. an interval of no more than a few seconds.

In this study only the limitation due to voltage instability was considered. The limitation due to harmonic instability was considered by Ainsworth [38] and will be mentioned in a later section dealing with an actual test when the Cross-channel d.c. link was connected to a weak a.c. system.

3.2.1 Description of system

The system in this study was one terminal of a 2 - terminal h.v.d.c. link connected to a weak a.c. power system, and is shown in Figs. 3.1 and 3.2. The converter station bus was connected by an auto-transformer to the a.c. system which was represented as an impedance and an infinite bus at nominal voltage. The station bus also supplied a local load through a network which consisted mainly of underground cables. The cable capacitance was represented as a lumped capacitance. The station bus supplied a converter bus having two converter transformers and a filter. A 6-pulse converter bridge was fed from each converter transformer, and the two bridges were connected in series on the d.c. side to form a converter group which can be operated either as a rectifier or as an inverter. For steady state the direct voltage of the link was kept constant at its nominal value by tap change on the converter transformers at the inverter end. When the converter was rectifying the firing angle should be kept within a range between 10° and 20° by tap changing of the converter transformers. When inverting the extinction angle should be kept constant at 17°.

The relevant data of this scheme is presented below:

A.C. Side

Infinite bus voltage	400 kV (1 p.u.)
Converter station bus nominal voltage	132 kV
Auto-transformer tap range	± 15%

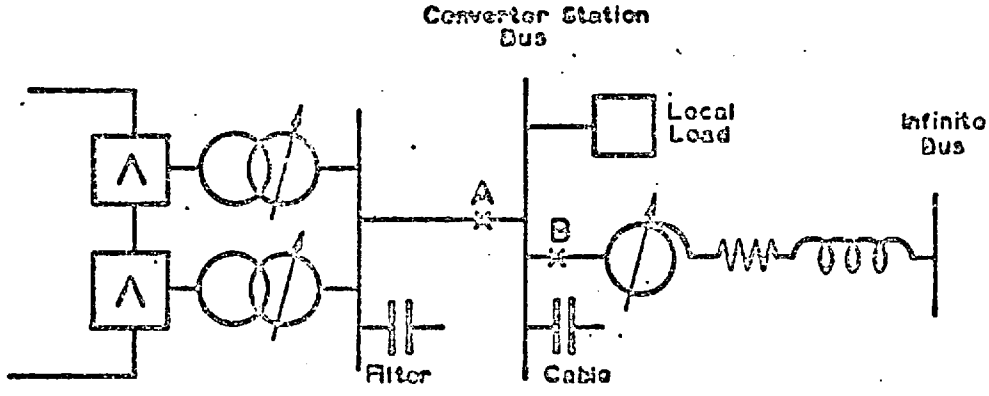

FIG. 3.1 SYSTEM AT ONE TERMINAL OF A 2-TERMINAL DC LINK

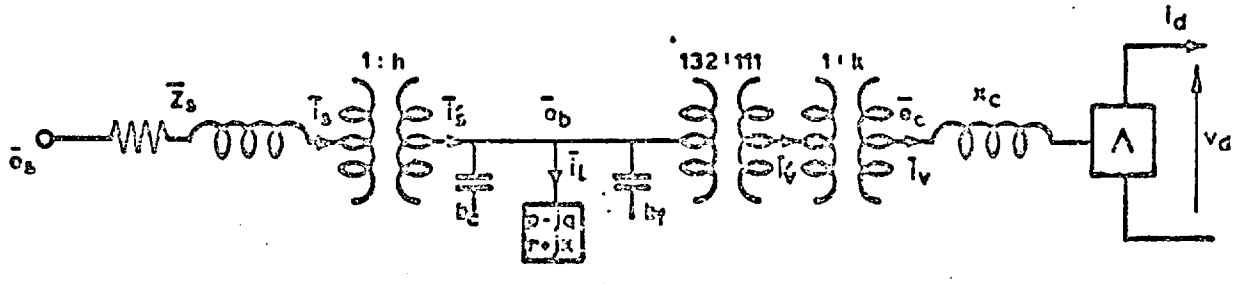

FIG 3.2 EQUIVALENT CIRCUIT OF SYSTEM IN FIG 3.1

Converter transformer tap range	+ 16%, - 10%
" " rating	189 MVA
Converter transformer voltage ratio	132/111 kV
Converter transformer reactance	15.6%
Filter rating	70 MVAr
Lumped capacitance of cable network	60 MVAr
Short circuit levels to be considered	3500, 2000 and 1000 MVA
Local a.c. load	500 MW max. 50 MW min. P/Q ratio = 5
D.C. Side	
Power rating	320 MW
Direct voltage	266 kV
Range of firing angle	$\alpha = 15^\circ \pm 5^\circ$ $\alpha_{min} = 7^\circ$ $\alpha = 17^\circ$

3.2.2 Computational details

In this study the converter representation and the equations and per unit systems used were those suggested by Gavrilovic and Taylor [13] and described in Chapter 2. With the data given in the last section the per unit base values are as follows:

A.C. Side

Voltage base $E_{cB} = 132$ kV

MVA base $P_{cB} = 2 \times 189$ MVA $= 378$ MVA

Current base $I_{cB} = \frac{P_{cB}}{\sqrt{3} E_{cB}} = 1.66$ kA

D.C. Side

Voltage base $\quad VdB = \frac{3\sqrt{2}}{\pi} \times 2 \times \frac{111}{132} \times 132 = 300$ kV

MVA base $\quad PdB = 2 \times 189$ MVA $= 378$ MVA

Current base $\quad IdB = \frac{PdB}{VdB} = 1.26$ kA

The converter equations in per unit are

$$v_d = e_c \cos\alpha - \frac{\pi}{6} \cdot x_c i_d \qquad (3.1)$$

$$i_p = v_d i_d / e_c \qquad (3.2)$$

$$i_v = i_d \qquad (3.3)$$

$$i_q = (i_v^2 - i_p^2)^{\frac{1}{2}} \qquad (3.4)$$

$$\bar{i}_v = i_p - j i_q \qquad (3.5)$$

where x_c = converter transformer reactance

$\bar{i}_v$ = equivalent converter current on the a.c. side with components.

e_i = commutating voltage

The filter and cable capacitances were represented as constant susceptances as:

$b_f = Q_f/PcB$

$b_c = Qc/PcB$

The local a.c. load were represented in two ways, first as constant P and Q and alternatively as constant R and X.

Different types of changes and disturbances were studied by means of the digital computer. In the following sections the procedures of computation are briefly described and the results are presented. A detailed description of the programs were given in Reference 39.

3.2.3 Changes in local a.c. load and d.c. power transfer

This study investigated the effect of changes in local a.c. load and d.c. power transfer on the steady-state operating conditions of the a.c./d.c. system. The converter bus voltage was maintained to within $\pm$ 10% of nominal value by tap-changing on the converter transformer or the auto-transformer. At the beginning of computation the commutating voltage e_c was calculated from Eq. 3.1 as follows:

$$e_c = \frac{1}{\cos\alpha}\left(v_d + \frac{\Pi}{6} x_c i_d\right)$$

where v_d = rated direct voltage

$\alpha = 15^o$

The converter bus voltage was then obtained as

$$e_b = \frac{1}{k}\, e_c$$

where k = converter transformer tap ratio and the total current from the system was

$$\bar{i}_s = h\,[k\bar{i}_v + je_b\,(b_f + b_c) + \bar{i}_e]$$

where $\bar{i}_v$ is given by Eq. 3.5 and

$\bar{i}_e$ = local a.c. load current

$$= \frac{p - jq}{e_b} \quad \left(\text{or } \frac{e_b}{r+jx}\right)$$

h = auto-transformer tap ratio

and the infinite bus voltage es is given by

$$\bar{e}_s = \frac{1}{h}\, e_b + \bar{Z}_s \bar{i}_s$$

where $\bar{Z}_s$ = system impedance

An iterative process was required to satisfy the boundary condition of

$$|e_s| = 1.0$$

Different system short circuit fault levels were used and the results are summarised in Table 3.1 and Fig. 3.3 and 3.4 from which the following conclusions are drawn:

(a) The maximum permissible power import or export of the d.c. link can be increased by raising the auto-transformer tap, while the converter transformer tap is used to keep the firing angle or direct voltage within specified limits.

(b) A reduction in local a.c. load does not allow the power export of the d.c. link to be increased by the same amount. This is due to the difference between the P/Q ratio of the load (=5) and that of the converter ($\doteq$2)

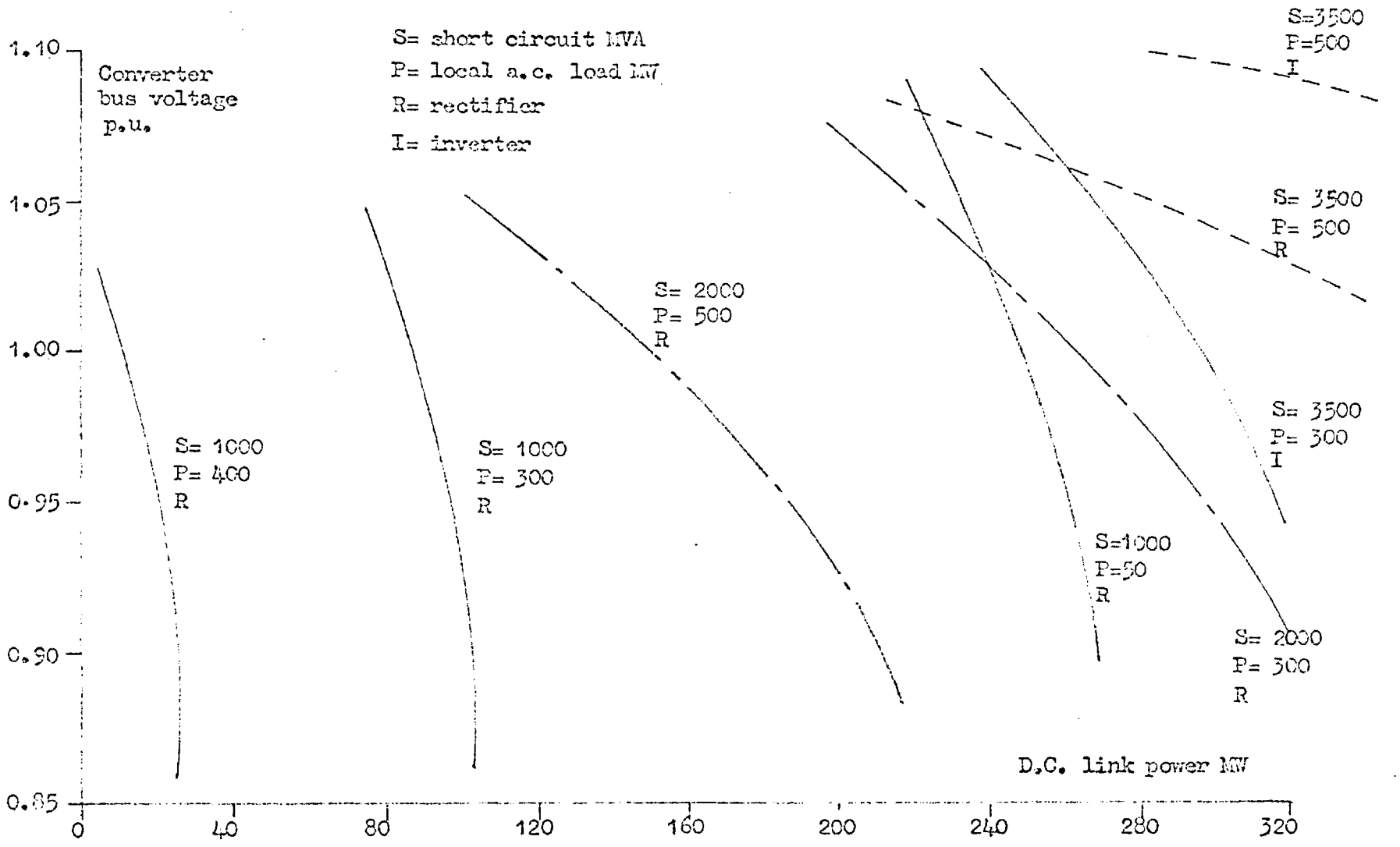

Fig. 3.3 Converter bus voltage vs. d.c. link power for different a.c. system conditions

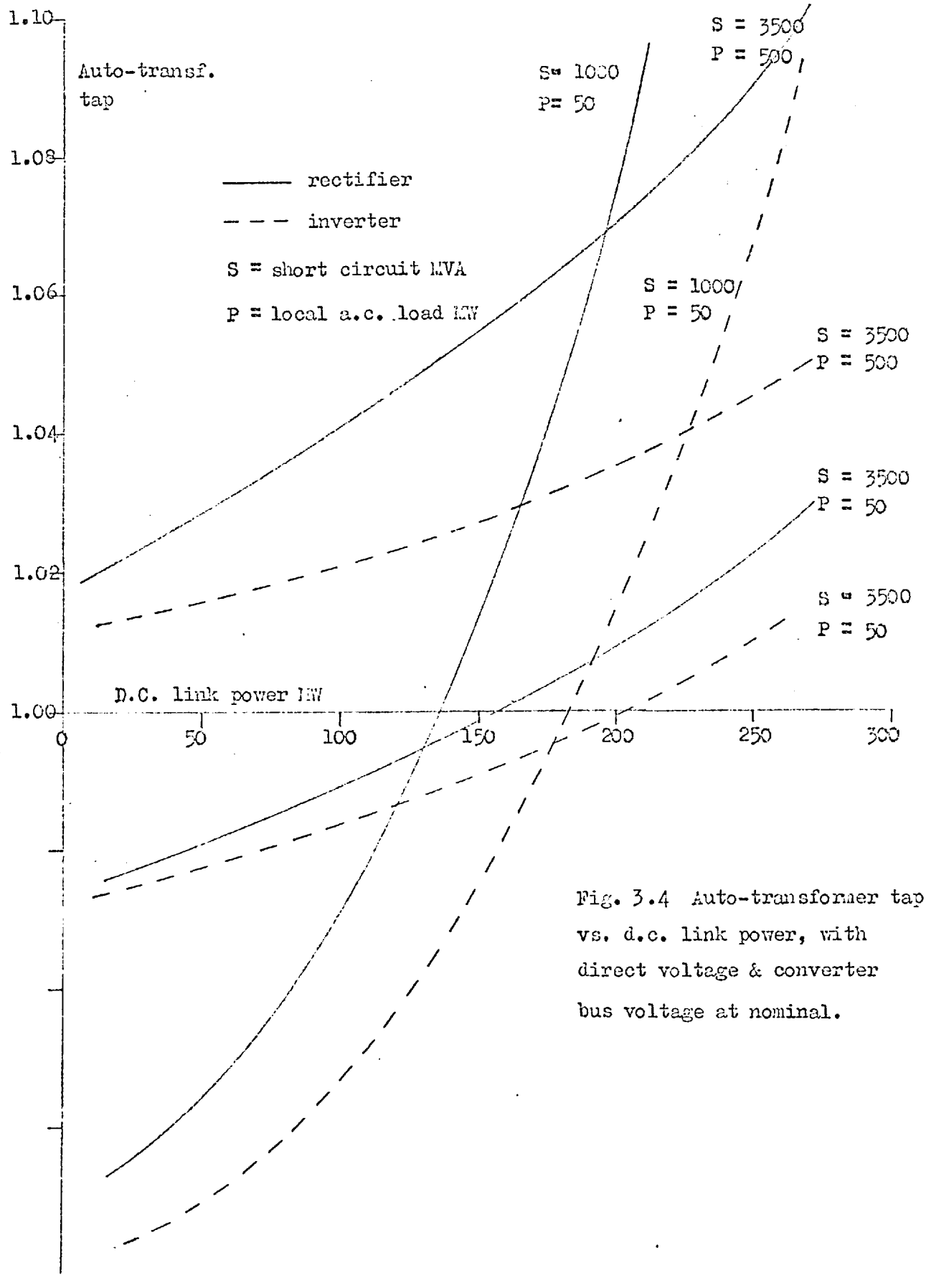

Fig. 3.4 Auto-transformer tap vs. d.c. link power, with direct voltage & converter bus voltage at nominal.

Short-Circuit Level MVA	Auto-transf. Tap	Con-transf. Tap	Local a.c. Load MW	D.C. Power Export MW	D.C. Power Import MW
3500	1.15	0.96	500	320	>320
	"	"	400	343	"
	"	"	300	368	"
2000	1.15	1.00	500	206	"
	"	"	400	257	"
	"	"	300	303	"
	"	"	200	338	"
1000	1.15	1.00	400	61	"
	"	"	300	135	"
	"	"	200	201	"
	"	"	100	260	"
	"	"	50	288	"

Table 3.1

The above results are based on the following parameters:-

(a) $\alpha = \gamma = 17^{\circ}$

(b) Converter bus voltage at $1.0 \pm 10\%$.

(c) Figs. 3.3 and 3.4 show that rectifier operation produces higher voltage regulation than inverter operation, so that emergency power reversal from import to export may possibly cause voltage instability in some cases.

(d) Fig. 3.4 shows that the converter bus voltage rises as power import or export is decreased. In cases of d.c. outage with one or more bridges blocked the converter bus voltage will rise, and the effect would be enhanced by the reactive power generated by the filter. If it exceeds the permissible level this voltage rise would place a limit on the maximum d.c. link power transfer.

The relationship between the auto-transformer tap and the converter transformer tap is discussed in Section 3.2.6.

3.2.4 Local disturbances

This disturbance was assumed to take the form of line switching at or near the terminal under consideration and produce a change in the short circuit fault level at the converter bus. The study only considered the interval of time after such an event but before tap changer operation; thus it may be considered as a semi-steady-state study. The tap positions used were established for an initial power import or export of 320 MW. The computational procedure was similar to that in the last section.

In the case of inverter operation constant extinction angle control was assumed so that the extinction angle was not effected by the change of short circuit level. For rectifier operation, however, there were two possibilities. If the converter bus voltage rises it will be necessary to increase the firing angle α so as to keep the direct current constant. On the other hand a fall in converter bus voltage may be sufficient to cause margin cross so that the inverter takes over current control and the rectifier operates with a minimum firing angle α min. (7°).

Constant power control and constant current control with different current margins were considered. The results were summarised in Table 3.2 and selectively shown in Fig. 3.5, 3.6, 3.7 and 3.8.

Only reductions in short circuit fault level were considered since this is the more onerous condition. Table 3.3 shows that when this occurs there is always a limit to the maximum power import or export with a corresponding drop in converter bus voltage. Normally the voltage is not allowed to drop below 10% following a disturbance, and Table 3.2 gives the correct current margin to use for constant current control to satisfy this requirement when the a.c. system fault level is expected to be reduced.

It can be seen from Table 3.2 that a constant P and Q representation of the local a.c. load gives more pessimistic results than a constant R and X representation.

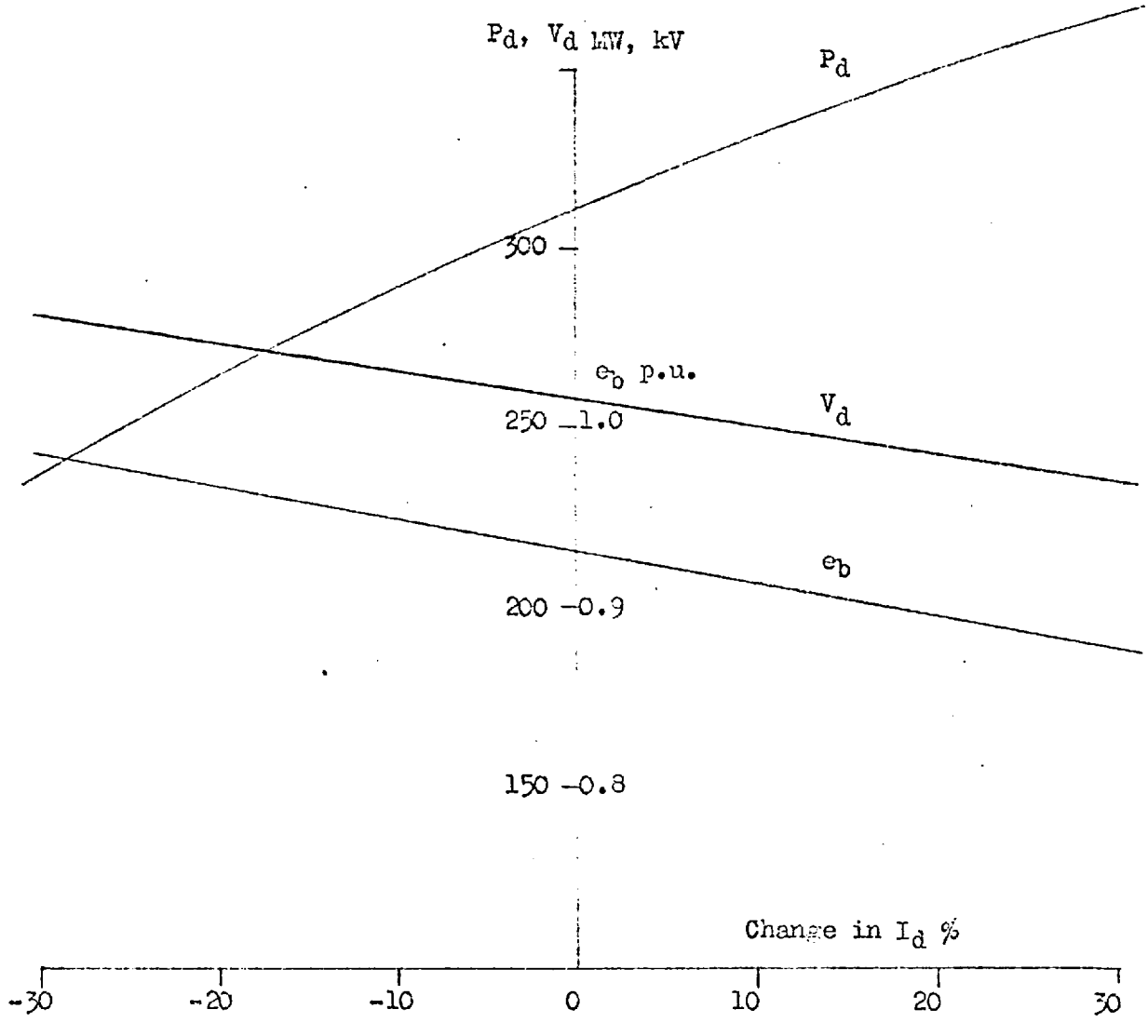

Fig. 3.5 Local disturbance : short circuit level changed from 3500 to 2000 MVA. RECTIFIER
Local a.c. load = 300 MW

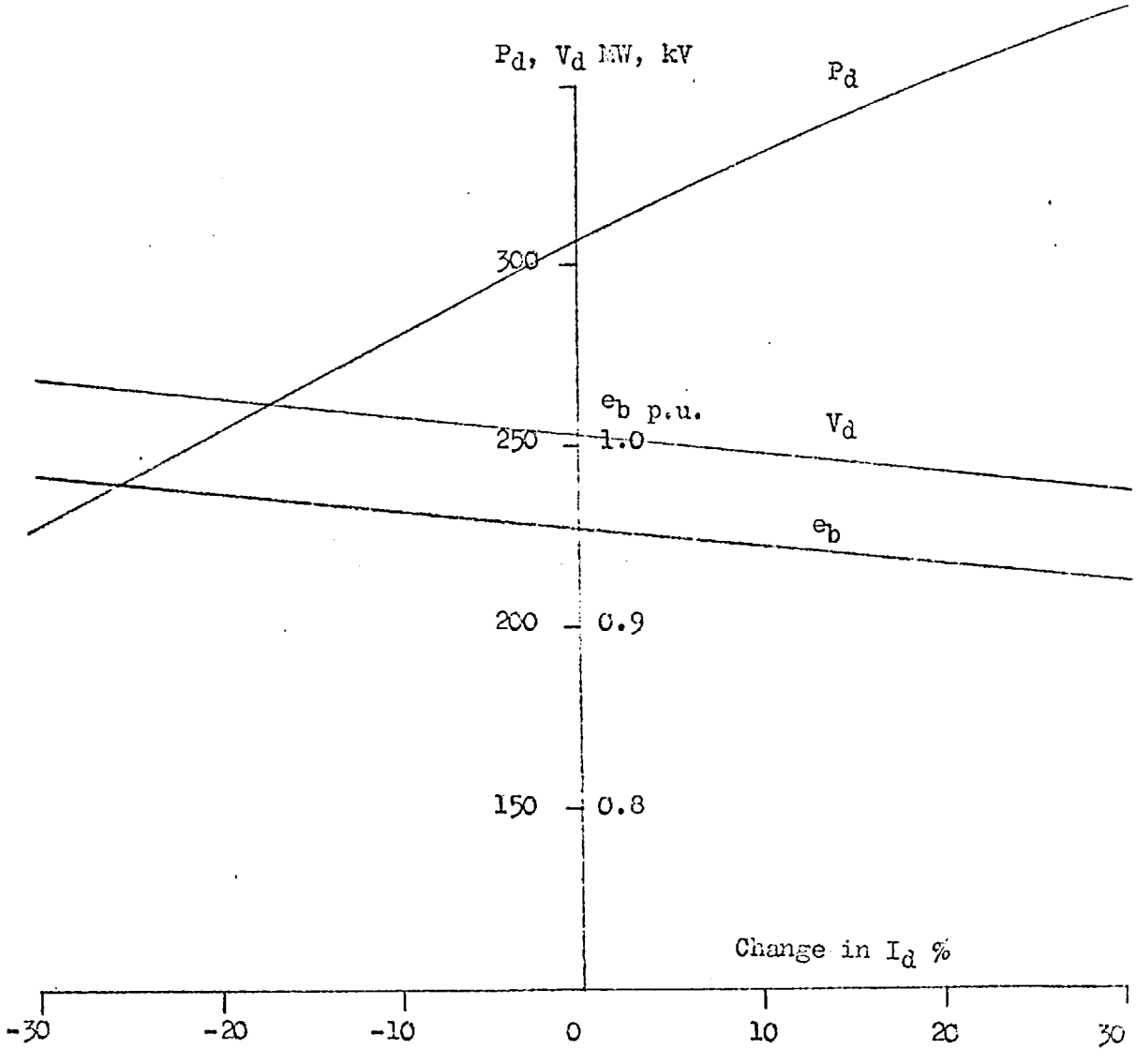

Fig. 3.6 Local disturbance : short circuit level changed from 3500 to 2000 MVA. INVERTER
Local a.c. load = 500 MW

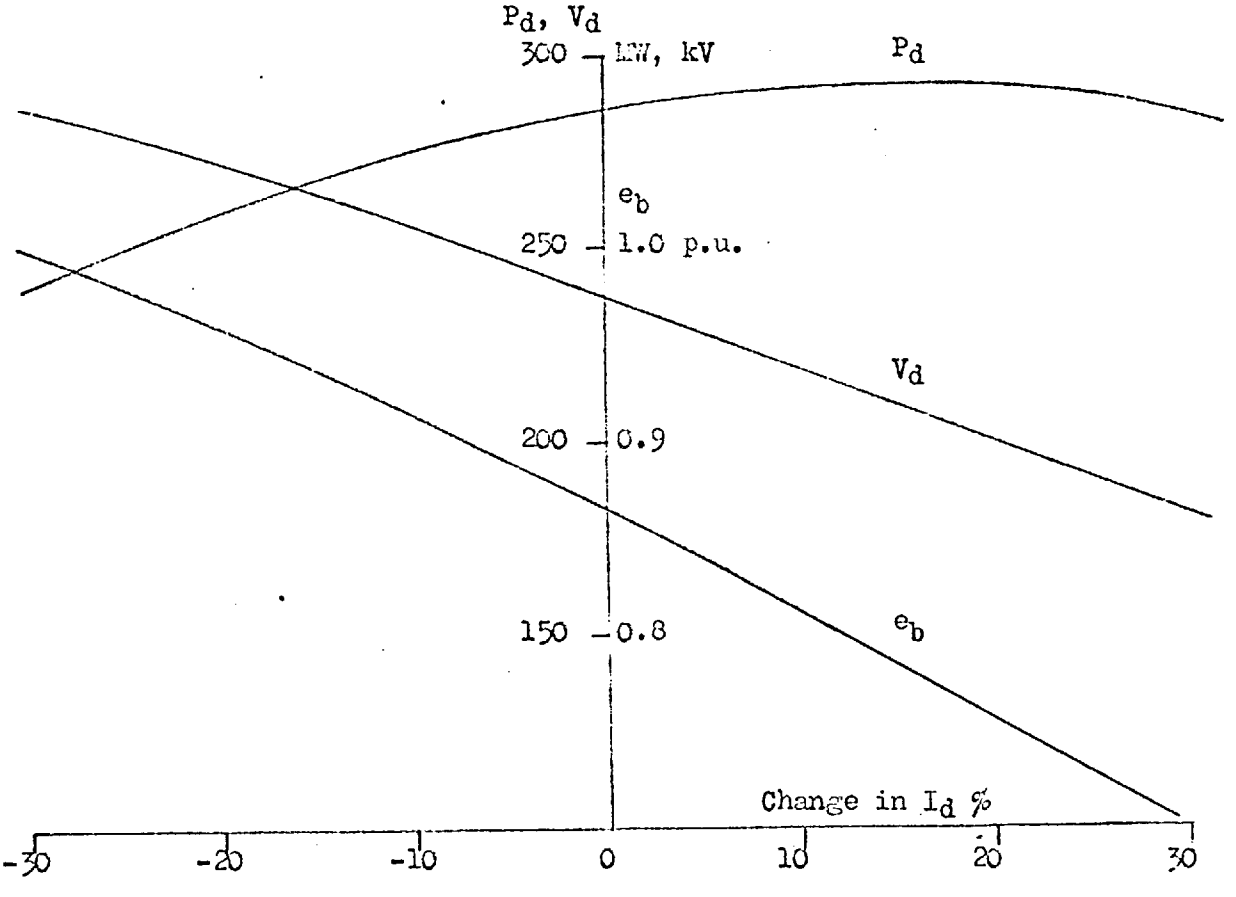

Fig. 3.7 Local disturbance : short circuit level changed from 2000 to 1000 MVA. RECTIFIER
Local a.c. load = 100 MW

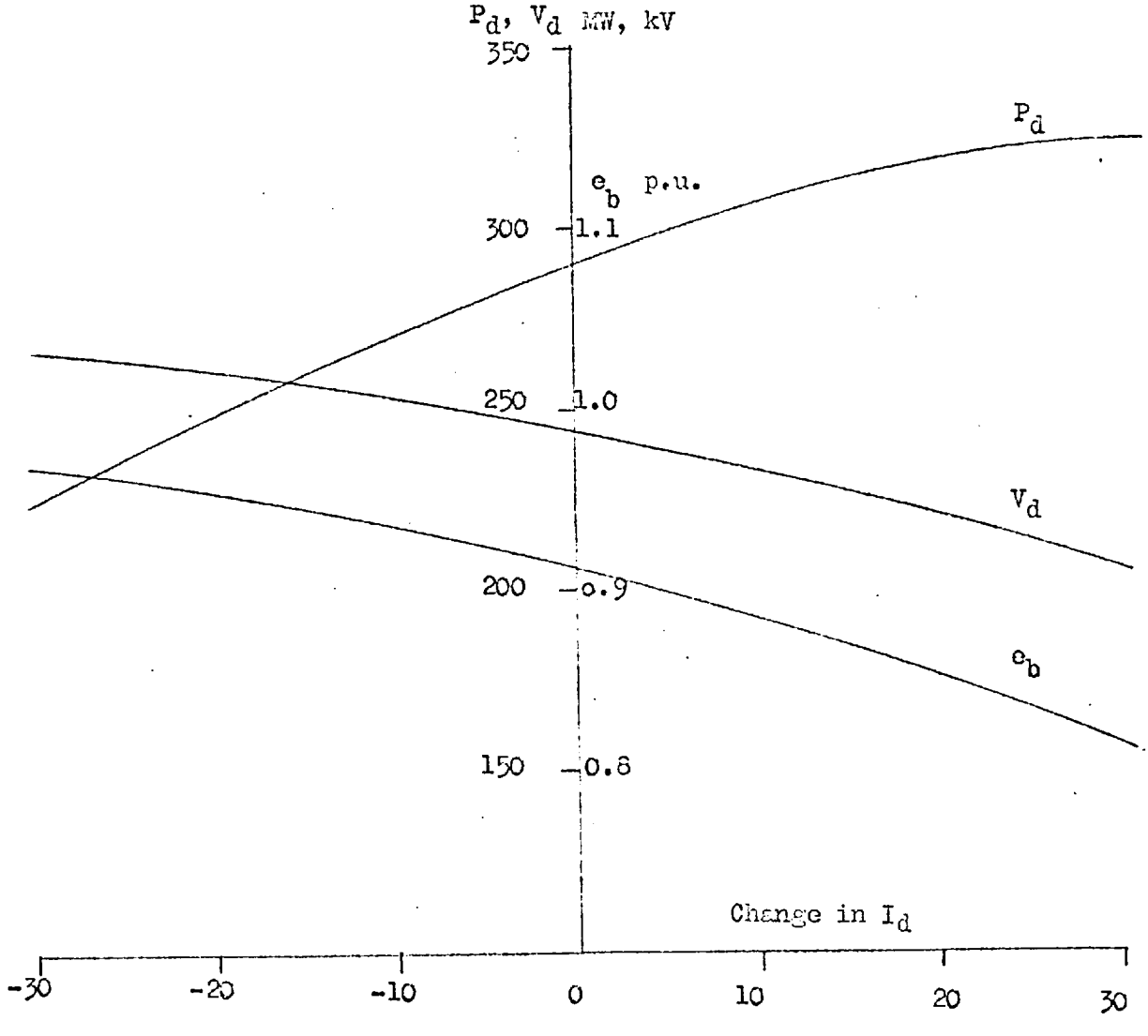

Fig. 3.8 Local disturbance: short circuit level changed from 2000 to 1000 MVA. INVERTER
Local a.c. load = 400 MW

Operation Mode	Change of short Circuit Level MVA	Local a.c. Load MW	Maximum d.c. Power Transfer MW	e_b p.u.	ΔId %
(A) Constant P & Q representation of local a.c. load					
Rectifier	3500/2000	300	Up to 320	0.89	+ 10
Inverter	"	500	Up to 320	0.935	+ 7
Rectifier	2000/1000	100	Up to 272	0.825	.0
"	"	"	267	0.90	-11.8*
Inverter	"	400	Up to 283	0.795	+ 15
"	"	"	257	0.90	- 11*
(B) Constant R & X representation of local a.c. load					
Rectifier	3500/2000	300	Up to 326	0.925	+ 4
Inverter	"	500	Up to 320	0.947	+ 5.5
Rectifier	2000/1000	100	Up to 292	0.778	+ 16
"	"	"	277	0.90	- 7.5*
Inverter	"	400	Up to 320	0.846	+ 22

Table 3.2a Local disturbances

e_b = converter busbar voltage

ΔId = change in direct current

* Marks correct current margin to keep $e_b \geq 0.90$ p.u.

Initial conditions shown in Table 3.2b

Operation Mode	Short Circuit Level MVA	Local a.c. Load MW	Tap h	Tap k	ℓ_b p.u.	α or γ	Vd kV	Id kA
Rectifier	3500	300	1.054	1.018	0.992	17°	266	1.203
Inverter	"	500	1.042	"	"	"	"	"
Rectifier	2000	100	1.069	"	"	"	"	"
Inverter	"	400	1.067	"	"	"	"	"

Table 3.2b Initial conditions before local disturbances

3.2.5 Remote disturbance

This disturbance was assumed to be a rise or fall in the direct voltage as a result of a fault in the a.c. or d.c. system at the remote end of the d.c. link and it was desired to determine the effect this had on the local end under consideration. The change in direct voltage v_d was assumed (e.g. 10% increase or decrease on the rated value) and it was necessary to find the corresponding firing angle by using Eq. 3.1 in the form:

$$\cos\alpha = \frac{1}{e_c}\left(v_d + \frac{\pi}{6} x_c i_d\right)$$

where the value of e_c was obtained as before by iteration to satisfy the boundary condition of $|e_s| = 1.0$ p.u. at the infinite busbar.

Both constant current and constant power control were studied and results are given in Fig. 3.9, 3.10, 3.11 and 3.12 which show only cases of reduced v_d as these are more likely and more onerous (causing margin cross). From these results the following conclusions are possible.

(a) Constant current control gives better voltage regulation than constant power control when the direct voltage at the remote end is reduced.

(b) Inverter operation produces higher voltage regulation when current margin is crossed.

3.2.6 Relationship between tap ratios of auto-transformer and converter transformer

Referring to Fig. 3.2 it is possible to develop a simple relationship between the tap ratios h and k of the two transformers. For a given set of p_d v_d and α the commutating voltage e_c and converter current i_v are fixed, and the following equations relate the various voltages and currents which are all referred to e_c

$$e_b = \frac{1}{k} e_c$$

$$\bar{i}_s = h\left[k\bar{i}_v + k\frac{p - jq}{e_c} + j\frac{1}{k} e_c (b_c + b_f)\right]$$

where the local a.c. load is represented as constant P and Q.

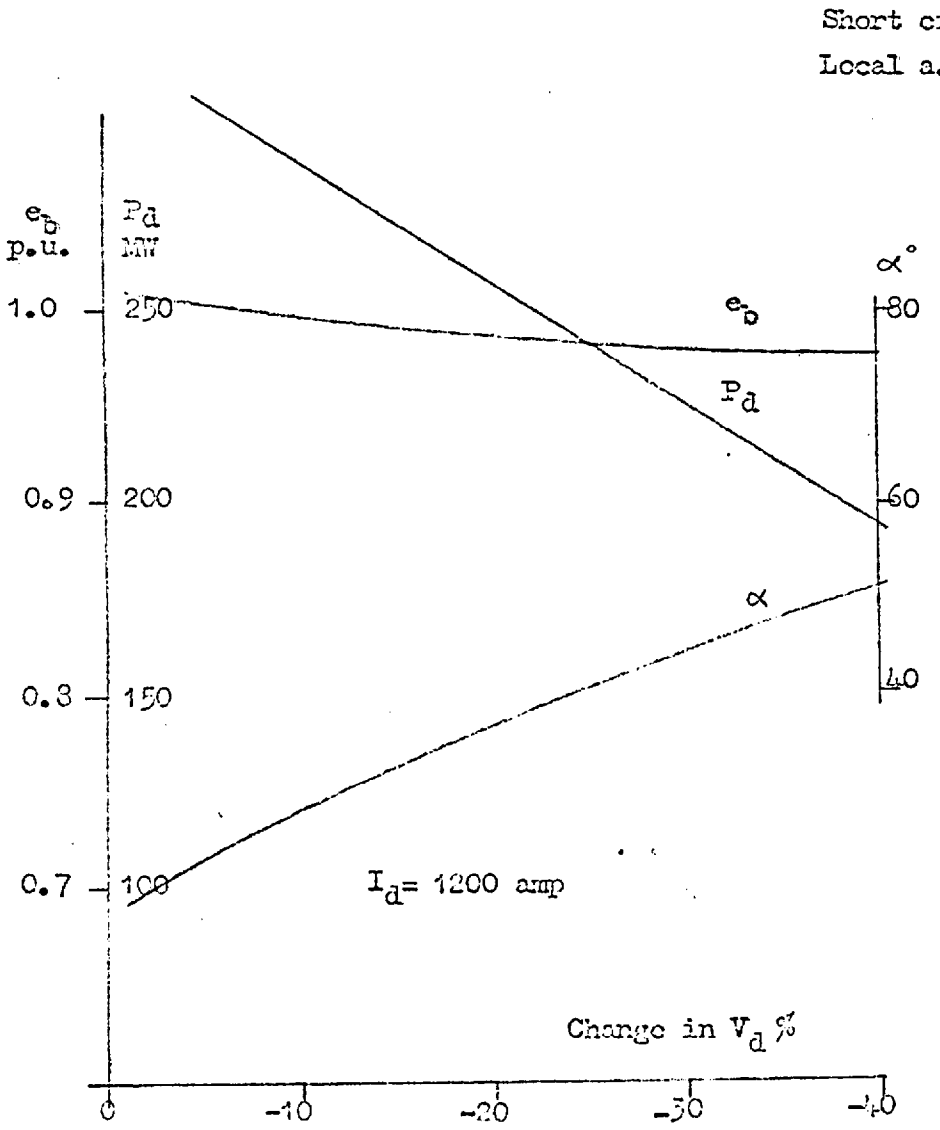

Fig. 3.9 Remote disturbances as reductions in d.c. link voltage. RECTIFIER END Constant current control.

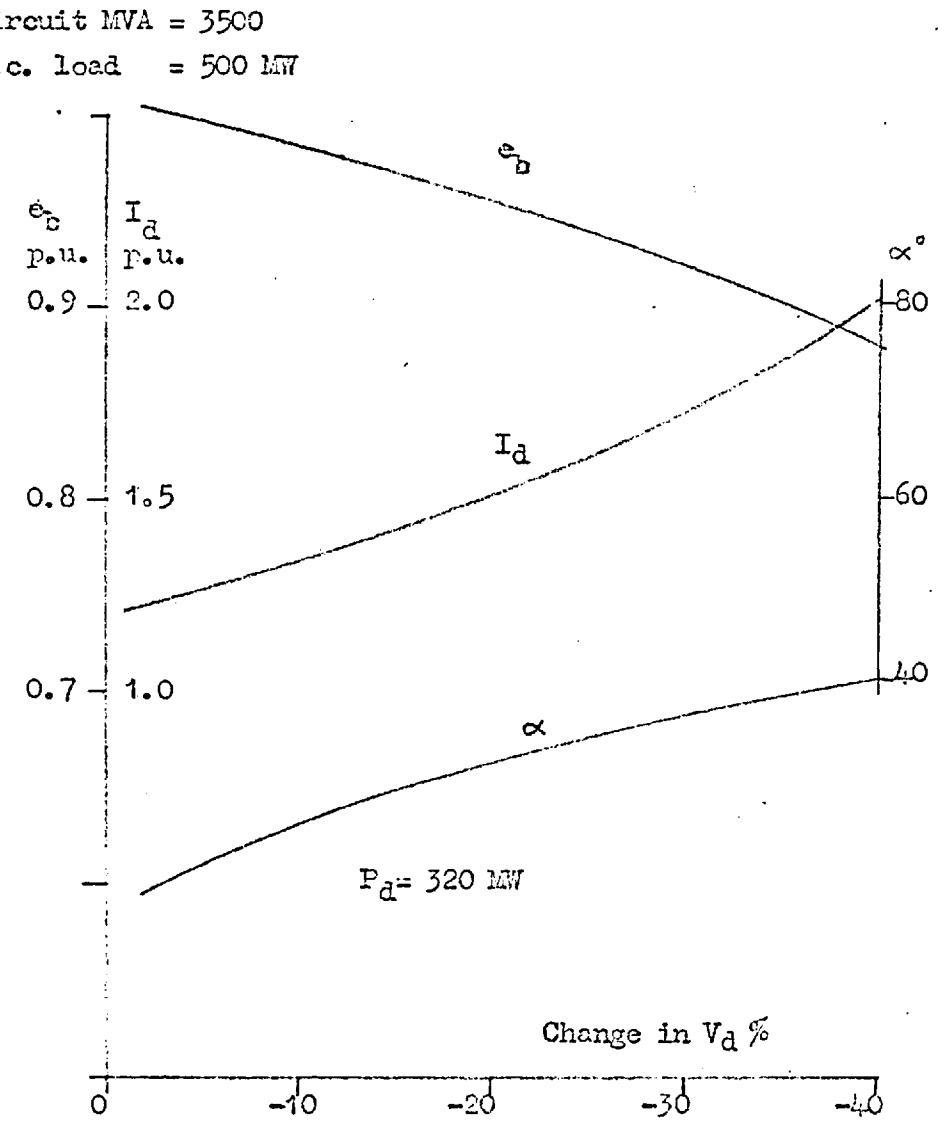

Fig. 3.10 Remote disturbances as reductions in d.c. link voltage. RECTIFIER END Constant power control.

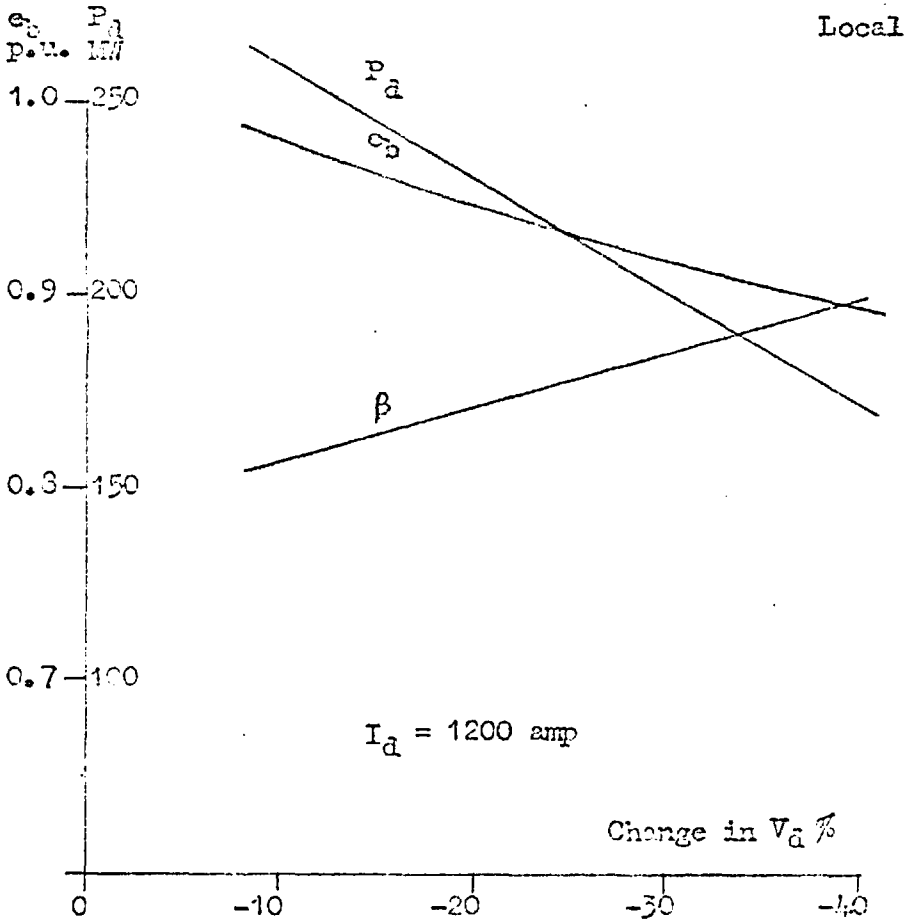

Fig. 3.11 Remote disturbances as reductions in d.c. link voltage. INVERTER END Constant current control.

Short circuit MVA = 1000
Local a.c. load = 50 MW

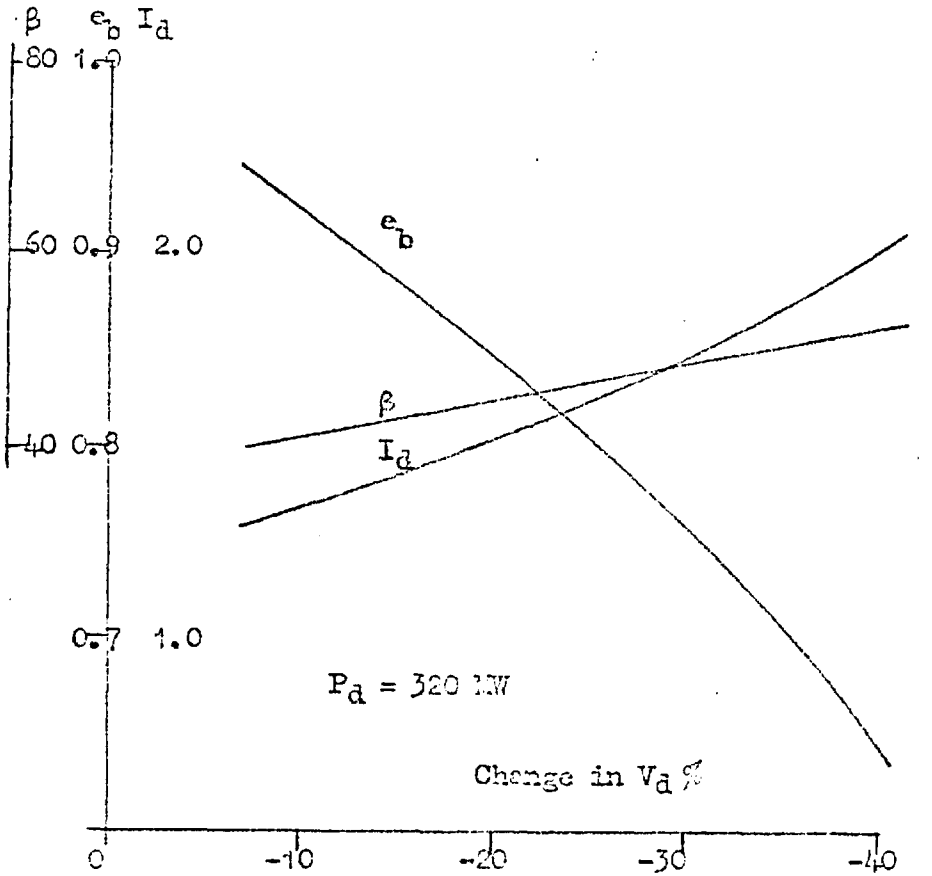

Fig. 3.12 Remote disturbances as reductions in d.c. link voltage. INVERTER END constant power control

$$\therefore \bar{e}_b' = \bar{e}_s - h\left(\bar{a}k + \bar{b}\,\frac{1}{k}\right)\bar{Z}_s = \frac{1}{h}\,e_b = \frac{1}{hk}\,e_c$$

where $\bar{a} = \bar{i}_v + \frac{1}{e_c}\,(p - jq)$

$\bar{b} = je_c\,(b_c + b_f)$

$$\therefore h^2\left(\bar{a}k^2 + \bar{b}\right)\bar{Z}_s - hk\bar{e}_s + \bar{e}_c = 0$$

and $$h = \frac{k\bar{e}_s \pm \left[k^2\bar{e}_s^2 - 4\left(\bar{a}k^2 + \bar{b}\right)\bar{Z}_s\bar{e}_s\right]^{\frac{1}{2}}}{2\left(\bar{a}k^2 + \bar{b}\right)\bar{Z}_s}$$

By taking the positive square root and the real part only of the R.H.S. the value of h for a given value of k can be obtained by iteration with $|e_s| = 1.0$ as the boundary condition. The general form of this relationship is shown in Fig. 3.13, with two different values of the system fault level. The value of this relationship is that by considering the extremes of expected system fault level, local a.c. load, direct power transfer and firing angle etc., it is possible to select matching ranges of tap ratio of the auto-transformer and converter transformer. For the scheme used in this study it was found that:

for auto transformer + 15%; - 10% and

for converter transformer + 15%; - 10%

are compatible, so that the actual range of the auto-transformer tap (± 15%) is slightly more than required to match that of the converter transformer. (+ 16%, - 10%).

It is interesting to note that, for high system ~~fault level~~ impedance, there is a minimum in the h - k curve. This is due to the increase in primary current when the transformer tap is raised to increase the voltage on the secondary side of the transformer. A point would be reached when the extra voltage drop in the system impedance due to the increased current depresses the voltage at the primary so much that there is no voltage increase on the secondary, and this point corresponds to the minimum in the curve.

Another relationship between the tap ratios concerns the power transfer across the d.c. link and is shown in Fig. 3.14. The d.c. power is plotted against auto-transformer tap ratio h with the converter transformer tap k and short circuit fault level as parameters. Lines of constant direct voltage v_d are also included. When the system fault level suddenly changes

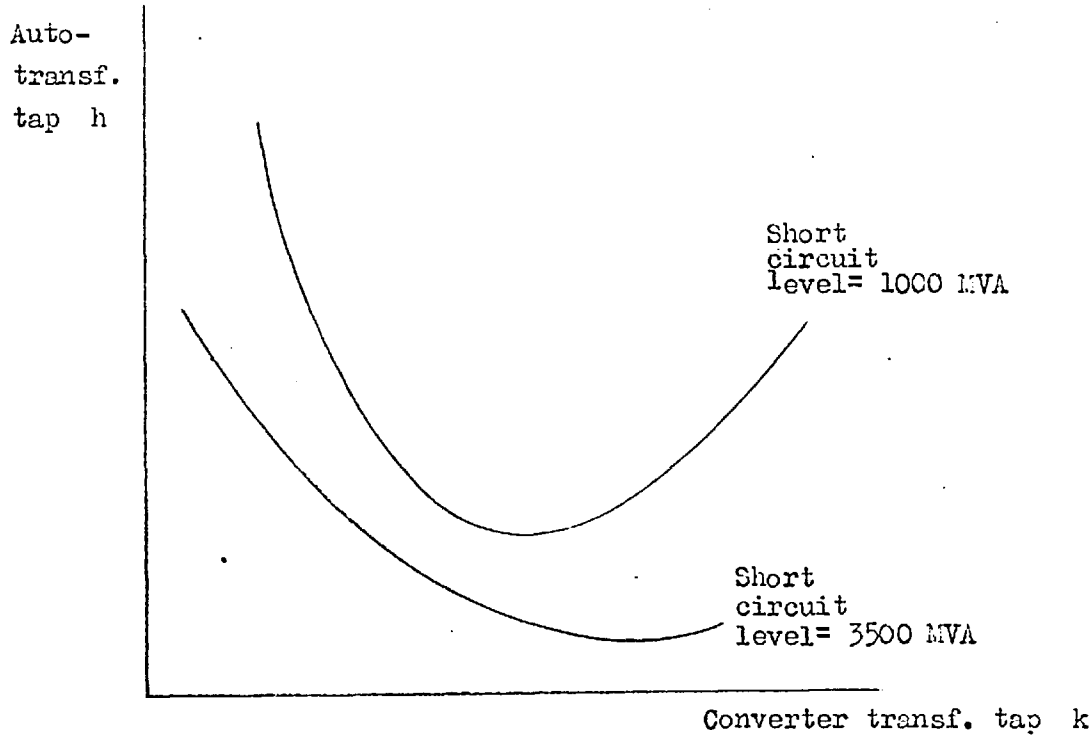

Fig. 3.13 Relatioship between auto- and converter tranformer taps.

Direct power transfer = 320 MW

Local a. c. load = 500 MW

Rectifier firing angle= 10 deg.

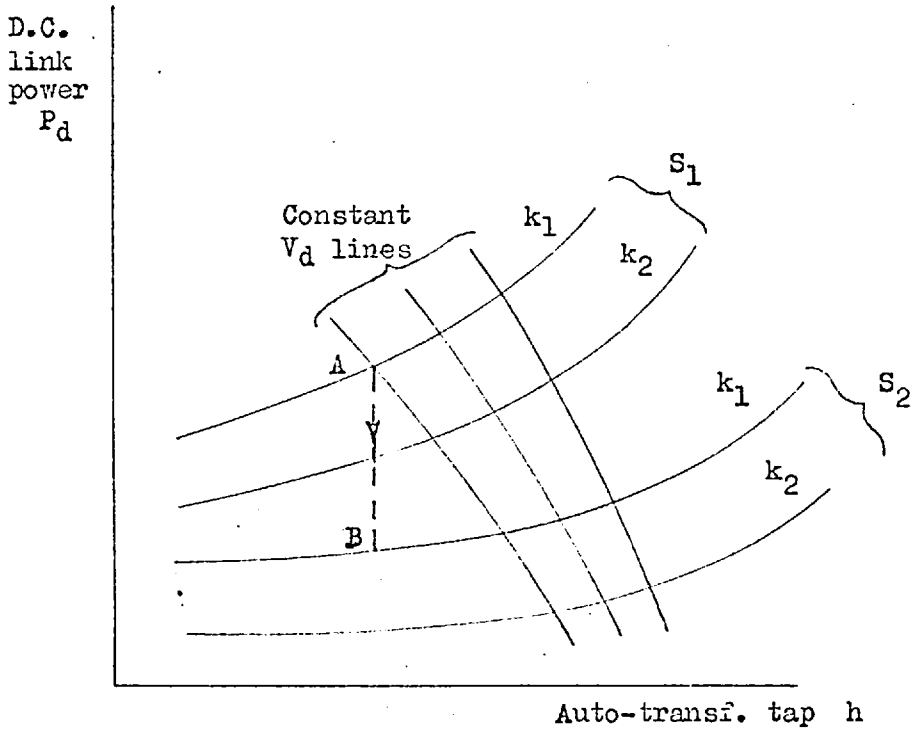

Fig. 3.14 D.C. link power as function of auto-transformer tap.

S_1, S_2 = short circuit levels

k_1, k_2 = converter tranformer taps

V_d = d.c. link voltage

from s_1 to s_2, the power transfer is reduced from A to B. To restore the power transfer either h or k or both may be adjusted according to the curves on the p_d - h plane.

3.3 Steady-state characteristics of a d.c. power transmission system

There are two main steady state characteristics of a d.c. transmission system: one is the direct voltage as a function of the direct current, and the other is the active and reactive power of the converters as functions of the a.c. system voltage. These characteristics have different forms for the rectifier and inverter, and depend on the methods of control of the d.c. link.

3.3.1 Converter voltage and current characteristics

Reider [23] had established some important rules for the steady-state stability of a d.c. link which can be summarised as follows:

(a) Operation of a d.c. link is stable for all conditions with one current controller at the rectifier,

(b) Operation with constant extinction angle control (compounding) only at the inverter is not stable, and

(c) Operation with both the controls together, viz. current control at the rectifier and constant extinction angle at the inverter, is stable.

The last principle of control is in fact adopted in all d.c. links in operation since it demands the minimum amount of reactive power at the inverter. In addition, the inverter characteristic is usually modified by a minimum current controller to prevent accidental shut-down of d.c. transmission as shown by Adamson and Hingorani.[40] The characteristics for a d.c. transmission system is therefore as shown in Fig. 3.15. Where Curves 1 and 2 form the rectifier characteristic and 3 and 4 the inverter characteristic. Curve 1 is known as the natural voltage characteristic of the rectifier where the firing angle α is constant at a usually small value

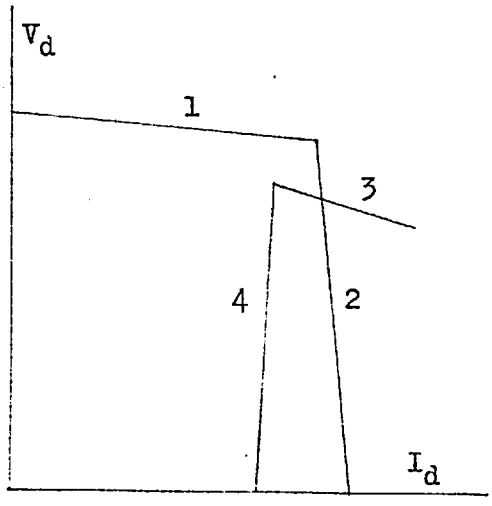

Fig. 3.15 Inverter on constant extinction angle control.

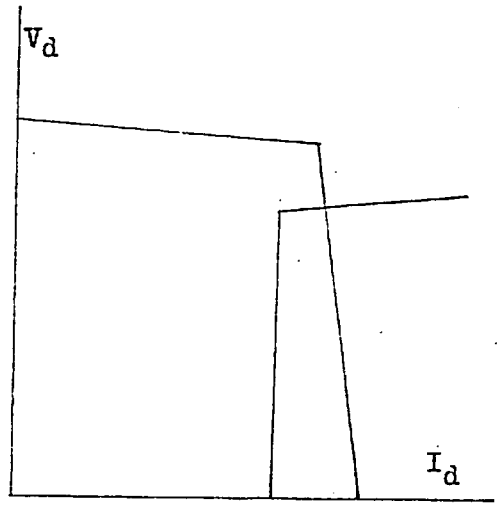

Fig. 3.16 Inverter on constant firing angle control.

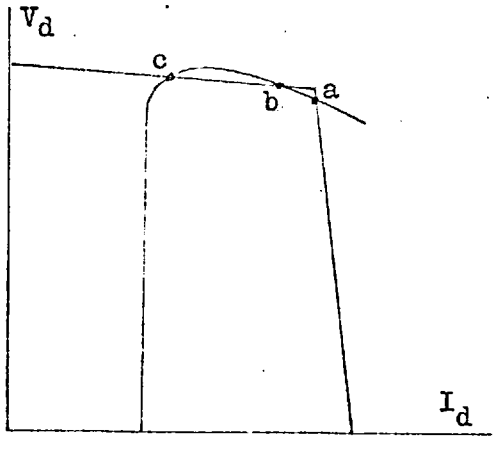

Fig. 3.17 Converter characteristic for possible power oscillations.

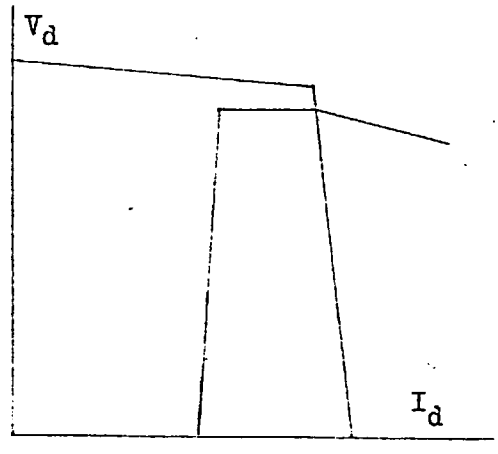

Fig. 3.18 Converter characteristic to avoid power oscillations.

(about 5°). Curve 3 is the constant extinction angle characteristic of the inverter with the extinction angle at a value of about 15°. Curve 2 is the constant current characteristic of the rectifier and is separated by a current margin from the minimum current characteristic, curve 4, of the inverter.

When the inverter is not compounded and operates with a constant firing angle with minimum current control the converter characteristics are as shown in Fig. 3.16. If however the extinction angle is maintained constant only within a certain range of conditions closed to the nominal conditions, then the inverter characteristic will be intermediate between the ideal constant extinction and constant firing angle characteristics as shown in Fig. 3.17. There are 3 distinct intersections at A, B and C between the two characteristics and there is a possibility of aperiodic power oscillations. The normal operating point is at A but a slight increase in rectifier voltage or a slight fall in inverter voltage would bring the operating point to B. However B is not a stable operating point because of its negative slope so that stable operation would be finally established at C. Here the rectifier operates at reduced active and reactive power so that the a.c. system voltage would rise and push the operating point back to A from where the whole process may begin once again, causing an aperiodic power oscillation in the d.c. transmission. To avoid this trouble the obvious way is to raise the taps of the converter transformers on the rectifier side to provide sufficient clearance between the rectifier natural voltage characteristic and the inverter characteristic, but the rectifier would be running at high firing angles and absorbs excessive reactive power. Alternatively the inverter characteristic may be modified to become more or less flat for currents less than the current order of the rectifier as shown in Fig.3.18.

Another possibility of power oscillations arises if the current margin is small so that the separation between the rectifier constant current characteristic and the inverter minimum current characteristic barely exists. A slight reduction in the rectifier voltage will cause a margin cross so that the rectifier now operates on the natural voltage characteristic with substantially the same current. The net result is a slight drop in the reactive power demanded by the rectifier, and therefore an increase in rectifier voltage which may be sufficient to restore the original operating point, i.e. with the rectifier on current control. The rectifier then operates at a higher firing angle thereby demanding more reactive power from the sending a.c. system and lowering the rectifier voltage once again, thus causing oscillations in power transmission. The same phenomenon may be brought on by a slight increase in inverter voltage. A margin cross again occurs with the inverter working at increased angle of advance β and demanding higher reactive power from the receiving a.c. system. The inverter voltage therefore drops and the current margin is re-crossed to restore the initial operating point. The inverter then operates with constant extinction angle control absorbing less reactive power. This gives the inverter voltage a chance to rise and cause another margin cross, again resulting in power oscillations.

The occurrence of power oscillations caused by insufficient current margin was observed in an actual test described in Section 3.5. To avoid such oscillations the normal practice is to use a current margin of about 10% of rated direct current.

3.3.2 Converter active and reactive power characteristics

Having discussed the steady-state control principle of the d.c. system it is now possible to derive qualitatively active and reactive power characteristics of the converters as functions of the a.c. system voltage. When the control is as shown in Fig. 3.15 the power characteristics for the rectifier and inverter take the form of Figs. 3.19 and 3.20. For the rectifier when the a.c. system voltage rises the active power increases only slightly, being limited by the constant current controller, while the reactive

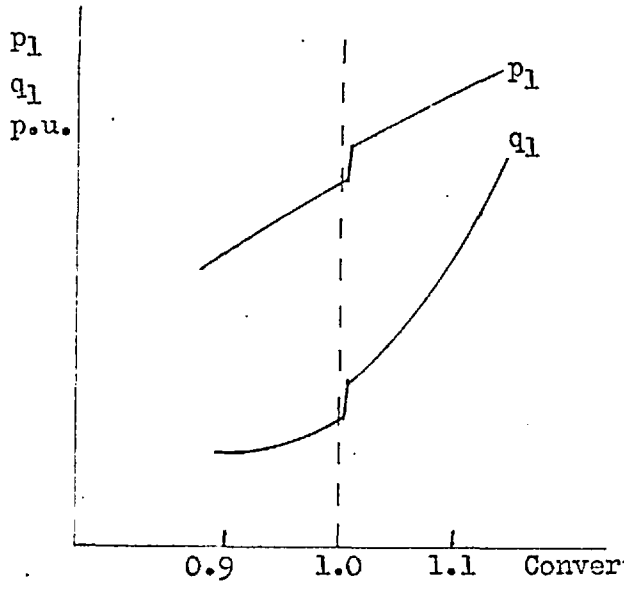

Fig. 3.19 Rectifier active & reactive power characteristics

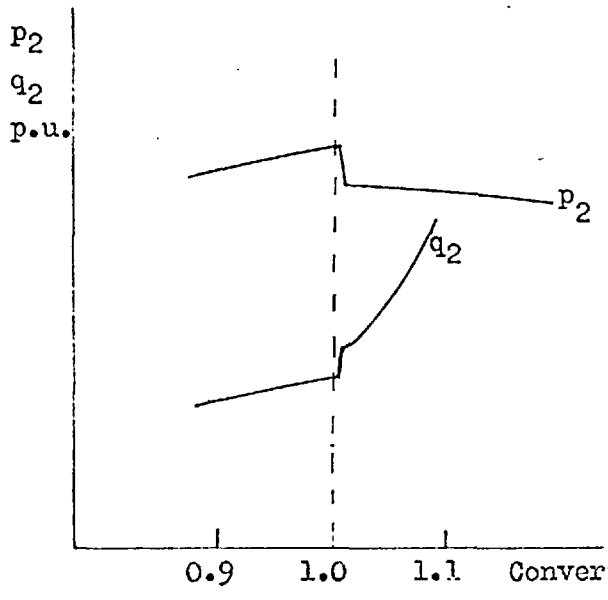

Fig. 3.20 Inverter active & reactive power characteristics

power increases more rapidly due to the high firing angles now required. When the a.c. system voltage of the rectifier drops sufficiently the current margin is crossed and there is a sudden but slight reduction of active and reactive power, after which the current is limited by the minimum current controller of the inverter. The reactive power of the rectifier for further reduction in a.c. system voltage decreases less than the active power because the commutation angle increases with decreasing a.c. voltage, although the firing angle is smaller. The net effect would be a lower power factor for the rectifier.

At the inverter end a rise in a.c. system voltage would cause a margin cross with the direct current limited by the minimum current control so that there is a sharp and slight reduction in active power and an increase in reactive power due to the increased firing angle. Thereafter the active power decreases slightly while the reactive power increases more rapidly with increasing a.c. voltage. When the a.c. voltage falls the direct current is maintained nearly constant by the rectifier so that both active and reactive power only decrease slightly.

Without the minimum current control at the inverter the flow of power across the d.c. link will cease if there is sufficient rise or fall of a.c. system voltage at the inverter or rectifier respectively. To the left of the dotted line on Fig. 3.19 the p and q curves will drop sharply to zero for the rectifier. On Fig. 3.20 the inverter characteristic will do likewise to the right of the dotted line.

3.4 Steady-state stability of d.c. transmission

Bower et al [41] had demonstrated the use of circle diagrams to analyse voltage stability of a d.c. link connected to a simple a.c. system represented as an infinite bus. By neglecting the resistive component of the system impedance the circle diagrams, shown in Fig. 3.21, can be described by the equation:

$$p + jq = (ve \quad \exp(-j\theta) - v^2) \exp\left(j\frac{\pi}{2}\right)$$

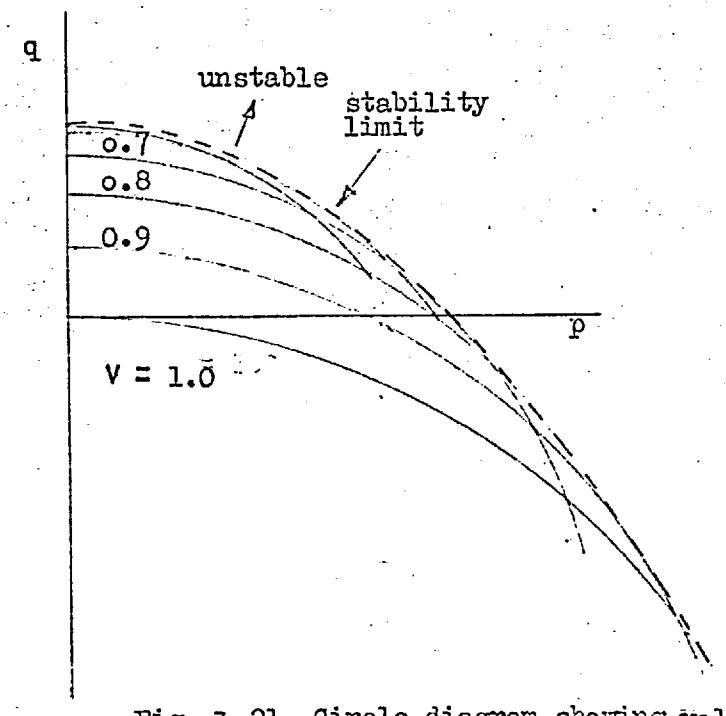

Fig. 3.21 Circle diagram showing voltage stability limit at receiving end.

where p and q are in per unit of the system short circuit fault level

e = sending end voltage in per unit = 1.0

v = receiving and voltage in per unit

θ = angle between e & v.

From this equation, it can be shown that

$$q = [(ve)^2 - p^2]^{\frac{1}{2}} - v^2$$

and the envelope of the circle diagrams marking the voltage stability limit is obtained by putting

$$\frac{\partial f}{\partial V} = 0$$

where $f(p,q,v) = [(ve)^2 - p^2]^{\frac{1}{2}} - v^2 - q = 0$

Hence, the envelope is given by the relation

$$q = \frac{1}{4}e^2 - \frac{1}{e^2}p^2$$

and this represents the maximum q for a given p.

By making use of this relationship and the p - q characteristics given in Section 3.3.2 the voltage stability limit of converter operation can be established.

3.5 Actual weak a.c. system tests with a d.c. link

Actual system tests with the cross-channel d.c. link were carried out to study the stability of the link when inverting into a weak a.c. system at Lydd, and also to investigate the effect of margin cross on system voltage (Reference 42). The system configuration was as shown in Fig. 3.22 and the short circuit fault level at the 275 kV terminals at Lydd was 730 MVA, which was 4.56 times the rated d.c. link power of 160 MW.

The results of the voltage stability study are summarised in Figs. 3.23 and 3.24 which are curves of d.c. link power and direct voltage against direct current. These show that voltage-wise the link was stable up to rated current. Voltage regulation was slightly higher when the inverter (Lydd) controlled the current as was expected from the higher reactive power absorption. When the link was on 6-pulse working, i.e. with one bridge blocked at each end, voltage regulation at Lydd was better than 12-pulse working because the primary windings of two converter windings were connected in parallel through the tertiary windings.

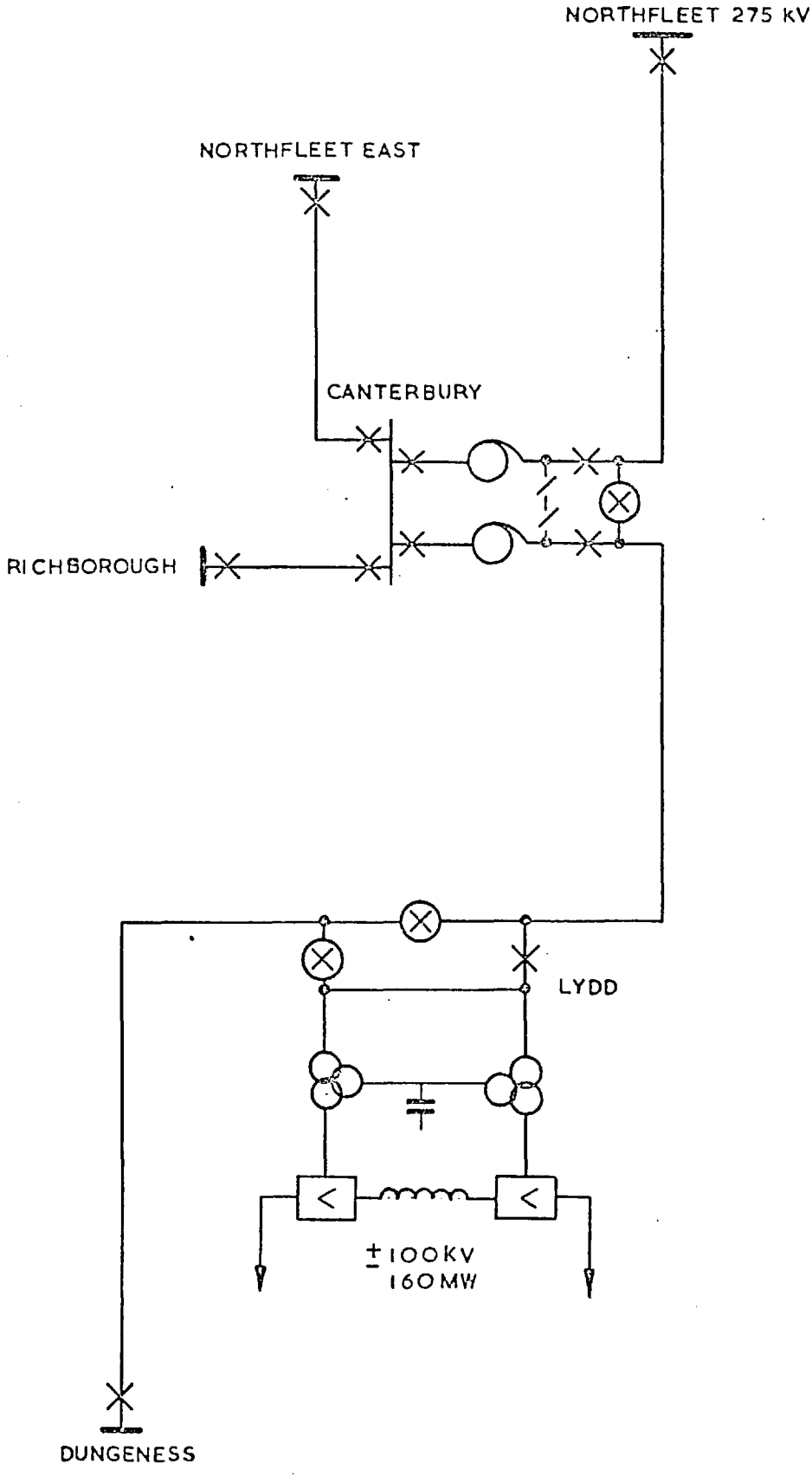

FIG 3.22 WEAK A.C. SYSTEM FOR LYDD TEST.

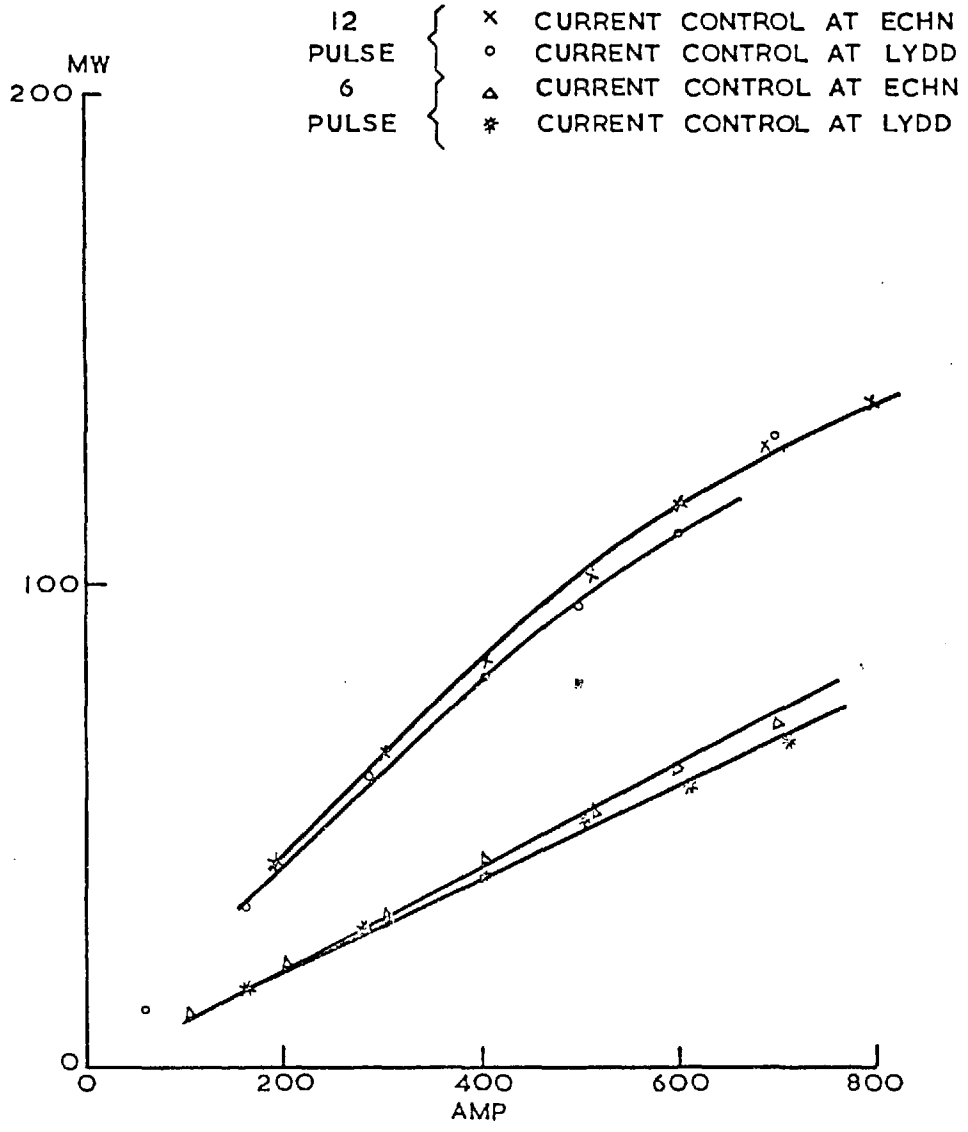

FIG 3.23 D.C. LINK POWER VS. DIRECT CURRENT.

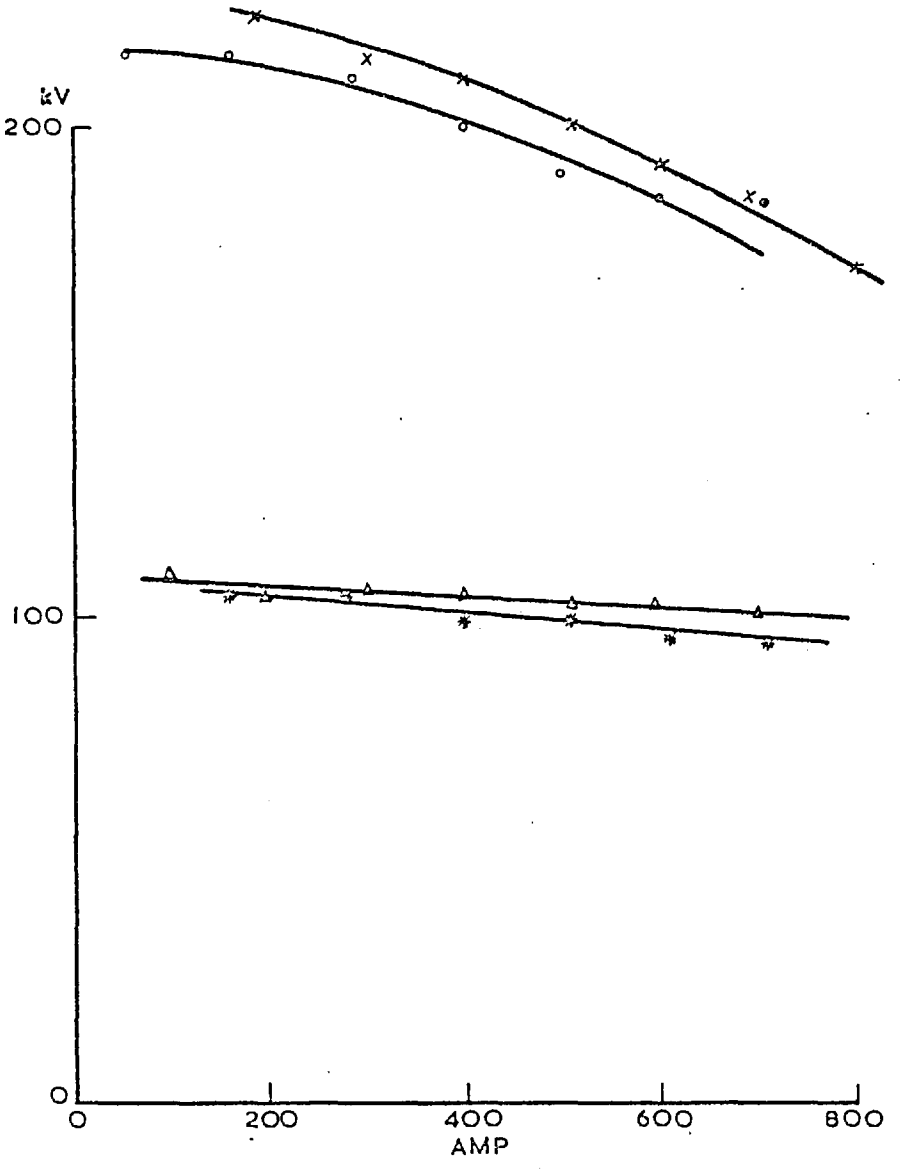

FIG 3.24 DIRECT VOLTAGE VS. DIRECT CURRENT.

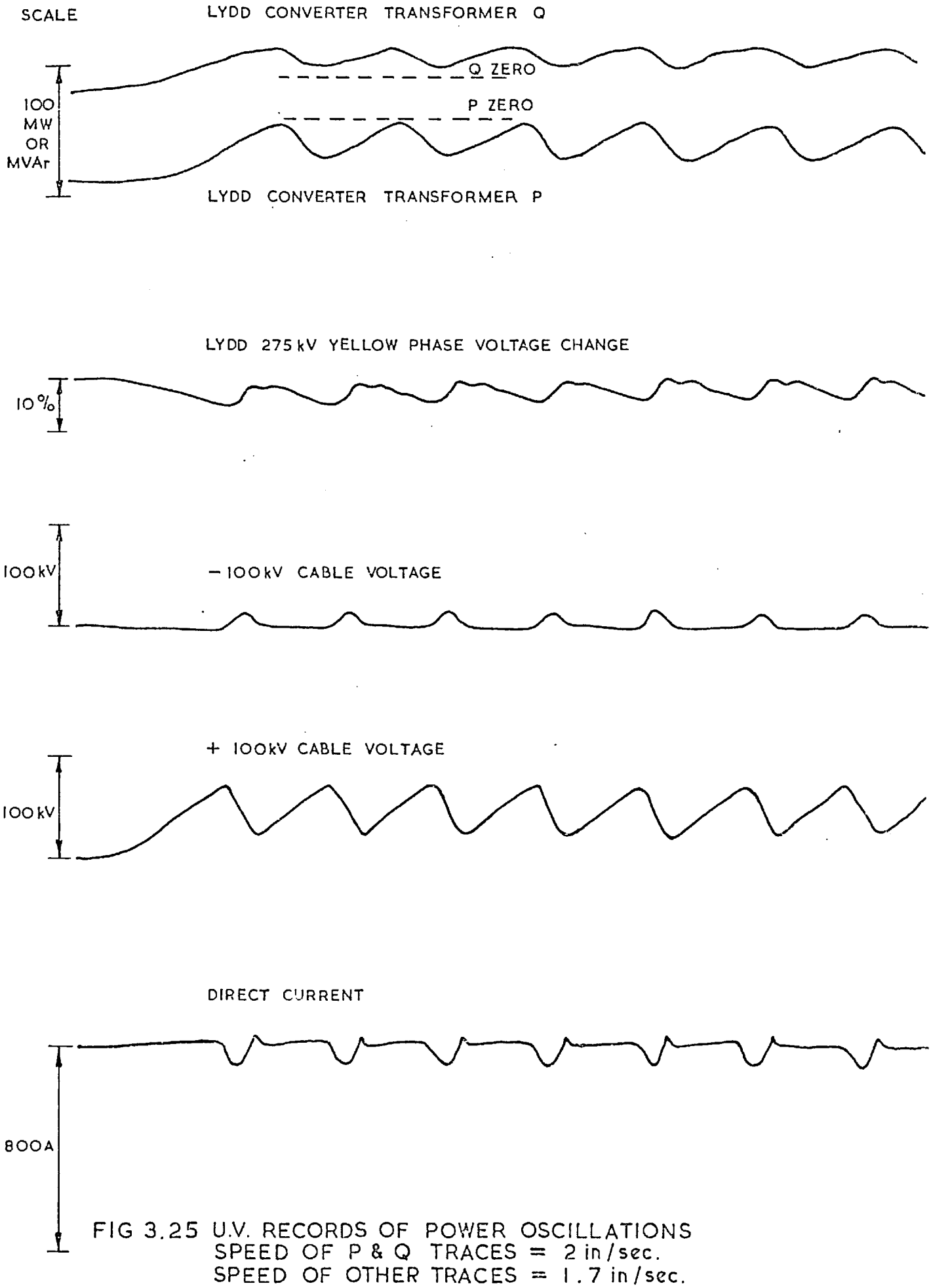

FIG 3.25 U.V. RECORDS OF POWER OSCILLATIONS
SPEED OF P & Q TRACES = 2 in/sec.
SPEED OF OTHER TRACES = 1.7 in/sec.

During these tests no harmonic instability occurred as evidenced by the absence of excessive harmonics in the voltage waveforms and no repeated commutation failures. This can be attributed to the effectiveness of the third harmonic filters at Lydd. It is of interest to note that in the Kingsnorth scheme no third harmonic filters would be installed, and harmonic instability is expected to be avoided by using the new phase-locked oscillator Control [43].

Two types of margin cross tests were performed: in the first the link was on 6-pulse working and margin cross was induced by tapping up the converter transformers at the inverter (Lydd) a few steps until the direct current suddenly dropped; in the second the link was on 12-pulse working and one valve group at the rectifier (Echinghen) was blocked to produce a fast margin cross. Therefore the two types may be regarded as simulating small and large disturbances on the inverters. The results were summarised in Table 3.3:

Direct Current (Amp)	Current Margin (Amp)	Direct Voltage of Positive Pole (kV)	Lydd Converter Transformer MW	Lydd Converter Transformer MVAr	Lydd 275 kV Voltage Change %	Canterbury 132 kV Voltage Change %
(a) Slow Margin Cross						
800(780)	20	101(101)	76(74)	-14(-14)	0	0
800(740)	60	97 (97)	74(70)	-16(-20)	+0.5	+0.125
800(670)	130	101(106)	76(66)	-14(-28)	+0.75	+0.375
400(360)	40	101(102)	38(36)	-42(-46)	+0.5	+0.05
400(300)	100	101(106)	36(30)	-42(-50)	+0.6	+0.15
400(260)	140	101(106)	38(28)	-44(-52)	+0.75	+0.25
(b) Fast Margin Cross						
800(780)	20	88 (97)	136(70)	42 (88)	-6	-2.25
800(720)	80	92 (97)	136(64)	40 (80)	-5	-1.62
800(660)	140	92(100)	140(64)	34 (64)	-2.2	-1

Figures in brackets are readings after margin cross.

- sign indicates leading MVAr

Table 3.3 Voltage change after margin cross

It is seen from this table that small current margins result in lower voltage fluctuation when the margin cross was caused by small disturbances. When margin cross was caused by a large disturbance a low current margin results in a large change in voltage. A high current margin, on the other hand, has the opposite effect, i.e. large voltage change for small disturbances and small voltage change for large disturbances. Therefore a medium current margin is most suitable, in this case about 100A. As explained in Section 3.3 a small current margin has the additional hazard that it may give rise to accidental power oscillations. This was in fact observed during one of the above tests when current margin was erroneously set to below 10A and the resulting power oscillations, which were illustrated in Fig. 3.25, were removed simply by increasing the current margin.

CHAPTER 4

A.C./D.C. LOAD FLOW PROGRAM

4.1 Purpose of program

The load flow problem is one of the major topics in power system analysis and its solution provides vital information for the design, planning and operation of power systems. The solution obtained is essentially one of steady-state, but a load flow program can be used to study the effects of faults by running it once before these are applied and once after. It also provides the initial conditions required for a transient study, and, if necessary, the end conditions after system faults that the regulation or control equipments have to aim at. The a.c./d.c. load flow program described in this chapter was developed with this object in mind.

4.2 Scope of program

The a.c./d.c. load flow program developed could handle an a.c./d.c. system with 30 buses and 5 single-pole two-terminal d.c. links or 3 single-pole links plus one double-pole link. Each link was provided with full conventional control, i.e. constant current, constant power, and constant extinction angle control. The tap changers on converter transformers were included as part of the d.c. link control and were used to keep the rectifier firing angles and d.c. line voltage within specified limits, and to ensure as far as possible constant current control at the rectifier.

In this program d.c. converters were treated as current injections as shown by Gavrilovri and Taylor[13] and Hingorani and Mountford[11]. In this way the d.c. system can be written as a subroutine and incorporated into most existing a.c. load flow programs with little modification required. In the present case an a.c. load flow program based on the method of Glimn and Stagg[14] was used. Harmonic filters, cable capacitance and static compensators were treated as pure capacitances at the fundamental frequency, while synchronous compensators were treated as sources of reactive power.

In order to study semi-steady-state conditions, i.e. those existing during the period after a disturbance but before operation of converter tap changers, the program was provided with facilities for locking the taps and blocking converter groups.

4.3 Survey of existing methods

The solution of load flow problem in an a.c./d.c. system can be obtained in three ways - by a model h.v.d.c. transmission system[45], by a network analyser[8,16,46], or by means of a digital computer[11,47,48]. Since the use of models and network analysers for a.c. load flow has been almost relegated to teaching and other special purposes, and digital computer programs for solving load flow problems are well established and a great deal of active research work is continuing in this direction, it is almost certainthat a.c./d.c. load flow problem will only be solved by means of digital computers. For this reason it is worthwhile to review the methods which have been published.

The first publication on this subject was by Horigome and Ito[48], in which the d.c. converters were represented by an equivalent circuit. The method was developed to deal only with the case of two independent a.c. systems connected by a single pole two-terminal d.c. link, and the sending end system was analysed separately from the receiving end system. The converters and the d.c. link were represented as equivalent voltage sources behind equivalent impedances. This method is sound in principle but appears to be difficult to apply. The main difficulty is that there were 11 variable such as firing angles, converter phase angles etc. to be found iteratively for each main iteration in the program. Inclusion of d.c. link control and converter transformer tap changer action would be possible but rather difficult.

The paper by Hingorani and Mountford[11] described a more straightforward method of including h.v.d.c. links in an a.c. load flow program. Only single-pole two-terminal links were described but more than one link may be present anywhere in the a.c. network. The converters were represented as equivalent current generators, and the value of the currents were calculated without iteration from the d.c. line voltage drop equation the converter characteristics and current orders, with the a.c. voltages at the converter terminals, available at each iteration. This method is therefore easily included as a subroutine in an a.c. load flow program which calculates voltages from nodal current injections. One feature of this paper was that conventional d.c. link controls were easily included in the form of converter voltage/current characteristics from which simple geometrical calculations were made during the iterative process to determine the voltage and current of a d.c. link as well as the firing angles of the converters. A tap changer subroutine was also given, but this was found to be incomplete and did not cover all possible operating conditions of a d.c. link. However, in view of the simplicity of the d.c. representation the method described in that paper was adopted in the present program, which extended the work of that paper by the inclusion of double-pole d.c. links of the Kingsnorth type and a new and more comprehensive tap changer subroutine capable of meeting all normal operating conditions of a d.c. link. These are described in detail in later sections.

Since Hingorani and Mountford's paper, Barker[47], and, more recently, Sato and Arrillaga[49] also described their a.c./d.c. load flow programs. The significant point is that both papers followed the method in Hingorani's paper to determine the direct current without iteration by using the a.c. voltages at each end of the d.c. link available from the last iteration. Both included a tertiary winding in the converter transformers to allow for the connection of filters or synchronous compensators, with the result that a secondary iterative cycle was required to determine the commutating voltage when the primary voltage of

the converter transformer was known from the main iterative cycle. Barker placed the converter transformer tap changer subroutine in an additional loop outside the main a.c. and d.c. iterative cycle on the ground that, if the a.c. system at either end of the d.c. link is weak compared with the d.c. link, this would avoid non-convergence. He also concluded that there was an insignificant difference between the rate of convergence of an a.c./d.c. system study (containing one d.c. link) and a corresponding study on the same system with the d.c. link replaced by an a.c. line. Sato and Arrillaga, by contrast, put the tap changer subroutine, which was, incidentally, an improved version over previous ones in that optimum tap positions were established by interpolation rather than by a stepwise procedure, in an inner loop together with the d.c. subroutine, and did not report any trouble with convergence. They concluded, quite contradictory to Barker, that substitution of an a.c. line by a d.c. link increased computing time by 30%. Because of these divergences in view these two aspects of the a.c./d.c. load flow problem seem worthy of attention in any future work.

In all papers a multi-bridge converter was treated as an equivalent single bridge fed by one converter transformer. This is based on the assumption that the transformers of a multi-bridge converter are normally on the same tap and tap-changes together.

4.4 Per unit system

The per unit system of Gavrilovri and Taylor[13] quoted in Chapter 2 was adopted in the present program. This per unit system is based on the number of bridges in a converter, and in order to simulate the blocking of one or more bridges at a converter, the converter voltage equation must be multiplied by the ratio of the number of bridges remaining in service at the converter to the original number of bridges used to define the per unit base. These numbers are represented by the symbols N' and N respectively in the following list of symbols.

4.4.1 List of symbols

E_{cb}	A.C. side base voltage r.m.s. line, kV
P_{cb}	" " " MVA
I_{cb}	" " " current
Z_{cb}	" " " impedance
E_{db}	D.C. " " voltage, kV
P_{db}	" " " MVA
I_{db}	" " " current
Z_{db}	" " " resistance
M_t	Rating of 1 converter transformer, MVA
E_p	Converter transformer primary voltage, r.m.s. line, kV
E_s	" " secondary " " " "
N	Rated number of bridges in converter group
N'	Actual " " " " " " in service
X_t	Converter transformer reactance, ohms/phase
R_t	" " resistance, " "
R_ℓ	D.C. line loop resistance, ohms
A	Equivalent resistance of converter characteristic slope, ohms
V_d	Direct voltage
I_d	Direct current
I_{ds}	Current order
I_{dm}	Current margin
V_o	Converter open circuit terminal voltage
n	Converter transformer tap ratio
n_ℓ	Bottom tap position
n_h	Top tap position
n_s	Tap step
α	Valve firing angle
α_o	Minimum value of
α_ℓ	Minimum for normal operation
α_h	Maximum " " "
γ	Extinction angle

4.5 A.C. and D.C. system equations

4.5.1 D.C. System Equations

Hingorani's paper[11] on a.c./d.c. load flow showed an elegant and simple way to describe in full the conventional d.c. converter $V_d - I_d$ characteristic with its usual constant current and constant extinction angle controls. The rectifier simplified $V_d - I_d$ characteristic of the rectifier consists simply of portions of three straight lines whose equations are easily derived as shown in Fig. 4.1, that of the inverter is similar but is drawn upside down on the $V_d - I_d$ plane because of the reversed polarity of inverter voltage (Fig. 4.2). The operating point of the d.c. transmission is given by the intersection of the rectifier and inverter characteristics.

The current order I_{ds} is measured from the corner between the constant current control and constant extinction angle control characteristics for both rectifier and inverter. With simplified converter characteristics this is satisfactory, but actual characteristics may be more complicated as shown by Ainsworth and Martin[50] and reproduced in Fig. 4.3 and it would be more convenient to reckon the current order at the rectifier from the corner between the natural voltage and constant current characteristics and similarly at the inverter using the constant current and c.e.a. characteristics. In this way the current orders I_{ds1} and I_{ds2} fix one part of the converter characteristic, and I'_{ds1} and I'_{ds2} the other.

Adopting Hingorani's notation, the following equations apply:-

(a) Current control at rectifier:-

$$V_{d1} = N'\left[n_1 V_{o1} \cos \alpha_o - \left\{\frac{3X_{t1}}{\pi} + 2R_{t1}\right\} I_d + A_1(I_d - I_{ds1})\right] - \tfrac{1}{2}R_\ell I_d \qquad (4.1)$$

$$V_{d2} = N'\left[n_2 V_{o2} \cos \gamma + \left\{\frac{3X_{t2}}{\pi} + 2R_{t2}\right\} I_d\right] + \tfrac{1}{2} R_\ell I_d \qquad (4.2)$$

(b) Current control at inverter:-

$$V'_{d1} = N'\left[n_1 V_{o1} \cos \alpha_o - \left\{\frac{3X_{t1}}{\pi} + 2R_{t1}\right\} I_d\right] - \tfrac{1}{2}R_\ell I_d \qquad (4.3)$$

$$V'_{d2} = N'\left[n_2 V_{o2} \cos \gamma + \left\{\frac{3X_{t2}}{\pi} + 2R_{t2}\right\} I_d + A_2(I_d - I_{ds2})\right] + \tfrac{1}{2}R_\ell I_d \qquad (4.4)$$

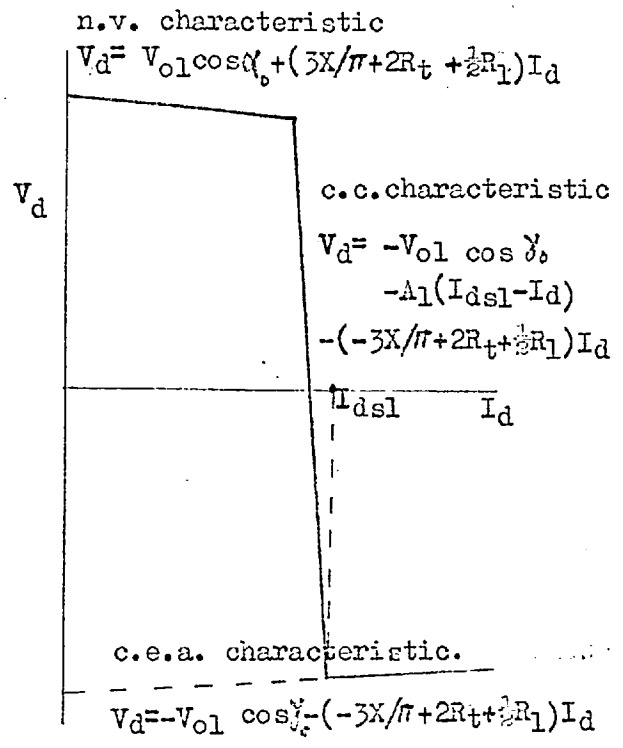

Fig. 4.1 One converter characteristic

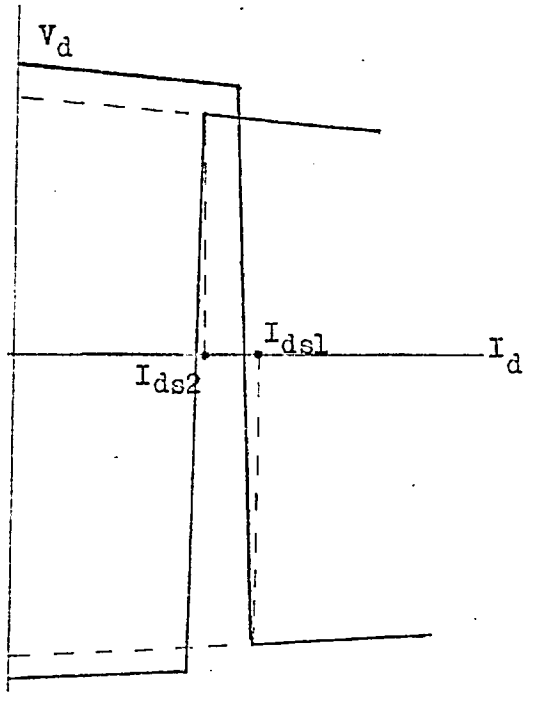

Fig. 4.2 Two converter compound characteristic

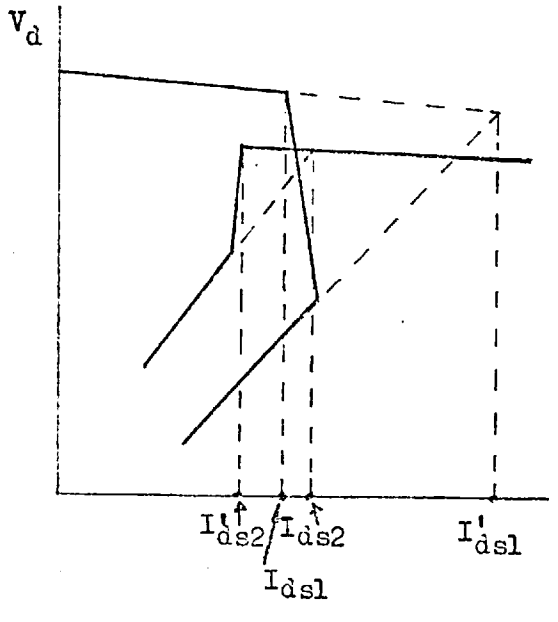

Fig. 4.3 Method of describing more complicated characteristics

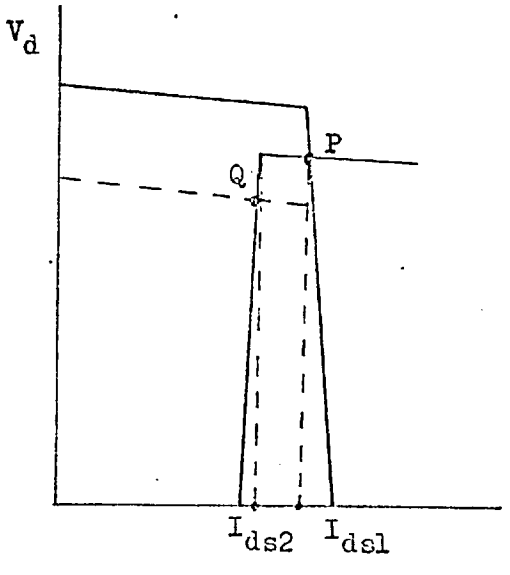

Fig. 4.4 Characteristics showing current control at rectifier or inverter.

In these equations A_1 and A_2 are signed, i.e. they are positive or negative according to the slope of the characteristic.

To determine I_d use the equation

$$V_{d1} = V_{d2} \tag{4.5}$$

to obtain

$$I_d = \frac{n_2 V_{02} \cos\gamma - n_1 V_{01} \cos\alpha_o + A_1 I_{ds1}}{A_1 - \left(\frac{3X_{t1}}{\pi} + 2R_{t1}\right) - \left(-\frac{3X_{t2}}{\pi} + 2R_{t2}\right) - \frac{R_\ell}{N'}} \tag{4.6}$$

To check whether the original assumption that the rectifier is on constant current is correct calculate the voltage on the natural voltage characteristic V_{d1}' from Eq. 4.3. If $V_{d1}' \geq V_{d1}$ the assumption is true and I_d is correct. If $V_{d1}' < V_{d1}$ the inverter is on constant current control and I_d ought to be found by using the equation

$$V_{d1}' = V_{d2}' \tag{4.7}$$

which gives

$$I_d = \frac{n_1 V_{01} \cos\alpha_o - n_2 V_{02} \cos\gamma + A_2 I_{ds2}}{A_2 - \left(\frac{3X_{t1}}{\pi} + 2R_{t1}\right) + \left(-\frac{3X_{t2}}{\pi} + 2R_{t2}\right) + \frac{R_\ell}{N'}} \tag{4.8}$$

A conventional converter characteristic is shown in Fig. 4.4 from which it can be seen that if the rectifier is on constant current control, the operating point is at P and $I_d > I_{ds1}$. If current control is at the inverter with operating point at Q, then $I_d < I_{ds2}$. Therefore a check can be made to see if a proper operating point is obtained.

Once I_d is known, the magnitude of the converter currents can be obtained,

$$\left|I_1\right| = N'n_1 \frac{\sqrt{6}}{\pi} I_d \tag{4.9}$$

$$\left|I_2\right| = N'n_2 \frac{\sqrt{6}}{\pi} I_d \tag{4.10}$$

The equivalent terminal voltage at the converters are given by

$$V_{dl1} = V_{d1} + N(2R_{t1})\, I_d + \tfrac{1}{2}R_\ell I_d \tag{4.11}$$

$$V_{d22} = V_{d2} + N(2R_{t2})\, I_d + \tfrac{1}{2}R_\ell I_d \tag{4.12}$$

if rectifier is on constant current control; or

$$V_{dll} = V'_{dl} + N(2R_{tl})\, I_d + \tfrac{1}{2}R\, I_d \tag{4.13}$$

$$V_{d22} = V'_{d2} + N(2R_{t2})\, I_d + \tfrac{1}{2}R\, I_d \tag{4.14}$$

if inverter is on constant current control.

The power factors of the converter currents with respect to the converter bus voltages are obtained from the approximate equations:-

$$V_{dll} = Nn_1\, V_{01} \cos\phi_1 \tag{4.15}$$

$$V_{d22} = Nn_2\, V_{02} \cos\phi_2 \tag{4.16}$$

The converter currents are related to the reference phasor through the convention shown in Fig. 4.5.

$$\bar{I}_1 = |I_1| \left[\cos(\phi_1 - \theta_1) - j \sin(\phi_1 - \theta_1)\right] \tag{4.17}$$

$$\bar{I}_2 = |I_2| \left[\cos(\phi_2 - \theta_2) - j \sin(\phi_2 - \theta_2)\right] \tag{4.18}$$

The equations in this section can be written in per unit form as:

$$v_{dl} = \frac{N'}{N}\left[n_1\, e_1 \cos\alpha_o - \left(\frac{\Pi}{6} x_{tl} + \frac{\Pi^2}{9} r_{tl}\right) i_d - Na_{dl}(i_d - i_{dsl})\right] - \tfrac{1}{2} r_\ell\, i_d \tag{4.19}$$

$$v_{d2} = \frac{N'}{N}\left[n_2\, e_2 \cos\gamma + \left(-\frac{\Pi}{6} x_{t2} + \frac{\Pi^2}{9} r_{t2}\right) i_d\right] + \tfrac{1}{2} r_\ell\, i_d \tag{4.20}$$

$$v'_{dl} = \frac{N'}{N}\left[n_1\, e_1 \cos\alpha_o - \left(\frac{\Pi}{6} x \quad + \frac{\Pi^2}{9} r_{tl}\right) i_d\right] - \tfrac{1}{2} r_\ell\, i_d \tag{4.21}$$

$$v'_{d2} = \frac{N'}{N}\left[n_2\, e_2 \cos\gamma + \left(-\frac{\Pi}{6} x_{t2} + \frac{\Pi^2}{9} r_{t2}\right) i_d + Na_{d2}(i_d - i_{ds2})\right] + \tfrac{1}{2} r_\ell\, i_d \tag{4.22}$$

$$i_d = \frac{n_2\, e_2 \cos\gamma - n_1\, e_1 \cos\alpha_o + Na_{dl}\, i_{dsl}}{Na_{dl} - \left(\frac{\Pi}{6} x_{tl} + \frac{\Pi^2}{9} r_{tl}\right) - \left(-\frac{\Pi}{6} x_{t2} + \frac{\Pi^2}{9} r_{t2}\right) - \frac{N}{N'} r_\ell} \tag{4.23}$$

or

$$i_d = \frac{n_1\, e_1 \cos\alpha_o - n_2\, e_2 \cos\gamma + Na_{ds2}}{Na_{d2} + \left(\frac{\Pi}{6} x_{tl} + \frac{\Pi^2}{9} r_{tl}\right) + \left(-\frac{\Pi}{6} x_{t2} + \frac{\Pi^2}{9} r_{t2}\right) + \frac{N}{N'} r_\ell} \tag{4.24}$$

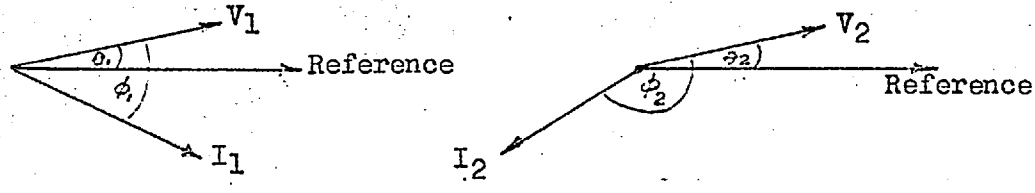

(a) Rectifier (b) Inverter

Fig. 4.5 Converter current phase angle

$$\left|i_1\right| = \frac{N'}{N} n_1 i_d \tag{4.25}$$

$$\left|i_2\right| \quad \frac{N'}{N} n_2 i_d \tag{4.26}$$

where

$$x_t = \frac{M_t}{E_p^2} X_t$$

$$r_t = \frac{M_t}{E_p^2} R_t$$

$$r_\ell = \frac{R_\ell}{Z_{db}}$$

$$a_d = \frac{A}{Z_{db}}$$

4.5.2 A.C. System Equations

Glimm and Stagg[44] uses a general equation of the form

$$E_p = \frac{\frac{P_p - jQ_p}{E_p^*} + \sum_q Y^{pq} E_q}{\sum_q Y^{pq}} \tag{4.27}$$

to calculate the voltage at node p, and q are all the other nodes.

The sign convention for P and Q is that power leaving a node is negative, and lagging reactive power is positive. Coupled with the sign convention for the converter current on the a.c. side the above equation was modified to

$$E_p = \frac{\frac{P_p - jQ_p}{E_p^*} + \sum_q Y^{pq} E_q + \bar{I}_d}{\sum_q Y^{pq}} \tag{4.28}$$

for a d.c. node where $\bar{I}_d$ is the converter current in complex form.

4.5.3 Organisation of Program

During each iteration cycle in the a.c. load flow program a node was checked to see if it was one terminal of a d.c. link. If it was then the most recent voltages at this node and the node at the other end of the

d.c. link were used in the main d.c. subroutine. A rectifier node was distinguished from an inverter by the higher current order assigned to it.

The organisation of the program is presented in Fig. 4.6.

4.6 Converter Transformer Tap Changer Subroutine

4.6.1 General Description

The tap changers of converter transformers form an integral part of the control of d.c. transmission. In normal operation the rectifier is on constant current control and its firing angles are regulated by the tap changers to within certain limits. The direct voltage on the d.c. line is maintained to a certain limit by the tap changers at the inverter which is on constant extinction angle control. The reference point for voltage regulation purpose is usually the mid-point of the d.c. line.

In the event of excessive drop in rectifier bus voltage or blocking of one rectifier bridge, the current margin of the converter characteristics is crossed. The inverter is now on constant current control and the rectifier controls the d.c. line voltage with firing angle α at α_0, i.e. on the natural voltage characteristic. This is not a normal mode of operation and causes high reactive power consumption at the inverter. For normal operation, therefore, the tap changers at both the rectifier and inverter ends should co-operate to maintain constant current control at the rectifier.

In this subroutine whenever the inverter was on current control the tap changer at the rectifier would step up to raise the natural voltage characteristic and tried to regain current control at the rectifier. Of course the tap changer was limited by the top tap position and in some cases it was inevitable that the inverter would have current control. Therefore this subroutine was divided into two sections, one for the case of current control at the rectifier, the other at the inverter.

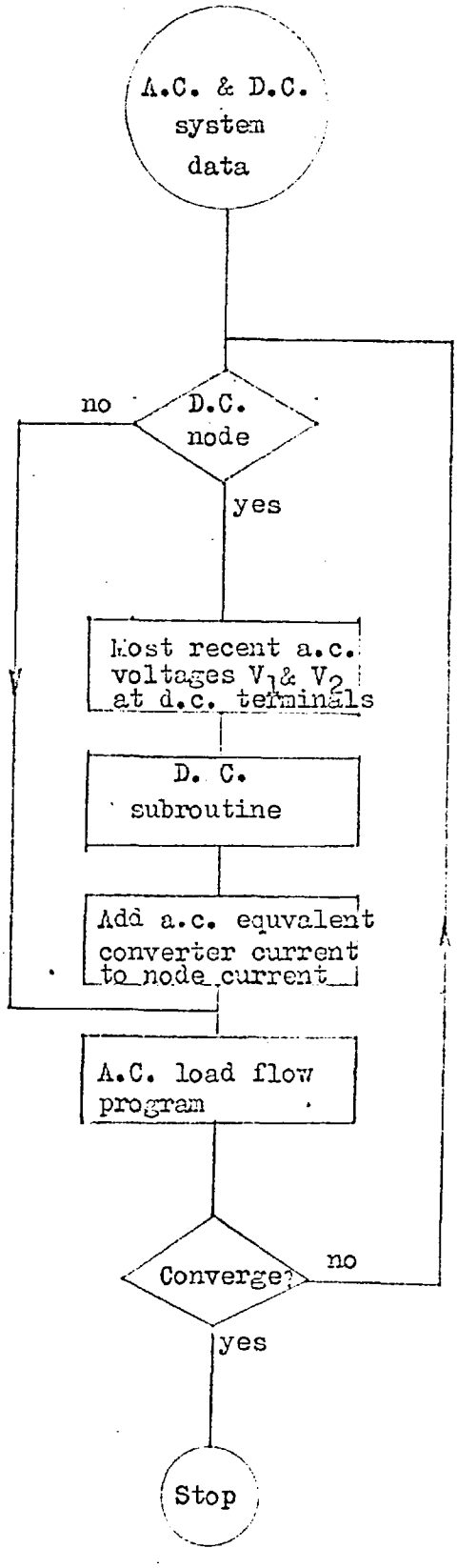

Fig.4.6a A.C./D.C. load flow program

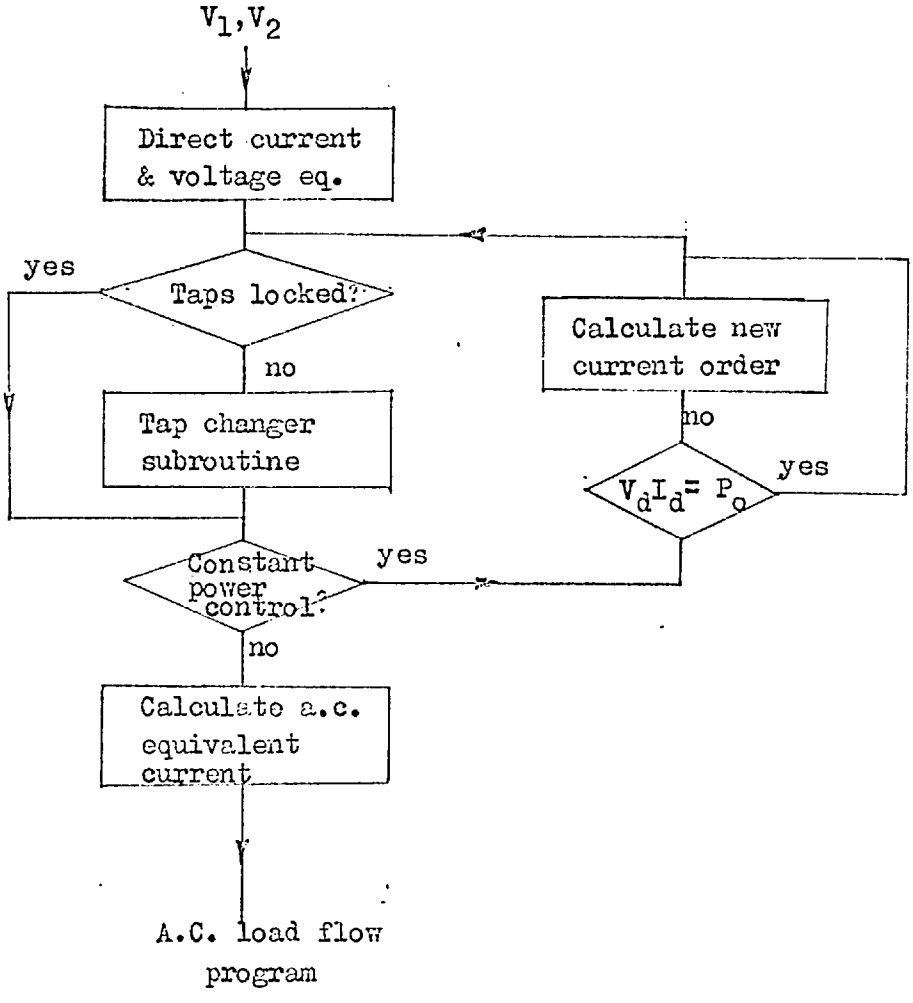

Fig. 4.6 b D.C. subroutine

4.6.2 Current Control at Rectifier

In this section the following equations were repeatedly used to find the voltage at the mid-point of the d.c. line, the firing angle of the rectifier, and the tap positions at both rectifier and inverter.

$$v_d = \frac{N'}{N}\left[n_2\, e_2 \cos\gamma + \left(-\frac{\Pi}{6}x_{t2} + \frac{\Pi^2}{9}r_{t2}\right) i_d\right] + \tfrac{1}{2}r_\ell i_d \qquad (4.29)$$

$$n_2 = \left[\frac{N}{N'}\, v_d - \left(-\frac{\Pi}{6}x_{t2} + \frac{\Pi}{9}x_{t2}\right) i_d - \tfrac{1}{2}\frac{N}{N'}r_\ell i_d\right] \Big/ (e_2 \cos\gamma) \qquad (4.30)$$

$$\cos\alpha = \left[\frac{N}{N'}\, v_d + \left(\frac{\Pi}{6}x_{t1} + \frac{\Pi^2}{9}r_{t1}\right) i_d + \tfrac{1}{2}\frac{N}{N'}r_\ell i_d\right] \Big/ (n_1\, e_1) \qquad (4.31)$$

$$n_1 = \left[\frac{N}{N'}\, v_d + \left(\frac{\Pi}{6}x_{t1} + \frac{\Pi^2}{9}r_{t1}\right) i_d + \tfrac{1}{2}\frac{N}{N'}r_\ell i_d\right] \Big/ (e_1 \cos\alpha) \qquad (4.32)$$

The tap positions obtained from Eqs. 4.30 and 4.32 may not be an actual position and were therefore rounded off to the nearest actual tap position.

The functions of this section were summarised as follows:

(1) If v_d from d.c. subroutine $v_{d\ell} \leq v_d \leq v_{dh}$ go to (9)

(2) If $v_d < v_{d\ell}$ or $v_d > v_{dh}$ set

$$v_d = \tfrac{1}{2}(v_{d\ell} + v_{dh})$$

(3) Compute n_2 with Eq. 4.30 and round off

(4) If $n_2 < n_{2\ell}$ set $n_2 = n_{2\ell}$

(5) If $n_2 > n_{2h}$ set $n_2 = n_{2h}$

(6) Compute v_d with Eq. 4.29

(7) If $v_d < v_{d\ell}$ and $n_2 < n_{2h}$ step up n_2 by n_{s2} and repeat (6)

(8) If $v_d > v_{dh}$ and $n_2 > n_{2\ell}$ step down n_2 by n_{s2} and repeat (6)

(9) Compute α with Eq. 4.31 using v_d from (1) or (6)

(10) If $\alpha_\ell < \alpha < \alpha_h$ exit from subroutine since both v_d and α line inside their limits.

(11) If $\alpha < \alpha_\ell$ or $\alpha > \alpha_h$ set

$$\alpha = \tfrac{1}{2}(\alpha_\ell + \alpha_h)$$

(12) Compute n_1 with Eq. 4.32 and round off

(13) If $n_1 < n_{1\ell}$ set $n_1 = n_{1\ell}$

(14) If $n_1 > n_{1h}$ set $n_1 = n_{1h}$

(15) Compute α with Eq. 4.30

(16) If $n_1 \leq n_{1\ell}$ or $n_1 \geq n_{1h}$ go to (20)

(17) If $\alpha < \alpha_\ell$ step up n_1 by n_{s1} and repeat (15)

(18) If $\alpha > \alpha_h$ step down n_1 by n_{s1} and repeat (15)

(19) If $\alpha_\ell < \alpha < \alpha_h$ exit from subroutine

(20) If $\alpha < \alpha_\ell$ step up n_2 by n_{s2}, compute v_d with Eq. 4.29 and repeat (15)

(21) If $\alpha > \alpha_h$ step down n_2 by n_{s2}, compute v_d with Eq. 4.29 and repeat (15)

(22) If $n_2 \leq n_2$ or $n_2 \geq n_{2h}$ exit from subroutine

Steps (20) to (22) call upon the inverter tap changer to operate and help to keep the rectifier firing angles within limits at the expense of the D.C. line voltage. This is justified on the ground that the rectifier valves operate most satisfactorily when the firing angles are within limits.

4.6.3 Current Control at Inverter

The following equations are used in this section:

$$n_1' = \left[1.1\,\frac{N}{N'}\,v_{dl} + \left(\frac{\Pi}{6}\,x_{t1} + \frac{\Pi^2}{9}\,r_{t1}\right) i_d + \tfrac{1}{2}\frac{N}{N'} r_\ell i_d\right] \Big/ (e_1 \cos\alpha_o) \qquad (4.33)$$

$$v_d = \frac{N'}{N}\left[n_2\, e_2 \cos\gamma + \left(-\frac{\Pi}{6}\,x_{t2} + \frac{\Pi^2}{9}\,r_{t2}\right) i_d + Na_{d2}(i_d - i_{ds2})\right] + \tfrac{1}{2} r_\ell i_d \qquad (4.34)$$

$$n_2 = \left[\frac{N}{N'}\,v_d - \left(-\frac{\Pi}{6}\,x_{t2} + \frac{\Pi^2}{9}\,r_{t2}\right) i_d - Na_{d2}(i_d - i_{ds2}) - \tfrac{1}{2}\frac{N}{N'} r_\ell i_d\right] \Big/ (e_2 \cos\gamma) \qquad (4.35)$$

$$v_d = \frac{N'}{N}\left[n_1 e_1 \cos\alpha_o - \left(\frac{\Pi}{6} x_{t1} + \frac{\Pi^2}{9} r_{t1}\right) i_d\right] - \tfrac{1}{2} r_\ell i_d \qquad (4.36)$$

$$n_1 = \left[\frac{N}{N'} v_d + \left(\frac{\Pi}{6} x_{t1} + \frac{\Pi^2}{9} r_{t1}\right) i_d + \tfrac{1}{2}\frac{N}{N'} r_\ell i_d\right] \Big/ (e_1 \cos\alpha_o) \qquad (4.37)$$

$$\cos\beta = -\left\{\frac{N}{N'} v_d - \left(\frac{\Pi}{6} x_{t2} + \frac{\Pi^2}{9} r_{t2}\right) i_d - \tfrac{1}{2}\frac{N}{N'} r_\ell i_d\right\} \Big/ (n_2 e_2) \qquad (4.38)$$

$$v_d = \frac{N'}{N}\left[n_2 e_2 \cos(180 - \beta) + \left(\frac{\Pi}{6} x_{t2} + \frac{\Pi^2}{9} r_{t2}\right) i_d\right] - \tfrac{1}{2} r_\ell i_d \qquad (4.39)$$

If the main d.c. subroutine showed that the current margin was crossed and current control was transferred to the inverter, it might be possible to restore it to the rectifier by tapping up at the rectifier end.

When the program entered this section of the tap changer subroutine Eq. 4.33 was used to establish the rectifier tap n_1 required to produce 110% v_d. The extra 10% was arbitrary to give a margin between the natural voltage characteristic and operating point. The rest of the actions are described below.

(1) Find rectifier tap n_1' required to produce v_d as obtained from main d.c. subroutine plus 10%. (The 10% is to provide arbitrary margin between voltages of the natural characteristic and the actual operation point)

(2) If $n_1' < n_{1h}$ set $n_1 = n_1'$ and go to section 1 of this subroutine.

(3) If $n_1' > n_{1h}$ set $n_1 = n_{1h}$ and go to section 1 of this subroutine, so that the rectifier can try to regain current control with highest tap. A counter is started to limit thenumber of such trials to say, 10, after which current control is assigned to the inverter and the program proceeds to (4). The limit on the number of trials is necessary to prevent the current control shifting between rectifier and inverter.

(4) If $v_{d\ell} < v_d < v_{dh}$ go to (11)

(5) If $v_d < v_{d\ell}$ or $v_d > v_{dh}$ set

$$v_d = \tfrac{1}{2}(v_{d\ell} + v_{dh})$$

(6) Find n_1 by Eq. 4.37 and round off

(7) Find v_d by Eq. 4.36

(8) If $n_1 \leq n_{1\ell}$ or $n_1 \geq n_{1h}$ go to (11)

(9) If $v_d < v_{d\ell}$, step up n_1 by n_{1s} and repeat (7)

(10) If $v_d > v_{dh}$ step down n_1 by n_{1s} and repeat (7). In the last two steps the rectifier transformer tap is used to control v_d since current control is at inverter.

(11) Find n_2 by Eq. 4.35 using v_d from previous steps and round off.

(12) Find v_d by Eq. 4.34

(13) If $n_{1\ell} \leq n_1 \leq n_{1h}$ go to (17)

(14) If $n_{2\ell} \leq n_2 \leq n_{2h}$ go to (19)

(15) If $n_2 < n_{2\ell}$ step up n_1 by n_{1s}

(16) If $n_2 > n_{2h}$ step down n_1 by n_{1s}

(17) Find v_d by Eq. 4.36 using new value of n_1 from the last two steps and repeat (11).

The last 3 steps uses the rectifier transformer tap to regulate v_d such that n_2 will come into range.

(18) Find β by Eq. 4.38

(19) Program leaves this subroutine.

(20) If $v_d < v_{d\ell}$ step up n_1 by n_{1s} and go to (16).

(21) If $v_d > v_{dh}$ step down n_1 by n_{1s} and go to (16).

In this section the rectifier transformer tap was used both to adjust v_d and to maintain the inverter transformer tap within range. The latter is a hard constraint which must be satisfied and, in some cases only be achieved by sacrificing the soft constraint on v_d and allowing it to exceed limits.

4.7 Other Features of Program

4.7.1 Constant Power Control

This was a slight extension of the constant current control. At the end of each calculation in the d.c. subroutine I_d and V_{d1} are known. If V_{d1} is the voltage at the mid-point of the D.C. line chosen as the reference for constant power control, then the power order P_o should be given by

$$P_o = V_{d1} I_d$$

If this is not so, new current orders must be calculated as follows:

(i) When rectifier is on constant current control

$$I'_{ds1} = \frac{P_o}{V_{d1} I_d} I_{ds1}$$

$$I'_{ds2} = I'_{ds1} - I_{dm}$$

(ii) When inverter is on constant current control

$$I'_{ds2} = \frac{P_o}{V_{d1} I_d} I_{ds2}$$

$$I'_{ds1} = I'_{ds2} + I_{dm}$$

With these new current orders the calculation in the d.c. subroutine was repeated until the power order was satisfied.

4.7.2 Harmonic Filters, Cable Capacitance, and Synchronous Compensators

Harmonic filters and cable capacitance were represented at fundamental frequency as a capacitor of fixed capacitance. Static compensators were treated in the same way. Synchronous compensators, however, usually supply constant reactive power at steady state, and were therefore represented as sources of constant reactive power.

4.7.3 Double-Pole D.C. Link

Equations for single pole d.c. links shown in previous sections are basically also applicable to double-pole d.c. links. The only

difference is that a loop resistance R_ℓ can no longer be used to calculate the voltage drop along the D.C. line, because there is now a common section of neutral line or cable shared by the two poles as shown by Fig. 4.7.

Eqs. 4.19-4.22 of Section 4.5.1 were modified as follows:-

For the upper pole, with rectifier on current control,

$$v_{dl1} = \frac{N'}{N}\left[n_{l1}\, e_{l1}\, \cos\alpha_o - \left(\frac{\Pi}{6} x_{tl1} + \frac{\Pi^2}{9} r_{tl1}\right) i_{dl} - Na_{dl1}(i_{dl} - i_{dsl1})\right] - r_{l1} i_{dl} + r_{nl} i_{d2} \qquad (4.40)$$

$$v_{dl2} = \frac{N'}{N}\left[n_{l2}\, e_{l2}\, \cos\gamma - \left(\frac{\Pi}{6} x_{tl2} + \frac{\Pi^2}{9} r_{tl2}\right) i_{dl}\right] + r_{l2} i_{dl} - (r_{n2} + r_{n3})\, i_{d2} \qquad (4.41)$$

with inverter on current control,

$$v'_{dl1} = \frac{N'}{N}\left[n_{l1}\, e_{l1}\, \cos\alpha_o - \left(\frac{\Pi}{6} x_{tl1} + \frac{\Pi^2}{9} r_{tl1}\right) i_{dl}\right] - r_{l1} i_d + r_{nl} i_{d2} \qquad (4.42)$$

$$v'_{dl2} = \frac{N'}{N}\left[n_{l2}\, e_{l2}\, \cos\gamma + \left(-\frac{\Pi}{6} x_{tl2} + \frac{\Pi^2}{9} r_{t22}\right) i_{dl} + Na_{dl2}(i_{dl} - i_{ds2})\right] + r_{l2} i_{dl} - (r_{n2} + r_{n3})\, i_{d2} \qquad (4.43)$$

Similarly modifications must be applied to the lower pole.

The first digit in the double subscript indicates the pole (1 for upper pole, 2 for lower pole), the second digit denotes rectifier or inverter as before.

The equations used in the tap changer subroutine were also altered in accordance with these new equations.

When calculations were being made for one pole the current in the other pole was required, e.g. Eq. 4.40 contains a $r_{nl} i_{d2}$ term. This current had been obtained from the last calculations made for that pole. When the calculations first start, this current was taken as the current order for that pole.

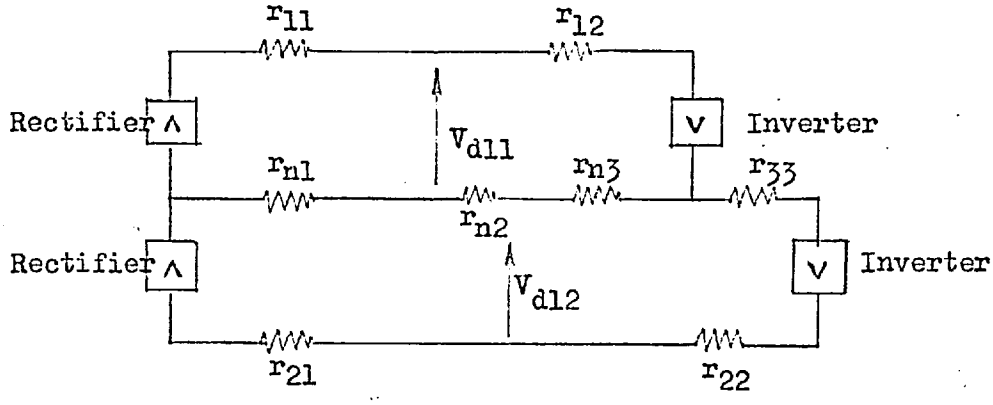

Fig. 4.7 Double pole d.c. link

4.7.4 Load Flow for Semi-Steady State

When there is a change in the normal network condition, e.g. line outage, blocking of converter bridges, transient voltages and currents are produced. Usually these transients die down fairly rapidly, but more time may elapse before any regulation equipment operates to adjust the network conditions in some prescribed manner, e.g. tap changers step up or down to maintain voltage level. This time interval between disturbances and corrective apparatus operation may be referred to as semi-steady state. Although a load flow program is essentially for steady state it can also be used to calculate voltages and power flows during the semi-steady state period since there is no change in the network.

Two facilities were included in the program:-

(i) Locking of converter transformer tap changers

This is used to study the condition of the a.c./d.c. system after a disturbance, e.g. outage of a.c. line, but before the tap changers of the converter transformers have time to operate. If this facility was requested, the tap changer subroutine was not called and the taps remained the same.

(ii) Blocking of converter bridges

This was used to study the conditions of the a.c./d.c. system when one or more bridges in a converter group were blocked at either the rectifier or inverter end or both. The values of N' in the relevant equations were set in accordance to the number of bridges remaining in service.

4.8 Experience with a.c./d.c. Load Flow Program

4.8.1 Results from Test System

An A.E.P. 14 bus test system[63] was used to check out the program. The original system, details of which are shown in Table 4.1 and Fig. 4.8, was modified by replacing the line between bus 4 and 5 with a single-pole

Line Node-Node		R (p.u.)	X (p.u.)	B (p.u.)	Tap Setting
1	2	0.01938	0.05917	0.0528	
1	5	0.05403	0.22304	0.0492	
2	3	0.04699	0.19797	0.0438	
2	4	0.05811	0.17632	0.0374	
2	5	0.05695	0.17388	0.0340	
3	4	0.06701	0.17103	0.0346	
4	5	0.01335	0.04211	0.0128	
4	7	0	0.20912	0	0.978
4	9	0	0.55618	0	0.969
5	6	0	0.25202	0	0.932
6	11	0.09498	0.19890	0	
6	12	0.12291	0.25581	0	
6	13	0.06615	0.13027	0	
7	8	0	0.17615	0	
7	9	0	0.11001	0	
9	10	0.03181	0.08450	0	
9	14	0.12711	0.27038	0	
10	11	0.08205	0.19207	0	
12	13	0.22092	0.19988	0	
13	14	0.17093	0.34802	0	
9	-	0	-5.26316	0	

Table 4.1

A.C. line data (on MVA base)

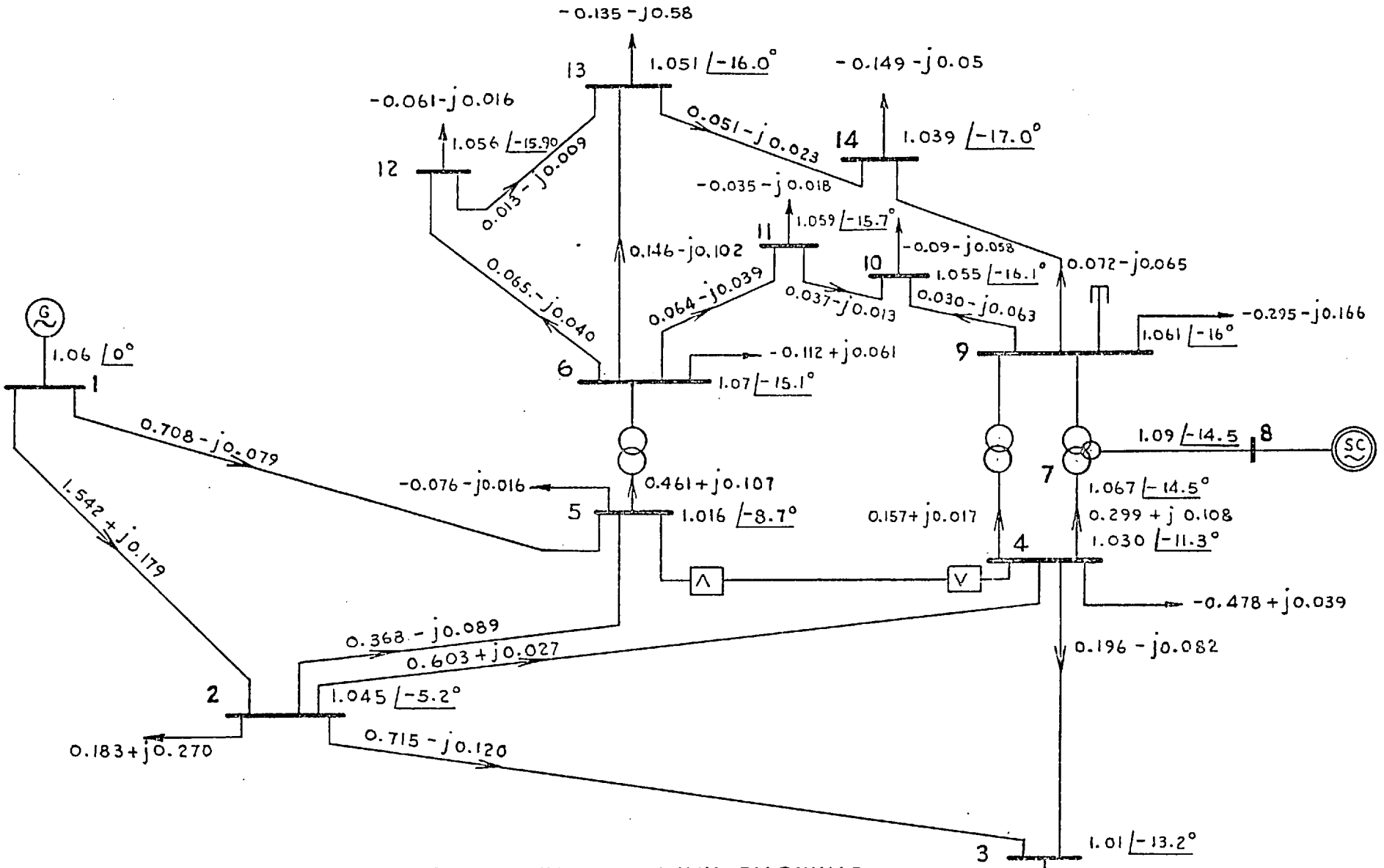

FIG. 4.8 A.E.P. TEST SYSTEM WITH 1 D.C. LINK SHOWING RESULTS OF A.C./D.C. LOAD FLOW. BASE MVA = 100

d.c. link. Details of the link are given in Table 4.2. Results of the a.c./d.c. load flow obtained with the program developed are shown in Table 4.3 and Fig. 4.8 . Convergence took 27 iterations and 1.2 min. on the IBM 7090 computer.

4.8.2 Effect of Slope of Converter Characteristics

The equation of the natural voltage characteristic is

$$V_d = V_{01} \cos\alpha_o - \left(\frac{3X_{t1}}{\pi} + 2R_t + \tfrac{1}{2}R_\ell\right) I_d$$

and that of the constant extinction angle is

$$V_d = V_{02} \cos\gamma + \left(-\frac{3X_{t2}}{\pi} + 2R_t + \tfrac{1}{2}R_\ell\right) I_d$$

If the line resistance R_ℓ is of the same order as the transformer reactance X_{t1} and X_{t2}, the two characteristics will have vastly different slopes, as shown in Fig. 4.9.

When the rectifier open circuit voltage is ${}_1V_{01}$ the intersection of 1 and 4 produces a proper operating point at A with rectifier on constant current control.

If ${}_1V_{01}$ is changed to ${}_3V_{01}$, another proper operating point at B is also obtained at the intersection of 3 and 5, constant current control being at the inverter.

However, if the rectifier open circuit voltage is ${}_2V_{01}$ Eq. 4.8 would produce an operating point at C which is the intersection between 2 and the extension of 5. This is obviously not a proper operating point, and is detected by noting the current I_d at C is greater than I_{ds2}.

To obtain a proper operating point, the following actions are possible:-

(i) Increase I_{ds2} to I'_{ds2} and get a proper operating point D.

(ii) Raise or lower tap changer at rectifier end.

(iii) Raise tap changer at inverter end.

	Rectifier	Inverter
Converter transformer rating	189 MVA	189 MVA
Converter transformer reactance	0.156 p.u.	0.156 p.u.
Number of tap positions	19	19
Regulation range	±15%	±15%
Number of bridges	2	2
Slope of converter characteristic	63.8 p.u.	63.8 p.u.
Minimum firing angle	7^{o}	
Minimum extinction angle		17^{o}
Resistance of d.c. line	5 ohms	
Direct voltage range	0.88 - 0.90 p.u.	

Table 4.2

D.C. link data

Rectifier tap	= 1.0
Inverter tap	= 0.91
Direct voltage	= 0.893 p.u.
Direct current	= 0.621 p.u.
Firing angle, α	= 12.7^{o}
Extinction angle, γ	= 17^{o}

Table 4.3

D.C. link operating parameters from a.c./d.c. load flow

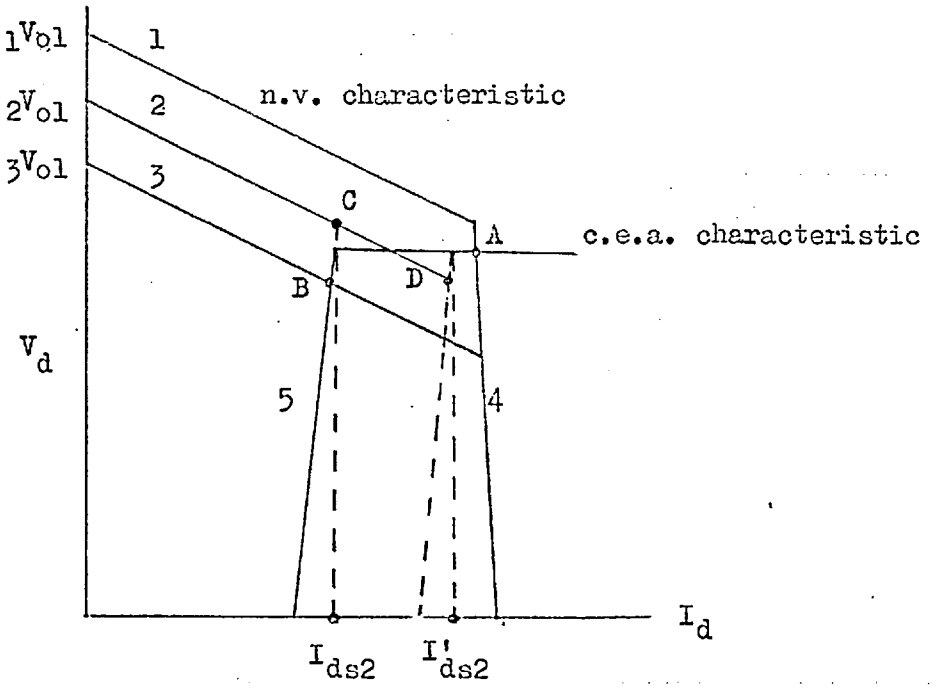

Fig. 4.9 Effect of slope of converter characteristic on operating point.

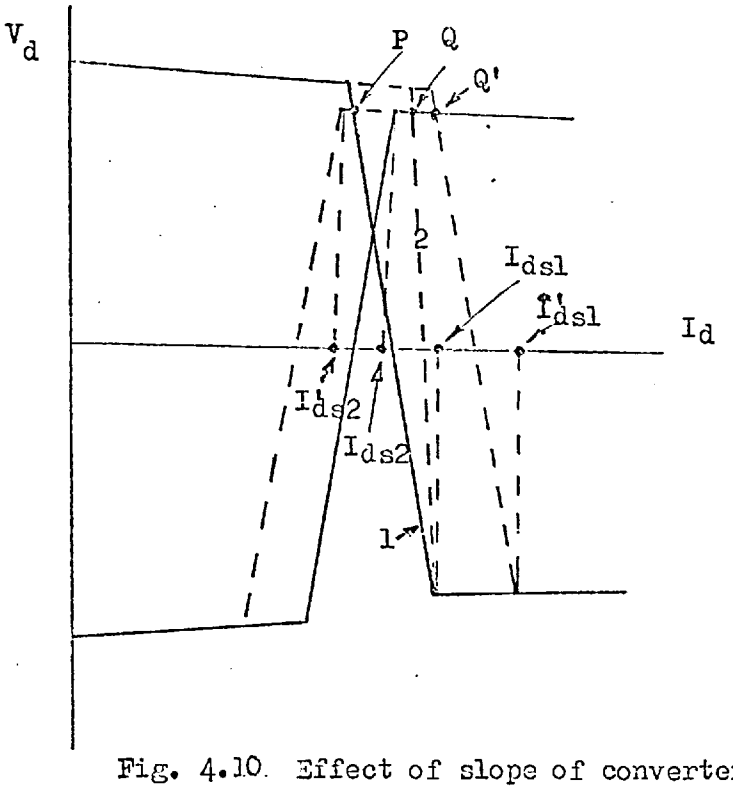

Fig. 4.10 Effect of slope of converter characteristic on operating point.

If Hingorani's convention of reckoning rectifier current order I_{dsl} from the corner of the c.e.a. characteristic was followed, false operating points may also be obtained as a result of ill-chosen values of the slope A_1 and current orders. This is illustrated in Fig. 4.10.

The full lines are the converter characteristics with current orders I_{dsl} and I_{ds2} and rectifier characteristic slope A_1 shown in line 1. Eq. 4.6 will produce a false operating point at P with current I_d less than I_{ds2} and constant current control at the rectifier.

A proper operating point at Q can be obtained by adjusting the value of A_1 to that shown by line 2. Altering the current order to I_{dsl}' or I_{ds2}' also results in proper operating points at P or Q'.

When adjusting the value of slope A_1 it is necessary to bear in mind the requirement for positive damping of the d.c. line as given by Adamson & Hingorani[40].

$$R_r' > \sqrt{\frac{L_d}{C_d}}$$

where $$R_r' = \left|A_1\right| + \tfrac{1}{2}R_\ell$$

L_d = inductance at rectifier or inverter

($\frac{1}{2}$ d.c. line inductance + smoothing reactor inductance)

C_d = capacitance of d.c. line

4.8.3 Problem of Non-Convergence Due to Repeated Margin Cross

An interesting phenomenon of repeated margin crossing of the converter characteristics had been observed in one application of the a.c./d.c. load flow program in the semi-steady-state mode with the tap changer of the converter transformers locked and with the d.c. link on constant current control. It can be explained by reference to Fig. 4.4 where P is a proper operating point with the tap positions of the converter transformers fixed by the load flow program used in the steady-state mode.

If an a.c. line near to the rectifier bus is removed to simulate outage, and if the connection of the rectifier bus to the a.c. system is weakened as a result, the rectifier bus voltage may fall sufficiently to cause a margin cross, i.e. constant current control passes from rectifier to inverter and operating point shifts to Q. The rectifier then draws less active power because of the reduced current and even less reactive power due to the improved power factor with $\alpha = \alpha_o$. The rectifier bus voltage may thus rise sufficiently to regain current control. The rectifier then draws its original current and runs at a lower p.f. with $\alpha > \alpha_o$. The bus voltage at the rectifier therefore falls again and may cause another margin cross, whence the previous process may be repeated, and the program would not converge. Fig. 4.11 illustrates this phenomenon which was obtained from the system described in Section 4.8.1 with the converter transformer taps locked at the values shown in Table 4.3. The program was re-run with the a.c. line between nodes 1-5 removed but other conditions were unchanged. The converter bus voltages can be seen to fluctuate, more at the inverter due to the higher swing in reactive power as the inverter changed from constant extinction angle control to constant current control. The program did not converge. The implication of this phenomenon is that with such an a.c. system configuration as would exist after the line outage operation of the d.c. link on constant current control will not be stable if the tap changers of the converter transformers are inoperative.

One solution which was found to be satisfactory in overcoming this difficulty of convergence is to use constant power control of the d.c. link. When the power order is constant, then after a margin cross the lower direct voltage would automatically force up the current order which would prevent the rectifier bus voltage rising to regain current control. This is shown in Fig. 4.11 where a constant power of 0.58 p.u. was ordered and the program

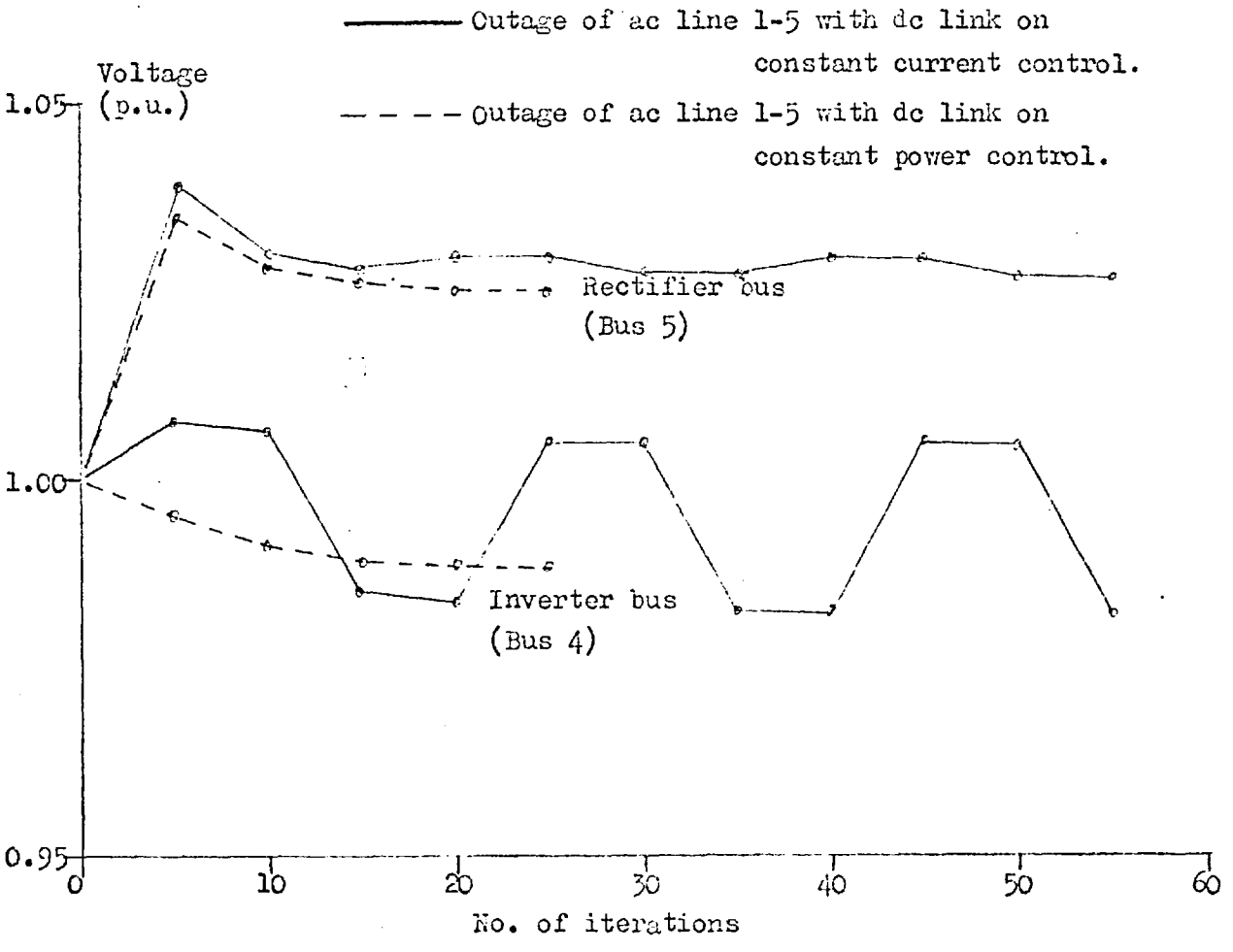

Fig. 4.11 Problem of non-convergence due to repeated margin cross. Converter bus voltages plotted every 5 iterations.

converged in 25 iterations. Alternatively the power order may be reduced so that the rectifier bus voltage is always sufficient to maintain current control.

When the tap changers finally operate, they should try to maintain a suitable power order with current control at the rectifier.

CHAPTER 5

TRANSIENT ANALYSIS OF A.C./D.C. SYSTEMS

5.1 Introduction

The last two chapters considered a.c./d.c. systems in the steady state. This chapter discusses the methods of analysis in the transient state. A fairly detailed description of the representation of generators, governors and automatic voltage regulator is given. On the d.c. side the representation of converters d.c. lines and their control is discussed. A method using matrix algebra was developed to link up the a.c. and d.c. systems, and was applied to a simple a.c./d.c. system for the study of disturbances.

In Chapter 2 it was mentioned that Hingorani et al[30] had developed a comprehensive dynamic representation of converters which produces actual waveforms of converter output voltage and instantaneous currents on the a.c. side. The draw-back of this method is the considerable programming effort and computing time required. In this chapter a simplified method is presented which is easier to program and requires less computing time although at the expense of some loss of generality of representation.

The transient behaviour of an a.c./d.c. system were formulated as sets of simultaneous first order differential equations. Digital solutions were obtained by the method of numerical integration using either plain FORTRAN programming language or the digital analog simulation languages MIMIC and DSL/90. Details of numerical integration methods and digital analog simulation languages are given in the Appendix. In this Chapter, however, an alternative method using transition matrix and recursive formulae requiring no integration is presented. This method has the merit of being both simple and fast with regard to computer application.

In this Chapter discussions are limited to symmetrical a.c. systems only.

5.2 Analysis of Generators

Three different methods of analysing generator transient behaviour were considered, each varying in accuracy of representation and ease of solution. All these methods are based on the two - axis general theory of electrical machines[34].

5.2.1 Full Representation

This representation, based on a mathematical model described by Shackshaft[51], includes the effects of damper windings, speed changes and rate of change of flux linkages. The voltage and flux linkage equations are as follows:

$$\psi_f = x_f i_f + x_{md} i_{kd} - x_{md} i_d \tag{5.1}$$

$$\psi_d = x_{md} i_f + x_{md} i_{kd} - x_d i_d \tag{5.2}$$

$$\psi_{kd} = x_{md} i_d + x_{kd} i_{kd} - x_{md} i_f \tag{5.3}$$

$$\psi_q = x_{mq} i_{kq} - x_q i_q \tag{5.4}$$

$$\psi_{kq} = x_{kq} i_{kq} - x_{mq} i_q \tag{5.5}$$

$$e_f = r_f i_f + \frac{1}{\omega_o} p\psi_f \tag{5.6}$$

$$e_d = \frac{1}{\omega_o} p\psi_d + \frac{\omega}{\omega_o}\psi_q - r_a i_d \tag{5.7}$$

$$e_q = \frac{\omega}{\omega_o}\psi_d + \frac{1}{\omega_o} p\psi_q - r_a i_q \tag{5.8}$$

$$o = r_{kd} i_{kd} + \frac{1}{\omega_o} p\psi_{kd} \tag{5.9}$$

$$o = r_{kq} i_{kq} + \frac{1}{\omega_o} p\psi_{kq} \tag{5.10}$$

where ω = actual angular speed of generator

ω_o = synchronous speed of generator

and the equation for electrical torque is

$$T_e = \psi_d i_q - \psi_q i_d \tag{5.11}$$

The flux linkage and voltage equations are re-arranged into the following form for solution:

$$p\psi_f = \omega_o(e_f - r_f i_f) \tag{5.12}$$

$$p\psi_d = \omega_o(e_d + r_a i_d + \frac{\omega}{\omega_o}\psi_q) \tag{5.13}$$

$$p\psi_{kd} = -\omega_o r_{kd} i_{kd} \tag{5.14}$$

$$p\psi_q = \omega_o(e_q + r_a i_q - \frac{\omega}{\omega_o}\psi_d) \tag{5.15}$$

$$p\psi_{kq} = -\omega_o r_{kq} i_{kq} \tag{5.16}$$

Thus the flux linkages are expressed as five first order differential equations in terms of voltages, currents and the flux linkages themselves. Knowing the flux linkages the currents are then calculated from Eq. 5.1 - 5.5, e.g.

$$i_f = \frac{\begin{vmatrix} \psi_f & x_{md} & -x_{md} \\ \psi_d & x_{md} & -x_d \\ \psi_{kd} & x_{kd} & -x_{md} \end{vmatrix}}{\begin{vmatrix} x_f & x_{md} & -x_{md} \\ x_{md} & x_{md} & -x_d \\ x_{md} & x_{kd} & -x_{md} \end{vmatrix}} \qquad (5.17)$$

Similar equations can be written for the other currents.

The direct and quadrature voltages e_d and e_q required in Eq. 5.13 and 5.15 are related to the rest of the a.c. system external to the generator, e.g. in the simple case of an infinite busbar of voltage V connected by an impedance $(r_t + jx_t)$ to the generator these voltages are given by

$$e_d = \sqrt{2}V_{bd} - \frac{x_t}{\omega_o} pi_d - r_t i_d - \frac{x_t}{\omega_o} i_q$$

$$e_q = \sqrt{2}V_{bq} - \frac{x_t}{\omega_o} pi_q - r_t i_q + \frac{x_t}{\omega_o} i_d$$

where $V_{bd} = V\sin\delta$

$V_{bq} = V\cos\delta$

in which δ = load angle of generator with respect to infinite bus.

The field voltage e_f is determined by the automatic voltage regulator and is discussed later.

5.2.2 Representation with $p\psi_d$, $p\psi_q$ terms neglected

By neglecting the $p\psi_d$ and $p\psi_q$ terms in Eq. 5.7 and 5.8 the five flux linkage equations Eq. 5.12 to 5.16 were transformed by Alford[52] as follows:-

$$p\psi_f = e_f + \frac{1}{T'_{do}}\left\{\frac{x''_d - x_a}{x'_d - x_a}\left(\frac{x_{md}}{\omega_o} i_d + \frac{x_{md}}{x_{kd}}\psi_{kd}\right) - \left[1 + \frac{(x''_d - x_a)x_{md}}{x_{kd}x_f}\right]\psi_f\right\} \qquad (5.18)$$

$$p\psi_{kd} = \frac{1}{T''_{do}}\left(\frac{x'_d - x_a}{\omega_o}\cdot i_d + \frac{x'_d - x_a}{x_{f\ell}}\cdot f - \psi_{kd}\right) \qquad (5.19)$$

$$p\psi_{kq} = \frac{1}{T''_{qo}} \left(\frac{x_{mq}}{\omega_o} \cdot i_q - \psi_{kq} \right) \qquad (5.20)$$

Thus the three remaining flux linkages are expressed as three simultaneous first order differential equations in terms of the field voltage e_f and the axis currents i_d and i_q. In conjunction with these equations the machine can be represented as a voltage behind its subtransient reactance with d and q components of:-

$$v''_d = - sx''_q i_q + \omega_o (x''_q - x_a) \frac{\psi_{kq}}{x_{kq}} \qquad (5.21)$$

$$v''_q = sx''_d i_d - \omega_o (1 - s) \left[(x''_d - x_a) \left(\frac{\psi_f}{x_{f\ell}} + \frac{kd}{x_{kd}} \right) \right] \qquad (5.22)$$

where s = slip of machine

This simplified representation is most useful for analysing small disturbances, but would not be very accurate under large transients, e.g. pole slipping, when the values of $p\psi_d$ and $p\psi_q$ are relatively high. The inaccuracies would be even higher when the machine has an exciter system with rectifiers. In this case the blocking action of the rectifiers during severe transients may cause sharp discontinuities in field current and voltage, and would require the retention of the $p\psi_d$ and $p\psi_q$ terms for an accurate analysis. Eq. 5.21 and 5.22 then becomes

$$v''_d = \frac{x''_d}{\omega} pi_d + (x''_d - x_a) \left(\frac{p\psi_f}{x_{f\ell}} + \frac{p\ kd}{x_{kd}} \right) - sx''_q i_q + \omega (x''_q - x_a) \frac{\psi_{kq}}{x_{kq}}$$

$$v''_q = \frac{x''_q}{\omega} pi_q + \frac{x''_q - x_a}{x_{kq}\ T''_{qo}} \left(\frac{x_{mq}}{\omega} pi_q - p\psi_{kq} \right) + sx''_d i_d - (1 - s) \left[(x''_d - x_a) \left(\frac{\psi_f}{x_{f\ell}} + \frac{\psi_{kd}}{x_{kd}} \right) \right]$$

5.2.3 More Simplified Representation

In cases where an accurate solution is not required or where it is desired to reduce the complexity of the problem, the machine equations can be further simplified by neglecting, in addition to the $p\psi_d$ and $p\psi_q$ terms, all subtransient effects, changes in machine speed and armature resistance. The machine can then be represented by a terminal voltage with components:-

$$e_d = x_q i_q \qquad (5.23)$$

$$e_q = \frac{1}{1 + T_{do} p} \cdot e_f - \frac{x_d + T_{do}\ x'_d p}{1 + T_{do} p} \cdot i_d \qquad (5.24)$$

as shown by Humpage and Stott[53]. In these equations p is the Laplace operator, and it is seen that only one first order differential equation is required to calculate the machine voltage.

This last representation was used for the simple system to be described in Section 5.4. The more accurate representation in Section 5.2.2 was used in Chapter 6 where the control of an isolated generator connected to a d.c. link is discussed. Reference 54 used the full representation described in Section 5.2.1 as a test case for investigating the application of digital analog simulation languages.

5.2.4. Per unit system for synchronous machines.

For the d-and q-axis coils the following per unit system is used:

Axis voltage base = Armature rated voltage, r.m.s. per phase

Axis current base = $\frac{3}{2}$ x armature rated current, r.m.s. per phase

Axis power base = $\frac{1}{2}$ x armature power base.

The per unit system for the field coil is obtained by considering it and the direct axis coil as magnetically coupled circuits with N_f and Nd turns respectively, hence

$$\left.\begin{aligned} \text{Field voltage base} &= \frac{N_f}{N_d} \times \text{axis voltage base} \\ &= \frac{N_f}{N_d} \times \text{armature rated voltage, r.m.s. per phase} \\ \text{Field current base} &= \frac{N_d}{N_f} \times \text{axis current base} \\ &= \frac{N_d}{N_f} \times \frac{3}{2} \text{ armature rated current, r.m.s.} \end{aligned}\right\} \quad (5.26)$$

Field power base = $\frac{1}{2}$ x armature power base.

Since Nd and Nf are not known, the field voltage and current base is calculated indirectly from the machine open circuit and short circuit characteristics as shown in Fig. 5.1. AB is the field current required to balance the MMF due to rated armature current and

$$\frac{OA}{OB} = \frac{AC}{BD}$$

$$\frac{OB - OA}{OB} = \frac{BD - AC}{BD}$$

$$\frac{AB}{OB} = \frac{X_d - X_\ell}{X_d} = \frac{X_{md}}{X_d} = \frac{X_{md}}{x_d}$$

But $\frac{OB}{OF} = x_d$

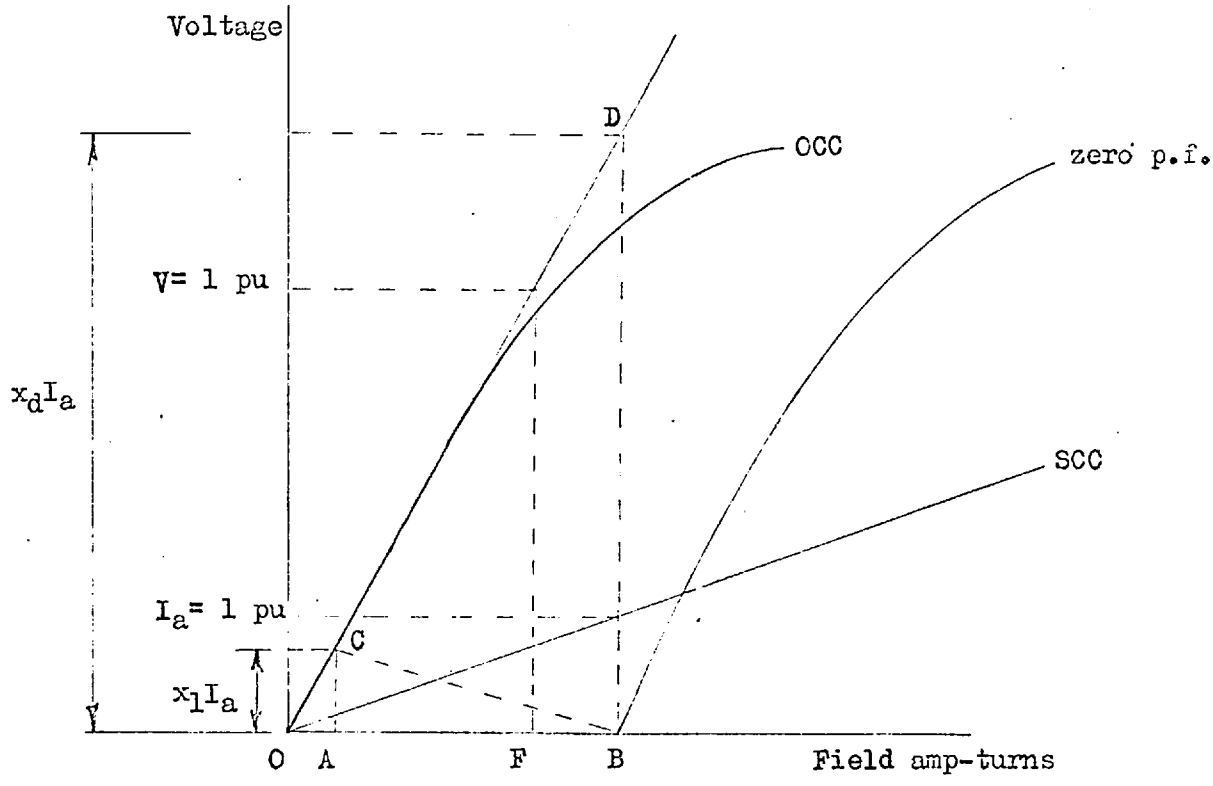

Fig. 5.1 Open circuit and short circuit characteristic of synchronous machine

OA- Field amp-turns for leakage reactance drop
OB- " " " rated armature current at zero p.f.
OF- " " to produce rated armature voltage on air-gap line

where OF = field current required to produce rated armature voltage on the air-gap line

$= I_{fv}$

$\therefore$ AB $= x_{md} I_{fv} = I_f$

Moreover Say[55] showed that the current I_f produces the same M.M.F. as the rated armature current I_a if

$$I_f = \sqrt{2} \frac{N_a}{N_f} \frac{3}{2} I_a$$

From Eq. 5.26,

$$\text{Field current base} = \frac{N_d}{N_f} \times \frac{3}{2} \text{ armature rated current}$$

$$= \sqrt{\tfrac{1}{2}}\, I_f \text{ because } N_a = N_d$$

$$= \sqrt{\tfrac{1}{2}}\, x_{md} I_{fv}$$

Using this per unit system the axis quantities are related to the phasor components of voltage and current as follows:-

$$e_d = \sqrt{2}\, E_d$$

$$e_q = \sqrt{2}\, E_q$$

$$i_d = \sqrt{2}\, I_d$$

$$i_q = \sqrt{2}\, I_q$$

where the quantities on the L.H.S. are axis quantities and those on the R.H.S. are phasor components.

5.2.5 Representation of automatic voltage regulator

Shackshaft[51] has presented an useful representation of a voltage regulator and excitation system which consists of an a.c. exciter supplying a rectifier, two magnetic amplifiers and two stabilizing circuits as shown in Fig. 5.2. The equation (in volts, amperes, and seconds) are:

Voltage - sensitive circuit

$$Vm_1 = -G_{vs} (Vm - Vr)$$

First magnetic amplifier

$$Vm_2 = \frac{Gm_1}{1 + Tm_1 P} (Vm_1 + V_{xs} + Vms) + Km_1$$

$$Vm_2 min \leq Vm_2 \leq Vm_2 max$$

Second magnetic amplifier

$$Vx = \frac{Gm_2}{1 + Tm_2 P} Vm_2 + Km_2$$

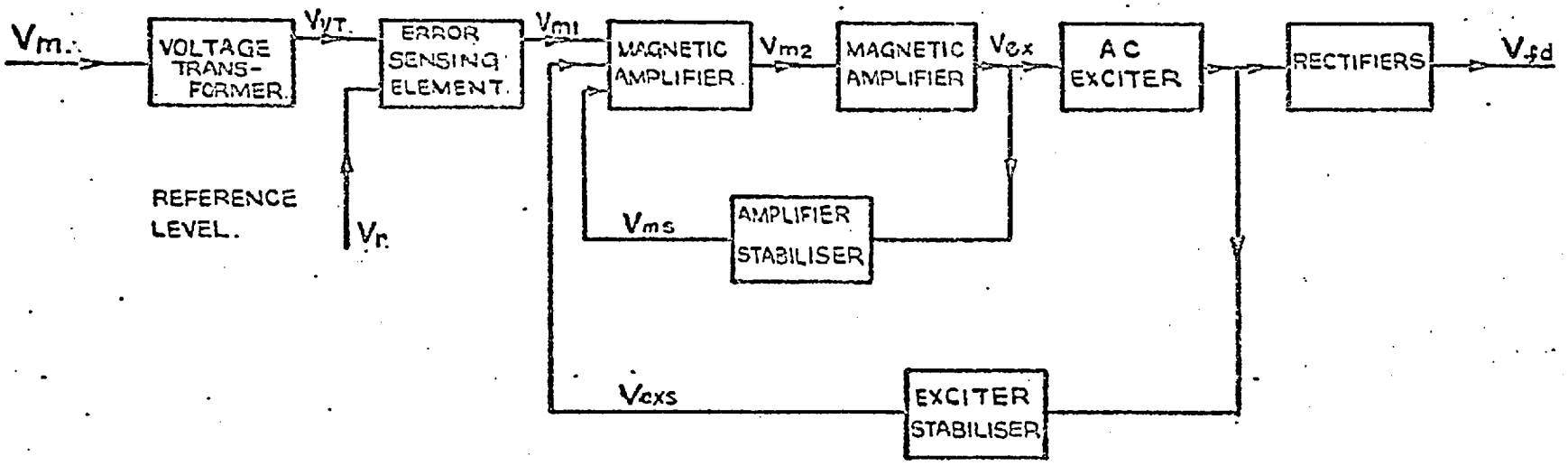

FIG 5.2 BLOCK DIAGRAM OF VOLTAGE REGULATOR.

$$V_{xmin} \leq V_x \leq V_{xmax}$$

Exciter

$$e_f = \frac{G_x}{1 + T_x P} \quad V_x + K_x$$

Amplifier stabiliser

$$V_{ms} = - \frac{G_{ms} T_{ms} P}{1 + T_{ms} P} V_x$$

Exciter stabiliser

$$V_{xs} = - \frac{G_{xs} T_{xs} P}{1 + T_{xs} P} \quad e_f$$

The calculation of the initial values of these variables are given in Reference 54.

5.2.6 Representation of governor and turbine

A simple representation of governor and turbine was also given by Shackshaft, and was based on an oil-servo type governor actuated by the speed of the machine or the speeder-gear motor. This governor and turbine is shown in block diagram form in Fig. 5.3 and described by the following equations (in per unit):

Centrifugal governor

The sleeve position Y is given by

$$Y = Y_o - G_1 P\delta$$

$$0 \leq Y \leq 1$$

where Y_o = initial setting

G_1 = governor slope

$p\delta$ = change in machine speed

Relays

The governor valve position Y_1 is given by

$$Y_1 = \frac{G_2}{(1 + T_1 P)(1 + T_2 P)} \quad Y + K_2$$

$$0 \leq Y \leq 1$$

Governor Valve

The steam power is assumed to be proportional to governor-valve opening, thus

$$P_s = G_3 Y_1$$

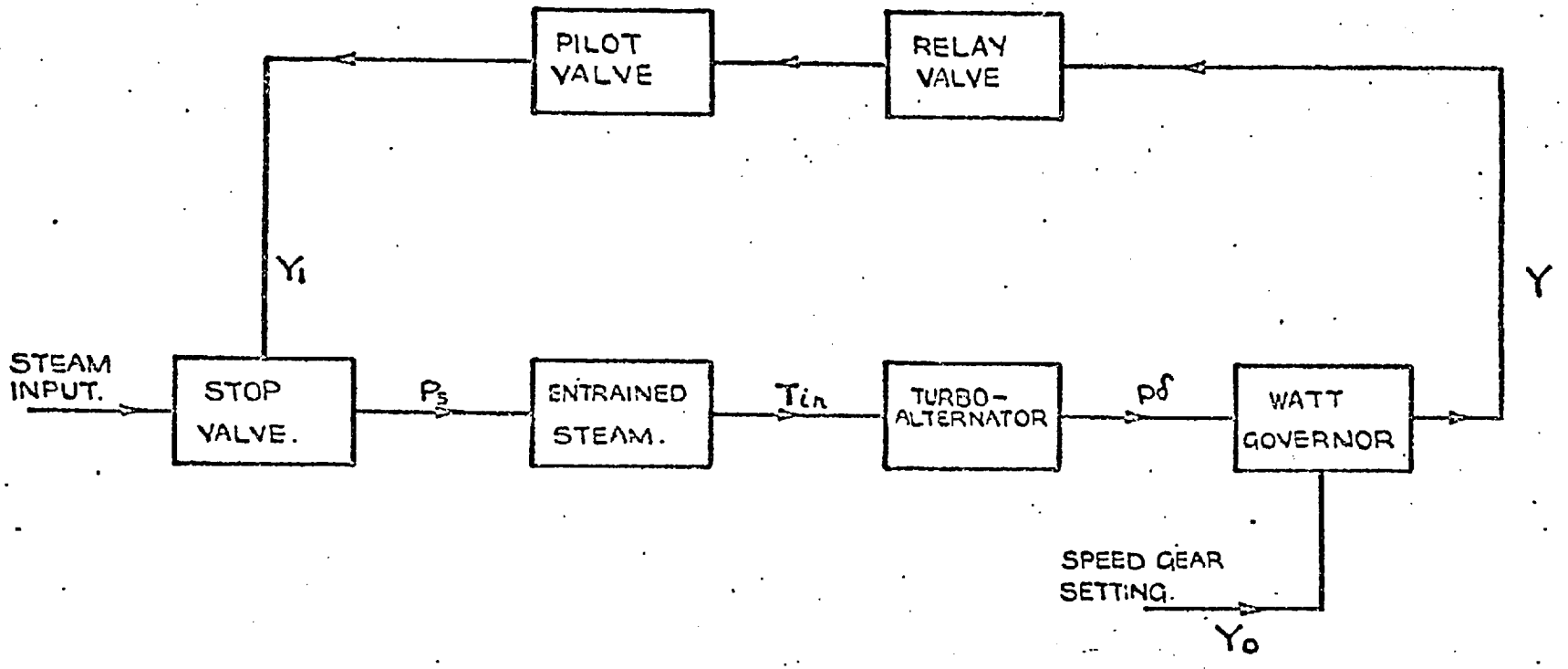

FIG 5.3 BLOCK DIAGRAM OF GOVERNING SYSTEM

Turbine

The turbine power and torque are

$$P_{in} = \frac{1}{1 + T_3 p} P_s$$

$$T_{in} = 1 - \frac{1}{p\delta/\omega_o} Pin$$

As before, the calculation of the initial values of these variables are given in Reference 54.

Acceleration of the machine is found by the well-known equation

$$p^2\delta = \frac{\omega_o}{2H} T_a$$

$$T_a = T_{in} - T_e - T_\ell$$

$$T_e = \psi d\, iq - \psi q\, id \text{ (electrical torque)}$$

T_ℓ = loss torque

A more detailed representation of governor and turbine is used in Chapter 6 when the control of an isolated generator connected to a d.c. link is considered.

5.3 Representation of d.c. links and their control

In this analysis the firing angles of the rectifier and inverter were assumed to be continuously controllable so that the converters were treated as a d.c. motor and generator respectively with no inertia. A detailed discussion of the various ways of representing converters was given in Chapter 2, but with the above assumptions it was sufficient to represent the converters as e.m.f.s. which were continuous functions of the firing angles.

Rectifier

$$Vd = N\left(\frac{3\sqrt{2}}{\Pi} E \cos\alpha - \frac{3X}{\Pi} I_d\right) \qquad (5.27)$$

Inverter

$$Vd = N\left(\frac{3\sqrt{2}}{\Pi} E \cos\gamma - \frac{3X}{\Pi} I_d\right) \qquad (5.28)$$

where N = number of bridges in service

X = commutating reactance

The equivalent current on the a.c. side of the converter is given in terms of its active and reactive components I_p and I_q as

$$I_p = M\, V_d I_d$$

$$\cos\alpha - \cos(a + u) = \frac{\sqrt{2}\, X\, I_d}{E}$$

$$I_q = I_p \left(\frac{2u + \sin 2a - \sin 2(a+u)}{2[\cos^2 a - \cos^2(a+u)]} \right)$$

$$I_v = I_p - jI_q$$

where M = 1 for rectifier, = -1 for inverter

a = α for rectifier, = γ for inverter

As explained in Chapter 2 this representation is due to Reider[23] who replaced the actual saw-tooth voltage waveform across a 1-bridge converter over a period of 60 electrical degrees with an equivalent step-voltage waveform. For a converter with two bridges a slight modification is necessary, viz. there is now, at steady state or slow transients, a commutation every 30 electrical degrees, with new firing angles preceeding each commutation. The total direct voltage can therefore be regarded as made up of two step-voltages in series each phase-shifted by 30 electrical degrees. Moreover new firing angles must be supplied for the valves of alternate bridges at 30 degrees intervals. The total converter current on the a.c. side is the phasor sum of the converter currents of the two bridges, with the phase angle of alternate converter currents calculated at each new firing angle.

The converters are controlled by their firing angles which are determined by the following relationships:-

Rectifier

$$\cos\alpha = \cos\alpha_o - \frac{A_1 (I_{ds1} - I_d)}{\frac{3\sqrt{2}}{\Pi} E_1} \qquad \text{for } I_d > I_{ds1}$$

$$= \cos\alpha_o \qquad \text{for } I_d < I_{ds1}$$

Inverter

$$\cos\alpha_2 = \cos\gamma_o + \frac{\sqrt{2}X\, I_d}{E_2} \qquad \text{for } I_d > I_{ds2}$$

$$= \cos\gamma_o + \frac{\sqrt{2}\, X\, I_d}{E_2} + \frac{A_2 (I_{ds2} - I_d)}{\frac{3\sqrt{2}}{\Pi} E_2} \qquad \text{for } I_d < I_{ds2}$$

where α_o = minimum rectifier delay angle

γ_o = minimum extinction angle

A_1, A_2 = slope of rectifier and inverter characteristics.

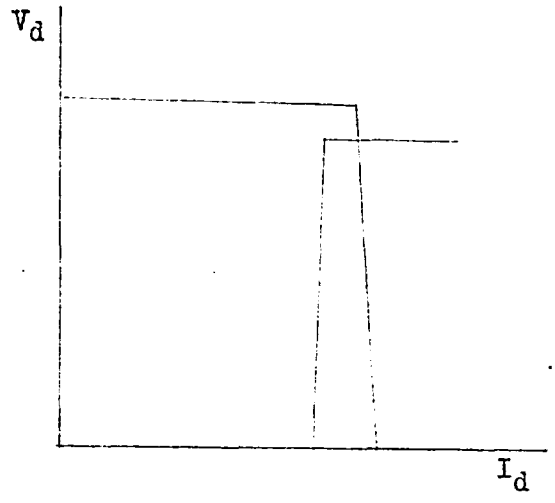

Fig. 5.4 Typical converter characteristic

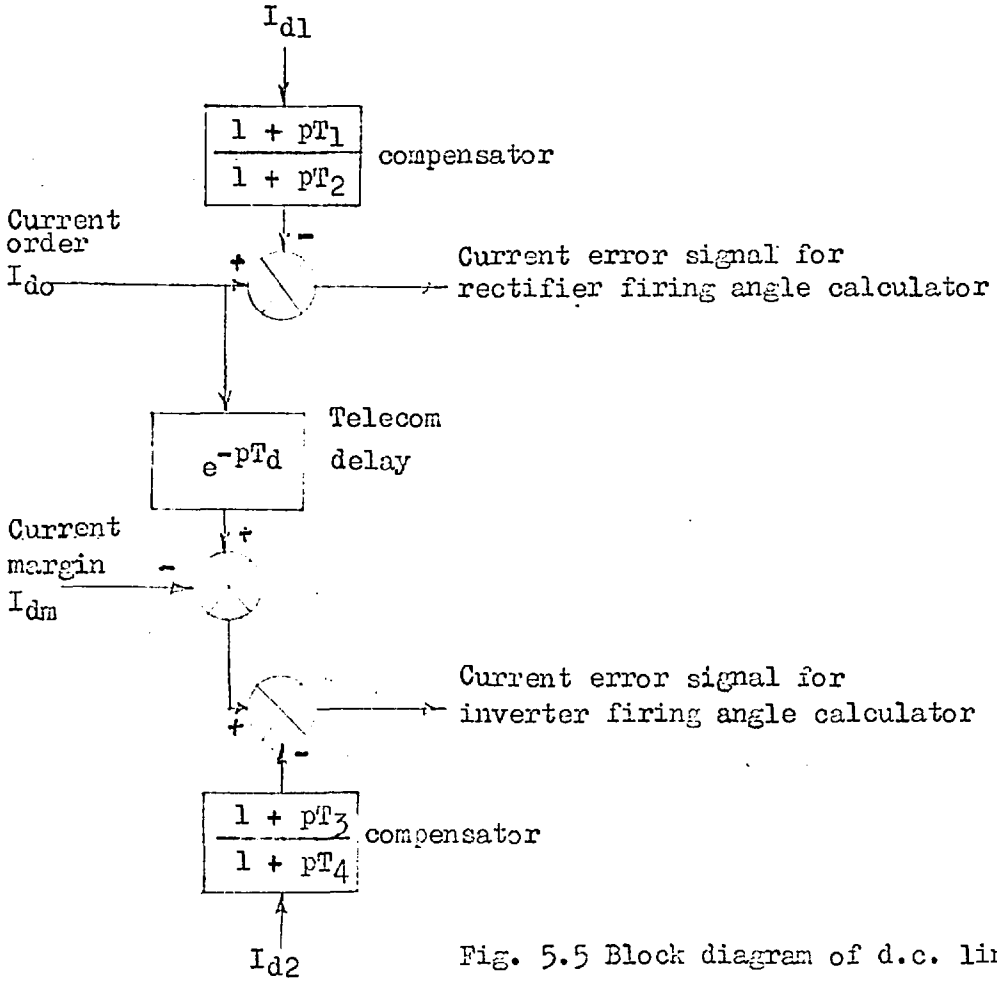

Fig. 5.5 Block diagram of d.c. link control

I_{ds1}, I_{ds2} = current order at rectifier and inverter

X = commutating reactance

E_1, E_2 = rectifier and inverter a.c. bus voltages

Fig. 5.4 shows typical converter characteristics, and Fig. 5.5 illustrates a block diagram of a d.c. link control with transfer functions of compensators and delay. The former represents the current measuring device which transmits a signal proportional to the direct current from the d.c. line to the firing angle calculator. The delay represents the telecommunication delay between the rectifier and inverter stations. These transfer functions are similar to those used by Breuer et al.[9] All the above equations are in practical units, for conversion to per unit the per unit system of Gavrilovic and Taylor shown in Chapter 2 was used.

The d.c. line was represented as a simple T- network which was sufficiently accurate for slow transients.

5.4 Analysis of simple parallel a.c./d.c. system

In order to gain some understanding of the transient operation of h.v.d.c. links working in an a.c. power system, and also to illustrate how the representations of a synchronous machine can be combined with that of converters to effect an analysis of a composite-system, a simple a.c./d.c. parallel transmission system was analysed. This system is shown in Fig. 5.6 and consists of an equivalent generator connected to an infinite busbar by an a.c. line in parallel with a single pole h.v.d.c. link having two bridges at each terminal.

The simplified representation of a synchronous machine of Section 5.2.3 and the representation of d.c. converters as continuously controllable e.m.f.s. as shown in Section 5.3 were used. The simplified machine representation was justified by the assumption that subtransient effects and speed changes are small. The local loads and filters at the converter buses were represented as constant impedances and susceptances respectively. The a.c. circuits were represented by their impedances at the fundamental frequency. The data for this study are as follows:-

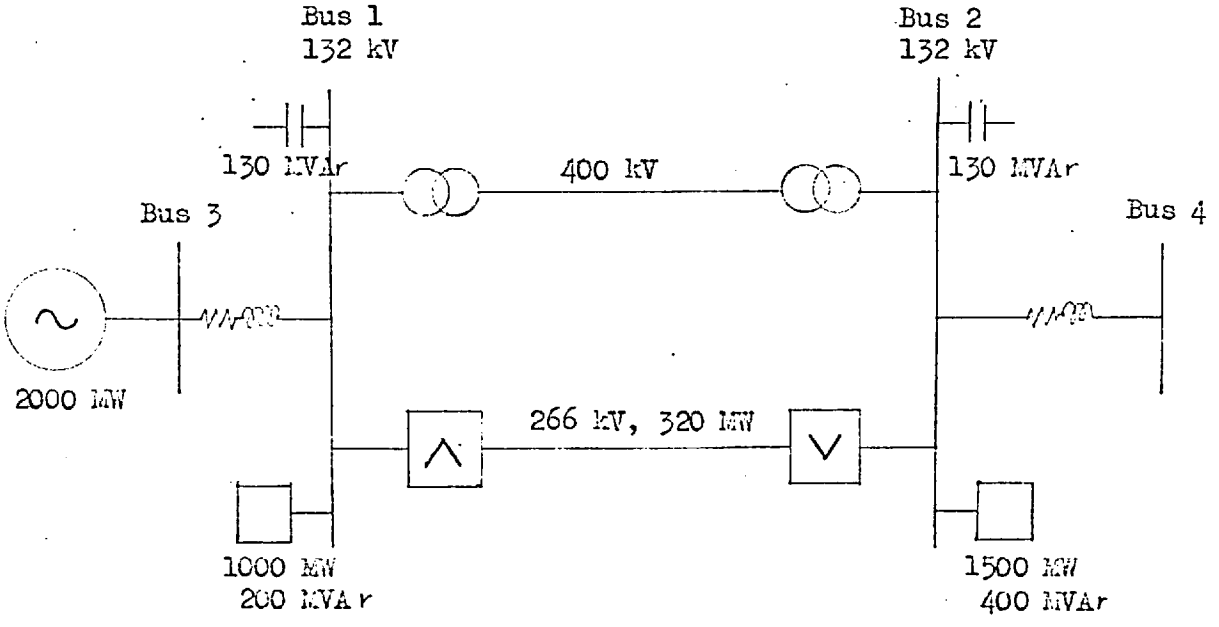

Fig. 5.6 Simple parallel a.c./d.c. system
Bus 4 as infinite busbar

Equivalent generator data

x_a = 0.00047 p.u.

x_d = 0.1039 p.u.

x_q = 0.0755 p.u.

x'_d = 0.0478 p.u.

H = 31.8 sec.

T_{do} = 6.36 sec.

Network data

Z_{13} = 0.0009+j0.0189 p.u.

Z_{12} = 0.0075+j0.26 p.u. (including 2 transformers)

Z_{24} = 0.0037+j0.0756 p.u.

D.C. line data

Half-line resistance 0.967 ohm

Half-line inductance 0.6 H

Line Capacitance 12.5 μF

D.C. link control data

$T_1 = T_3$ = 0.015 sec.

$T_2 = T_4$ = 0.1 sec.

T_d = 0.02 sec.

MVA base = 378

AVR data

G_{vs} = 0.00159

G_{m1} = 51

T_{m1} = 0.044 sec.

K_{m1} = 65.4V

V_{m2min} = 1.8V

V_{m2max} = 51.6V

G_{m2} = 12.2

T_{m2} = 0.1 sec.

K_{m2} = 146.7V

V_{xmin} = 0V

V_{xmax} = 227V

G_x = 3.06

T_x = 0.2 sec.

K_x = 15.0 sec.

G_{ms} = 0.00525

T_{ms} = 0.1 sec

G_{xs} = 0.0139

T_{xs} = 2.0 sec

Governor data

$G_1 = 0.00188$

$G_2 = 1.33$

$G_3 = 1.42$

$T_1 = 0.1$ sec

$T_2 = 0.188$ sec

$T_3 = 0.49$ sec

$K_2 = 0.267$

The busbar voltages v_1, v_2 and machine voltage v_3 and current i_3 were the unknowns in this network, for which the following matrix equation was written

$$\begin{bmatrix} y_{11} & y_{12} & 0 & -1 \\ y_{12} & y_{22} & 0 & 0 \\ 0 & 0 & 1 & -x \\ -1 & 0 & 1 & -x \end{bmatrix} \begin{bmatrix} v_1 \\ v_2 \\ v_3 \\ i_3 \end{bmatrix} = \begin{bmatrix} i_1 \\ i_2 - y_{24} y_4 \\ F \\ 0 \end{bmatrix} \qquad (5.29)$$

where i_1 and i_2 were the fundamental component of rectifier and inverter currents in per unit. And if all voltages and currents were expressed in terms of d- and q- components the above equation was expanded as follows:

$$\begin{bmatrix} g_{11} & b_{11} & g_{12} & b_{12} & 0 & 0 & -1 & 0 \\ -b_{11} & g_{11} & -b_{12} & g_{12} & 0 & 0 & 0 & -1 \\ g_{12} & b_{12} & g_{22} & b_{22} & 0 & 0 & 0 & 0 \\ -b_{12} & g_{12} & -b_{22} & g_{22} & 0 & 0 & 0 & 0 \\ 0 & 0 & 0 & 0 & 1 & 0 & & -xq \\ 0 & 0 & 0 & 0 & 0 & 1 & x'_d & 0 \\ -1 & 0 & 0 & 0 & 1 & 0 & -v_t & x_t \\ 0 & -1 & 0 & 0 & 0 & 1 & -x_t & -v_t \end{bmatrix} \begin{bmatrix} v_{1d} \\ v_{1q} \\ v_{2d} \\ v_{2q} \\ v_{3d} \\ v_{3q} \\ i_{3d} \\ i_{3q} \end{bmatrix} = \begin{bmatrix} i_{1d} \\ i_{1q} \\ i_{2d} - i \sin(\delta - \phi) \\ i_{2q} - i \cos(\delta - \phi) \\ 0 \\ f \\ 0 \\ 0 \end{bmatrix} \qquad (5.30)$$

where $|i| = |y_{24} v_4|$

$\phi = \tan^{-1}(i)$

δ = load angle between v_3 and v_4

f is an intermediate variable and is derived from Eq.5.24 such that

$$pf = \frac{1}{T_{do}} (e_f - V_{3q} - x_d i_{3d})$$

$$i_{1d} + ji_{1q} = |i_1| \exp(j\theta_1)$$

$$\theta_1 = \tan^{-1}(v_{1q}/v_{1d}) - \tan^{-1}(i_1)$$

$$i_{2d} + ji_{2q} = |i_2| \exp(j\theta_2)$$

$$\theta_2 = \tan^{-1}(v_{2q}/v_{2d}) - \tan^{-1}(i_2)$$

v_{1d}, v_{1q}, v_{2d}, and v_{2q} are the d- and q- components of v_1 and v_2.

Eq. 5.30 can be abbreviated to a matrix equation as

$$[A][B] = [C]$$

and is solved in the form

$$[B] = [A]^{-1}[C]$$

since [A] is a matrix of constants only one matrix inversion is required.

The converter current i_1 and i_2 (and hence their components i_{1d}, i_{1q}, i_{2d}, i_{2q}) depended on the voltages v_1 and v_2, therefore a process of iteration was required in which the above matrix equation is solved repeatedly with each new set of values of C until a convergent set of B is obtained. Experience showed that two or three iterations were sufficient for each step.

Figs. 5.7, 5.8 show the result of a change in current order from 0.98 to 1.1 p.u. and the effect of blocking one bridge at one terminal. They show that the d.c. system settled down to the new steady-states after 0.05 sec. in both cases with no excessive transients. It is interesting to note that the direct voltage appeared as smooth curves because the converters were treated as continuously controllable. By comparison the direct voltage obtained by Hingorani et al[30], who represented the converters faithfully on a firing by firing bases, appeared as the actual saw-tooth waveforms.

5.5 Simplified transient analysis of converters

As mentioned in Chapter 2 Hingorani et al[30] presented a rigorous and comprehensive dynamic representation of converters. Their representation produces the actual voltage waveform across a converter, and the instantaneous values of currents on the a.c. phases and on the d.c. line. Their method is simple in principle and is based on the

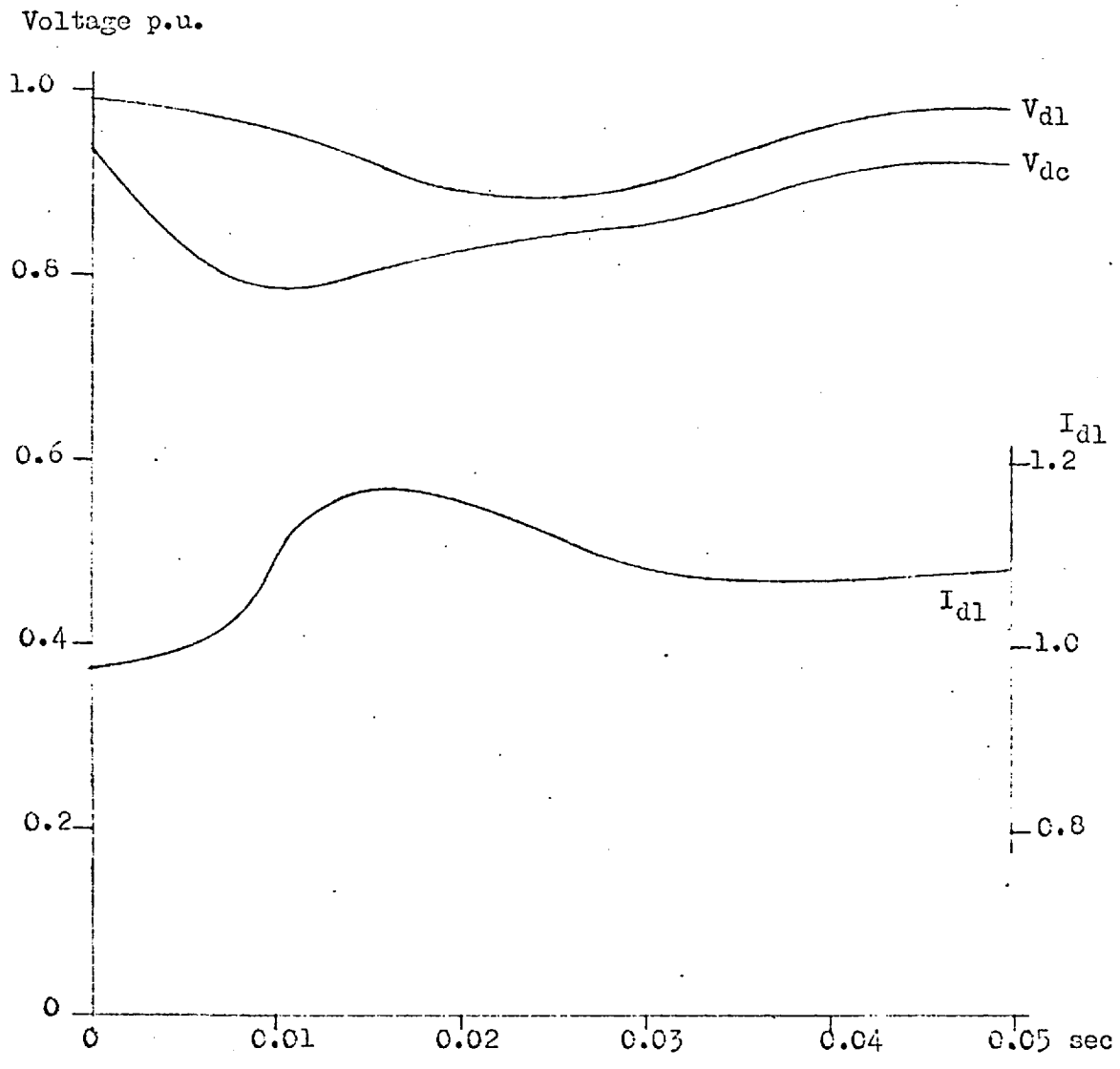

Fig. 5.7 Change of current order from 0.98 to 1.1 p.u.

V_{dl}, I_{dl} = rectifier side direct voltage & current

V_{dc} = d.c. line mid-point voltage

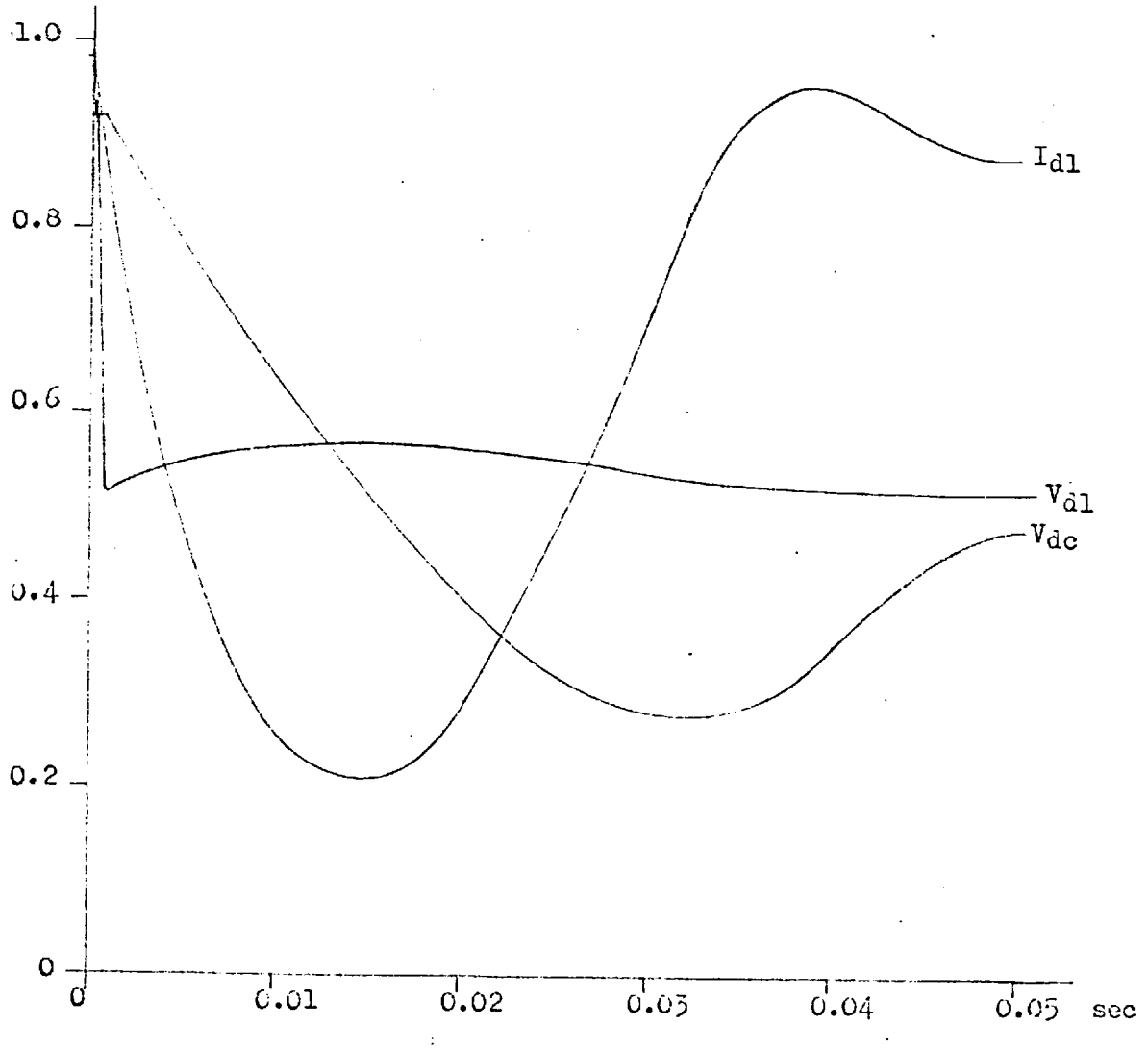

Fig. 5.8 Blocking one bridge at rectifier

V_{dl}, I_{dl} = rectifier side direct voltage & current

V_{dc} = d.c. line mid-point voltage

concept that converter operation is sequential in nature and normally either 2 or 3 values are conducting in each bridge, a process which the authors called "central process". However, the implementation of this representation requires considerable programming effort due to the intricate logics involved, and the finished program takes considerable computing time because of the small integration time step of 0.1 msec used (10 min. on KDF9 to simulate 20 msec). Considerable simplification is possible when the a.c. system e.m.f. is balanced and if the individual phase currents need not be identified. Then only three basic voltage waveforms are sufficient to describe the converter voltage waveform; these are (for a 1-bridge converter):-

$$e_1 = \sqrt{3}\ E \sin \omega t$$

$$e_2 = \sqrt{3}\ E \sin (\omega t - \frac{\pi}{3})$$

$$e_3 = \tfrac{1}{2} (e_1 + e_2) = \frac{3}{2} E \sin (\omega t - \frac{\pi}{6})$$

where E = r.m.s. line voltage. These voltages are shown in Fig. 5.9.

With two valves conducting, the converter output voltage is e_1 between a-b in Fig. 5.9(b) or e_2 between c-d. When three valves are conducting, i.e. during commutation, the output voltage is e_3 between b-c. If the direct current is not constant and the a.c. system resistance is not neglected, then the rectifier output voltage is modified by:

2-valves conducting

$$V_{dl} = e_1 - 2RI_{dl} - 2LpI_{dl}$$

$$\text{or} \quad = e_2 - 2RI_{dl} - 2LpI_{dl}$$

3-valves conducting

$$v_{dl} = e_3 - \frac{3}{2} RI_{dl} - \frac{3}{2} LpI_{dl}$$

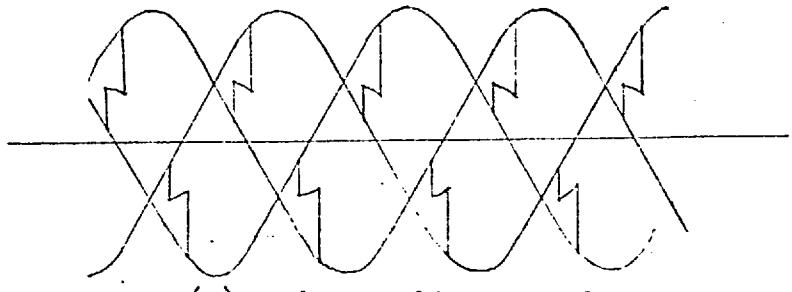

(a) 3-phase voltage waveform

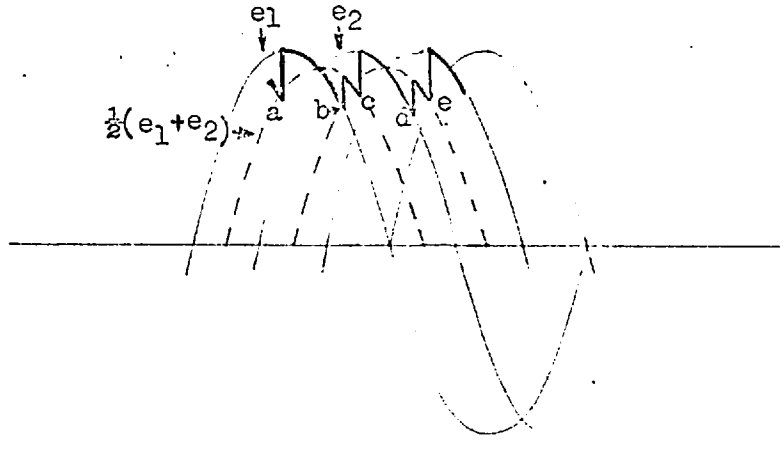

(b) Converter output voltage waveform from (a)

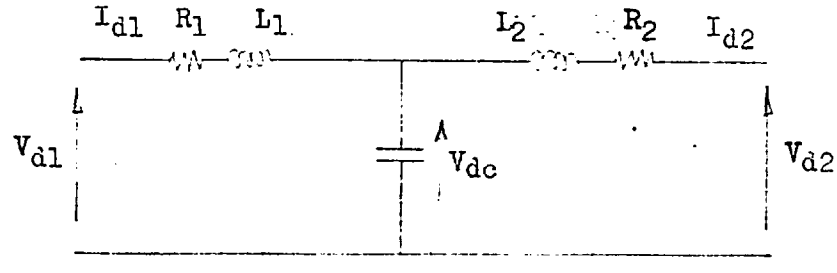

(c) D.C. line representation

Fig. 5.9 Simplified dynamic analysis of converters

where $pI_{dl} = \frac{1}{L_l} (V_{dl} - V_{dc} - R_l I_{dl})$

R,L = resistance and inductance per phase of a.c. system

R_l, L_l = resistance and inductance of half the d.c. line

The equation of commutation current is

$$e_1 = 2R\, i_1 + 2L\, pi_1 - R_l\, I_{dl} - L_l\, pI_{dl}$$

$$\therefore 2L\, pi_1 = e_1 - 2Ri_1 + R_l I_{dl} - \frac{L}{L_l}(V_{dl} - V_{dc} - R_l I_{dl})$$

and the end of commutation is detected by repeated forward and backward integration with reducing time steps until $i_1 - I_{dl} \leq 0.0001$ say.

The equations for inverter output voltage and commentation current are similar. To advance from one valve firing to the next, the voltages e_1, e_2, and e_3 are each advanced by 60 electrical degrees. Firing angles were determined by the controls described in Section 5.3.

One typical result from this simplified representation is given in Fig. 5.10. Typical computing time required was 1 min. on the IBM7090 to simulate 20 msec.

The differential equations in Sections 5.2 - 5.5 were solved by means of the Runge-Kutta integration routine or by using a digital analog simulation language as described in the Appendix. The next section describes an alternative method for solving the d.c. line differential equations and the control equations without using any numerical integration. This method makes use of the techniques of transistion matrix and recursive formulae, based on sampled-data control theory.

5.6 Application of transition matrix and sampled-data control theory to d.c. system analysis.

The transition matrix method, based on the theory of state-variables, offers an alternative way of solving the d.c. line differential equations, and the method of recursive formulae based on sampled-data control theory can determine the output from a transfer function at a given time step from the output at the previous time step. By combining these two methods the transient behaviour of a d.c. link including the effect of its firing angle controls can be

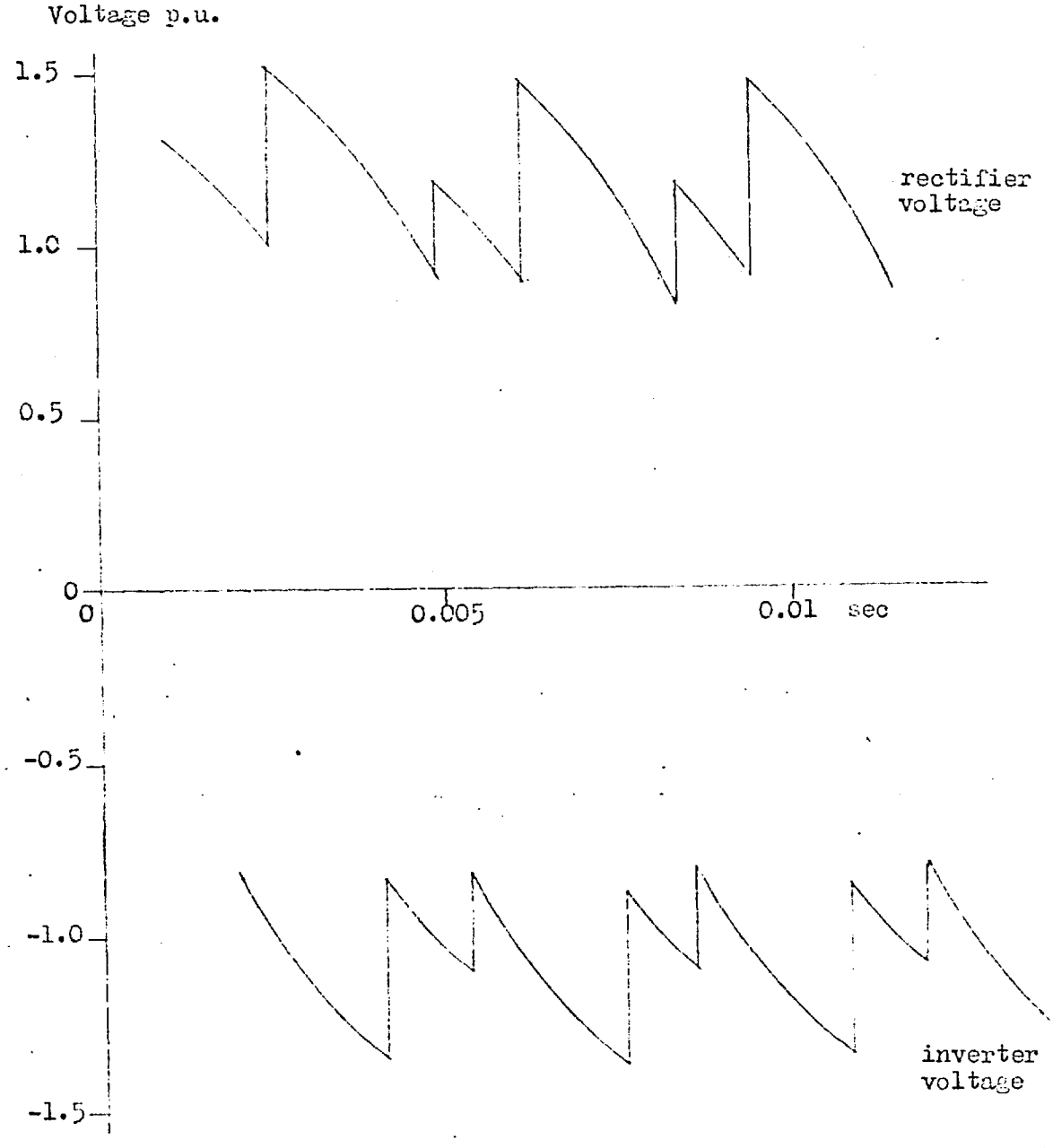

Fig. 5.10 Rectifier & inverter output voltage obtained by simplified analysis

studied without the formal solution of differential equations. This approach may be faster than the usual method of numerical integration if small integration time steps are required. Moreover the theory of state variables has become popular for the analysis of the transient behaviour of a.c. systems as shown, for example, by Iyer[58] and the present work shows that d.c. systems can be included in such analysis.

5.6.1 D.C. line linear state-space equation.

By assuming the d.c. line parameters to be linear, the currents and voltage of the equivalent T- circuit representing the d.c. line can be expressed as a set of linear state-space equations of the form

$$\dot{x}(t) = Ax(t) + Bu(t) \qquad (5.31)$$

where $x(t)$ are state variables and $u(t)$ forcing functions, in the following manner

$$\begin{bmatrix} I_{d1} \\ I_{d2} \\ V_{dc} \end{bmatrix} = \begin{bmatrix} -\frac{R_{11}}{L_{11}} & 0 & -\frac{1}{L_{11}} \\ 0 & -\frac{R_{22}}{L_{22}} & \frac{1}{L_{22}} \\ \frac{1}{C} & -\frac{1}{C} & 0 \end{bmatrix} \begin{bmatrix} I_{d1} \\ I_{d2} \\ V_{dc} \end{bmatrix} + \begin{bmatrix} \frac{1}{L_{11}} & 0 & 0 \\ 0 & -\frac{1}{L_{22}} & 0 \\ 0 & 0 & 0 \end{bmatrix} \begin{bmatrix} V_{d1} \\ V_{d2} \\ 0 \end{bmatrix} \qquad (5.32)$$

In this formulation the currents I_{d1}, I_{d2} and the voltage V_{dc} are the state variables and the converter terminal voltages V_{d1} and V_{d2} are the forcing functions.

The solution of Eq. 5.31 is, from Kuo and Kaiser[56], of the form:-

$$x(t) = e^{At}\, x(o) + e^{At} \int_o^t e^{-At}\, Bu(\tau)dt \qquad (5.33)$$

for a continuous system where e^{At} is the transition matrix. For a discrete system $t = nT$, where T is an increment of time and $n = 0,1,2$ etc., the solution is

$$x(nT) = e^{AnT}\, x(o) + e^{AnT} \int_o^{nT} e^{-At}\, Bu(\tau)dt \qquad (5.34)$$

Alternatively

$$x[(n+1)]T = e^{At}\, x(nT) + e^{A(n+1)T} \int_{nT}^{(n+1)T} e^{-At}\, Bu(\tau)dt \qquad (5.35)$$

which is a recursive equation for finding the response at $t = (n + 1)T$ in terms of the response at $t = nT$.

When the forcing function u(t) is constant during the interval $nT \leq t \leq (n + 1)T$ Eq. 5.35 becomes

$$x[(n + 1)T] = e^{AT} x(nT) + (e^{AT}-I)A^{-1}Bu(nT)$$

$$= Fx(nT) + Gu(nT) \qquad (5.36)$$

where $F = e^{AT}$

$G = (e^{AT}-I)\, A^{-1}B$

with I = identity matrix

When the forcing function u(t) is a delta function during the interval $nT \leq t \leq (n+1)T$, and if the increment of time T is sufficiently small so that the delta function can be treated as if it were at $t = nT$, then Eq. 5.35 becomes

$$x[(n + 1)T] \doteq e^{AT} x(nT) + e^{AT} Bu$$

$$= F[x(nT) + Bu] \qquad (5.37)$$

where u is a constant vector representing the magnitude of the delta function.

The matrix F and G in the above equations can be calculated once and for all at the beginning of computation and a procedure was given by Kuo and Kaiser[56] as follows:-

$$F = e^{AT} = \sum_{k=0}^{\infty} \frac{A^k t^k}{K!} \qquad (5.38)$$

$$G = T \left[\sum_{k=0}^{\infty} \frac{A^k t^k}{(k+1)!} \right] B \qquad (5.39)$$

Since both F and G are infinite series, they can be expanded to as many terms as necessary to give the required accuracy.

In Eq. 5.36, where the forcing function is constant during a given time interval, is suitable for solving the d.c. system equation (Eq. 5.32) where the converter terminal voltages are represented as voltage steps as in Reider.[23] Conversely, when the converter voltages are represented by delta functions, as in Norton and Cory,[26] then Eq. 5.37 is suitable, but the results obtained will then be the increments of the state variables as explained in the paper.

5.6.2 Representation of d.c. control system by recursive formulae

In Section 5.3 the d.c. control systems have been shown in Fig. 5.5 and the transfer functions were transformed into first order

differential equations and solved together with those of the machine and d.c. line equations. This section will show that the transfer functions can be expressed as recursive formulae so that the responses at a given time step can be calculated in terms of the responses at the previous time step. This method was presented by D'Angelo et al[57] and is based on the impulse response of the system, and the output is obtained in a sampled form.

Recursive formula for compensator

The transfer function of the compensator in Laplace operator form is

$$F(s) = K \frac{1 + sT_1}{1 + sT_2} \tag{5.40}$$

and the impulse response in the time domain is

$$\omega(t - \tau) = K \frac{T_1}{T_2} \delta(t - \tau) + \frac{K}{T_2} \left(1 - \frac{T_1}{T_2}\right) \exp\left(- \frac{t - \tau}{T_2}\right) \tag{5.41}$$

and the compensation sampled output y (mT) for an input x(mT) is given by

$$y(mT) = y_1(mT) + y_2(mT) \tag{5.42}$$

where $y_1(mT) = K\frac{T_1}{T_2} x(mT)$

$$y_2(mT) = K.\exp\left(- \frac{T}{T_2}\right) y_2 [(m - 1)T] + K\left(1 - \frac{T_1}{T_2}\right) [1 - \exp\left(- \frac{T}{T_2}\right) x[(m-1)T]$$

where T = sampling rate

Recursive formula for delay

The Laplace transform of the delay function is

$$F(s) = e^{-sT_d}$$

and its recursive equation is

$$y(mT) = y [(m - T_d)T]$$

where T_d = delay dead time

5.6.3 Combination of transition matrix and recursive methods.

By using the transition matrix method in Section 5.6.1 to solve the d.c. line transient equations and the recursive method to obtain the sampled response of the d.c. control system the entire transient behaviour of the d.c. system can be studied without solving directly the differential equations describing the system. A program

was written to simulate the d.c. system including controls as described in Section 5.3 with constant a.c. side voltages, and by choosing a value of T = 1.67 msec to correspond to 12-pulse operation this method of solution was found to be quite fast. It took 1.2 min. of IBM7090 computer time to simulate 1.36 sec. real time.

The alternative to express the compensator transfer function as a recursive equation is to treat the output from the compensator as a state variable and include the first order differential equation of the compensator in the state-space equation of the d.c. line. The advantage of the recursive method is that it can be applied to non-linear transfer functions, for example saturation, or backlash, that cannot be included in the state-space equations, which are only applicable to linear systems.

CHAPTER 6

CONTROL OF D.C. LINK IN THE ISOLATED GENERATOR MODE

6.1 Introduction

This chapter is devoted to the study of the behaviour and control of a generator which is normally connected to the supergrid network and is suddenly isolated so that it supplies only the rectifiers of a h.v.d.c. link. This situation is particularly relevant to the Kingsnorth scheme which is described in a recent paper by Calverley et al[59], where it was stated that studies are to be made into generator performance when connected only to a d.c. link. From such studies the feasibility of connecting an isolated generating station solely to a d.c. link can be assessed.

The present study deals mainly with the behaviour of the generator upon sudden isolation, as a result of which voltage and machine frequency are expected to change. Two different control strategies of the d.c. link are proposed and their effectiveness tested by means of simulation on a digital computer.

The Kingsnorth scheme as described by the above paper is chosen for this study. This is a double pole d.c. link from Kingsnorth to Beddington and Willesden with a total power rating of 640 MW. Fig. 6.1 shows this scheme, from which it is seen that by opening switch S Generator No. 3 will be isolated from the 400 kV system and then supplies the d.c. link alone.

Although this mode of operation, termed the isolated generator mode, is not a normal operating mode, it may arise from the following circumstances:-

(a) experimental purposes

(b) short term operation following certain filter faults in which d.c. transmission is continued with Generator No. 3 isolated to prevent out-flow of excessive harmonics

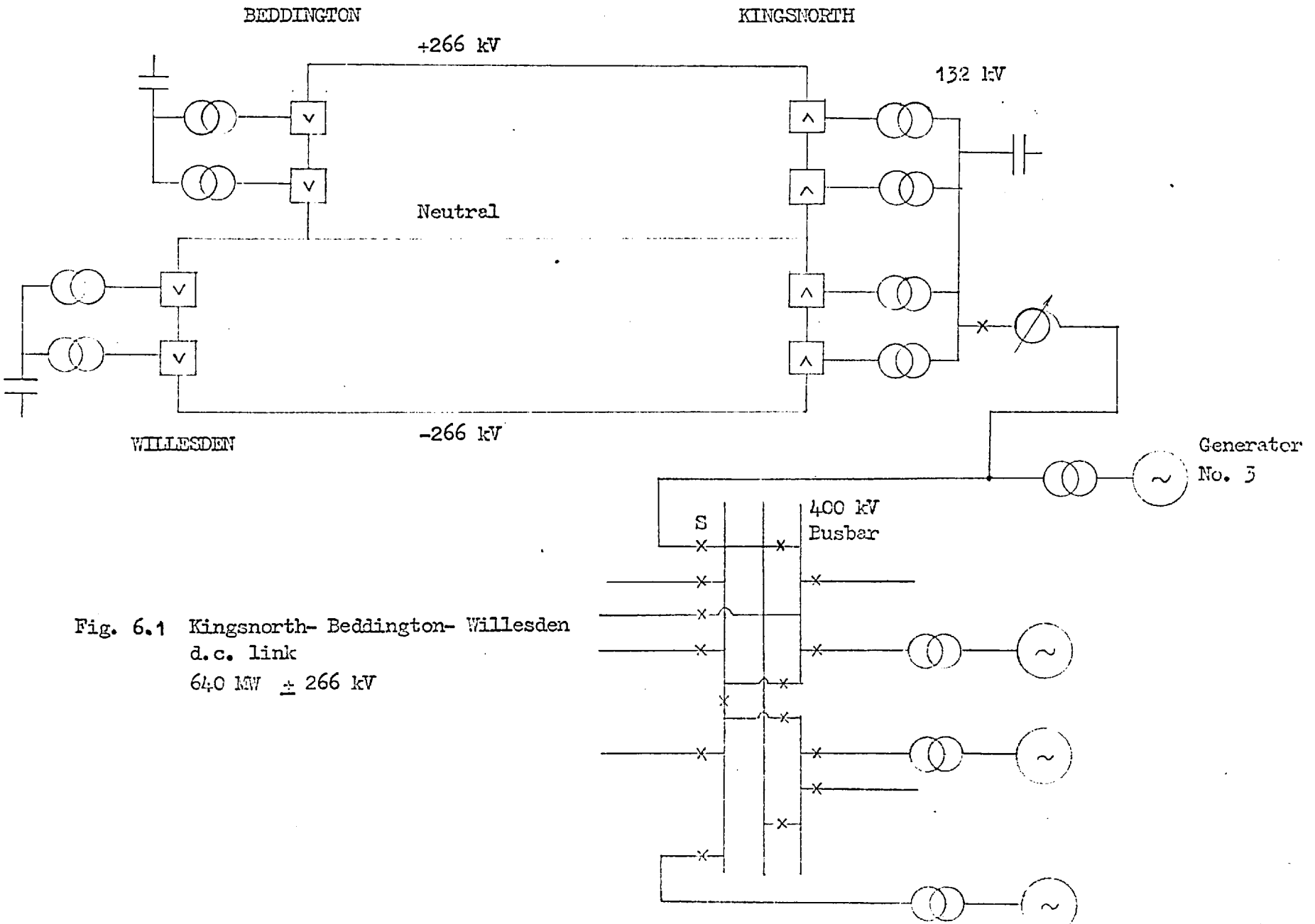

Fig. 6.1 Kingsnorth- Beddington- Willesden
d.c. link
640 MW ± 266 kV

(c) tripping of switch S following a busbar fault

(d) inadvertent tripping of switch S

In cases (a) and (b) the isolation of the generator is more or less planned so that the power order of the d.c. link and active and reactive power output of the machine can be adjusted beforehand to reduce disturbances upon isolation. In cases (c) and (d), however, the machine would be isolated suddenly and since the 500 MW rating of the machine is not the same as the 640 MW rating of the link, and the machine may operate at between 0.85 lagging and 0.98 leading power factor severe disturbances to machine frequency and voltage can be expected. The study and control of these disturbances forms the subject of this chapter.

Bower and Bradbury[60] studied the speed changes of the isolated generator and means of control by considering only the effect of real power and assuming constant busbar voltage at the rectifiers. It is well known, however, that the operation of converters is heavily dependent on voltage so that the assumption of constant voltage is really too drastic. This study considers both real and reactive power flows and no assumption is made of the rectifier busbar voltage. The busbar voltage was calculated from the generator voltage behind sub-transient reactance.

More recently Cladé and Persoz[61] carried out an analytical study of the dynamic behaviour of a generator connected to a d.c. link. Small signal analysis was used to determine the transfer functions relating direct current to generator field voltage, turbine throttle valve position and the firing angle of converters. Although some critical values of controller gain and time constants were presented, no control strategy of the converters was suggested. Moreover this study considered the effect of small perturbations when the generator was already operating steadily into the d.c. link and paid no attention to its behaviour in the short period after isolation.

6.2 Network Used in Study

In the present study the whole supergrid network for the year 1971/72 comprising some 300 nodes was reduced by means of a network reduction program to a network of 5 basic nodes, viz: the three D.C. terminals of Kingsnorth, Beddington and Willesden, plus Dungeness and Waltham Cross. These 5 nodes together with the lower voltage busbars at the three d.c. terminals form an 11 node study network as shown in Fig. 6.2. Although a larger network can be dealt with, the network adopted was thought to be of a convenient size which represents the Kingsnorth scheme adequately.

The a.c./d.c. load flow program described in Chapter 4 was used to establish the steady state conditions of the a.c. and d.c. systems, and selected result, are indicated in Table 6.1

Table 6.1

Kingsnorth 400 kV bus voltage	= 0.95 p.u.
Kingsnorth converter bus voltage	= 0.98 p.u.
D.C. link current of both poles	= 1200 amps
D.C. link voltage of both poles	= 266 kV
Firing angle of rectifiers	= 17°
Tap setting of Kingsnorth 400/132 kV autotransformer	= 1.1
Tap setting of Kingsnorth converter transformers	= 0.965

If the 400 kV circuit breaker S at Kingsnorth is opened Generator No. 3 becomes isolated from the system and is connected solely to the converters. Since the centre of interest lies in the behaviour of the generator upon isolation it is necessary only to consider the simple combination of the generator plus the d.c. link. A further simplification can be made by assuming that the Kingsnorth converters are controlled independently from the inverters. Generator No. 3 will then be feeding a controlled rectifier load, both independent of the rest of the system,

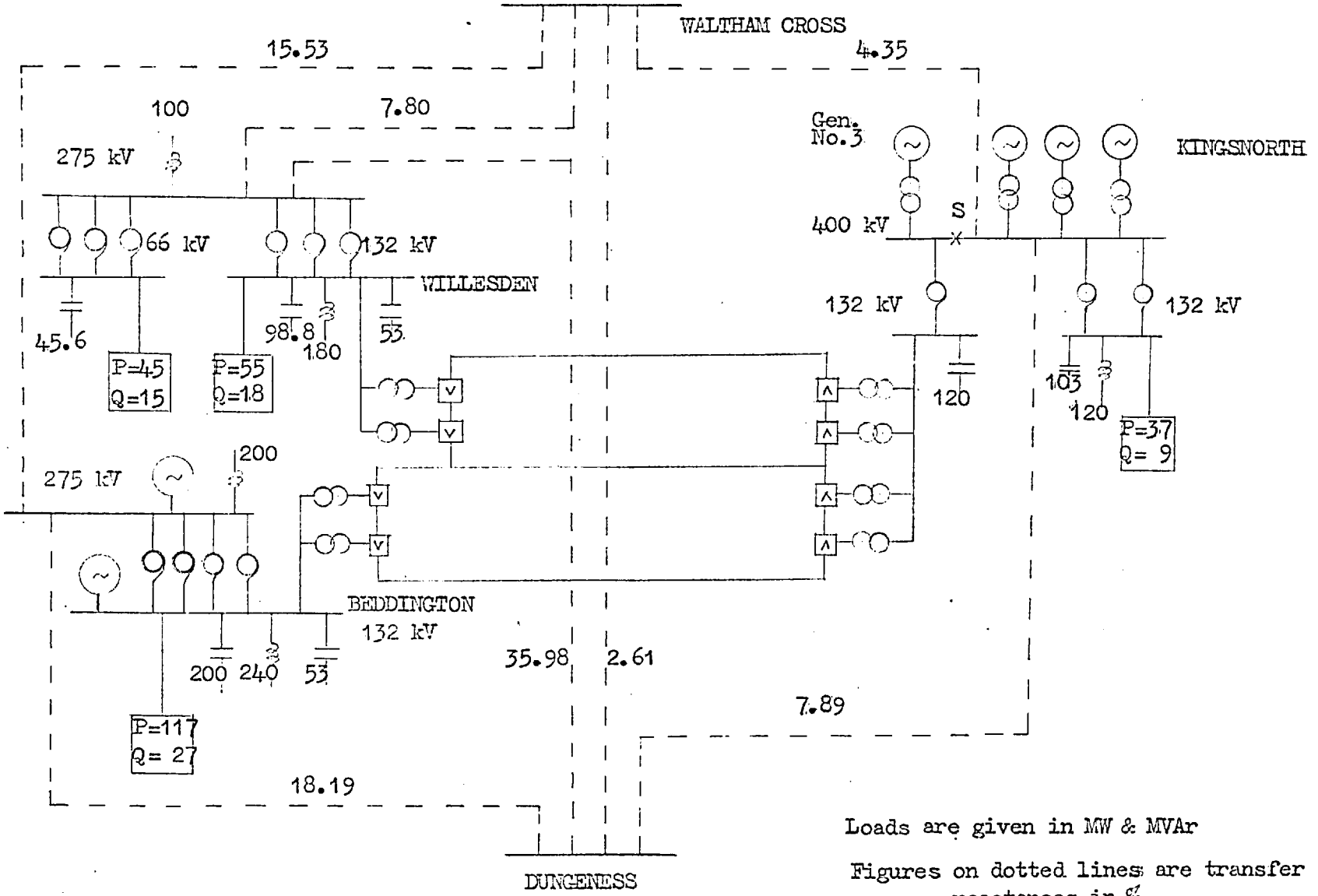

Loads are given in MW & MVAr

Figures on dotted lines are transfer reactances in %

Shunt reactors and cable capacitance are given in MVA

Fig. 6.2 Reduced network for study

which is ignored. Hence upon isolation only the generator and the rectifiers are considered; Fig. 6.3 shows this connection schematically.

6.3 Analysis of Generator Behaviour upon Isolation to d.c. Link

With the system to be studied simplified to a single generator feeding a controlled rectifier load greater attention could be paid to both. The generator was represented by voltage behind subtransient reactance, together with detailed representation of turbine, governor and a.v.r. The converters were represented as equivalent current sources, and to study the effect of the d.c. link in the behaviour of the generator upon isolation two control methods of the link, that of frequency control of current order and progressive block and deblock of converters, were tried.

The structure of the program used in this study is shown in Fig. 6.4. The representation of generator, turbine, governor, a.v.r. and converters are explained below.

Fig. 6.4 Structure of Program

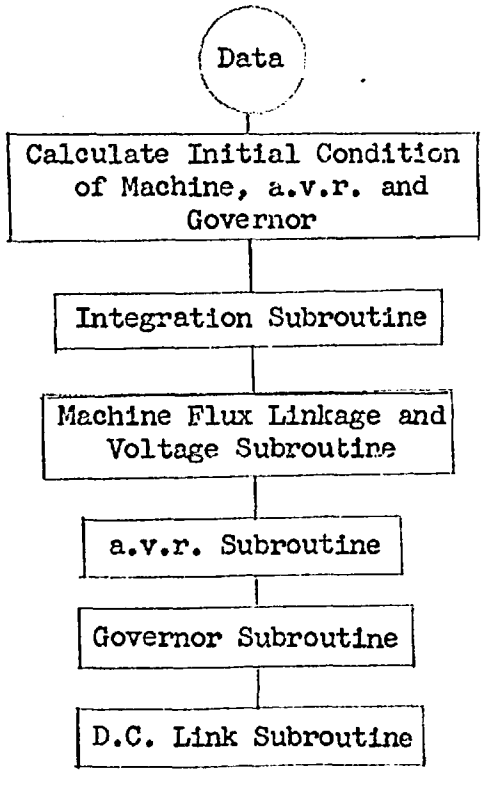

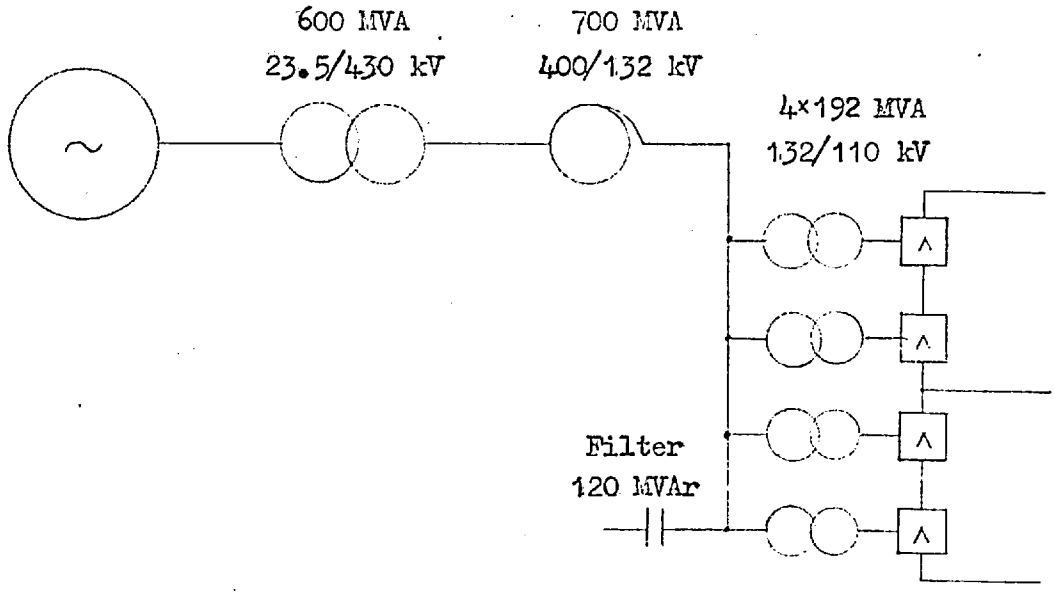

Fig. 6.3 Simplified circuit diagram of Generator No.3 supplying converters at Kingsnorth.

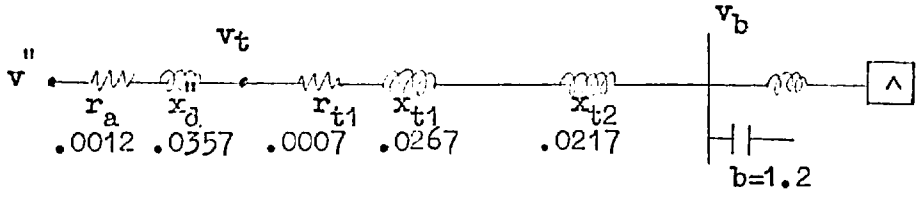

Fig.6.3a Parameters of above circuit in per unit on 100 MVA

6.3.1 Representation of Generator

The generator was represented by a voltage behind sub-transient reactance and the two-axis components were:

$$v_d'' = - sx_q'' i_q + \omega_o (x_q'' - x_a) \frac{\psi_{kq}}{x_{kq}} \tag{6.1}$$

$$v_q'' = sx_d'' i_d - \omega_c (1 - s) (x_d'' - x_a) \left(\frac{\psi_f}{x_{fl}} + \frac{\psi_{kd}}{x_{kd}}\right) \tag{6.2}$$

where s = slip and the corresponding voltages at the terminal were

$$v_d = v_d'' + r_a i_d - x_q'' i_q \tag{6.3}$$

$$v_q = v_q'' + x_d'' i_d + r_a i_q \tag{6.4}$$

The fluxes were given by the following equations:

$$p\psi_f = e_f + \frac{1}{T_{do}'} \left\{ \frac{x_d'' - x_a}{x_d' - x_a} \left(\frac{x_{md} i_d}{\omega_o} + \frac{x_{md} \psi_{kd}}{x_{kd}} \right) - \psi_f \left[1 + \frac{(x_d'' - x_a) x_{md}}{x_{fl} x_{kd}} \right] \right\} \tag{6.5}$$

$$p\psi_{kd} = \frac{1}{T_{do}''} \left[\frac{x_d' - x_a}{\omega_o} \cdot i_d + \frac{x_d' - x_a}{x_{fl}} \cdot \psi_f - \psi_{kd} \right] \tag{6.6}$$

$$p\psi_{kq} = \frac{1}{T_{qo}''} \left(\frac{x_{mq}}{\omega_o} \cdot i_q - \psi_{kq} \right) \tag{6.7}$$

and the flux linkages on the d - and q - axis were:

$$\psi_d = \frac{1}{\omega_o} \left[x_d'' i_d + \omega_o (x_d'' - x_a) \left(\frac{\psi_f}{x_f} + \frac{\psi_{kd}}{x_{kd}} \right) \right] \tag{6.8}$$

$$\psi_q = \frac{1}{\omega_o} \left[x_q'' i_q + \omega_o (x_q'' - x_a) \frac{\psi_{kq}}{x_{kq}} \right] \tag{6.9}$$

The electromagnetic torque was given by

$$T_e = \tfrac{1}{2} \left[(x_d'' - x_q'') i_d i_q - v_q'' i_q - v_d'' i_d \right] \tag{6.10}$$

The above equations neglect the $p\psi_d$ and $p\psi_q$ terms but include the effect of damping.

From given active power, power factor and terminal voltage a subroutine calculated the steady state values of axis voltages and currents, flux linkages and load angle as shown in Reference 54.

A subroutine calculated new values of v_d'', v_q'', v_d and v_q from the new values of flux linkages and currents.

The values of x_{kd}, x_{kq}, T_{do}', T_{do}'' and T_{qo}'' were calculated from the basic machine parameters shown in Table 6.2.

Table 6.2 Parameters of Kingsnorth Generator No. 3

Machine rating	588 MVA at 0.85 lagging p.f.	
Machine output voltage	23.5 kV	
Direct axis synchronous reactance	x_d	2.98 p.u.
Direct axis transient reactance	x_d'	0.25 p.u.
Direct axis sub-transient reactance	x_d''	0.17 p.u.
Quadrature axis synchronous reactance	x_q	2.6 p.u.
Quadrature axis sub-transient reactance	x_q''	0.21 p.u.
Armature resistance	r_a	0.00115 p.u.
Armature leakage reactance	x_a	0.17 p.u.
Rotor resistance	r_f	0.14 ohm
Direct axis transient short circuit time constant	T_d'	0.8 sec
Direct axis sub-transient short circuit time constant	T_d''	0.03 sec
Inertia constant of generator and turbine	H	3.48

6.3.2 Representation of a.v.r.

The a.v.r. on this generator has a magnetic amplifier and an a.c. main exciter whose output is rectified and supplied to the generator field; there is also a single stabilising feedback loop.

In this study the a.v.r. was represented by the model shown in Fig. 6.5 and was described by the following equations given by Fagg and Whorrod [62] :-

$$E_{smr} = - \frac{G_r (E_m - E_o)}{1 + pT_{sm}} \tag{6.11}$$

$$E_{fer} = \frac{G_a (E_{smr} + E_{str})}{1 + pT_d} \tag{6.12}$$

$$E_{fer}(min) \leq E_{fer} \leq E_{fer}(max) \tag{6.13}$$

$$I_{fer} = \frac{G_f E_{fer}}{1 + pT_f} \tag{6.14}$$

$$E_{str} = - \frac{pT_{st}}{1 + pT_{st}} I_{fer} \tag{6.15}$$

$$E_r = G_{ex} I_{fer} \tag{6.16}$$

The rotor voltage E_r, after conversion to per unit, became the voltage e_f required in Eq. 6.5.

The parameters of the a.v.r. are given in Table 6.3 below

Table 6.3 a.v.r. parameters

Voltage control input gain	G_r	0.025
Amplifier gain	G_a	9.3
Exciter field gain	G_f	1.61
Exciter gain	G_{ex}	6.0
Smoothing circuit time constant	T_{sm}	0.01 sec
Delay time constant	T_d	0.013 sec
Exciter field time constant	T_f	0.60 sec
Stabiliser time constant	T_{st}	2.0 sec
	$E_{fer}(min)$	0 V
	$E_{fer}(max)$	155 V

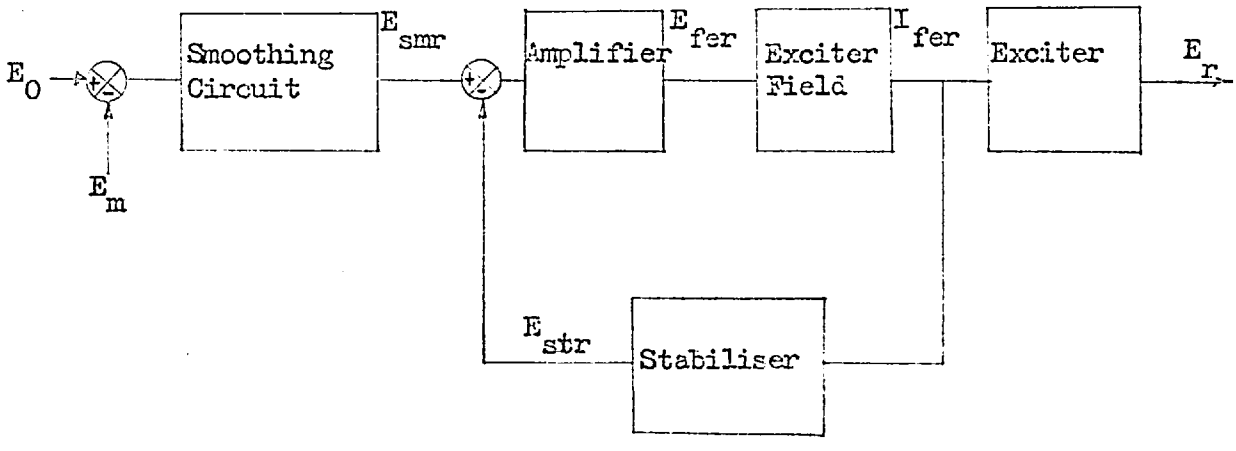

Fig. 6.5 Block diagram of avr

A subroutine calculated the steady state values of the variables used in the model and another subroutine calculated the voltage E_r for each integration step.

This a.v.r. model was verified by simulating an actual test on the generator where, with the machine open-circuited, the reference voltage E_o was given a step change from 22 kV to 24 kV. The computed and test results are shown in Fig. 6.6.

It was noticed, however, that for some of the studies described later the voltage E_r exceeded the a.v.r. rated voltage (590 V) and it was therefore necessary to apply a limit to E_r of 600 V. as a rough approximation to the effect of saturation in the main exciter.

6.3.3 Representation of turbine and Governor

A rather detailed representation of the turbine and governor was used in this simulation because it was realised that the operation of the throttle and interrupter valves would have a strong effect on the speed of the machine, particularly when working in the isolated mode.

This representation was taken from Bower and Bradbury[60] and is shown in Fig. 6.7.

The equations in per unit used were:

High pressure turbine

$$\varepsilon = f_{set} - f_g \tag{6.17}$$

$$Y'_h = Y_{ho} - G_1 \varepsilon \tag{6.18}$$

$$Y_h = F_h\,(Y'_h) \tag{6.19}$$

$$X_h = Y_h + A_g \tag{6.20}$$

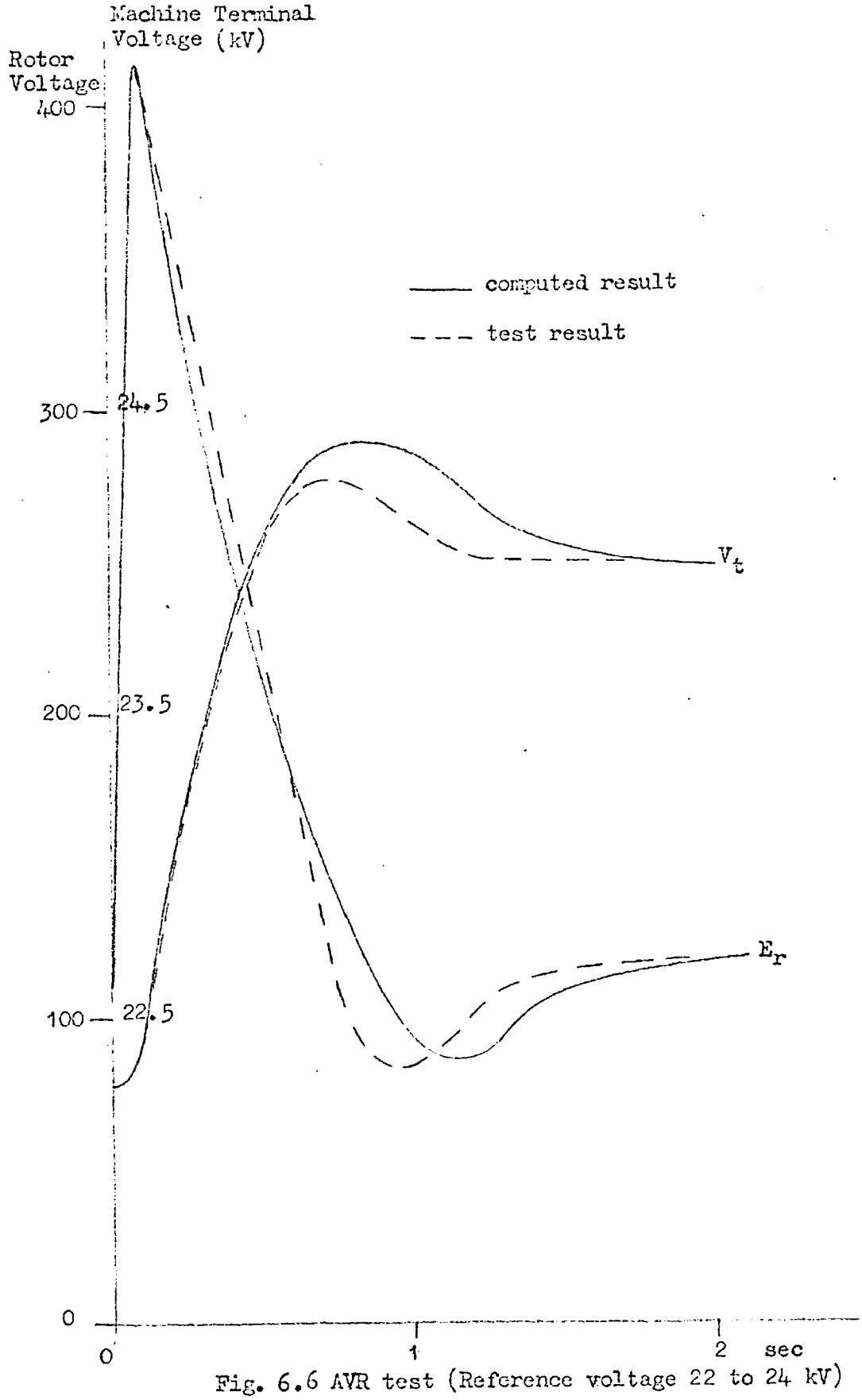

Fig. 6.6 AVR test (Reference voltage 22 to 24 kV)

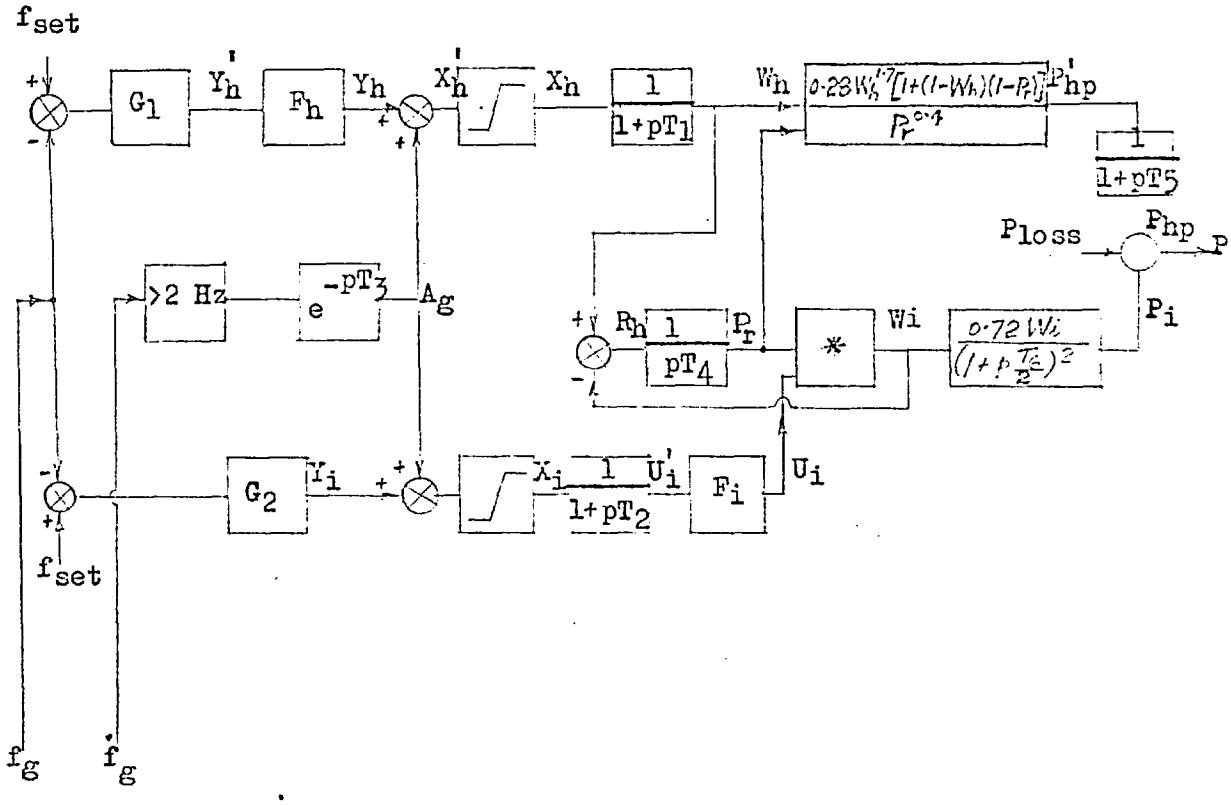

Fig. 6.7 Block diagram of Governor and Turbine

$$0 \leq X_h \leq 1 \tag{6.21}$$

$$W_h = \frac{1}{1 + pT_1} X_h \tag{6.22}$$

$$P_h' = \frac{0.28 W_h^{1.7} [1 + (1 - W_h)(1 - P_r)]}{P_r^{0.4}} \tag{6.23}$$

$$P_h = \frac{1}{1 + pT_5} P_h' \tag{6.24}$$

Intermediate and low pressure turbine

$$Y_i = Y_{io} - G_2 \varepsilon \tag{6.25}$$

$$X_i = Y_i + A_g \tag{6.26}$$

$$0 \leq X_i \leq 1 \tag{6.27}$$

$$U_i' = \frac{1}{1 + pT_2} X_i \tag{6.28}$$

$$U_i = F_i (U_i') \tag{6.29}$$

$$W_i = U_i P_r \tag{6.30}$$

$$P_i = \frac{0.72}{(1 + \frac{pT6}{2})\ 2} W_i \tag{6.31}$$

Acceleration governor

$$A_g = 0 \qquad \text{for } f_g < 2 \text{ Hz/sec} \tag{6.32}$$

$$A_g = f_g \exp^{-pT_3} \text{ for } f_g \geq 2 \text{ Hz/sec} \tag{6.33}$$

Reheat

$$P_r = \frac{1}{pT_4} (W_h - W_i) \tag{6.34}$$

where ε = frequency error

Y_h = governor position

Y_{ho} = initial governor position

F_h = function to represent non-linear governor characteristic

A_g = acceleration governor position

X_h = throttle valve position

W_h = high pressure steam mass flow

P_h = high pressure turbine output power

X_i, Y_i = intermediate variables

Y_{io} = initial value of Y_i

U_i = intercepter valve position

F_i = non-linear interception valve characteristic

W_i = intermediate and low pressure steam mass flow

P_i = IP and LP turbine output power

A_g = output from acceleration governor

P_r = reheat pressure

The parameters used are given in Table 6.4.

Table 6.4 Governor Parameters

Governor gain G_1	4%	
Intercepter value gain G_2	2%	
Throttle value time constant T_1	'close'	0.15 sec
	'open'	1.0 sec
Intercepter value time constant T_2	'close'	0.25 sec
	'open'	4.0 sec
Acceleration governor delay T_3	'operate'	0.14 sec
	'reset'	0.35 sec
Reheat time constant T_4		14.4 sec
H.P. cylinder time constant T_5		0.15 sec
IP & LP cylinder time constant T_6		0.51 sec

A subroutine calculated the steady state values of all the variables and another subroutine calculated their new values in each integration step. The validity of this model was checked against the manufacturer's curves and the comparison is shown in Fig. 6.8.

6.3.4 Representation of Converters

The converters were assumed to operate continuously by neglecting the effect of individual valve firing and were represented as equivalent current injections. If the direct current was i_d (p.u.) and the firing angle of the converters was α then the direct voltage v_d (p.u.) was given by

$$v_d = \frac{B'}{B}\left(n\, e_c \cos\alpha - \frac{\pi}{6} x_c\, i_d - \frac{\pi^2}{9} r_c i_d\right) \qquad (6.35)$$

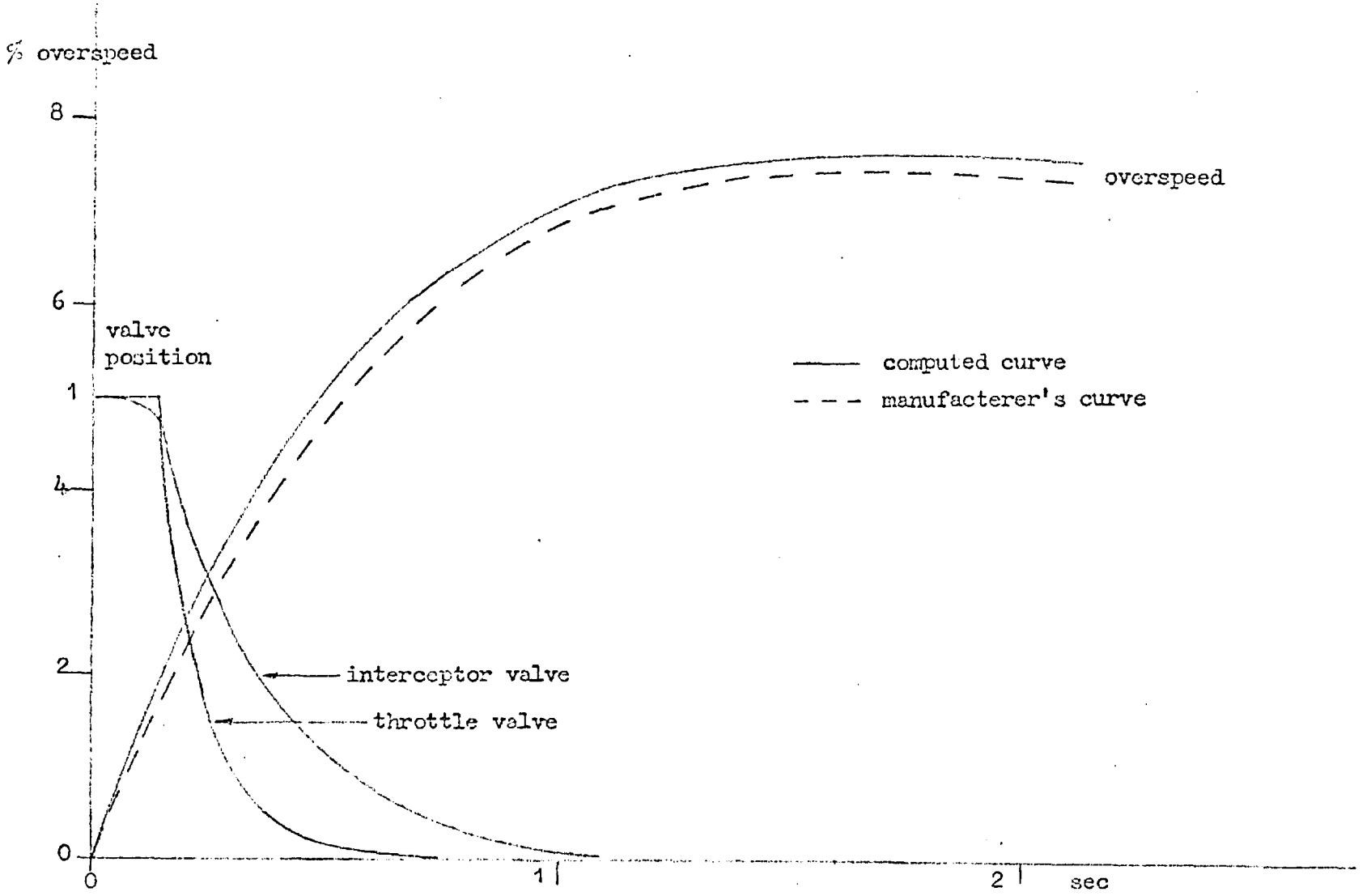

Fig. 6.8 Governor test (Full load rejection)

where B = number of valve groups in the per unit system used

B' = actual number of valve groups in service

n = tap ratio of converter transformer

e_c = commutating voltage = rectifier bus voltage (p.u.)

x_c = commutating reactance (p.u.)

r_c = commutating resistance (p.u.)

The in-phase and quadrature components of the equivalent converter current with reference to the commutating voltage e_c are given by

$$i_p = \frac{1}{e_c}\left(v_d\ i_d + \frac{2}{\pi} r_c\ i_d^{\,2}\right) \tag{6.36}$$

$$i_q = i_p \left\{ \frac{2u + \sin 2\alpha - \sin 2(\alpha + u)}{2\left[\cos^2\alpha - \cos^2(\alpha + u)\right]} \right\} \tag{6.37}$$

with u given by the relation

$$\cos\alpha - \cos(\alpha + u) = \frac{1}{ne_c}\ \frac{\pi}{3}\ x_c\ i_d \tag{6.38}$$

The equivalent converter current for each pole of the double-pole d.c. link was given by

$$\bar{i}_v = (i_p - j i_q) \tag{6.39}$$

At this stage only the voltage behind sub-transient reactance of the generator was known and the rectifier bus voltage e_c had to be found by the following iterative process. By assuming an initial value for e_c the total equivalent current at the converter terminal was

$$\bar{i} = \bar{i}_{v1} + \bar{i}_{v2} + jbe_c \tag{6.40}$$

where b = susceptence of filter capacitor at nominal frequency, and $\bar{i}_{v1}$ and $\bar{i}_{v2}$ were the equivalent converter currents of the first and second poles of the d.c. link.

From $\bar{i}$ and e_c the voltage $\bar{v}''$ behind sub-transient reactance was found. If the magnitude of $\bar{v}''$ was not equal to that obtained from the generator equations a process of linear interpolation was used to find a value of e_c to satisfy this condition.

The current $\bar{i}$ was now related to the d- and q- axis of the generator as follows:

$$i_d = - \bar{i} \sin \phi \tag{6.41}$$

$$i_q = - \bar{i} \cos \phi \tag{6.42}$$

$$\text{where } \phi = \tan^{-1} \frac{v_{d}''}{v_{q}''} - \tan^{-1} \bar{i} + \tan^{-1} (\bar{v}'') \tag{6.43}$$

with $\bar{i}$ and $\bar{v}''$ both referring to the same phasor e_c.

The current margin was assumed to be crossed when the direct voltage as obtained from Eq. 6.35 with $\alpha = \alpha_o = 7^o$ was less than the rated d.c. line voltage.

6.3.5 Control Schemes for d.c. link upon Generator Isolation

Two basic schemes for controlling the operation of the d.c. links were tested. These were:-

(a) frequency - control of current order

(b) progressive block and deblock of converters

6.3.5. (a) Frequency - Control of Current Order

The current order of the d.c. links was controlled by the frequency of the generator upon isolation, so that

$$I_{dc} = \frac{G}{1 + pT} (f_g - f_o) \tag{6.44}$$

where f_o and f_g are the reference frequency and actual generator frequency respectively , and

$$I_{dc} < I_{dc\ max} \tag{6.45}$$

6.3.5. (b) Progressive Block and Deblock of Converters

In this scheme the valve groups of the links were controlled by the converter bus voltage. If the voltage dropped upon isolation of the generator it was first assumed that the current margin was crossed and the firing angle of the converters was reduced to α_o (7^o). If the voltage continued to fall the valve groups were progressively blocked as follows: one group of one pole, then one group of the other pole, and finally the remaining group of both poles. The blocking of valve group or poles removed both active and reactive power demand from the generator and allowed the voltage to recover. At specified stages of voltage recovery the valve groups were deblocked in the reverse order of blocking. The block and deblock schedule in terms of converter bus voltage v_b used in this trial study was summarised below:-

$v_b < 0.75$ p.u. - block 1 group of first pole

$v_b > 0.8$ p.u. - deblock above group

$v_b < 0.65$ p.u. - block 1 group of second pole

$v_b > 0.7$ p.u. - deblock above group

$v_b < 0.55$ p.u. - block both poles

$v_b > 0.6$ p.u. - deblock both bridges of both poles

If both poles of the d.c. link were blocked, then on voltage recovery all valve groups were assumed to be deblocked simultaneously, the current order was assumed to be reinstated at a constant rate.

6.4 Computer Studies and Results

The two control schemes were applied to the d.c. link with the generater supplying its rated power of 500 MW at different power factors before isolation. The converters absorbed approximately 200 MVAr at full load after allowing for the reactive power generated by the filters.

If the machine delivers the same amount of reactive power to the converters at the moment of isolation the change in converter bus voltage would be small. On the other hand the voltage change would be high if the machine was absorbing reactive power just before isolation. The worst case occurred when it was operating at its design reactive capability at 0.98 leading power factor.

6.4.1 No control P = 500 MW, Q = 0 (Fig. 6.9)

This study was a trial and aimed at finding the response of the generator when there was no additional control applied to the converters other than the ordinary constant current control.

If the generator had been supplying full load (500 MW) at unity power factor at a terminal voltage of 1.02 p.u. and the converter bus voltage was 0.98 p.u., upon isolation the machine terminal voltage dropped to 0.82 and the converter bus voltage to 0.68, still rapidly falling. If the converters continued to operate at low bus voltage then the machine terminal voltage was seen to reach a minimum of 0.54 before it rose. Power transmitted by the rectifiers dropped because of the reduced bus voltage so that the machine accelerated and the frequency rose, reaching a maximum of 52.2 HZ. Both the main and intercepter valves closed rapidly. As voltage was gradually restored, power through the rectifier increased so that the machine slowed down and the main and intercepter valves opened. Eventually the voltage was restored but the machine frequency dropped below 41 HZ.

A study with the generater supplying full load at 0.98 leading power factor showed that the voltage drop was far worse than the above case, as can be expected from the bigger reactive power swing. The machine terminal voltage fell sharply to 0.47 p.u. in 0.1 sec after isolation, while the converter bus voltage dropped below 0.2 p.u. Computation was therefore discontinued.

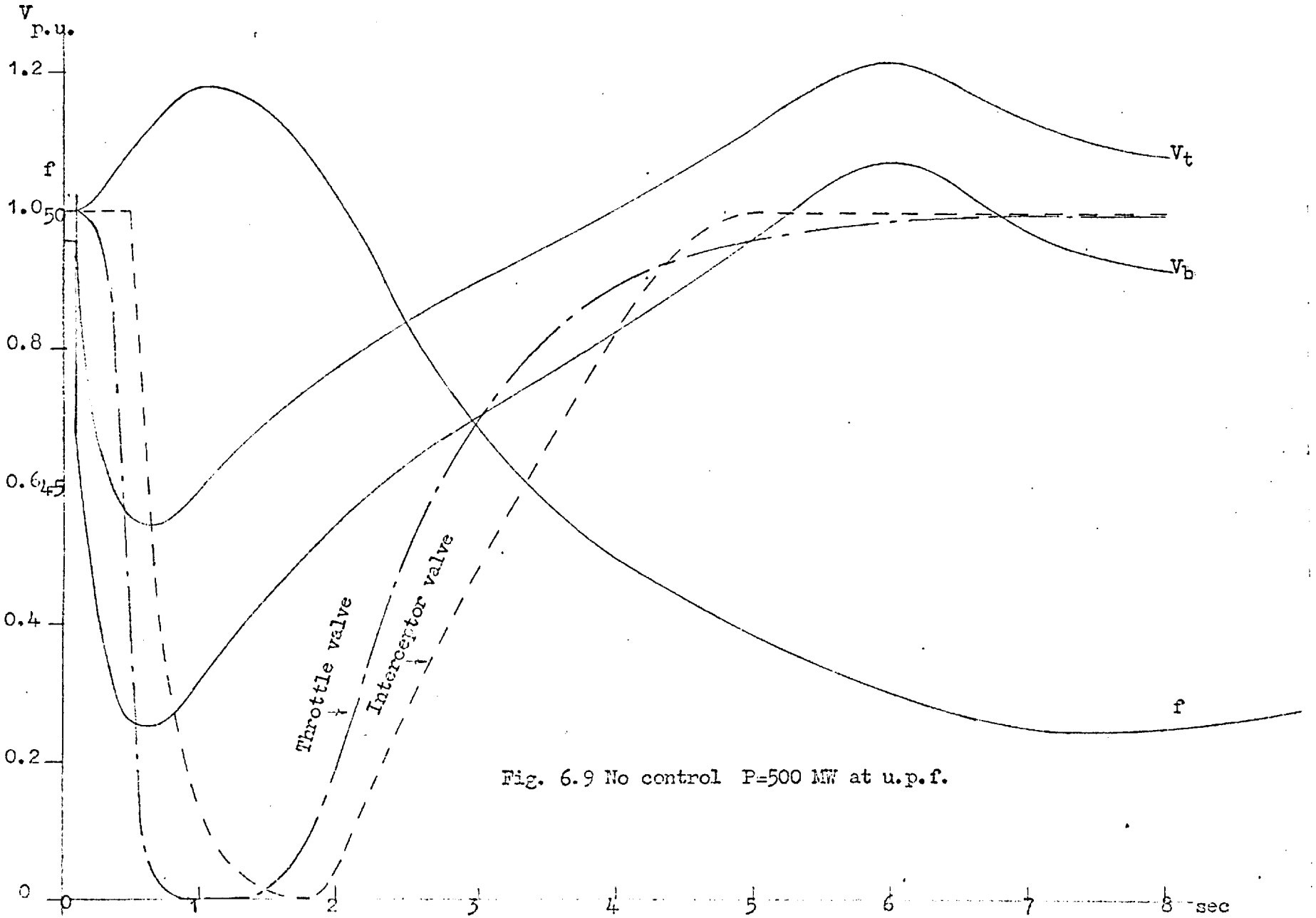

Fig. 6.9 No control P=500 MW at u.p.f.

6.4.2 Frequency control of current order I_{dc} (Fig. 6.10 - 6.12)

In these series of studies the direct current order I_{dc} was controlled by the frequency of the generator through a simple time delay.

The first study assumed the generator to be supplying full power at 0.85 power factor lagging with the frequency control having a gain of 1200 and a time constant of 0.01 seconds. Upon isolation the converter bus voltage fell immediately to 0.85 from an initial value of 0.98 (Fig. 6.10). The frequency control of I_{dc} was effective in reducing the fluctuation in machine frequency. Although the generator terminal voltage, converter bus voltage and I_{dc} oscillated, they showed a tendency to settle down in about 4 seconds after isolation.

A second study was made using the same gain and time constants for frequency control, but with the generator supplying full load at unity power factor (Fig. 6.11) showed that upon isolation there was a rapid fall in voltage and a corresponding drop in d.c. power transmission. The machine accelerated so that I_{dc} increased and caused the voltage to drop further. As the frequency of the generator swing to below 50 HZ the current order was rapidly reduced causing a sudden rise in voltage. The responses in this case were entirely unsatisfactory.

The parameters of the frequency control was therefore altered to a gain of 600 and a time constant of 0.05 second. Additionally in order to overcome the difficulty of increased current order when the voltages fell, I_{dc} was halved to 600 A from 1200 A upon isolation. The results in Fig. 6.12 shows that this scheme was effective in preventing any sudden changes in voltage and the frequency was kept fairly smooth.

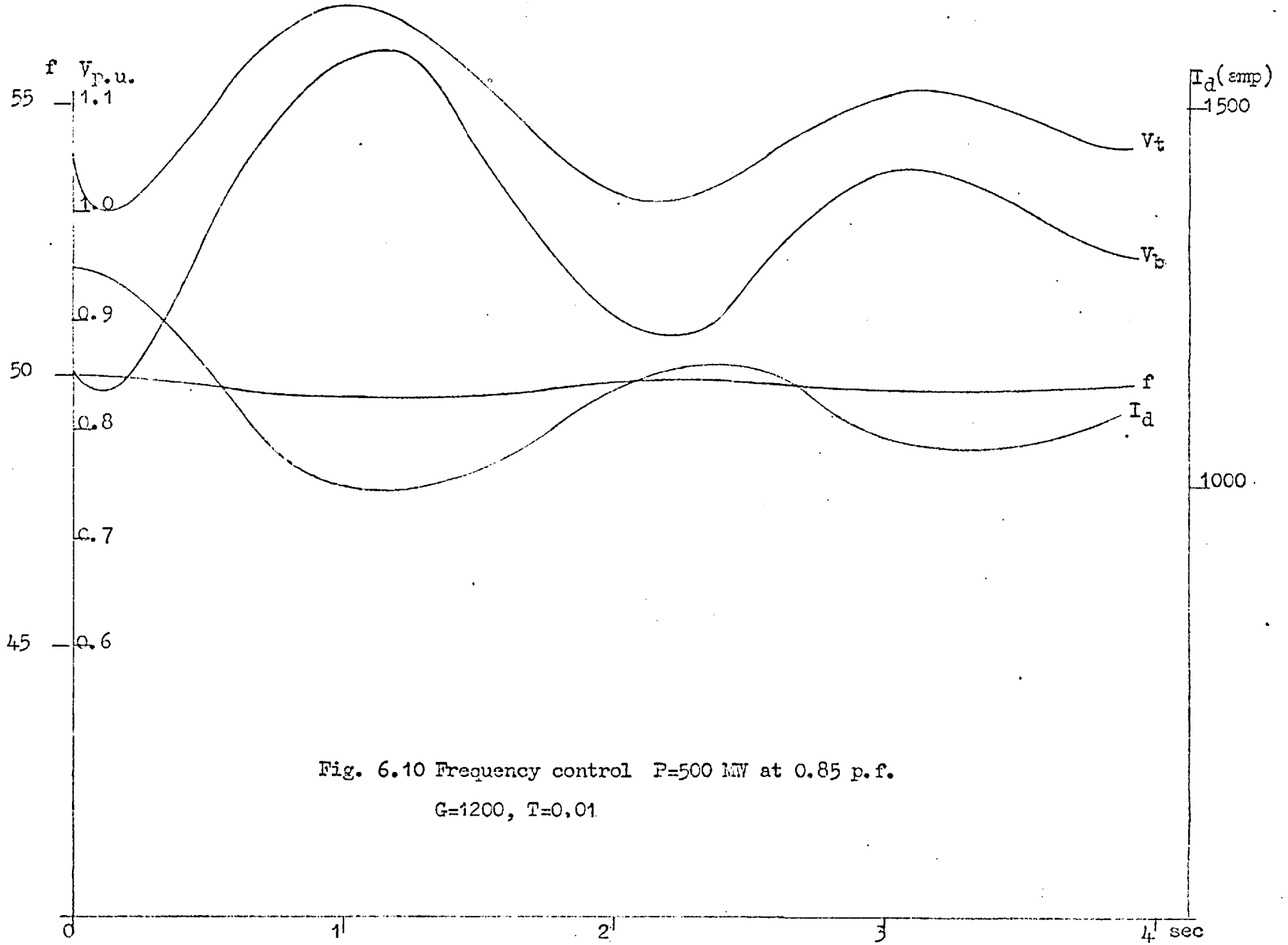

Fig. 6.10 Frequency control P=500 MW at 0.85 p.f.

G=1200, T=0.01

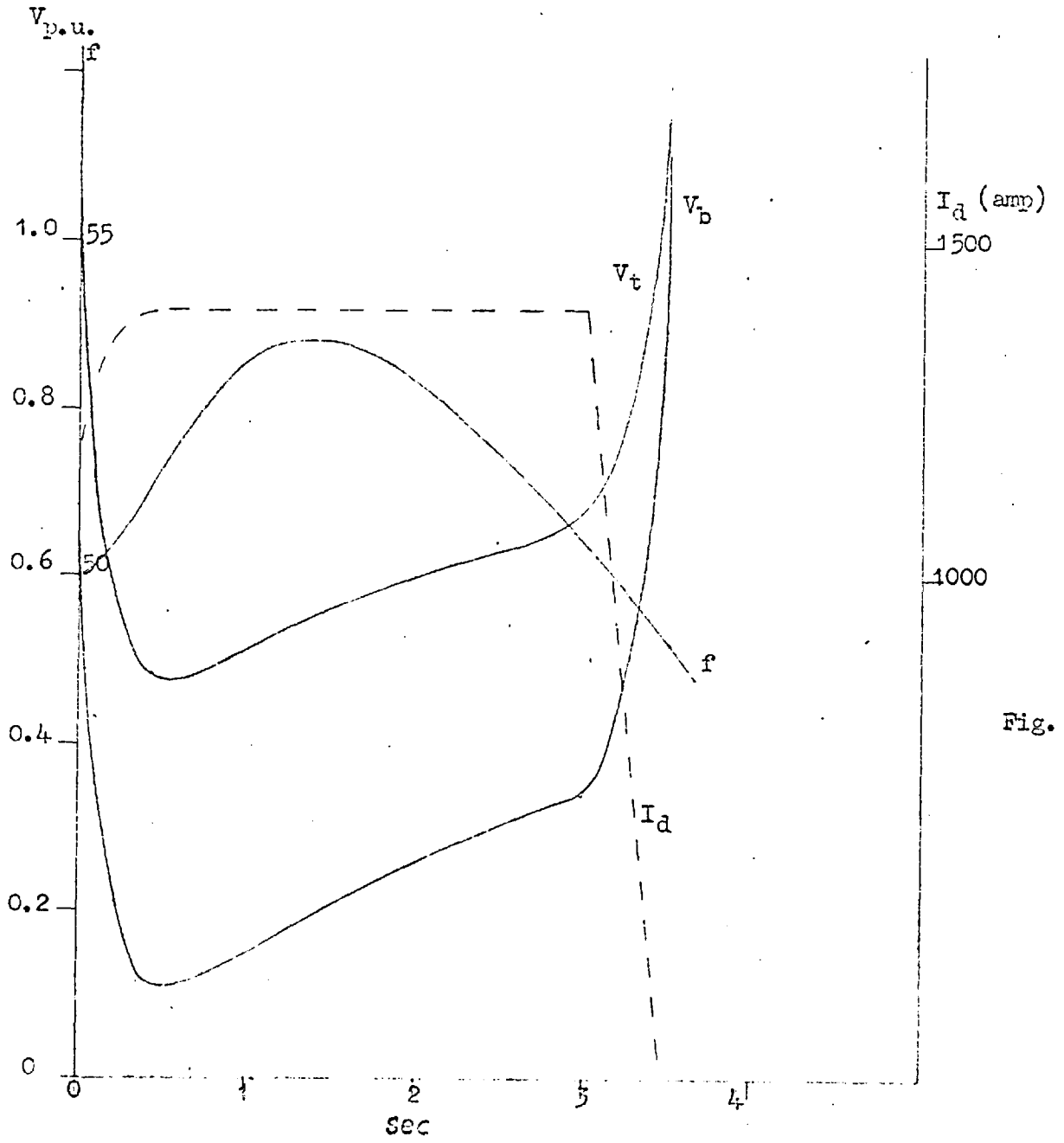

Fig. 6.11 Frequency control P=500 MW at u.p.f.
G=1200, T=0.01

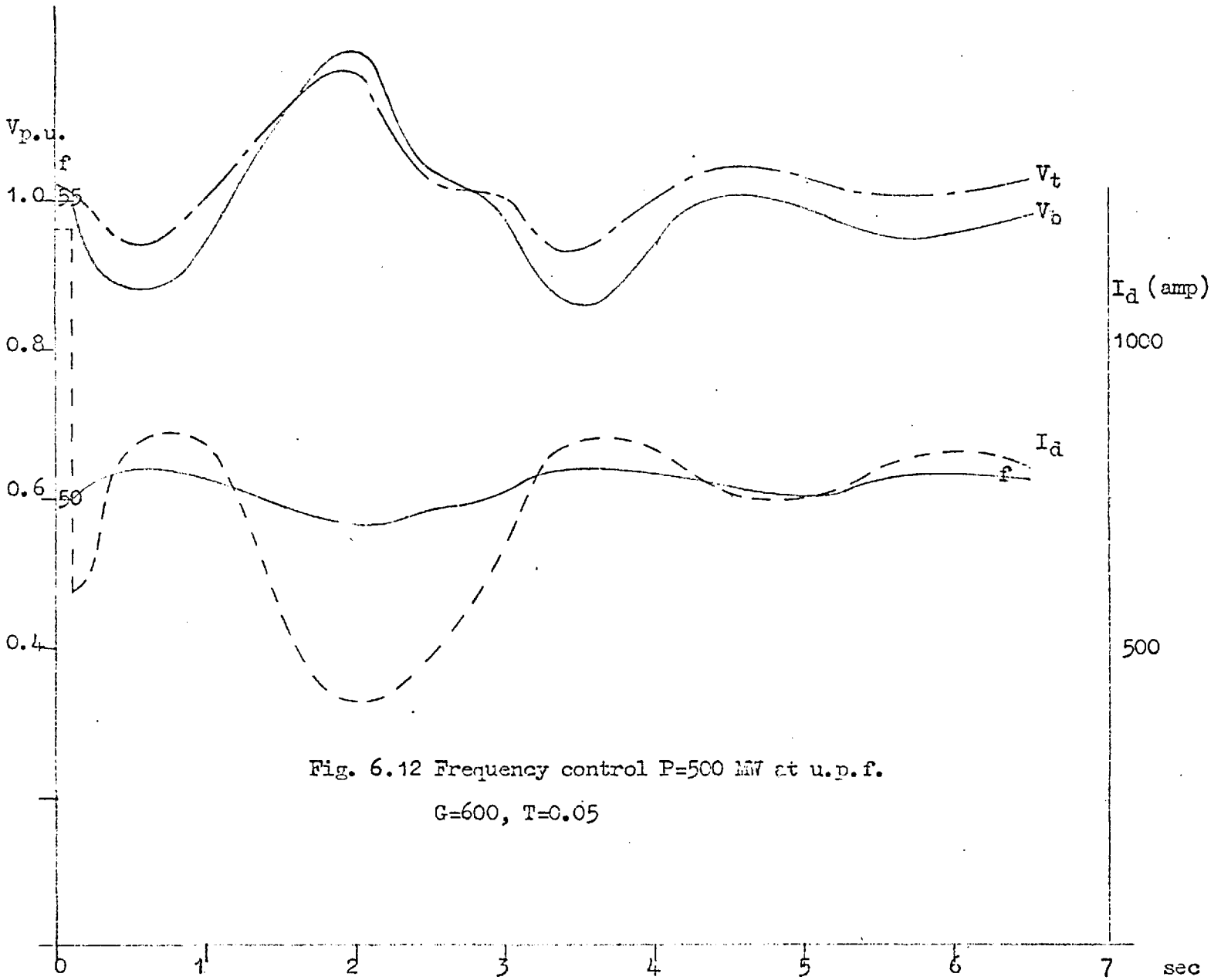

Fig. 6.12 Frequency control P=500 MW at u.p.f.

G=600, T=0.05

6.4.3 Progressive Block and Deblock (Figs. 6.13 - 6.16)

With the generator supplying full load at unity power factor, Fig. 6.13 shows that blocking one bridge quickly upon isolation was a very effective way of reducing fluctuations in the system which settled down in 4 seconds. The converter bus voltage fell upon isolation to 0.68 and showed a quick rise when the current margin was crossed.

For comparison a second study with the generator supplying full load at 0.85 lagging p.f. before isolation shows that, without blocking any bridge, the voltages recovered quite rapidly, but the machine frequency continued to fall as shown in Fig. 6.14.

Finally if the generator was supplying full load at 0.98 leading p.f. before isolation the drop in voltage was so severe upon isolation that both poles were progressively blocked starting with 1 bridge in each pole. As the voltages recovered the direct current order was assumed to be increased linearly at 1200 amp/sec. The result is shown in Fig. 6.15 from which it can be seen that this rate of current reinstatement was too rapid and caused excessive voltage and frequency reduction. Moreover, the maximum direct current in the isolated generator mode should have been limited to 940 A corresponding to a power transfer of 500 MW at rated direct voltage. This was incorporated in a second trial with a current reinstatement rate of 600 amp/sec, which produced better voltage and frequency responses as shown in Fig. 6.16.

6.4.4 Converters represented as constant R and X (Figs. 6.17 - 6.18)

For the purpose of comparison the cases of the generator supplying full load at unity power factor and 0.85 lagging power factor were repeated by representing the converter load as a constant impedance. In both cases as shown in Figs. 6.17 and 6.18 the voltage drops were less severe upon isolation due to the lower reactive power demand.

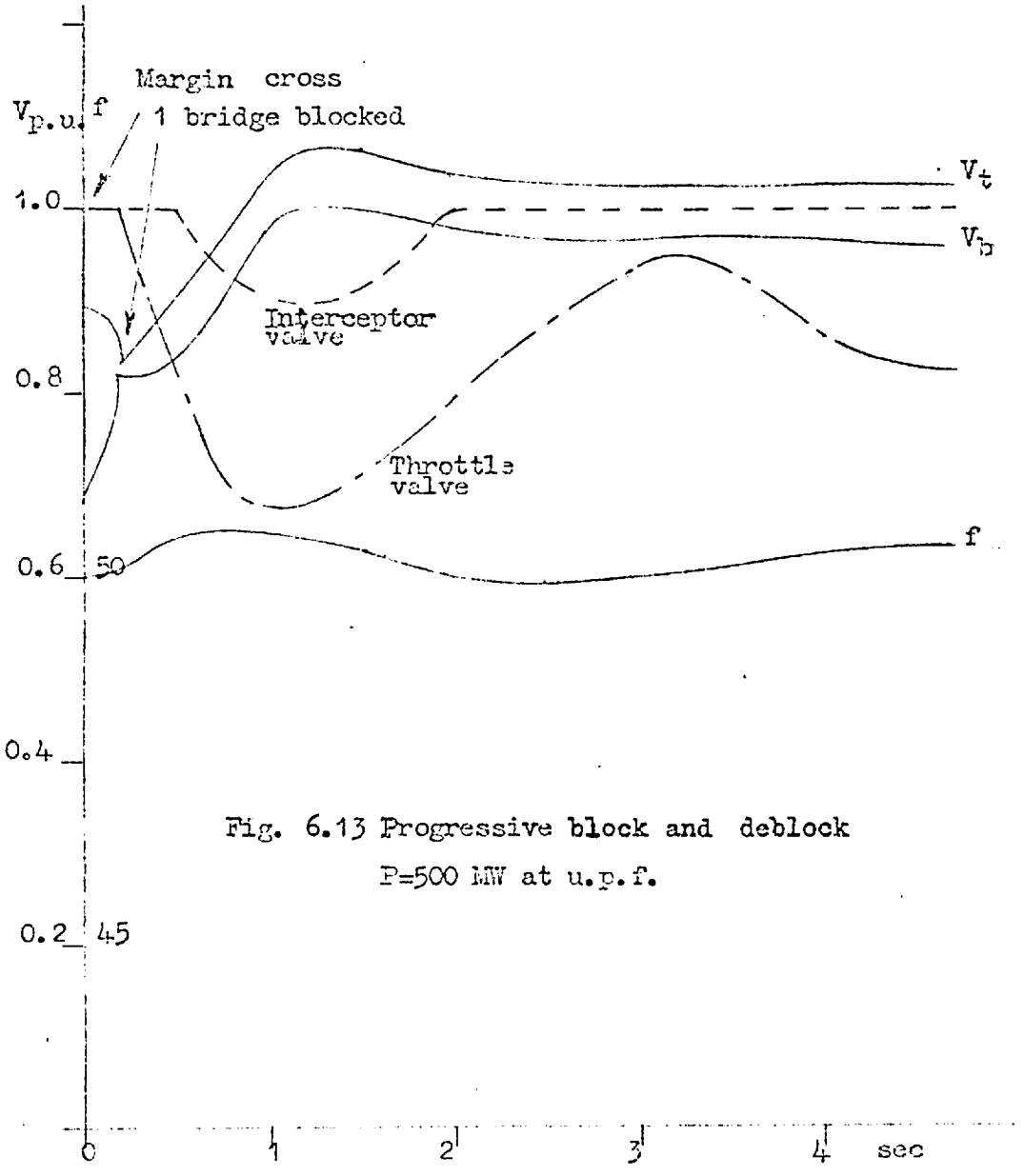

Fig. 6.13 Progressive block and deblock

P=500 MW at u.p.f.

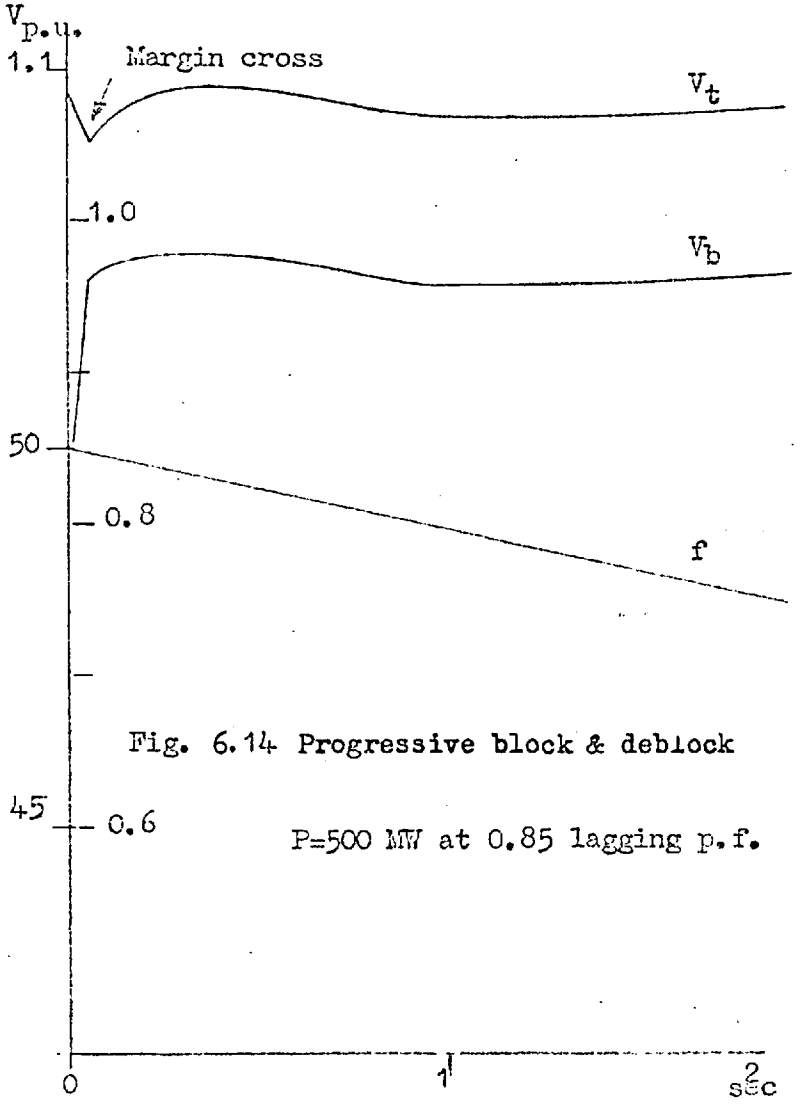

Fig. 6.14 Progressive block & deblock

P=500 MW at 0.85 lagging p.f.

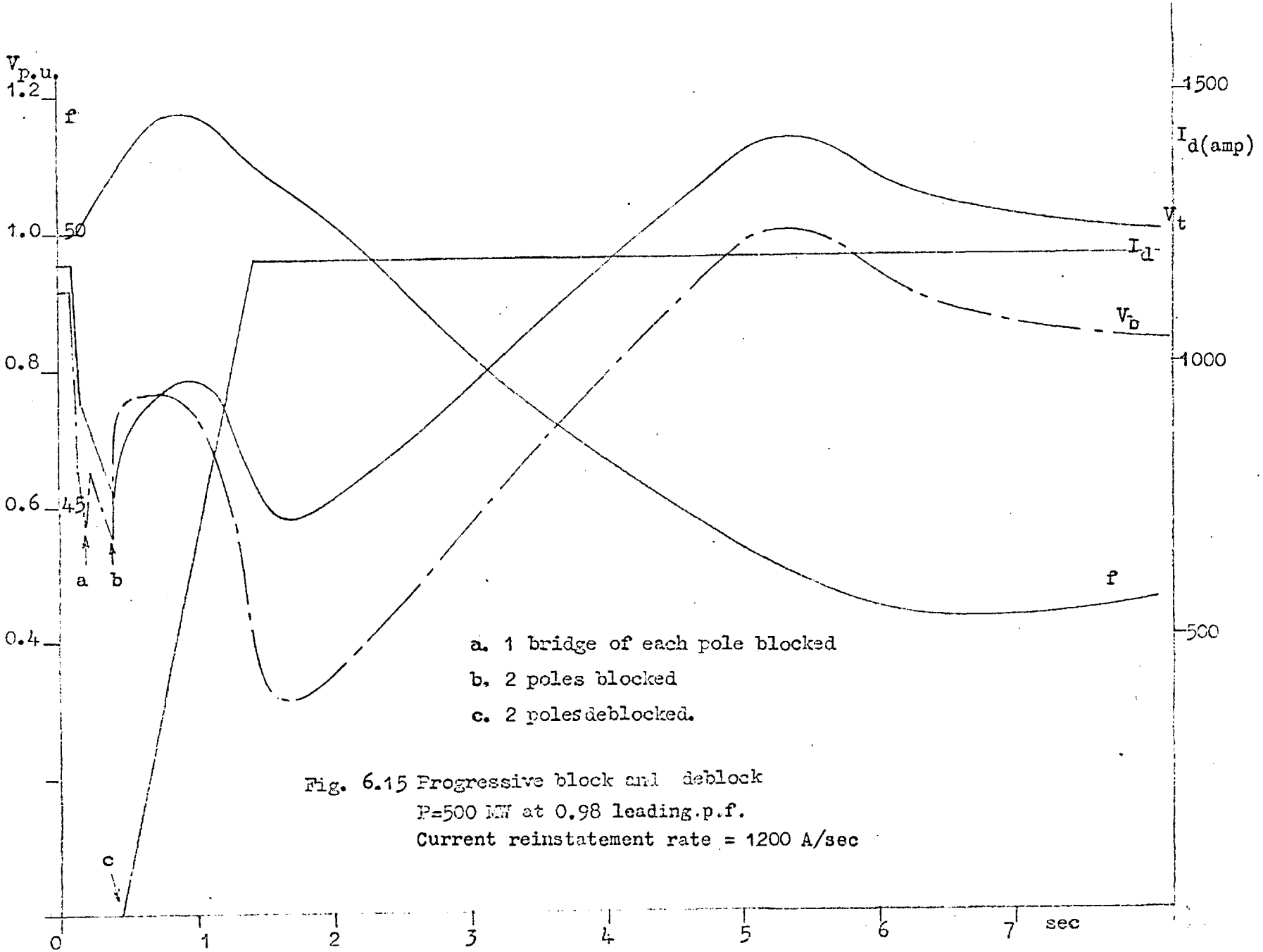

a. 1 bridge of each pole blocked

b. 2 poles blocked

c. 2 poles deblocked.

Fig. 6.15 Progressive block and deblock
P=500 MW at 0.98 leading.p.f.
Current reinstatement rate = 1200 A/sec

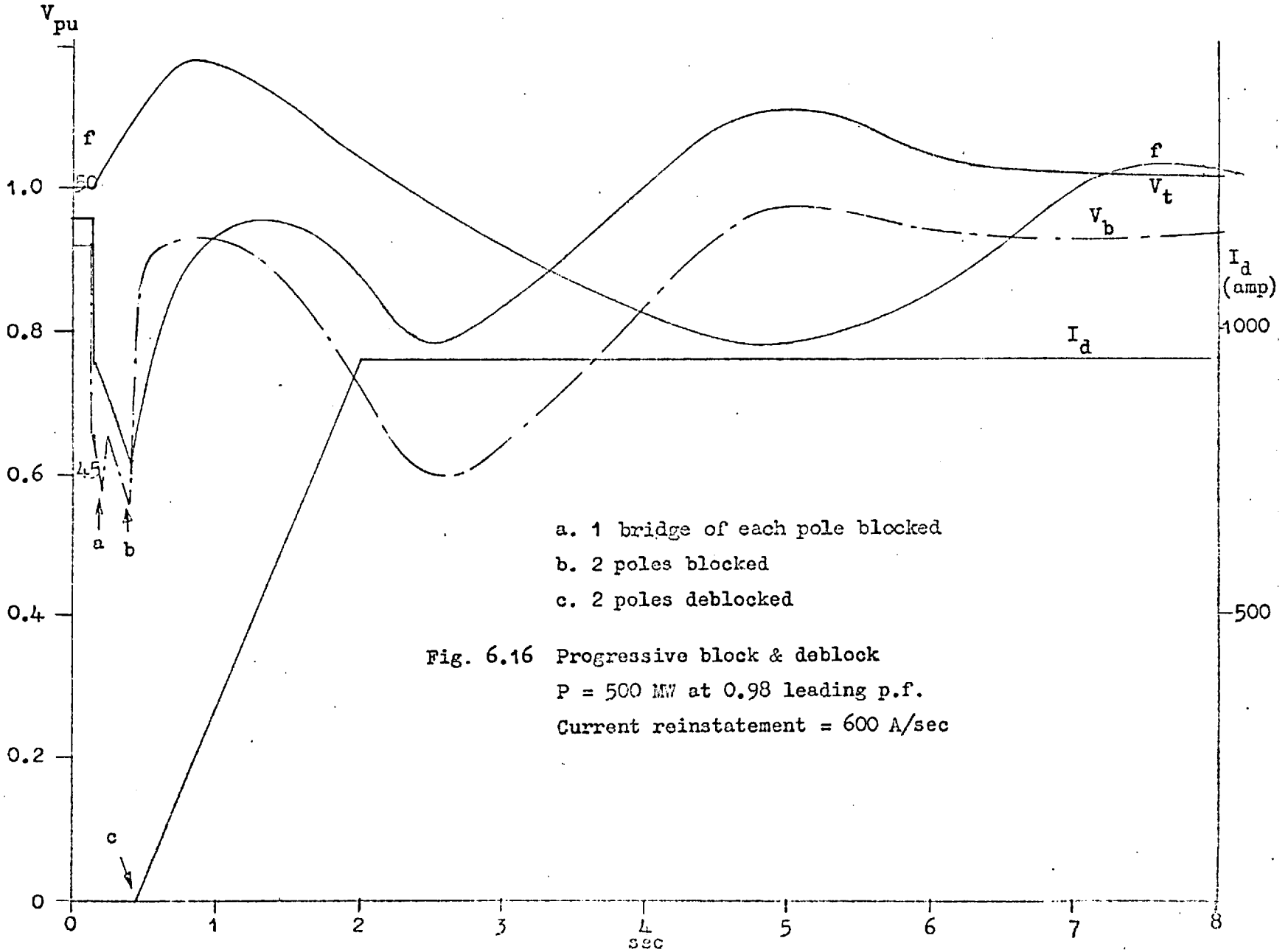

a. 1 bridge of each pole blocked
b. 2 poles blocked
c. 2 poles deblocked

Fig. 6.16 Progressive block & deblock
P = 500 MW at 0.98 leading p.f.
Current reinstatement = 600 A/sec

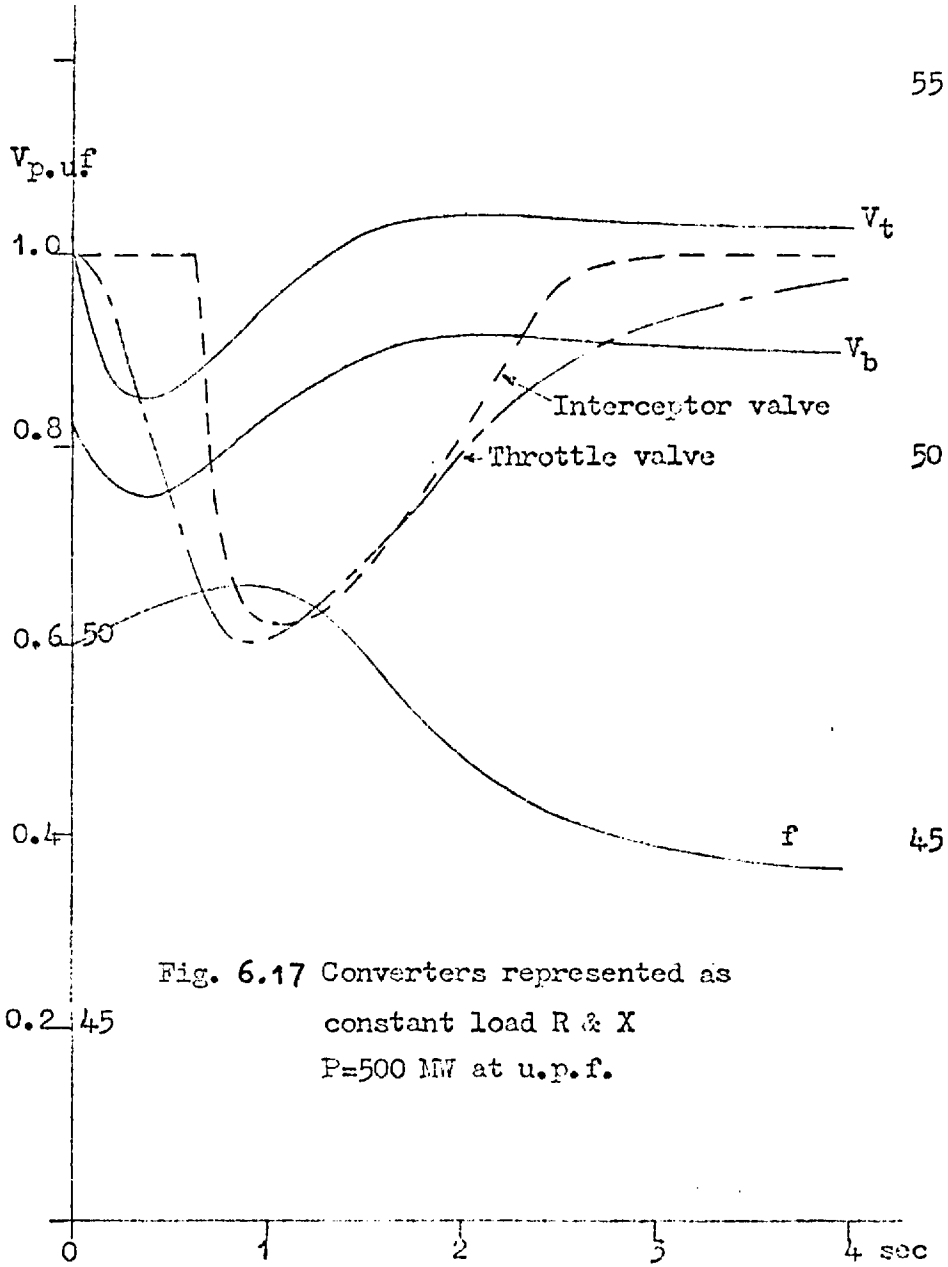

Fig. 6.17 Converters represented as constant load R & X
P=500 MW at u.p.f.

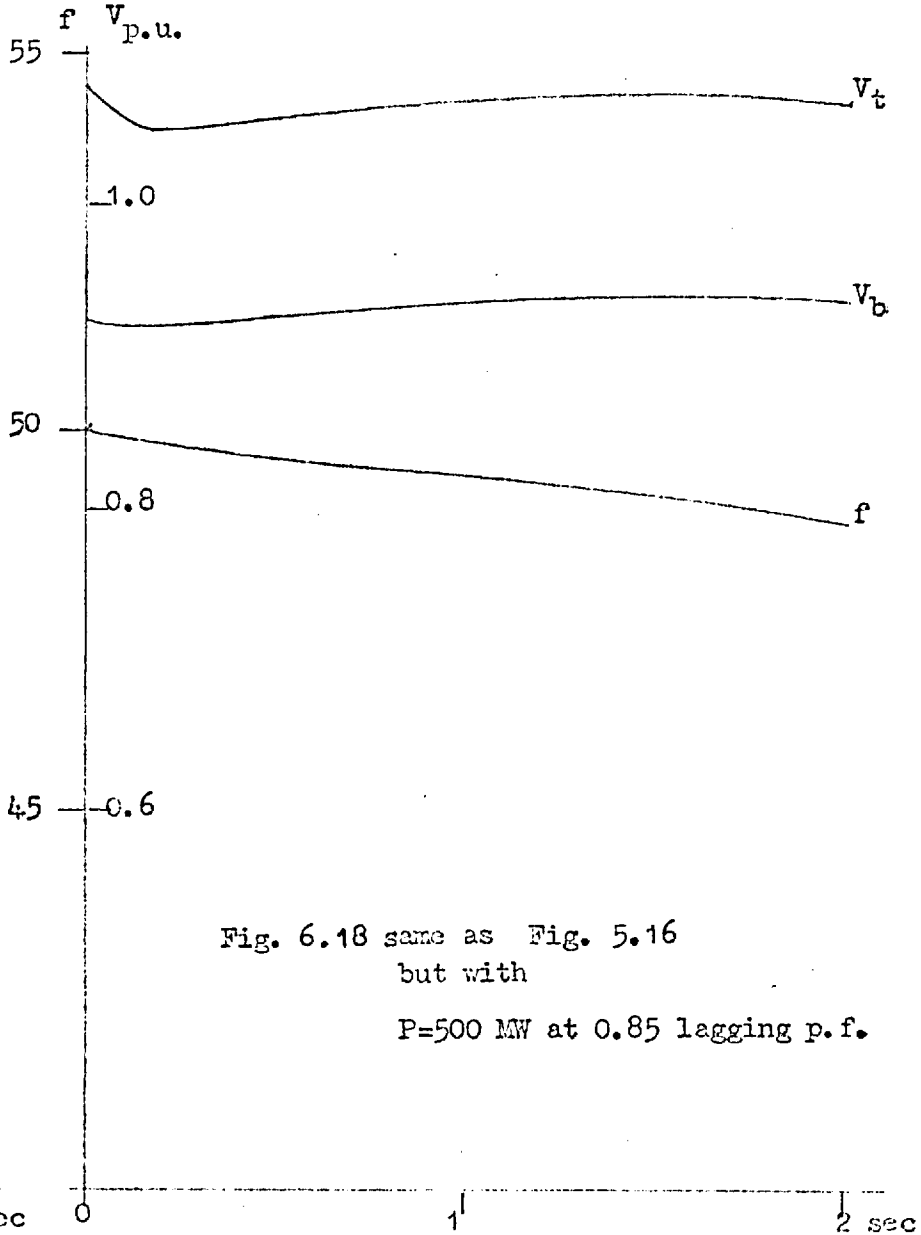

Fig. 6.18 same as Fig. 5.16 but with
P=500 MW at 0.85 lagging p.f.

6.5 Suggestion of Control of d.c. link in the isolated generator mode

The above studies have shown that both frequency control of direct current and progressive block and deblock are effective in preventing excessive voltage and speed changes when the generator is suddenly isolated with the d.c. link. Moreover certain desirable features can be postulated as a result of these studies.

(a) Frequency Control - The choice of gain and time constant is important (gain of 600 and time constant of 0.05 sec. seem satisfactory). To alleviate the voltage drop upon isolation the current order of the d.c. link should first be rapidly reduced by an amount which may be made, for example, proportional to the drop in converter bus voltage; frequency control can then take over.

(b) Progressive blocking and de-blocking - The voltage levels at which the converters are scheduled to be blocked and deblocked are important factors. If both poles are blocked then the rate of reinstating direct current after deblock is also important; a rate of 1200 amps/second was found to produce excessive voltage and frequency reduction, while halving the rate to 600 amp/second produced much better response.

From these results progressive block and deblock seems able to stabilise the changes in voltages and frequency more rapidly than frequency control. If these two controls are combined so that progressive blocking and deblocking plus suitable direct current reinstatement stablises the system soon after isolation, then frequency control can take over to provide damping for the post-isolation running of the machine.

To implement these controls it will be necessary to have an interlock with the 400 kV switches S connecting Generator No. 3 to the 400 kV busbar in order to detect isolation from the 400 kV system. In addition voltage and frequency sensing devices will be required in the 132 kV bus supplying the converters.

CHAPTER 7

CONCLUSIONS

7.1 Representation of Converters in the Analyses of a.c./d.c. Systems

After examining all known methods of representing converters in the steady and transient states under balanced and unbalanced conditions it was found that the simple representation of converters as continuously controllable motors and generators is suitable for both steady state and transient analyses. This representation applies only when the a.c. system is symmetrical and, strictly, only at steady state. However, since the time constants of d.c. converters and systems are small compared with those of a.c. machines it is permissible to neglect the individual firing of converter valves and to use average voltage values instead of the actual voltage waveform of the converters. Therefore this representation is assumed to be applicable to transient as well as steady state analysis. The work of Breuer et al[3], which showed good agreement between results of transient a.c./d.c. system analyses from a computer program based on this representation and those obtained from an a.c./d.c. system simulator, lent strong support to the validity of this assumption. This representation is, however, not applicable under unbalanced a.c. system conditions and is not suitable for analysing effects of valve faults. The dynamic representation of Hingorani et al[30] would be necessary in these circumstances.

7.2 Steady-State Stability of a.c./d.c. Systems

Various disturbances have been considered and indicated that voltage criterion considerations would place certain restrictions to the operation of a d.c. link, e.g. the power transfer across a link may have to be reduced during light load conditions, and emergency power reversal may cause voltage instability. The current margin should also be suitably chosen in order to limit the voltage change following a margin

cross. The relationship between tap ratios of system transformer and converter transformer was studied from which a method for co-ordinating the range of these ratios was developed. An operation chart relating d.c. link power, a.c. system short circuit level and the tap ratios was derived to indicate the required tap ratios at different a.c. system conditions. Converter characteristics were also considered and the desirable features were illustrated. Finally a voltage stability criterion was derived from the concept of circle diagrams which could be employed to indicate the limit of stable operation of d.c. links at steady-state.

7.3 A.C./D.C. Load Flow Program

An a.c./d.c. load flow program based on an equivalent current generator representation of converters incorporated into a Glimm-Stagg a.c. load flow program was described. Novel features of this program were that single - or double - pole d.c. links could be represented and a tap changer subroutine was developed to ensure proper operating conditions of a link i.e. with current control either at the rectifier or inverter. The effects of the slope of converter characteristics were investigated and found to affect the location of the operating point of a link. This program, by adjusting tap ratios of converter transformers, always ensured a proper operating point. The problem of non-convergence caused by simulating an outage of an a.c. line was also studied, and a solution was obtained by adjustment of the power order of the d.c. link.

7.4 Transient Analysis of a.c./d.c. Systems

On the strength of the work of Breuer et al[3], who showed results obtained from an a.c./d.c. simulator and those from a computer program which represented converters as d.c. motors and generators, it can be concluded that the steady-state representation of converters is equally applicable to the analysis of d.c. systems under transient conditions.

This is an important conclusion since it simplifies considerably the representation of converters required in the transient analysis of a.c./d.c. systems. Otherwise it would be necessary to use the comprehensive representation of converters suggested by Hingorani et al[30], which would increase considerably both the programming and computing times required; or alternatively the simplified representation suggested in Chapter 5 may be used, involving an assumption of balanced a.c. system e.m.f's, and some loss in generality in not identifying the conducting valves and phases.

As an alternative to the ordinary method of numerical integration a transition matrix method for solving the d.c. line equations had been used in conjunction with a recursive method of obtaining sampled responses from the transfer functions of the d.c. link control. The computing speed of this method was favourable compared with the method of numerical integration and has the advantage that it can be incorporated into a dynamic analysis of multi-machine systems using state variables.

7.5 Control of d.c. Link in the Isolated Generator Mode

The special problem of control of a double-pole d.c. link when a generator became suddenly isolated from the a.c. system and connected solely to the link was considered. With no control the machine voltage fell below 0.55 p.u. and frequency rose above 52 Hz. Two methods of control were tried and both were effective. The first method used the frequency of the machine to control the current order of the d.c. link. The second method progressively blocked and deblocked the converters as the converter bus voltage fell and recovered. The instrumentation required for these controls would be a device for positively identifying isolation of the machine plus a frequency sensing device for the frequency control method, or a voltage sensing device for the progressive blocking and deblocking method. The ideal control strategy is to use both frequency control and progressive block and deblock together. The latter provides fast control of voltage and machine frequency upon sudden isolation of the machine, while the former provides damping for the post-isolation running of the machine.

7.6 Numerical Integration and Digital Analog Simulation

The common methods of numerical integration for solving differential equations were presented. The problem of numerical instability and round-off errors were discussed, which led to the concept of centralised integration and sorting. Digital analog simulation techniques were introduced and their use illustrated with several of the most common simulation langauges. The desirable features of such languages were then listed and discussed. Two most common languages, MIMIC and DSL/90, had been used extensively in this thesis and were found to be entirely satisfactory so far as the simulation of machines, governors, a.v.r's and d.c. link controls were concerned. Unfortunately each of these languages had its own severe draw-back. MIMIC is a very simple language compared with DSL/90 but lacks many of the essential and desirable flexibilities required to simulate a complex system. DSL/90 on the other hand is a much more flexible language since it retains many features of FORTRAN. The worst disadvantage of DSL/90 is that it takes 1.8 min. on the IBM 7090 for loading and translation before an executable object program is produced from the user's source program. It also required three customer's magnetic tapes. As a result turn-round times from the computing environment as existed at Imperial College for DSL/90 programs were poor. In the end further dynamic problems were studied by using plain FORTRAN programs and a Runge-Kutta integration subroutine which resulted in faster turn-round and reduced computing times. However, experience with simulation languages led to the introduction of some programming features to ease the programming effort.

7.7 New Developments Considered in this Thesis

The review and classification of all known methods of representation of converter considered in Chapter 2 are new and would be useful as a starting reference for converter representations and as a guide when a suitable choice of representation has to be made. The study on steady-state stability revealed restrictions on the operation of a d.c. link when voltage criteria are applied. A method of co-ordinating the tap range of the system and converter transformers was developed, as well as a simple equation for determining voltage instability. With the load flow program described in Chapter 4 the problem of non-convergence when simulating an a.c. line outage was solved.

For the transient analysis of an a.c./d.c. system an important inference was made that the steady-state representation of converters, which treats converters as d.c. generators and motors with no inertia, can be used also as a simplified but effective representation in the analysis of a.c./d.c. systems under transient conditions. The use of the transition matrix to solve d.c. line equations and a recursive method to obtain the sampled responses from transfer functions of d.c. link control is new. The study in Chapter 6 of the problem of sudden isolation of a generator connected to a d.c. link is new, as is the method of progressive blocking and deblocking for the control of the link.

In the appendix a programming feature for easing the use of plain FORTRAN language for the numerical integration of differential equations is described.

REFERENCES

1. Ainsworth, J.D. and Bowles, J.P.: 'A h.v. d.c. transmission simulator suitable for both steady state and transient studies', I.E.E. Conf. Publ. 22, Sept., 1966.

2. Hano, I., Machida, T. and Sasaki, H.: 'Transient stability of a.c. system in case of fault on h.v. d.c. transmission line', paper presented at I.E.E.E. Winter Power Meeting, 1968.

3. Breuer, G.D., Pohl, R.V. and Young, C.C.: 'Comparison of h.v. d.c. simulator and digital computer results for a.c./d.c. system studies', paper presented at I.E.E.E. Winter Power Meeting, 1968.

4. Joetten, R. and Foerst, R.: 'Model plant tests on the behaviour of a h.v. d.c. transmission during a.c. and d.c. system disturbances', C.I.G.R.E., 1968.

5. Read, J.C.: 'The calculation of rectifier and inverter performance characteristic', J.I.E.E., 92, Pt.II, 1954.

6. Calverley, T.E.: 'The flow of power and reactive components in rectifier and inverter equipment', Pt. I & II, English Electric Journal, Vol. 13, 1954.

7. Uhlmann, E.: 'Alternating voltage, direct voltage regulation and power factor of converter stations operating on a.c. systems of finite short circuit capacity', Monograph I.E.E., May, 1955.

8. Uhlmann, E.: 'The representation of a h.v. d.c. link in a network analyser', C.I.G.R.E., 1960.

9. Breuer, G.D., Luini, J.F. and Young, C.C.: 'Studies of large a.c./d.c. systems on the digital computer', I.E.E.E. Trans., Vol. PAS-85, No. 11, 1966.

10. Breuer, G.D., Luini, J.F. and Young, C.C.: 'Studies of large a.c./d.c. systems on the digital computer', I.E.E. Conf. Publ. 22, Sept., 1966.

11. Hingorani, N.G. and Mountford, J.D.: 'Simulation of h.v. d.c. systems in a.c. load-flow analysis by digital computers', Proc. I.E.E., Vol. 113, No. 9, Sept., 1966.

12. Sasson, A.M. and Freris, L.L.: 'Investigation of the load flow problem', Proc. I.E.E. Vol. 115, No. 10, Oct., 1968.

13. Gavrilovic, A. and Taylor, D.G.: 'The calculation of the regulation characteristic of d.c. transmission system', I.E.E.E. Trans. Vol. PAS-83, No. 3, Mar., 1964.

14. Arrillaga, J. and Efthymiadis, A.E.: 'Simulation of converter performance under unbalanced conditions', Proc. I.E.E., Vol. 115, No. 12, Dec., 1968.

15. Horigome, T.: 'On the steady state equivalent circuit of a.c.-d.c.-a.c. interconnected transmission systems', Bulletin of Electrotechnical Laboratory (Japan), 1957.

16. Horigome, T. and Reeve, J.: 'Equivalent circuits of interconnected a.c.-d.c.-a.c. power transmission systems', International Journal of Electrical Engineering Education, Vol. 1, 1964.

17. Horigome, T. and Ito, N.: 'Digital computer method for the calculation of power flow in an a.c.-d.c. interconnected power system', Proc. I.E.E., Vol. 111, No. 6, June, 1964.

18. Horigome, T. and Adamson, C.: 'A.C. fault current in an a.c.-d.c.-a.c. interconnected power system', C.I.G.R.E. Study Committee No. 10, 1963.

19. Horigome, T. and Ito, N.: 'Digital computer method for the calculation of power flow in an a.c.-d.c. link during unsymmetrical fault in the a.c. system', C.I.G.R.E. Study Committee No. 10, 1965.

20. Phadke, A.G. and Harlow, J.H.: 'Unbalanced converter operation', I.E.E.E. Trans. Vol. PAS-85, No. 3, March, 1966.

21. Cahen, F.M., di Perna, A. and Gavrilovic, A.: 'The Sardinia - Italian mainland h.v. d.c. transmission scheme - frequency control of the Sardinia system', I.E.E. Conf. Publ. No. 22, Sept., 1966.

22. Casson, W.: 'Kingsnorth - London d.c. transmission interconnector', I.E.E. Conf. Publ. No. 22, Sept., 1966.

23. Reider, A.M.: 'Analysis of the stability of the control systems of the Kashira - Moscow direct current transmission line', Direct Current, Dec. 1957.

24. Berlin, E.M.: 'Steadiness of systems for regulating d.c. power transmission improved by altering the principle on which the inverter is compounded', Direct Current, Dec. 1962.

25. Norton, J.P. and Cory, B.J.: 'Digital simulation program for multiterminal h.v. d.c. systems', Proc. I.E.E. Vol. 115, No. 3 March, 1968.

26. Norton, J.P. and Cory, B.J.: 'Control-system stability in multiterminal h.v. d.c. systems', Proc. I.E.E., Vol. 115, No. 12 Dec., 1968.

27. Freris, L.L.: 'Effects of interaction among groups in a multigroup a.c.-d.c. converter', Proc. I.E.E., Vol. 114, No. 7, July, 1967.

28. Reeve, J: 'Logic behaviour of h.v. d.c. converters during normal and abnormal conditions', Proc. I.E.E., Vol. 114, No. 12, Dec., 1967.

29. Phadke, A.G., Reitan, D.K. and Peterson, H.A.: 'Transient fault currents in h.v. d.c. rectifiers', Paper presented at I.E.E.E. Summer Power Meeting, Portland, 1967.

30. Hingornai, N.G., Hay, J.L. and Crosbie, R.E.: 'Dynamic simulation of h.v. d.c. transmission systems on digital computers', Proc. I.E.E., Vol. 113, No. 5, May, 1966.

31. Hingorani, N.G. and Hay, J.L.: 'Dynamic simulation of an h.v. d.c. system on a digital computer', I.E.E. Conf. Publ. 22, Sept., 1966.

32. Hingorani, N.G. and Hay, J.L.: 'Representation of faults in the dynamic simulation of h.v. d.c. systems by digital computer', Proc. I.E.E., Vol. 114, No. 5, May, 1967.

33. Harley, R.G.: 'General aspects of transient stability', Power System Report No. 83, Imperial College of Science and Technology, 1968.

34. Adkins, B.: 'The general theory of electrical machines' (Chapman and Hall, 4th Ed., 1964).

35. Peterson, H.A. and Krause, P.C.: 'A direct and quadrature-axis representation of a parallel a.c. and d.c. power system', I.E.E.E.Trans. Vol. PAS-85, No. 3, March, 1966.

36. Peterson, H.A., Krause, P.C., Luini, J.F. and Thomas, C.H.: 'An analog computer study of a parallel a.c. and d.c. power system', I.E.E.E. Trans. Vol. PAS-85, No. 3, March, 1966.

37. Krause, P.C. and Carroll, D.P.: 'A hybrid computer study of a d.c. power system', I and II, I.E.E.E. Trans. Vol. PAS-87, No. 4, April, 1968.

38. Ainsworth, J.D.: 'Harmonic instability between controlled static converters and a.c. networks', Proc. I.E.E., Vol. 114, No. 5, May, 1967.

39. Tam, C.C.: 'Interaction of d.c. converters and weak a.c. systems', Power System Report No. 71, Electrical Engineering Department, Imperial College of Science and Technology, Sept., 1966.

40. Adamson, C. and Hingorani, N.G.: 'High voltage direct current power transmission', (Garraway, 1960).

41. Bower, J.B.C., Huddart, K.W. and Watson, W.G.: 'Reactive power requirements of a.c. systems and a.c./d.c. converters', I.E.E. Conf. Publ. No. 22, Sept., 1966.

42. Tam, C.C.: 'Weak a.c. system tests at Lydd', TDR 64, Transmission Development Branch report, C.E.G.B., May, 1969.

43. Ainsworth, J.D.: 'The phase-locked oscillator - A new control system for controlled static converters', I.E.E.E. Trans. Vol. PAS - 87, No. 3, March, 1968.

44. Glimn , A.F. and Stagg, G.W.: 'Automatic calculations of load flows', A.I.E.E. Trans., Pt. III, Vol. 76, 1957.

45. Busemann, F.: 'A model h.v. d.c. transmission system', E.R.A. Report V/T 104, 1949.

46. Cory, B.J. (Ed.): 'High voltage direct current converters and systems', (Macdonald, 1965).

47. Barker, I.E.: 'Load flow methods for a.c. system containing d.c. links', Paper presented at the Power System Load Flow Analysis symposium at the University of Manchester Institute of Science and Technology, 1967.

48. Horigome, T. and Ito, N.: 'Digital computer method for the calculation of power flow in an a.c.-d.c. interconnected power system', Proc. I.E.E., Vol. 111, No. 6, June, 1966.

49. Sato, H. and Arrillaga, J.: 'Improved load-flow techniques for integrated a.c.-d.c. systems', Proc. I.E.E. Vol. 116, No. 4, April, 1969.

50. Ainsworth, J.D. and Martin, C.J.B.: 'Principles of control for h.v. d.c. transmission', I.E.E. Conf. Publ. No. 22, Sept., 1966.

51. Shackshaft, G.: 'General-purpose turbo-alternator model', Proc. I.E.E., Vol. 110, No. 4, April, 1963.

52. Alford, R.J.: 'The stability of a synchronous generator associated with an induction motor load', Ph.D. thesis, London University, 1964.

53. Humpage, W.D. and Stott, B.: 'Effect of autoreclosing circuit breakers on transient stability in e.h.v. transmission systems', Proc. I.E.E., Vol.111, No. 7, July, 1964.

54. Tam, C.C.: 'Digital analogue method of simulating a turbo-alternator', Power System Report No. 75, Dept. of Electrical Engineering, Imperial College of Science and Technology, 1967.

55. Say, M.G.: 'Design and performance of a.c. machinery', (Pitman 1964).

56. Kuo, F.S. and Kaiser, J.: 'System analysis by digital computers', (Wiley 1966).

57. D'Angelo, H., Smilley, J.D. and Higgins, T.J.: 'Time-domain analysis of a class of discrete non-linear time varying systems', Proceedings, J.A.C.C. 1967.

58. Iyer, S.N.: 'State space techniques applied to power system stability studies', Power System Report No. 84, Dept. of Electrical Engineering, Imperial College of Science and Technology, 1969.

59. Calverley, T.E., Gavrilovic, A., Last, F.H. and Mott, C.W.: 'The Kingsnorth-Beddington-Willesden d.c. link', C.I.G.R.E. 1968.

60. Bower, J.B.C. and Bradbury, K.J.: 'D.C. link isolated generator-real power control', I.E.E. Conf. Publ. No. 22, 1966.

61. Clade, J.J. and Persoz,H.: 'Calculation of dynamic behaviour of generators connected to a d.c. link', I.E.E.E. Trans. Vol. PAS-87, No. 7, July, 1968.

62. Fagg, A.R. and Whorrod, R.B.: 'A comparative analogue simulation study of conventional and divided-winding rotor 500 MW turbo-generators', C.E.G.B. Report No. SSD/SE/RR 30/68, Jan., 1969.

63. I.E.E.E. Computer Applications Sub-Committee standard test system, American Electric Power Services Corporation, 1962.

64. John, M.N.: 'SLC - an automatic resonance link', Electrical Times 29 Aug., 1968.

65. Brewer, G.L. and Fraser, K.G.: 'D.C. transmission in a.c. distribution systems', I.E.E. Conf. Publ. No. 22, Sept., 1966.

66. Brewer, G.L. and Kidd, D.A.: 'A technical and economic appraisal of thyristor equipment for h.v. d.c. for reinforcing a.c. distribution systems', I.E.E. Conf. Publ. No. 53, Power Thyristors and their Applications, May, 1969.

67. Jones, K.M., et al.: 'The prospects of using thyristor strings in distribution system development', I.E.E. Conf. Publ. No. 53, Power Thyristors and their Applications, May, 1969.

68. Knight, U.G.: 'Study of fault levels on supply networks', Proc. I.E.E., Vol. 115, No. 7, July, 1968.

69. Bainbridge, G.R.: 'Obsolete nuclear power stations - no major problems in demolition', C.E.G.B. Newsletter No. 72, Nov., 1966.

70. Calverley, T.E.: 'Mercury arc and thyristor valves for h.v. d.c. transmission', Direct Current, April, 1969.

71. Gavrilovic, A., et al: 'Application of thyristor converters to h.v. d.c. transmission', I.E.E. Conf. Publ. No. 53, Power Thyristors and their Applications, May, 1969.

72. Lane, F.J.: 'Engineering unlimited', Chairman's address to the I.E.E. Power Division, Proc. I.E.E., Vol. 116, No. 1, Jan. 1969.

73. Electrical Times, 19 June 1969.

74. Electrical World, 19 May, 1969.

75. Grois, E.S., Kolpakova, A.I. and Rokotyan, S.S.: 'Prospects for development of d.c. transmission when creating the power pool system of the U.S.S.R.', C.I.G.R.E. Study Committee No. 14, 1969.

76. Scott, E.M.: 'The selection of ± 450 kV h.v. d.c. transmission for the Nelson River', paper presented to the American Power Conference, April, 1967.

APPENDIX

NUMERICAL INTEGRATION AND DIGITAL ANALOG SIMULATION

A.1 Summary of Appendix

This Appendix outlines the methods of numerical integration used to solve the dynamic problems in this thesis. Some of these problems were programmed in plain FORTRAN, others in digital analog simulation languages. These two programming techniques are described, followed by an assessment of the desirable features of a simulation language. Finally a method of improvising a digital analog simulation language is given.

A.2 Introduction

The behaviour of a dynamic system is usually described by differential equations. In a power system dynamic variations are present in machines, transformers, transmission lines, etc., as well as their respective protection and control equipment. With all dynamic systems an analytic solution in closed form can be obtained only when the system is simple and is described by simple differential equations. Examples are the fault currents of a suddenly short-circuited machine and the charging and discharging of a capacitor or inductor. When the system is complicated and is described by a high order (above third) differential equation or, alternatively, by a set of simultaneous first order differential equations, a closed form analytic solution would be difficult if not impossible, and computing aid in the form of analog or digital computer is required.

The analog computer is made up of high gain operation amplifiers wired to function as integrators, adders, multiplier etc. forming the computing units or blocks of the computer. To study the dynamics of a system a mathematical model of the system is built in an analog computer by connecting the computing blocks in accordance with the differential equation(s) of the system. Amplifier gains and input magnitude are adjusted through potentiometers, and the form of the input can be chosen

from a range of function generators. Since input and output of all computing blocks are virtually instantaneous operation of the analog computer may be described as parallel. Speed of computation can be varied by changing the time constant of the integrators to produce responses at real time, or slower or faster than real time. Input parameters can be changed by adjusting potentiometers. Output is usually from a X-Y plotter. The analog computer therefore has the advantage of high computing speed, easy parameter change, graphical output and direct interaction between user and his problem. Hence it is very useful and cheap when a large number of runs are required with different parameters, or when the user wants to develop a 'feel' of the system.

The analog computer, however, has some draw-backs. In the first place it is often a time-consuming and tedious job to connect up, or patch, the various computing blocks to simulate a system, and once dismantled, the whole patching process has to be repeated if even a single more run is required. Secondly before a problem is run on the analog computer it may be necessary to carry out time and amplitude scaling: time scaling involves adjustments of integrator time constants to produce solutions in the desired time scale at reasonable computing speed, and amplitude scaling involves adjustments of potentiometers and amplifier gains to limit any computing block output to below the ceiling voltage of the computer. Both tasks are also time-consuming. The actual hardware of the analog computer has its own limitations, too: e.g. there may be drift or unbalance in the operational amplifiers during computation, introducing some unknown inaccuracy, and there are also limitations in the accuracy with which parameters may be set and outputs presented. Furthermore the size of the problem that can be studied is limited by the number of computing blocks available on the computer. In spite of these, however, the analog computer has been the best tool for solving dynamic problems for many years until the digital computer becomes more wide-spread.

Whereas the analog computer is only suitable for dealing with dynamic problems, the digital computer has almost unlimited applications and has therefore become more popular. Moreover the digital computer performs arithmetic operations with far higher accuracy and consistency than the analog, the only draw-back is that, due to the sequential nature of its operation, as against the analog's parallel operation, it would inevitably be slower in computing speed. To perform integration, it must proceed on a step by step basis using a numerical integration formula. This discrete solution of differential equations introduces round-off errors and stability problems which is outlined in a later section. One great advantage of using digital computers is that modern programming languages such as FORTRAN and ALGOL are equipped with a wealth of library functions (e.g. trigonometric functions, square roots etc.) and logical operations which allows a great degree of flexibility and high power of analysis far exceeding that of the analog computer.

A fair knowledge and skill of these programming languages is essential, however, before their power and facilities can be correctly and efficiently exploited. Whilst such knowledge and skill are not difficult to acquire, they do need practice and time, particularly when the object is to study the dynamic behaviour of systems. It was soon realised that it is possible to simulate the operation of an analog computer on a digital computer, through suitable programming, so that the block structure of the analog computer is retained and there is no need for the user to know much computer programming. Simulation of analog computer through programming has since become known as digital analog simulation, and the programs are known as digital analog simulation languages. There are more than ten such languages in existence, and the more common ones will be discussed in a later section.

When these languages had been proved successful and easily used, it was once thought that analog computers would rapidly disappear. But this is not so. It was soon realised that, in spite of the fantastic speed of modern third generation computers, solving dynamic problems on digital computers requires excessive computing time and therefore money, particularly when many runs with different parameters are required. There is therefore a renewed interest in the analog computer due to its inherent fast speed in solving differential equations, and this culminates in the appearance of hybrid computers. A hybrid computer is an analog computer linked to a digital computer through suitable interface equipments forming an integral computing system. Such a machine has the speed of the analog computer and the analytical and logical power of the digital computer. It represents an union between the two types of computers through hardware (the interface) as against the digital analog simulation languages which joins the two through software (the programs). Blake et al[1] compared the cost of making 3,000 runs of a nuclear reactor simulation using simulation languages on the IBM 360/50/75 with the cost of making the same number of runs on a EAI 8900 hybrid computer and gave a figure of £2M as against £41,600. The hybrid computer, therefore, has a clear economic advantage in applications such as this.

A.3 Numerical Integration

The digital computer can be programmed to solve differential equations by using ordinary programming languages like FORTRAN, ALGOL or PL/1 and one of the numerical integration formulae. The choice of programming language is particular to the computer installation, while the choice of integration formula is governed by considerations such as ease of programming, accuracy, speed, storage etc. The most commonly used formulae are, from[2]:-

(a) Simpson's rule (2nd order)

$$x_{t+h} = x_t + \frac{h}{6}(\dot{x}_t + 4\dot{x}_{t+\frac{1}{2}h} + \dot{x}_{t+h})$$

(b) Runge-Kutta (4th order)

$$x_{t+h} = x_t + \frac{1}{6}(k_1 + 2k_2 + 3k_3 + k_4)$$

with $k_1 = h \cdot f(t, x_t)$

$k_2 = h \cdot f(t + \frac{1}{2}h, x + \frac{1}{2}k_1)$

$k_3 = h \cdot f(t + \frac{1}{2}h, x + \frac{1}{2}k_2)$

$k_4 = h \cdot f(t + h, x + k_3)$

(c) Milne predictor-corrector (5th order)

Predictor

$$x^p_{t+h} = x_{t-h} + \frac{h}{3}(8\dot{x}_t - 5\dot{x}_{t-h} + 4\dot{x}_{t-2h} - \dot{x}_{t-3h})$$

Corrector

$$x^c_{t+h} = \frac{1}{8}(x_t + 7x_{t-h}) + \frac{1}{192}h(65\dot{x}_{t+h} + 243\dot{x}_t + 51\dot{x}_{t-h} + \dot{x}_{t-2h})$$

$$x_{t+h} = 0.96116x^c_{t+h} + 0.03884x^p_{t+h}$$

where h = integration step

$\dot{x} = \frac{dx}{dt} = f(t, x)$

x = state variable (single element or vector)

All integration formulae are approximations to the power series of the true solution, and is therefore only accurate to varying degrees. The problems of round-off errors and numerical instability have been discussed in Reference 2, and Piggott and Smale[3] have derived stability boundaries of some common integration formulae for a second order system. In general these problems can be avoided if a fixed integration step less than the smallest time constant of the system is used. If the program running time is made excessive because of a very small time constant, then the suggestions of Ewart and de Mello[4] may be used. First if the time constant is very small compared with the others it can be deleted from the system equations and substituted by an algebraic equation. When this is not justified then the differential equation in question, which usually appears in the form:-

$$x = \frac{K}{1 + pT} u$$

and solved in the usual integral form:-

$$x = \frac{1}{T}\int (Ku - x)dt$$

can be solved in the differential form:-

$$x = Ku - T\frac{dx}{dt}$$

where $$\left.\frac{dx}{dt}\right|_t = \frac{1}{T}(x_t - x_{t-h})$$

h = integration step

Alternatively the differential equation can be replaced by an equivalent difference equation. For instance the differential form of the original equation can be written as

$$\frac{x_{t+h} + x_t}{2} = K\left(\frac{u_{t+h} + u_t}{2}\right) - (x_{t+h} - x_t)\frac{T}{h}$$

from which

$$x_{t+h} = \frac{K(u_{t+h} + u_t) - x_t(1 - 2\frac{T}{h})}{1 + 2\frac{T}{h}}$$

In some cases solution speed can be increased by varying the integration step while maintaining a specified accuracy. For this purpose the accuracy is specified in terms of an absolute error and/or a relative error. The absolute error is the difference between two values of the dependant valuable x, e.g. using the 5th order Milne predictor-corrector formulae the absolute error is the difference between the corrected and the predicted values, i.e. $E_a = x^c - x^p$; the relative error is the ratio of absolute error to the value of the variable, i.e. in the same example, $E_r = 1 - x^p/x^c$. At the end of each integration step the errors are checked against the specified values. If the actual error is smaller than that allowed, the next integration step is doubled; conversely if it is greater the integration is repeated with half the step. Naturally the error

checking and step adjustment adds extra computation to each step, and a faster overall solution is obtained only when the steps are doubled more often than they are halved and this depends on the system and the disturbances under study. Hughes and Brameller[5] in fact concluded that over a wide range of systems it is faster to use fixed step integration.

Another important point to note is that when a set of simultaneous first order differential equations is used to describe a system, these equations must be solved simultaneously. With an analog computer this is inherent in the parallel nature of its operation. With the digital computer a special technique known as centralised integration is necessary in view of the sequential operation of the machine. At the beginning of each integration step the derivative term forming the input to an integrator is calculated using the value of all the variables existing at that time and then stored. This process is repeated for all integrators. Then the numerical integration formula is used to advance one step by calculating the outputs of all integrators one by one. This is as close to simultaneous integration as is possible with a digital computer. Fig. A.1 shows a FORTRAN subroutine suitable for centralised integration using the Runge-Kutta formula. Note that all derivative terms are calculated at the same time by CALL PLANT statement, where PLANT is another subroutine which contains all the differential equations $\dot{x} = f(t, x)$, x being the vector of all the state variables. The application of this subroutine is illustrated by a program shown in Fig. A.2 to solve the AVR equation described in Chapter 6. The elements x(1), x(2), x(3) and x(4) represent the variables E_{smr}, I_{fer}, R_{efi} and E_{fer} in Fig. 6.5. These same elements of x must be used everywhere else in the program to denote these variables.

```
      SUBROUTINE INTEG(T,DELT,N,X,XDOT,PLANT)
C T = TIME, DELT = INTEGRATION STEP, N = NUMBER OF FIRST ORDER DIFFERENTIAL
C     EQUATIONS TO BE SOLVED, X = VECTOR OF STATE VARIABLES, XDOT =
C     VECTOR OF DERIVATIVES OF X, PLANT = SUBROUTINE FOR CALCULATING XDOT
      DIMENSION X(30),XDOT(30),FK1(30),FK2(30),FK3(30),FK4(30),XN(30)
C SPECIFY DIMENSION OF X AS 30.  THIS CAN BE INCREASED TO SUIT
      DELT2 = DELT/2.0
C CALCULATE K1 IN RUNGE-KUTTA FORMULA
      CALL PLANT(T,N,X,XDOT)
      DO 10 M = 1,N
      FK1(M) = DELT*XDOT(M)
   10 XN(M) = X(M) + FK1(M)/2.0
      T1 = T + DELT2
C CALCULATE K2 IN RUNGE-KUTTA FORMULA
      CALL PLANT(T1,N,XN,XDOT)
      DO 20 M = 1,N
      FK2(M) = DELT*XDOT(M)
   20 XN(M) = X(M) + FK2(M)/2.0
C CALCULATE K3 IN RUNGE-KUTTA FORMULA
      CALL PLANT(T1,N,XN,XDOT)
      DO 30 M = 1,N
      FK3(M) = DELT*XDOT(M)
   30 XN(M) = X(M) + FK3(M)
      T = T + DELT
C CALCULATE K4 IN RUNGE-KUTTA FORMULA
      CALL PLANT(T,N,XN,XDOT)
      DO 40 M = 1,N
   40 FK4(M) = DELT*XDOT(M)
```

```
C UPDATE X BY DELT
      DO 50 M = 1,N
   50 X(M) = X(M) + (FK1(M) + FK4(m) + 2.0*(FK2(M) + FK3(M)))/6.0

      RETURN

      END
```

Fig. A.1 FORTRAN subroutine for centralised integration using the Runge-Kutta formula.

```
      SUBROUTINE PLANT(T,N,X,XDOT)
      DIMENSION X(30),XDOT(30)

C VARIABLES A1, A2 ETC. OBTAINED FROM MAIN PROGRAM THROUGH COMMON
C     BLOCK/MAIN/
      COMMON/MAIN/A1,A2,A3,A4,GR,GF,GA,EM,DO,ESTR

      XDOT(1) = A1*(GR*(EM-EO) + X(1))
      XDOT(2) = A2*(GF*X(4) - X(2))
      XDOT(3) = A3*(X(2) - X(3))
      XDOT(4) = A4*(GA*(X(1) + ESTR) - X(4))

      RETURN
      END
```

Fig. A.2 Subroutine PLANT for calculating derivatives of a.v.r.

This example shows that a fair amount of programming skill is required to arrange the transfer functions describing the AVR into first order differential equations which are then programmed into the subroutine PLANT. Another difficulty is that the state variables in the system can only be identified as elements of the x vector, whereas it is much more convenient if they can be identified by a mnemonic name. Digital analog simulation languages are designed to remove most the programming effort from the user, and in some of the modern simulation languages state variables are easily identified by mnemonics.

A.4 Digital Analog Simulation

Digital analog simulation is accomplished by a special computer program, known as a digital analog simulation language, which simulates the operation of an analog computer. The block diagram concept of the analog computer is preserved, and the simulation language converts the block diagram into sets of differential and algebraic equations suitable for numerical solution. Thus the tedious task of connecting up an analog computer is replaced by one of programming in a digital analog simulation language which is, for a well designed language, easier. Once the program is written and proved, it is always available for further use at a later date. Simulation language also eliminates the need for time and amplitude scaling, and non-linearities can also be included far easier than on the analog computer.

One disadvantage of this digital method of solving dynamic problems is that there is no direct relationship between user and the machine such as that possible with the analog computer. With the advent of CRT display and multi-access real time computing facility this disadvantage should disappear. The more serious draw-back is the computing time required. In general for problems with about 10 first order differential equations the ratio of computing time to problem time

is well in excess of 10 on the IBM 7090. For this reason, if a large number of runs has to be made with different parameters the digital computer will not be economic. As mentioned before an analog or hybrid computer would provide the solutions cheaper and faster.

In the course of the work described in this thesis two modern simulation languages had been used. These are MIMIC and DSL/90 which are available at Imperial College on the IBM 7090 and 7094 computers. The following discussions on the structure, operation and desirable features of simulation languages refer particularly to these, but other well-known languages will also be discussed, notably SAM[5], KALDAS[8], MIDAS[9] and CSMP[3]. The latter is actually a version of DSL/90 for running on IBM 360 computers.

A.4.1 Structure and Operation of Digital Analog Simulation Languages

Early digital analog simulation languages such as SAM, KALDAS and MIDAS preserved explicitly the block structure of the analog computer with the function of each block identified by a mnemonic code, and blocks of the same function are identified by a number. The blocks are then connected together by means of a patching list. Using the example from Reference 3 the MIDAS program for a simple second order differential equation

$$\ddot{x} + 2\xi\omega\dot{x} + \omega^2 x = f(t)$$

is

```
NEG2 = I2          (sign reversal)
M2 = C2, NEG2      (multiplier)
NEG1 = I1          (sign reversal)
M1 = C1, NEG1      (multiplier)
S1 = F, M1, M2     (summer)
I1 = S1            (integrator)
I2 = I1            (integrator)
```

corresponding to the block diagram shown in Fig. A.3 where C1 = $2\xi\omega$ and C2 = ω^2. A block is identified by a code name and serial number and appears on the left hand side of a statement, while its inputs appear on the right hand side; if there are two or more inputs these are separated by commas. It is interesting to note that in MIDAS the block identification (e.g. I2) also serves to identify the input and output variables.

Modern simulation languages like MIMIC, DSL/90 and CSMP do not have an explicit block structure and therefore can be used to program the equations describing a system directly without the aid of a block diagram. Moreover the ordinary arithmetic operators (+, -, *, ÷) are retained and need not be treated as function blocks. Special functions are denoted by mnemonic names. In DSL/90, for example, there is a large selection of these functions including integrators, simple time constants, lead-lag compensators, zero order hold etc. With these modern simulation languages, the program statements are very similar to FORTRAN statements and can be readily understood. The above second order system can be programmed in MIMIC as

```
XDØT    INT (F-2.0*ETA*W*XDØT-W*W*X, XDØTO)
X       INT (XDØT, XO)
```

so that the second order differential equation is solved as two first order equations. The first statement solves for $\dot{x}$ (XDØT) and the second for x. The function INT denotes an integrator and the integrand, which may be a single variable or composite expression, appears as the first term inside the bracket and is separated by a comma from the second term which is the initial value of the integral. An imaginary equal sign connects the L.H.S. of the statement with the R.H.S.

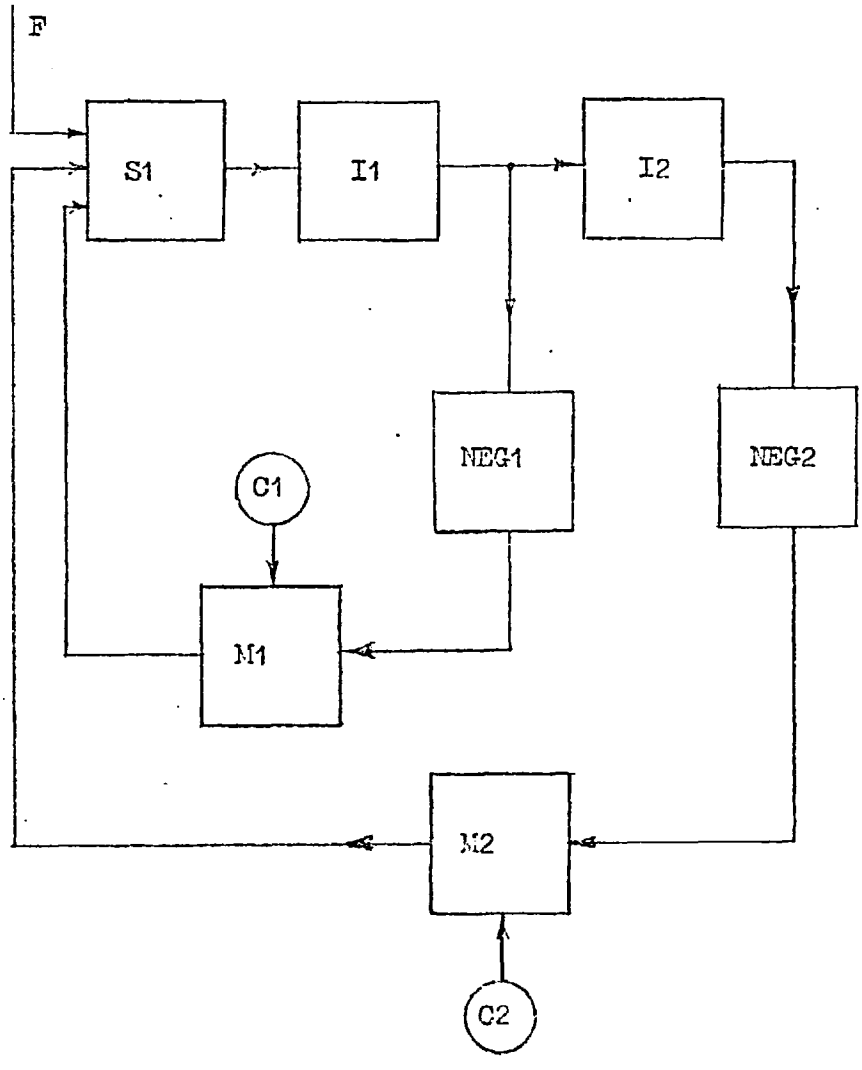

Fig. A.3 Block diagram for MIDAS program of second order differential equation

$$\ddot{x} + 2\zeta w\dot{x} + w^2 x = f(t)$$

The DSL/90 program for the same problem is similar and can be written as follows

```
XDØT = INTGRL (XDØT, F-2.0*ETA*W*XDØT-W*W*X)
X    = INTGRL (XO, XDØT)
```

It can be seen that the form of the statements is very close to FORTRAN statements and, like MIMIC, the integrand can also be a composite expression as well as a single variable. The advantage of using a composite expression as the integrand is that programming is much neater and faster, and this is a feature absent in early simulation languages.

From the system operation point of view, simulation languages can be classified as either an interpreter or compiler program. The former, of which MIDAS is an example, translates every function block of the same type in the user's source program into a block of machine instructions with the appropriate inputs and output and the program is then executed at the machine language level. Since there is only one block of instructions for each type of function block multiplexing of inputs and outputs is required when more than one block of the same type occurs in the program. Although there is only one translation phase from the user's source program to the object program for execution, the overall running of the program is slowed down by the multiplexing operation. Therefore this type of simulation program is only suitable for problems with short running times.

A compiler program does not produce an object program for execution. It translates the user's source program wirtten in the simulation language into a high level langauge program which in turn has to be translated into machine language by the appropriate compiler. For instance DSL/90 translates a source program into a FORTRAN program which is then translated by the FORTRAN compiler for execution. This two phase operation may seem a waste of time, but there are two advantages. First, the resultant machine language object program is more efficient than that of an interpretive

program. This is particularly important if several runs of the same problem are to be made with different parameters, because the saving in time for each run will outweigh the extra time needed for the compilation. The second advantage is that, using the FORTRAN compiler under the control of the IBSYS monitor for the final translation, all the special functions like sine, cosine, square root etc. available in the FORTRAN library, as well as most of the FORTRAN logical operations, become accessible to the DSL/90 user. Thus in DSL/90 and CSMP the flexibility and logical power of the FORTRAN language is retained, in fact FORTRAN statements can be mixed with DSL/90 and CSMP statements. In all previous simulation languages, e.g. KALDAS and MIMIC, the power of the 'mother languages' in which they were written was completely lost. This then leads to the following discussion on the desirable features of digital analog simulation languages.

A.4.2 Desirable Features of Digital Analog Simulation Languages

(a) Easy to learn and to use

This is obvious as the first reason for the development of simulation languages is to enable people with little skill in programming to solve fairly complex dynamic problems. Most simulation languages are made easy to learn mainly by forfeiting many of the flexibility and facilities of the ordinary programming languages, e.g. inputs and outputs are usually in fixed formats so that the user has only to learn one fixed format of input and accepts whatever output format the program provides. DSL/90 and CSMP retain most of the flexibility and power of FORTRAN and are therefore more difficult to learn. After learning there still is the question of how easy it is to use. The earlier languages like MIDAS and KALDAS are not suitable for programming directly from the equations describing the dynamic system and work better from a block diagram incorporating these equations as shown in the previous examples. In both

of these languages the connection between blocks is established by listing all the inputs to a block. SAM requires a connection list and a function list for this purpose. The modern languages (MIMIC, DSL/90, CSMP) are easy to use once the rules are mastered. There is no need for a block diagram and the program can be written directly from the system equations. Moreover the program statements are similar to FORTRAN statements and therefore easier to check and correct. As mentioned before composite expressions with complicated arithmetic or functional operations can be used as inputs to a block thereby reducing programming effort.

(b) Sorting and centralised integration

In early simulation languages, e.g. DAS[10], the order of computations at each time step was established from the order in which the functional blocks occurred in the user's source program; no attempt was made to organise it in accordance with the logical sequence of signal flow among the blocks. Thus there was the possibility of introducing inadvertent time delays between blocks. Later languages like MIDAS, MIMIC and DSL/90 correct this by providing a sorting facility which organises the source program so that the inputs to all functional blocks at the beginning of each time step are calculated from the latest values of the variables. In particular all statements which compute the variables necessary to calculate inputs to an integrator are formed into a loop ending with the integrator. With sorting, the simulation language becomes non-procedural and the statements of the user's source program may be written in any order.

Having safeguarded against inadvertent time delays it is just as necessary to prevent erroneous time advance. This may occur if the output from an integrator is calculated before the input to a following integrator is determined, since the first integrator will have advanced one time step before the second. The problem is avoided by using a centralised integration technique mentioned before. In this case the derivative term

of an integrator is calculated and stored until all integrators are covered, then the output from each integrator is calculated one by one. In an analog computer these operations take place virtually simultaneously in all integrators, and centralised integration is a digital computer's equivalent to such action.

(c) Change of parameters and parameter optimisation

Very often it is required to study the responses of a dynamic system with different parameters. More than one run with the same program must be made with one or more parameters altered each time. With DSL/90 this can easily be done simply by inputting as many sets of parameters values as the number of runs desired. Runs can be repeated from time zero or the same run may continue but with the parameters changed at any intermediate stage. Usually the different parameters are specified before the program is run and entered as part of the input data, which requires the user either to know in advance what he is looking for or to make an inspired guess. It would be highly desirable if the parameters can be optimised by the program during execution. Naturally this means the program must be able to perform logical operations; however most early simulation languages had no logical operations and only modern ones such as MIMIC and DSL/90 provides this facility.

(d) Change of system configuration during execution

In an actual system some paths may exist which can be switched in and out of the system by means of relays or other switching devices under the control of some variables of the system. For instance the acceleration governor in the governor system of the steam turbine used in Chapter 6 is switched in by a frequency sensitive relay. The configuration of this kind of system is therefore not fixed but variable, depending on the state of the system. Hence, to simulate the variable configurations of a system the simulation language must again be able to perform logical operations.

(e) Flexibility and functions library

Ordinary programming languages such as FORTRAN and ALGOL possess considerable flexibility in program formulation as well as input and output. The more important facilities includes logical operations, subroutines and nesting (DO loops in FORTRAN). Besides, these languages are also equipped with a huge library of all the common functions like sine, cosine, square roots etc. Digital analog simulation languages, on the other hand, have to satisfy the requirement of easy to learn and use, and most chose to achieve this by forfeiting most of the flexibility and functions library of the 'mother language' in which they were written. DSL/90 is unique amongst all simulation languages by retaining most of the original facilities and power of FORTRAN, although this naturally makes it more difficult to learn. One feature which is absent in all simulation languages but which is highly desirable is the ability to form an array of integrators. When there is a set of first order differential equations similar in form and differing only in the indices of some of the input variables the technique of nesting should reduce the programming considerably if an integrator is put inside a nest with subscripted inputs and outputs. With present day simulation languages this technique is not available, and each differential equation must be explicitly related to one integrator, so that there are as many integration statements as differential equations. A possible solution is described in section A.5.

(f) Implicit functions

One of the commonest troubles with a program written in a digital analog simulation langauge is the inadvertent formation of an algebraic loop of the form $x = f(x, t)$ enclosing no integrators. Without special programming this equation cannot be solved. Several simulation languages including MIDAS, MIMIC and DSL/90 are equipped with a special subroutine for solving this kind of equation iteratively.

(g) Graphical output

The advantage of this is obvious, particularly when several runs are made with different parameters, because a system response in graphical form is much easier to assimulate than a row of numbers. With a digital computer graphical output can be obtained either by using a plotting routine to produce graphical output from the line printer along with the alpha-numeric output, or by using a Calcomp plotter which can produce more accurate graphs. MIMIC produces graphs in the first manner, and DSL/90 the second. The use of CRT driven by a multi-access real-time computer will no doubt add a new dimension to the method of output.

(h) Diagnostics

When a program does not work it is most important for the user to know what is wrong. Ordinary programming languages like FORTRAN has a rich repertoire of diagnostic messages and the appropriate ones are output to tell the user his mistakes. This facility is, surprisingly, not very common in simulation languages, probably due to the formidable extra programming required. MIMIC has a limited diagnostic facility while DSL/90 has a much wider range of such facility. The most useful diagnostic message is one concerning closed algebraic loops, since this is most common and most difficult to check manually. Once this error is discovered, the solution is simply to use the implicit function facility mentioned in (f). DSL/90 also has a useful diagnostic message to tell the user when the integration step size he specifies is too large and causes the specified error limit to be exceeded.

(i) Fast turn-round

This is essential during the program development stage and desirable when production runs are made, and is just as true for programs written in simulation language as for those written in an ordinary programming language. Most computer installations operate under the control of a master monitor

which runs programs in batches under sub-monitors. Therefore for fast turn-round simulation programs must be acceptable to the same master and sub-monitors so that they can be run along with the other ordinary programs. At Imperial College most FORTRAN programs are run under the IBSYS monitor and the IBJOB sub-monitor. Both MIMIC and DSL/90 are designed to run under these monitors so that their programs can be run along with any other FORTRAN programs. Some unforeseen restrictions arose, however, and are discussed in the next section.

A.4.3 Actual Experience with MIMIC and DSL/90

At Imperial College during 1965-1968 when the work of this thesis was carried out the Computing Unit had to process hundreds of individual jobs daily on the IBM 7090 and, later, the 7094 computers. To achieve maximum efficiency and fast turn-round it was found expedient to classify all FORTRAN jobs into 3 groups according to their expected running times and amounts of output (in term of lines output expected) as follows:-

(1) Short jobs (maximum 0.5 min. running time, 300 lines output, no customers magnetic tapes) - run under PUFFT sub-monitor. 2-3 hours turn-round.

(2) Medium jobs (maximum 3 min. running time, 3000 lines output) - run under IBJOB sub-monitor. 4-12 hours turn-round.

(3) Long jobs (exceeding medium time and output) - run under IBJOB sub-monitor. Over 24 hours turn-round.

MIMIC programs required one magnetic tape (the MIMIC system tape) and DSL/90 three (one DSL/90 system tape, one scratch tape and one tape for Calcomp plotter) so that they did not qualify for short jobs. Moreover, the loading time of the MIMIC and DSL/90 system tapes and the times taken to translate and sort the user's source program proved to be fairly substantial. For MIMIC a total of about 0.8 min. was necessary for all these operations, while DSL/90 took 1.8 min. These times represented a fixed overhead and

were virtually independent of the size of the system simulated. Run as a medium job a DSL/90 simulation program in fact had only 1.2 min. run time. Experience with the problem described in Chapter 5 showed that this was enough only to simulate about 0.05 sec. of a system with 10-15 integrators using an integration step of 0.0005 sec. DSL/90 also produces about 500 lines of various internal tables and core storage maps which are only of trivial interest to the user. Since DSL/90 is more flexible and powerful than MIMIC most of the program used in this thesis had been written in DSL/90. Unfortunately the above-mentioned draw-back of excessive overhead time and unnecessary output severely restricted the development and production running of the programs. In the end it was decided that an alternative was necessary and a return to using ordinary programming language was made. The problem described in Chapter 6 was programmed in FORTRAN and integration was performed by a Runge-Kutta centralised integration routine. A new feature to ease the effort of programming the differential equations was devised and is described below.

A.5 Improvised Digital Analog Simulation

Having used MIMIC and DSL/90 hind-sight suggested that they are not really suitable for a computing environment as existed at Imperial College due to the restrictions in computing time and size of output. Programming in plain FORTRAN using the method of centralised integration was resorted to and further improved. Programming in this way also allowed rapid turn-rounds at the development stage using PUFFT, which, of course, is the whole point of the PUFFT system.

The centralised integrations method described in Section A.3 was improved by adding a facility for easier identification of the state variables. It will be recalled that with ordinary integration routines all variables are formed into an array of X and each variable identified as an element in the array. Although this is not a serious restriction it

does cause considerable confusion. It would be more convenient to represent a state variable by a mnemonic, e.g. to denote a voltage by ER rather than X(10). In FORTRAN this facility can be provided by using the COMMON and EQUIVALENCE statements. All state variables,which are in mnemonics, are placed in a COMMON block in the main program and all subroutines except the integration routine which still operates on an array X. To identify the variables with the elements of X it is only necessary to make the first variable in the COMMON block equivalent to the first element of the X array by putting an EQUIVALENCE statement with these as arguments in the main program. By this single EQUIVALENCE statement the elements of the X array is made equivalent to the variables in the COMMON block in the order in which they occur. Similarly the derivatives of these variables are identified with elements of the $\dot{X}$ array. Referring to the a.v.r. example in Section A.3 the necessary statements are

```
COMMON/A/ESMR,IFER,REFI,EREC,/B/PESMR,PIFER,PREFI,PEFER
EQUIVALENCE/ESMR,X(1)/,/PESMR,XDOT(1)/
```

and the derivative subroutine PLANT was written as shown in Fig. A.4. The mnemonic names ESMR(E_{smr}), IFER(I_{fer}) etc. could be used throughout the program, allowing much easier identification. Experience with the problem described in Chapter 6 confirmed the convenience of this method. Moreover there was a significant improvement in computing time, which was 1.8 min. to simulate 6.5 sec. using a time step of 0.01 sec.

By using plain FORTRAN as the programming language it is now possible to integrate a set of simultaneous differential equations with subscripted state variables simply by declaring an array of variables in the COMMON block. The derivatives of these state variables may be calculated simply in a DO loop in the derivative subroutine PLANT. As mentioned before this facility is not available in any existing simulation languages, but which is most useful when there are many differential

```
      SUBROUTINE PLANT(T,N,X,XDOT)
      DIMENSION X(30),XDOT(30)
      CALL PAVR(X(1),X(2),X(3),X(4),XDOT(1),XDOT(2),XDOT(3),XDOT(4))
      RETURN
      END

      SUBROUTINE PAVR(ESMR,IFER,REFI,EFER,PESMR,PIFER,PREFI,PEFER)
C     STATE VARIABLES ESMR,IFER ETC. MADE EQUIVALENT TO X(1), X(2) ETC.
C           THROUGH ARGUMENT LIST

      COMMON/MAIN/A1,A2,A3,A4,GR,GF,GA,EM,EO,ESTR
C     VARIABLES A1, A2 ETC. OBTAINED FROM MAIN PROGRAM THROUGH COMMON
C           BLOCK MAIN

      PESMR = A1*(GR*(EM-DO) + ESMR)
      PIFER = A2*(GF*EFER - IFER)
      PREFI = A3*(IFER - REFI)
      PEFER = A4*(GA*(ESMR + ESTR) - EFER)

      RETURN
      END
```

Fig. A.4 Subroutine PLANT acting as dummy to call Subroutine PAVR which calculates derivatives of a.v.r. equations. Equivalence between the state variables and the x array, and then derivatives and the $\dot{x}$ array, are established through the argument list of the subroutine PAVR.

e.g. ESMR = X(1)

PESMR = XDOT(1) etc.

equations having a similar form, e.g. the differential equations describing the action of distillation columns in a large chemical plant.

It has been mentioned that a high order differential equation or transfer function must be converted into a set of simultaneous first order differential equations before the method of numerical integration can be applied. For instance a second order transfer function

$$x = \frac{1}{s^2 + a^2} u$$

is transformed into

$$\dot{x}_1 = u - a^2 x_2$$

$$\dot{x}_2 = x_1$$

Conversion procedure for this and other common transfer functions can be mechanised by programming into subroutines, which are then used as blocks in a simulation language. This approach has the advantage that these kind of special subroutines can be developed as required, and the user has the choice of including only those subroutines which are actually used in his program. In contrast a simulation language has to supply all the subroutines representing the function blocks in its specification, and they must all be loaded into the computer even though most of them may not be used, hence the long loading time.

References to Appendix

1. Blake, R.G., Piggott, P.M., Smale, R.J., et al: 'Hybrid computer simulation of Dungeness B power station' CEGB Computing Branch Report RD/C/R52 May 1967.

2. National Physical Laboratory: 'Modern computing methods', (H.M.S.O. 1961)

3. Piggott, P.M. Smale, R.J.: 'Assessment of digital simulation languages', CEGB Computing Branch Report RD/C/R53, 1968.

4. Ewart, D.N., de Mello, F.P. : 'FACE - a digital dynamic analysis program', Proceedings, 5th Power Industry Computer Application Conference, Pittsburg, 1967.

5. Hughes, F.M., Brameller, A. = 'Digital simulation of analogue method', Computer Journal, May, 1966.

6. Sansom, F.J., Peterson, H.E., Warshawsky, L.M. = 'MIMIC - a digital simulator program', SESCA Internal Memo 65-12, Systems Engineering Group, Wright-Patterson Air Force Base, Ohio.

7. DSL/90 - Digital Simulation Language, IBM SHARE General Program Library PA 3358, 1965.

8. Dineley, J.L., Preece, C. = 'KALDAS, an algorithmically based digital simulation of analogue computation', Computer Journal, August 1966.

9. Brennan, R.D., Linebarger, R.N. = 'A survey of digital simulation - digital analog simulator programs', Simulation, December 1964.

10. Gaskill, R.A., Harris, J.W., McKnight, A.L. = 'DAS - a digital analog simulator', Proceedings Spring Joint Computer Conference, 1963.

INTERACTIONS OF D.C. CONVERTERS AND WEAK A.C. SYSTEMS

C.C. Tan, Imperial College, London

SUMMARY

This paper describes a study into the interaction between d.c. convertors and weak a.c. power system. For this purpose a point-to-point H.V.D.C. link with one end connected to a weak a.c. power system has been chosen. The operation of the a.c./d.c. terminal at this end is simulated on a digital computer.

One object of the study is to find the permissible d.c. power import or export from the a.c./d.c. terminal. In order to make the study more general, a local a.c. load is also supplied from the convertor station bus.

The permissible d.c. power transfer depends on the method of control as well as on the a.c. system conditions. A second object of this study, therefore, is to determine the necessary control requirements to suit existing or anticipated a.c. system conditions.

The operation of the d.c. link is considered under both steady-state and semi-steady-state conditions. The former refers to the condition when the a.c. system, local a.c. load and d.c. power transfer are fixed. The latter refers to the interval of time after a local or remote a.c. system disturbance but before transformer tap-changer operation.

(The term "remote a.c. system" means the effect of a disturbance on the a.c. system at one end of the d.c. link on the a.c./d.c. terminal at the other end.)

Presented at the 2nd Power System Conference, Glasgow, 1967.

1. INTRODUCTION

A number of papers have been written about the operation and performance of HVDC links in an a.c. power system. In many of these the power rating of the d.c. link is small compared with the short circuit fault infeed of the a.c. system.

Very little study has been made with a d.c. link rectifying from, or inverting into, a weak a.c. system. By the term "weak a.c. system" is meant an a.c. system whose short circuit fault infeed is not very great compared with the power transfer rating of the d.c. link, say 5 times.

When a large a.c. load is also connected to the convertor station bus the sum of the d.c. and a.c. power demand may also cause the a.c. system to appear weak.

When a d.c. link is connected to such an a.c. system, the a.c. system impedance and load have a strong influence on the maximum possible d.c. power transfer and on voltage stability at the convertor bus.

The need to investigate the operation of d.c. links connected to weak a.c. systems is stimulated by the possibility of reinforcing the power supply to large load centres economically with d.c.

2. DESCRIPTION OF SCHEME (Fig. 1)

The H.V.D.C. scheme in this study is taken as a simple point-to-point link with one end connected to a weak a.c. power system. The main interest of the study is in the voltage regulation on the a.c./d.c. terminal at this end, and the permissible d.c. power transfer across the link.

The convertor station bus is connected to the a.c. system, represented as an infinite bus at nominal voltage, through a system transformers and switch B. The transformer is fitted with a tap changer. The station bus also supplies a variable local load through a network which consists mainly of underground cables. The cable capacitance is represented by a lumped capacitive load.

The station bus supplies a second bus through switch A as shown. This second bus is connected to two identical convertor transformers and a filter. Both transformers are provided with tap changers having the same range. A 6-pulse convertor bridge is fed from each convertor transformer. The two bridges are connected in series on the d.c. side to form a convertor group which can be operated either as a rectifier or as an inverter. For steady state the terminal voltage of the convertor is to be kept constant at its nominal value by tap change on the convertor transformers at the inverter end.

When the convertor is rectifying the firing angle should be kept within a specified range (say between 10° and 20°) by means of tap change on the convertor transformers. When inverting the extinction angle should be kept constant at a suitable value (about 17°).

3. SYSTEM PARAMETERS

A.C. side

Infinite bus voltage		1.0 per unit
Convertor station bus nominal voltage		132 kV
System transformer tap range		±15%
Convertor transformer tap range		+16%, -10%
	rating	189 MVA
	voltage ratio	132/111 kV
	leakage reactance	15.6%
Filter rating		70 MVAR
Lumped capacitance to represent cable network		60 MVAR
Short circuit levels to be considered:		3500, 2000, and 1000 MVA
Local a.c. load		500 MW max. 50 MW min. P/Q ratio = 5

D.C. side

Direct power rating 320 MW

Direct power rating 266 kV

Range of firing angle $\alpha = 15^\circ \pm 5^\circ$ on constant current characteristic

$\alpha_{min} = 7^\circ$ on natural voltage characteristic

$\gamma = 17^\circ$

4. DESCRIPTION OF WORK

The whole study is divided into four parts, each dealing with one form of change or disturbance in the a.c./d.c. system. Operation of the convertor both as a rectifier and as an inverter is considered in each case.

For steady state operation the convertor station bus voltage must be kept within a suitable range (say ± 10%) by tap change on the system transformer. The d.c. power transfers at nominal direct voltage is governed by this requirement, and have been calculated for different tap positions of the system transformer.

For semi-steady state responses of the a.c./d.c. terminal, that is before tap-changer operation, an a.c. system outage is assumed and this is represented as a change of short circuit fault infeed.

The local a.c. load is represented either as a constant real and reactive power sink (constant P and Q) or as a constant series impedance (constant R and X). Its power factor (determined by P/Q ratio) is assumed constant.

.1 Change in Local A.C. Load

This study determines the effect of changes in local a.c. load on the steady-state operating conditions of the a.c./d.c. system.

The d.c. power transfer is taken to be the rated value, and for any firing angles within the given range it is possible to calculate the tap positions of the convertor and system transformers.

If the total power demand at the convertor bus, i.e. the sum of the d.c. power transfer and the local a.c. load, exceeds the power transfer limit set by a.c. system short circuit fault infeed, the system transformer tap is set at the bottom tap, nominal tap, and top tap in turn to find the permissible d.c. power transfer in each case.

.2 Change in D.C. Power Transfer

This study is similar to the previous one, the variable in this case is the d.c. power transfer. The local a.c. load is kept constant.

.3 Local Disturbance

This is a semi-steady state study and the term "local" applies to the a.c. system connected to the a.c./d.c. terminal under consideration.

In the case of inverter operation, constant extinction angle control is assumed so that the extinction angle is not affected by the change of short circuit level. For rectifier operation, however, there are two possibilities. Depending on both the local a.c load and d.c. power transfer at the time of the disturbance, the convertor bus voltage may rise or fall. (From results of 4.2) If this voltage rises, it will be necessary to increase the firing angle α so as to keep the direct voltage constant. On the other hand, a fall in convertor bus voltage may fall down the direct voltage so that the rectifier characteristic crossess the current margin. The inverter at the remote end of the d.c. link takes over constant current control, and the rectifier operates with a minimum firing angle α min (about 7°).

For this purpose different current margin settings have been used. Constant power and constant current control of the d.c. transmission have been studied.

4.4. Remote Disturbance

In this part, a disturbance is assumed to occur in the a.c. system connected to the far end of the d.c. link, and it is required to find the response of the a.c./d.c. terminal of the near end. The result of the disturbance is assumed to be a change in the direct voltage V_d of the d.c. link, but the nature of the disturbance need not be specified.

Since the direct voltage is specified (e.g. 10% increase or decrease on the rated value) it is now required to find the new firing angle α for a rectifier or the advance angle β for an inverter. (The advance angle β is required because the inverter is no longer on constant extinction angle control when the current margin is crossed if the direct voltage V_d is reduced).

5. RESULTS AND SELECTED GRAPHS

The following results apply to a local a.c. load P/Q ratio of 5.

(1) Effect of a.c. system short circuit level (Fig. 3)

The effect of short circuit level on d.c. power transfer is summarised as follows:-

Short Circuit Level MVA	Local A.C. Load MW	D.C. Power MW	
		Export	Import
3500	500	>320	>320
	50	>320	"
2000	500	>260	"
	50	>320	"
1000	400	>66 *	"
	50	>310	"

* Voltage instability may occur.

The above results are based on the following parameters:-

(i) $\alpha = \gamma = 17^{\circ}$

(ii) Convertor bus voltage at nominal $\pm$ 10%.

(iii) System transformer at highest tap of +15% (h = 1.15). This gives the maximum power transfer.

(2) Effect of a.c. load change (Fig. 3)

A reduction in local load does not allow the direct power export to be increased by the same amount without tap changing.

(3) Effect of D.C. Outage (Fig. 4)

Outage of the d.c. link, which may be caused by blocking, can cause voltage rise or fall at the converter bus, depending upon a.c. load and d.c. power transfer.

(4) D.C. Power Reversal (Fig. 4)

Fig. 4 shows that rectifier operation causes higher voltage regulation than inverter operation. Therefore cases will arise in which full d.c. power reversal is not possible unless the convertor transformers change taps.

(5) Local Disturbance (Fig. 5-8)

From the figures it can be seen that the a.c. system short circuit fault infeed governs the maximum possible d.c. power transfer. With constant power control, therefore, the power setting must conform with the existing and anticipated a.c. system conditions.

When the rectifier characteristic crosses the current margin, the convertor bus voltage should not fall below - 10%. A suitable current margin to achieve this can be obtained from curves of convertor bus voltage against direct current. ($e_b - I_d$).

A constant R and X representation of the local a.c. load gives a better voltage regulation than a constant P and Q representation.

(6) Remote Disturbance (Figs. 9-12)

The figures generally suggest that constant current control gives a better voltage regulation on the convertor bus than constant power control.

Acknowledgement

The author wishes to thank his supervisor at Imperial College, Mr. B.J. Cory, Senior Lecturer in Power System, who gave advice and encouragement, and Mr. W.G. Watson of C.E.G.B. who provided valuable suggestions. He also wishes to express his gratitude to C.E.G.B. for sponsoring the project.

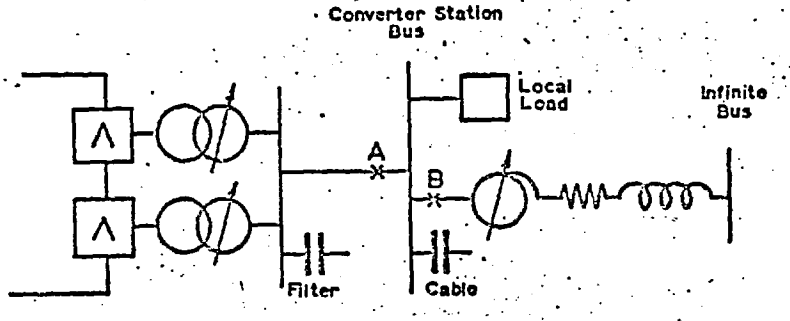
Converter Station Bus
Local Load
Infinite Bus
A
B
Filter
Cable

FIG. 1

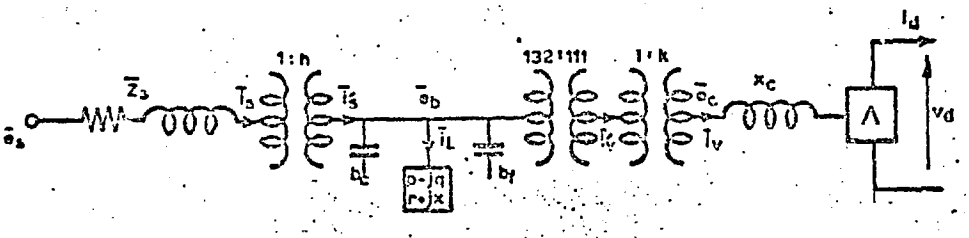
1:n
1321111
1:k
$\bar{z}_s$
$\bar{e}_b$
$\bar{i}_L$
p-jq
r+jx
x_c
I_d
V_d

FIG. 2

Converter Bus Voltage p.u.
1.10
1.05
1.00
0.95
0.90
0.85
0.80
Converter Bus Voltage vs Direct Power Transfer
α = γ = 17°
h = +15%
Inverting
Rectifying
3500
P=2500
P=4000
P=1500
P=500
P=50
P=500
P=50
P=500
P=50
P=300
P=50
V=500
Direct Power Transfer M.W.
0
40
80
120
160
200
240
280
320
-211-

Fig 3.1

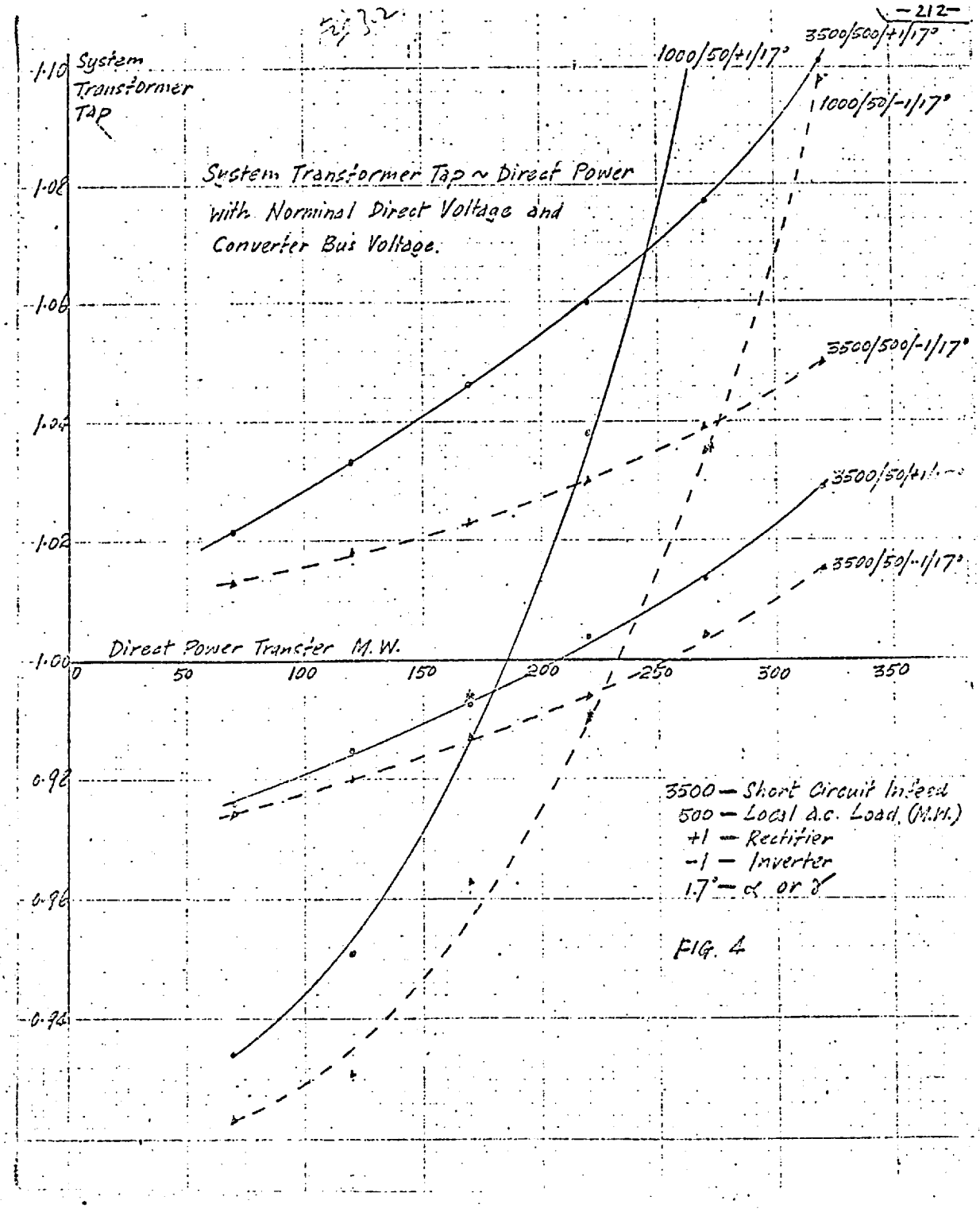
System Transformer Tap
1.10
1.08
1.06
1.04
1.02
1.00
0.98
0.96
0.94
System Transformer Tap ~ Direct Power
With Nominal Direct Voltage and
Converter Bus Voltage.
1000/50/+1/17°
3500/500/+1/17°
1000/50/-1/17°
3500/500/-1/17°
3500/50/+1/17°
3500/50/-1/17°
Direct Power Transfer M.W.
0
50
100
150
200
250
300
350
3500 — Short Circuit Infeed
500 — Local a.c. Load (M.W.)
+1 — Rectifier
-1 — Inverter
17° — α or δ

FIG. 4

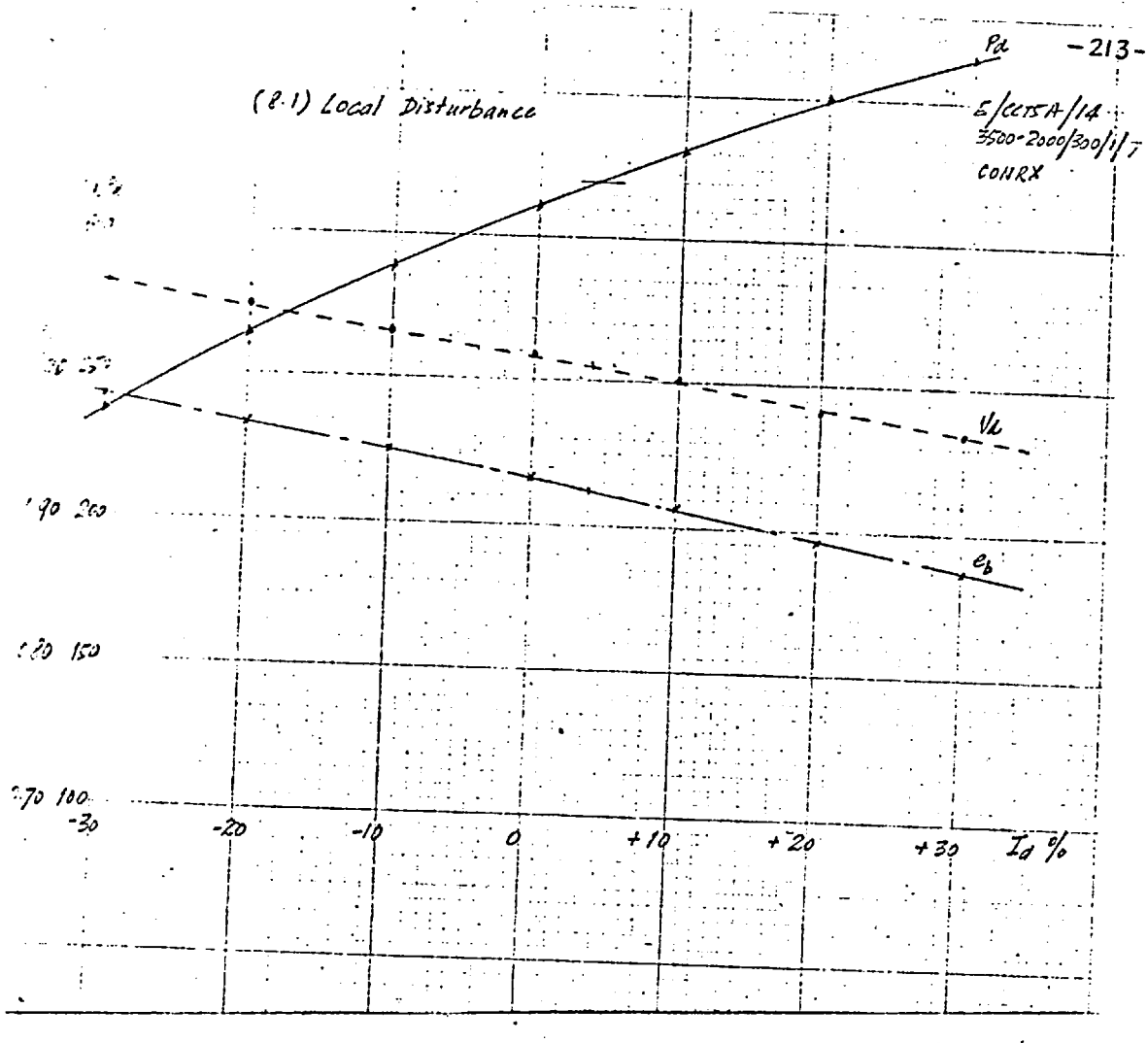

FIG 5 Rectifying

Change of Short Circuit Infeed 3500 - 2000 MVA.

e_b = Converter Bus Voltage

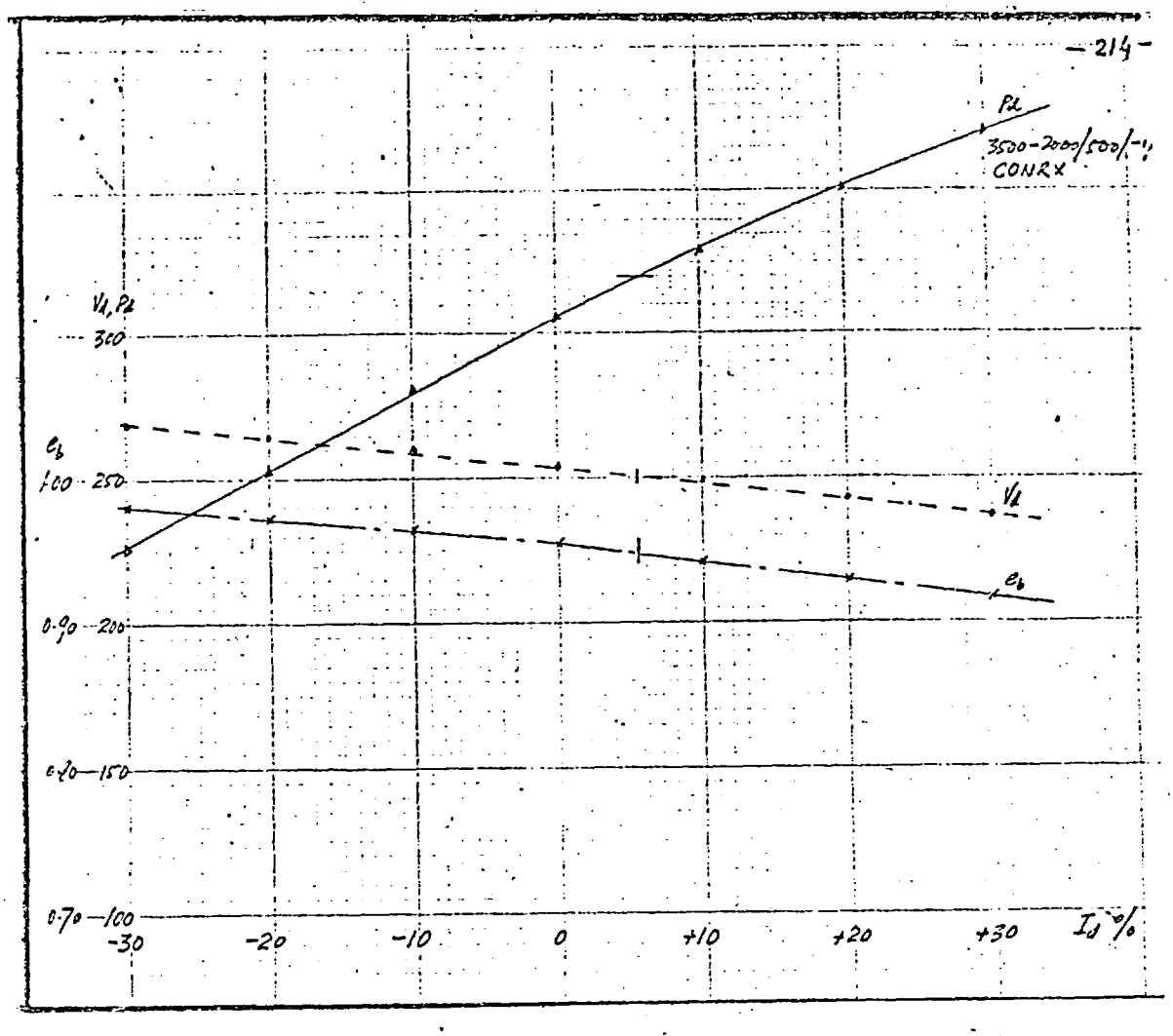

FIG. 6 Inverting

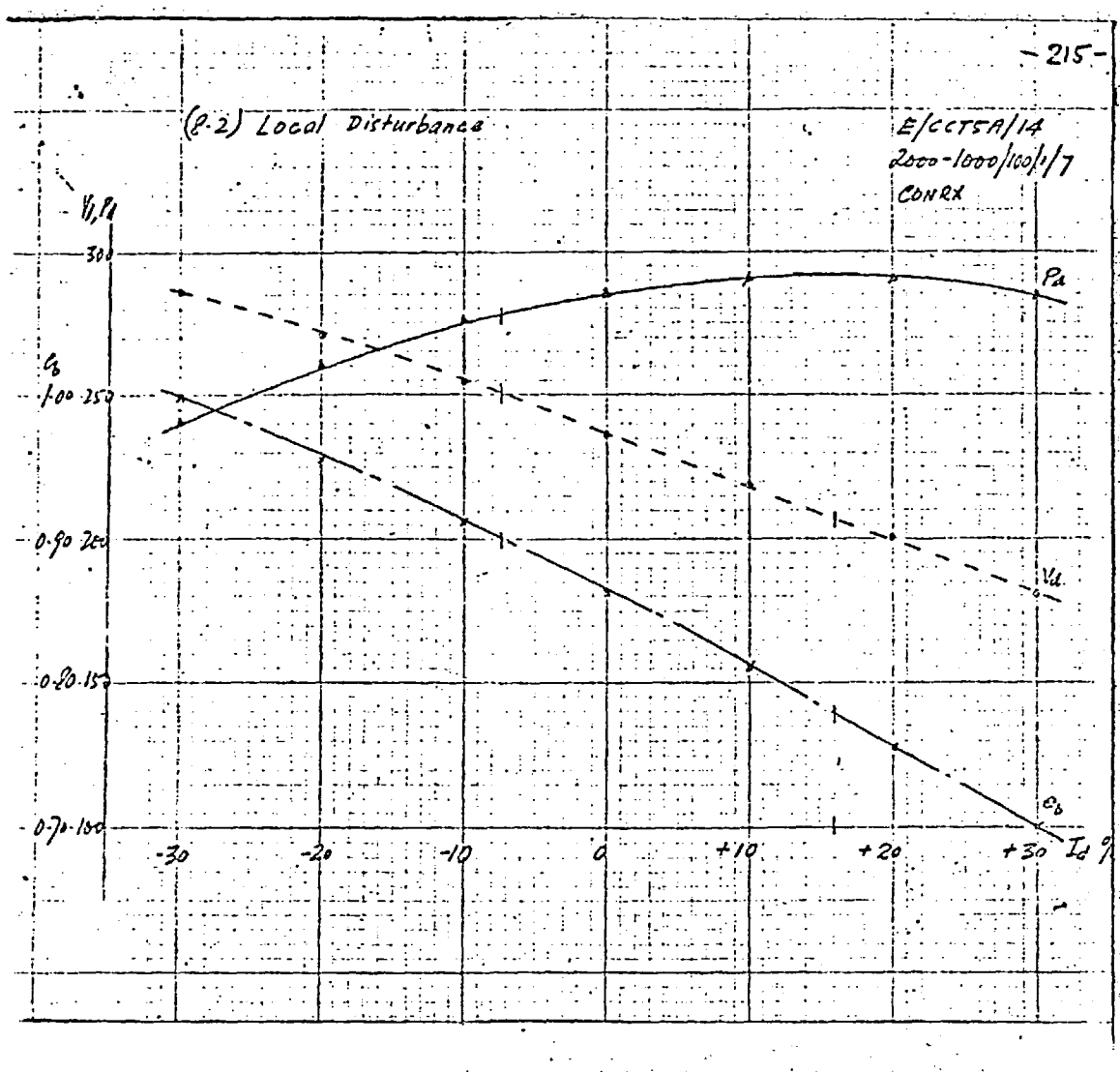

FIG. 7 Rectifying
Change of Short Circuit Infeed 2000-1000 MVA

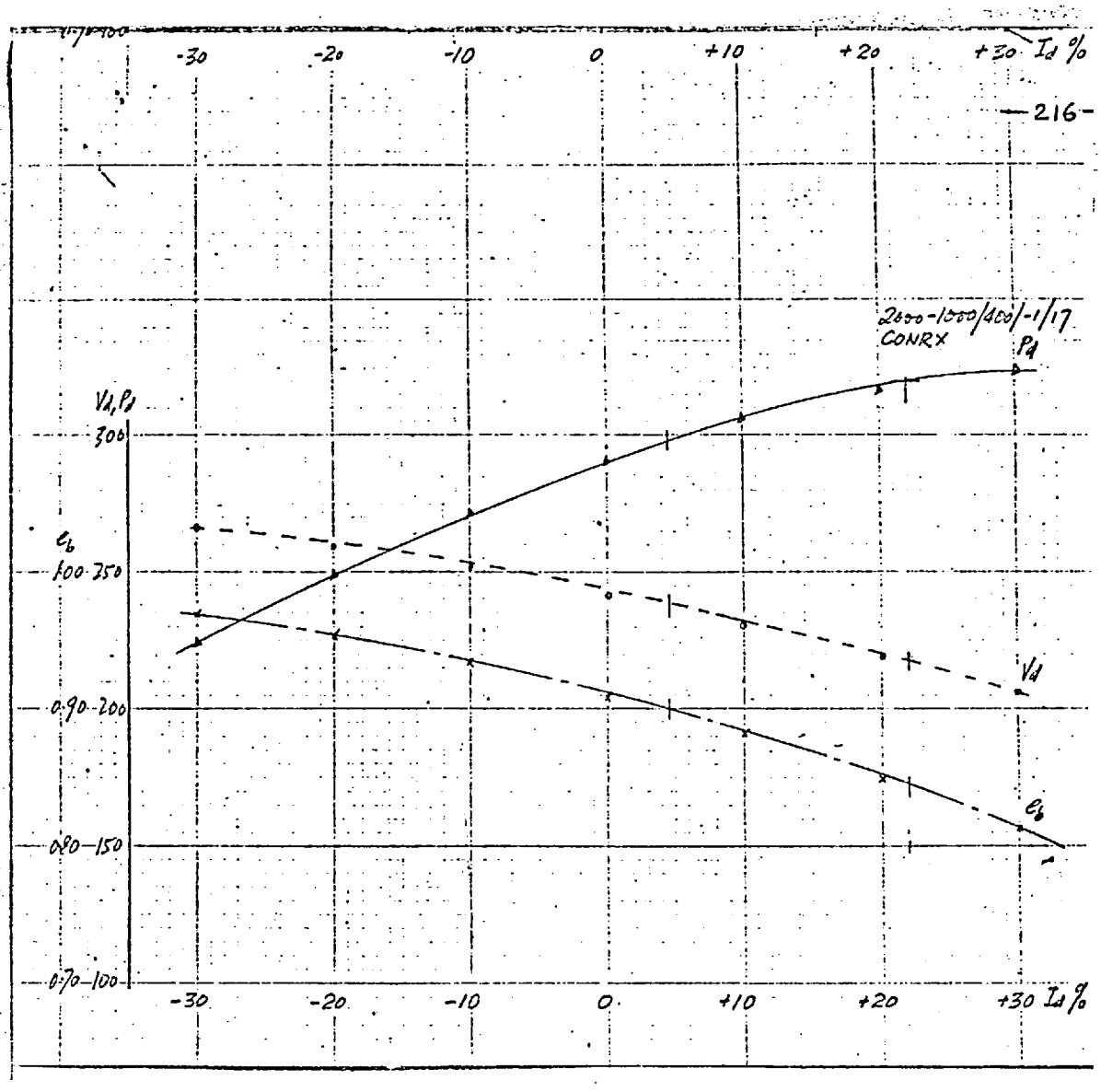

FIG 8 Inverting

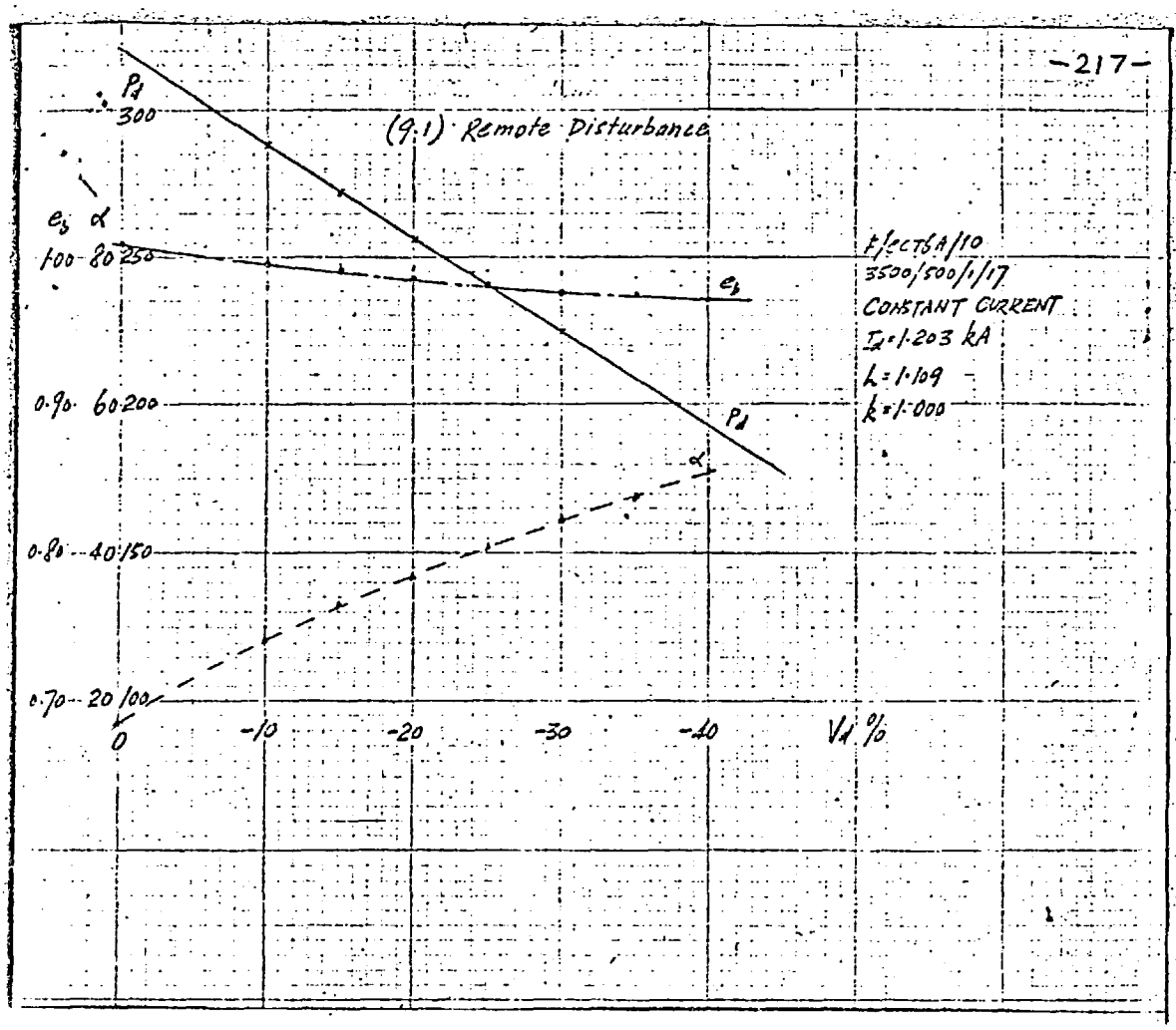
(9.1) Remote Disturbance
P_d
300
e_b α
100 80 250
0·90 60 200
0·80 40 150
0·70 20 100
0
-10
-20
-30
-40
V_d %
e_b
P_d
α
E/ECTBA/10
3500/500/1/17
CONSTANT CURRENT
I_d = 1·203 kA
L = 1·109
k = 1·000

FIG. 9.

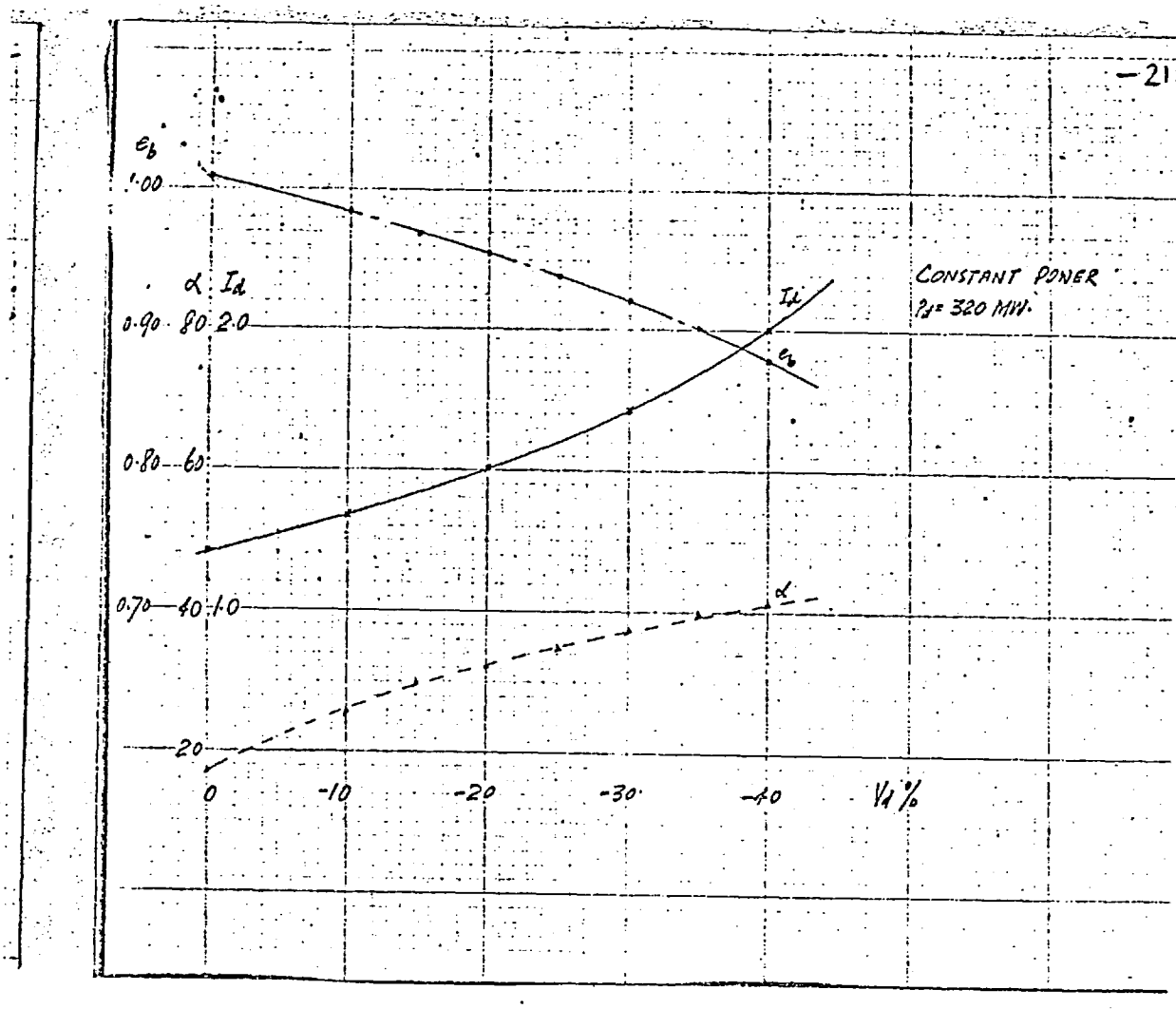
e_b
1·00
α I_d
0·90 80 2·0
0·80 60
0·70 40 1·0
20
0
-10
-20
-30
-40
V_d %
I_d
e_b
α
CONSTANT POWER
P_d = 320 MW.

FIG. 10

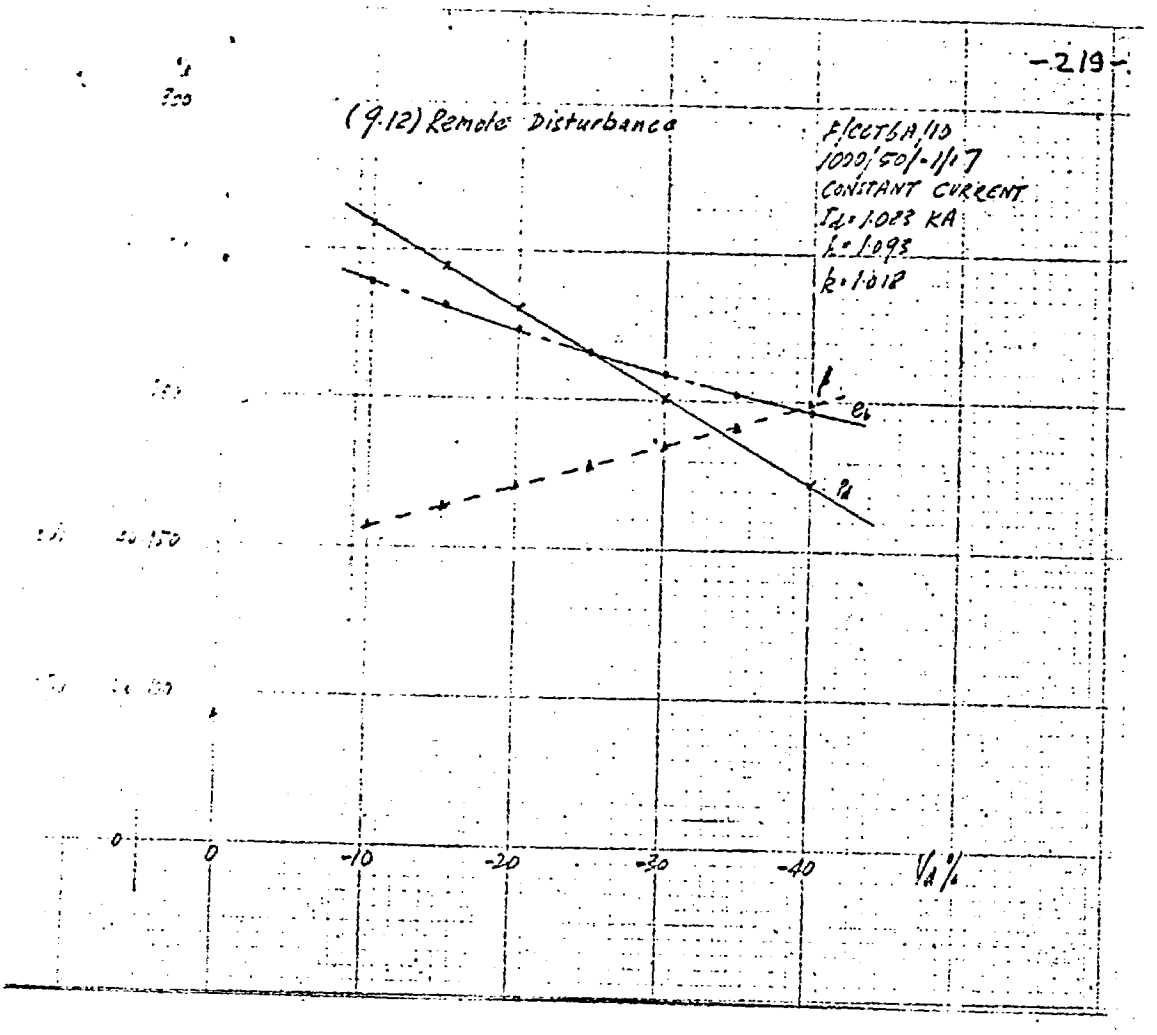
(9.12) Remote Disturbance
ELECTRA 110
1000, 50/-1/17
CONSTANT CURRENT
I_d = 1.023 KA
L = 1.093
k = 1.018
e_t
e_d
0
-10
-20
-30
-40
V_d %

FIG. 11

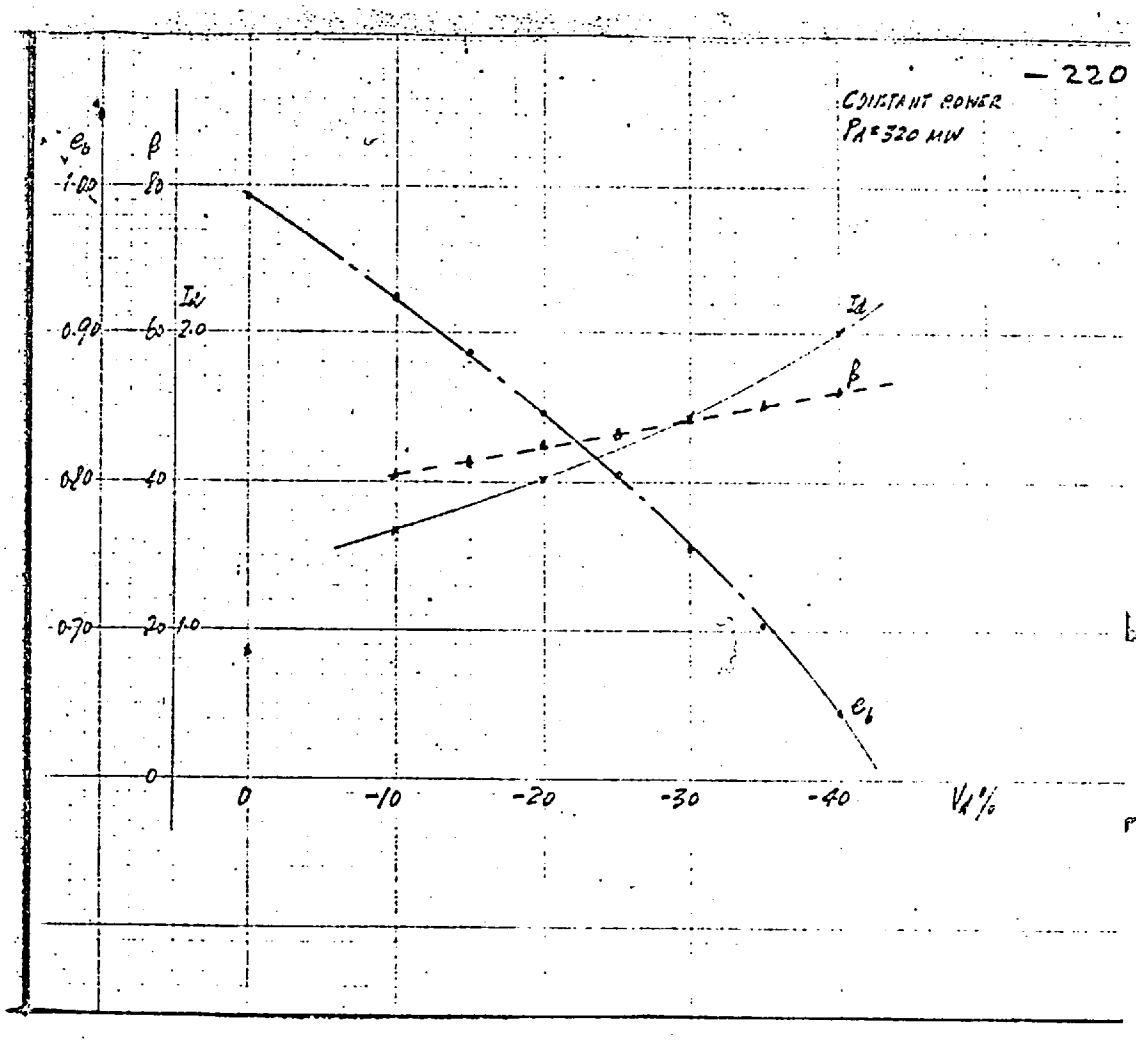
— 220
CONSTANT POWER
PA = 320 MW
e_b
β
1.00
80
I_d
0.90
60
2.0
I_d
β
0.80
40
0.70
20
1.0
e_b
0
0
-10
-20
-30
-40
V_d %

FIG. 12